Determination of the Composition and Architecture of the Mitochondrial Ubiquitome in PINK1/Parkin Mitophagy

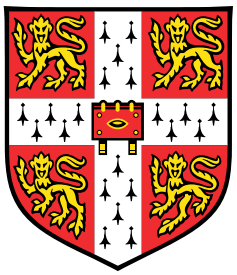

Joanne Louise Usher

MRC Laboratory of Molecular Biology
University of Cambridge

This thesis is submitted for the degree of
Doctor of Philosophy

Peterhouse July 2020

Declaration

This thesis is the result of my own work and includes nothing which is the outcome of work done in collaboration except as declared in the Preface and specified in the text. It is not substantially the same as any that I have submitted, or, is being concurrently submitted for a degree or diploma or other qualification at the University of Cambridge or any other University or similar institution except as declared in the Preface and specified in the text. I further state that no substantial part of my thesis has already been submitted, or, is being concurrently submitted for any such degree, diploma or other qualification at the University of Cambridge or any other University or similar institution except as declared in the Preface and specified in the text. It does not exceed the prescribed word limit for the relevant Degree Committee.

Joanne Louise Usher
July 2020

Acknowledgements

I would first like to acknowledge my supervisory team. To my main supervisors: David Komander, thank you for welcoming me to the lab, and giving me the opportunity to pursue this excellent project; Alex Whitworth, thank you for stepping in at relatively short notice, and giving me the opportunity to take the work in a new direction. To my second supervisor Julian Sale and my university supervisor Heike Laman, thank you for being a constant through all of this. To my whole supervisory team, thank you for your mentorship, and for helping me to get to this point.

I would like to thank all the former members of the Komander lab alongside whom I had the pleasure of working: Rune Busk Damgaard, Paul Elliott, Malte Gersch, Christina Gladkova, Anja Kück, Tycho Mevissen, Martin Michel, Jonathan Pruneda, Alex Schubert, Yuri Shibata, Michal Šimíček and Kirby Swatek. Thank you all for your mentorship, help around the lab, and good times outside too. Special thanks go to Kirby, for your help with the mass spectrometry side of things; to Christina, for performing the *in vitro* assembly assays; to Martin, for helping me with expression and purification of recombinant proteins; to Rune, for your company and guidance for your last several months at the LMB; to Paul, for your guidance and supply of proteins for the UbiCRest assays; and to Jonathan, for your guidance in how best to address the reviewer comments for our Ub-clipping paper. I would also like to give my thanks to the Whitworth lab: Simonetta Andreazza, Wing Hei Au, Tom Gleeson, Victoria Hewitt, Juliette Lee, Aitor Martinez Zarate, Leonor Miller-Fleming, Alvaro Sanchez-Martinez, Ana Terriente-Felix, Roberta Tufi, and Natalie Welsh. Thank you all for welcoming me into the lab, and for teaching me how to work with *Drosophila*. Special thanks go to Alvaro, for always being willing to help me develop this project, and to Aitor, for rewarding discussions about the project and associated biology.

Thank you to the mass spectrometrists who have taught me all I know. In the LMB mass spectrometry facility, particular thanks go to Sarah Maslen, for helping me out of many a sticky situation; to Mark Skehel, for your guidance when I thought I had reached a dead end;

and to Sew Peak Chew, for useful discussions about using and procuring StageTips. I would also like to thank Andrew Webb at the Walter and Eliza Hall Institute for taking me under your wing for a month: without your valuable teaching I most certainly would not have been able to complete this project.

My thanks go out to the people who make up the huge scientific support structure at the LMB: the media kitchen, the Stores personnel, the IT team, and the Domestic Services staff, who together make the LMB the most amazing place to work. Particular thanks go to Michele Kidd at the animal facility for providing mouse brain samples. I would also like to thank the students' administrative team, both at the LMB and the MBU, for all of your help throughout the years. Thank you to Gates Cambridge, both for the scholarship that has allowed me to pursue this opportunity, but also for the community of amazing students to whom you have introduced me. To the Peterhouse community: thank you to my fellow students, and college staff, both academic and non-academic, for making Peterhouse my home away from home. I would particularly like to thank the members of the Peterhouse Chapel Choir, and the MCR, for being my family outside the lab. I would also like to thank the members of CUMPC, for providing such a supportive, encouraging environment outside of academic work.

Finally, to my partner, friends and family, thank you all for your support throughout all of this. I hope to celebrate in person with all of you before too long.

Abstract

Parkinson's Disease is the second most common age-related neurodegenerative disorder, with multiple lines of evidence suggesting that mitochondrial dysfunction may underlie the etiology of the disease. The kinase PINK1, and the ubiquitin (Ub) E3 ligase Parkin, function in a pathway to maintain mitochondrial quality control through the engulfment of mitochondria by the autophagy system, in a process termed mitophagy. Through a positive feedback loop centred on the production of S65-phosphorylated Ub, PINK1 and Parkin work in concert to ubiquitinate proteins on the outer mitochondrial membrane, leading to the recognition, engulfment, and eventual destruction of the damaged mitochondria by the autophagy machinery. While significant work has been done to establish the substrates and chain type composition of the Ub placed on mitochondrial substrates by Parkin, little work has been done to establish the broader Ub chain architecture: the degree of chain branching, and the relationship between phosphorylation and chain formation in the context of a single ubiquitin moiety. Further, while *Drosophila melanogaster* has been successfully used as a model organism to understand that PINK1 and Parkin function in a common pathway, the chain composition of mitochondrial Ub has not been explored in this model. Using a novel mass spectrometry-based technique, Ub-clipping, combined with biochemical methods for understanding Ub biology, this thesis explores the composition and architecture of the mitochondrial ubiquitome. Using a depolarisation-induced HeLa cell model, it was found that Parkin predominantly produces mono- and short chain-ubiquitination of integral mitochondrial membrane proteins, and that mono- and distal Ub moieties are preferentially phosphorylated. Further, significant method development was performed to enable detection of the lowly abundant mitochondrial Ub in *Drosophila*, and it was found that treatment of flies with the oxidant paraquat robustly induces formation of pS65-Ub in the presence of endogenous levels of PINK1 and Parkin. These results further our understanding of the precise nature of Parkin-mediated ubiquitination events, and provide the first evidence that the feedforward production of pS65-Ub occurs in response to the induction of mitochondrial damage in *Drosophila*. The paraquat model for inducing PINK1 and Parkin activation will form a basis for future studies understanding the role of PINK1 and Parkin, in enabling the

study of other players in the PINK1/Parkin pathway, and in determining the downstream fate of pS65-ubiquitinated mitochondria, in the context of an organism.

Table of contents

List of figures

List of tables

Acronyms and Abbreviations

λPP	λ phosphatase
ACN	Acetonitrile
ACT	Activating element
AQUA	Absolute quantification
ATP	Adenosine triphosphate
BME	β-mercaptoethanol
CCCP	Carbonyl cyanide m-chlorophenyl hydrazone
CTR	C-terminal region
CV	Column volume
Cyt *c*	Cytochrome *c*
DMEM	Dulbecco's modified Eagle medium
DMSO	Dimethyl sulfoxide
DNA	Deoxyribonucleic acid
Drp1	Dynamin-related protein 1
DTT	Dithiothreitol
DUB	Deubiquitinase
EDTA	Ethylene-diamine-tetraacetic acid
FA	Formic acid

FBS	Fetal bovine serum
FMDV	Foot and mouth disease virus
GAPDH	Glyceraldehyde 3-phosphate dehydrogenase
GST	Glutathione-S-transferase
GTP	Guanosine triphosphate
HA	Haemagglutinin
HCD	Higher-energy collisional dissociation
HECT	Homologous to E6AP C-terminus
HRP	Horseradish peroxidase
IBR	In-between-RING
IMM	Inner mitochondrial membrane
IMS	Intermembrane space
IPTG	Isopropyl β-d-1-thiogalactopyranoside
ISG	Interferon-stimulated gene
Lb^{pro}	Leader protease
LC-MS	Liquid chromatrography-mass spectrometry
LDS	Lithium dodecyl sulfate
LIR	LC3-interacting region
LPS	Lipopolysaccharide
MDV	Mitochondria-derived vesicle
MES	2-(N-morpholino)ethanesulfonic acid
Mfn	Mitofusin
MHC	Major histocompatibility complex

MPP^+	1-methyl-4-phenylpyridinium
MPP	Mitochondrial processing peptidase
MPTP	1-methyl-4-phenyl-1,2,3,6-tetrahydropyridine
MS	Mass spectrometry
mtDNA	Mitochondrial DNA
MTS	Mitochondrial targeting sequence
MUL1	Mitochondrial Ub E3 ligase 1
MW	Molecular weight
NDP52	Nuclear dot protein 52 kDa
Ni-NTA	Nickel-nitrilotriacetic acid
NLS	Nuclear localisation sequence
OA	Oligomycin and Antimycin A
OMMAD	OMM-associated degradation
OMM	Outer mitochondrial membrane
OMS	OMM localisation sequence
OPA1	Optic atrophy 1
OPTN	Optineurin
OTC	Ornithine transcarbamylase
OXPHOS	Oxidative phosphorylation
P/S	Penicillin-streptomycin
PAA	PA artefact
PA	Perchloric acid
PARL	Presenilin-associated rhomboid-like protein

PBS	Phosphate-buffered saline
PBST	Phosphate-buffered saline with Tween 20
PD	Parkinson's Disease
PE	Phosphatidylethanolamine
PINK1	PTEN-induced putative kinase 1
PK	Proteinase K
PMS	Post-mitochondrial supernatant
PQ	Paraquat
PRM	Parallel reaction monitoring
PTM	Post-translational modification
PVDF	Polyvinylidene difluoride
RBR	RING-IBR-RING
RING	Really interesting new gene
ROS	Reactive oxygen species
SAM	Sorting and assembly machinery
SDS-PAGE	Sodium dodecyl sulfate- polyacrylamide gel electrophoresis
StageTips	Stop-and-go extraction tips
STING	Stimulator of interferon genes
TAX1BP1	TAX1-binding protein 1
TIM	Translocase of the inner membrane
TMS	Transmembrane sequence
TOM	Translocase of the outer membrane
TUBE	Tandem Ub binding entity

Ub-CR	Ub C-terminally retracted
UBA	Ub-associated
UBD	Ub-binding domain
UbiCRest	Ubiquitin Chain Restriction
Ubl	Ub-like
Ub	Ubiquitin
UIM	Ub-interacting motif
UPD	Unique Parkin domain
UPS	Ub-proteasome system
USP	Ub-specific protease
VDAC	Voltage-dependent anion channel
WT	Wild-type

Chapter 1

Introduction

1.1 Mitochondria are hubs of cellular metabolism

Mitochondria are highly dynamic organelles that contribute to a plethora of cellular functions, including ATP generation, synthesis of important cofactors such as iron-sulfur clusters, immune signalling, and apoptosis [267, 171]. Additionally, mitochondria are a major source of reactive oxygen species (ROS), which perform vital signalling functions but can result in damage to proteins, lipids and DNA [267, 171]. Mitochondria are believed to have arisen from an endosymbiotic event involving the engulfment of an early α-proteobacterium by an archaeal ancestor [69, 153]. Mitochondria therefore contain multiple vestiges of their bacterial ancestry, including their own circular DNA chromosome (mtDNA) and an inner and outer mitochondrial membrane (IMM and OMM respectively) that predominantly contain α-helical and β-barrel structures, respectively [69, 280, 94, 293]. A brief summary of several of the vital processes performed by mitochondria follows.

1.1.1 The OXPHOS system

The best-appreciated function of mitochondria is their role in generating ATP, the energy currency of the cell. This is achieved through the oxidative phosphorylation (OXPHOS) system, consisting of a series of five IMM-embedded multi-subunit complexes. In brief, Complexes I through IV generate an electrochemical proton gradient, consisting of $\Delta\Psi$m and ΔpH, across the IMM through a series of oxidative reactions that are coupled with the pumping of protons from the matrix to the intermembrane space (IMS), resulting in the reduction of molecular oxygen. Complex V then facilitates the energetically favourable transfer of protons accross the IMM back into the matrix to generate ATP from ADP and

inorganic phosphate. The OXPHOS system is dependent on the tightly controlled transport of metabolites across the IMM, which is achieved through the action of a range of membrane-embedded carrier proteins for substrates that include ADP, ATP, phosphate and pyruvate among others [133]. Complex I (NADH:ubiquinone oxidoreductase) is the largest of the OXPHOS complexes, consisting of 45 subunits in humans [19, 174]. Complex I is the major source of mitochondrial ROS, and mutations in many subunits and assembly factors have been reported to be causative in childhood-onset neuromuscular disorders [182, 174]. Further, exposure to chemicals that induce ROS generation through Complex I has been associated with neurodegenerative disease [278], as described further in Section 1.3.

1.1.2 Mitochondrial protein import

The mitochondrion can be divided into four compartments: the OMM, the IMM, the IMS and the matrix. Of the approximately 1,000 proteins in the mitochondrial proteome, only 13 are encoded by the mitochondrial genome, translated in the mitochondrial matrix, and directly assembled alongside nuclear-encoded subunits into the IMM-resident OXPHOS Complexes I, III, IV, and V [181]. The remaining proteins are encoded by the nuclear genome, translated in the cytosol, and imported post-translationally into the mitochondria where they must localise to the correct sub-mitochondrial compartment [11]. All nuclear-encoded proteins, with the exception of some single pass OMM proteins, are imported via the translocon of the outer membrane (TOM) complex, which in humans consists of the β-barrel pore-forming TOMM40 subunit, the receptors TOMM20, TOMM22, and TOMM70, and the small TOM proteins TOMM5, TOMM6, and TOMM7 [87, 108, 11, 290]. Translocation of nuclear-encoded mitochondrial proteins through the TOMM40 pore usually occurs from the N-terminus and requires the protein to be either unfolded or in a single loop conformation, which is aided by binding of the precursor to cytosolic chaperones [290, 11]. OMM-targeted proteins either diffuse laterally into the OMM from the TOM complex [75], or are transported through the IMS and assembled in the OMM by the sorting and assembly machinery (SAM) complex [11]. Matrix- or IMM-targeted proteins containing an amphipathic presequence are imported via the translocase of the inner membrane 23 (TIM23) complex, while IMM-integral carrier proteins are imported via the TIM22 complex [229, 11]. Import that occurs through the TIM23 complex requires an intact mitochondrial membrane potential ($\Delta\Psi$m), which is generated by the OXPHOS system [11]. Following import, the protein's amphipathic presequence is cleaved by the mitochondrial processing peptidase (MPP) to form a mature

protein [11]. The reliance on $\Delta\Psi m$ for mitochondrial protein import causes OXPHOS and mitochondrial protein import to be closely coupled.

1.1.3 Mitochondrial homeostasis

The maintenance of the correct abundance, distribution, and functioning of mitochondria within the cell requires a number of interweaving homeostatic mechanisms. These include mitochondrial dynamics, biogenesis, and turnover of proteins and whole organelles. Mitochondria constantly fuse and divide; changes in the balance of mitochondrial fission and fusion occur in response to or concurrent with changes in metabolic demands, or in response to mitochondrial insults [218]. Mitochondrial fission relies on Drp1, a large Dynamin family GTPase that is recruited from the cytosol to scission sites through binding of OMM-resident adapters [262, 205]. Mitochondrial fusion is mediated by the mitofusins (Mfn1 and Mfn2 in humans), which mediate OMM fusion, and OPA1, which mediates IMM fusion [24, 72]. The mitofusins and OPA1 are integral OMM (facing the cytosol) and IMM (facing the IMS) proteins respectively [73, 199]. Many functions of mitochondrial fission have been proposed, including in aiding mitochondrial motility, particularly along axons [98], improved release of Cytochome *c* during apoptosis [155], and segregation and degradation of damaged mitochondria by autophagy [291], a process described further in Section 1.3. Conversely, mitochondrial fusion has been implicated in efficient energy generation via OXPHOS [175], and in protecting mitochondria from destruction by mitophagy [67, 226]. Further maintaining mitochondrial homeostasis are mitochondrial transport, biogenesis and degradation, and disruption of this delicate balance of processes can lead to numerous diseases [143, 147].

Several interconnected and partially overlapping modes of mitochondrial quality control exist, in different physiological contexts and in response to different inputs. One such pathway is the destruction of mitochondria by autophagy, termed mitophagy, in response to mitochondrial damage. An important step in the signalling for the autophagic destruction of damaged mitochondria is the labelling of the organelle with ubiquitin (Ub), a small protein modifier discussed further below. This chapter will explore the process of mitophagy, and specifically the Ub-dependent process initiated by the enzymes PINK1 and Parkin. First, a discussion of the Ub system is presented, including methods that have been developed for analysing ubiquitination in cells. Next, the role of PINK1 and Parkin in mitochondrial quality control in health and neurodegenerative disease will be discussed, followed by a review of the animal models of PINK1 and Parkin deficiency.

1.2 The Ub system

Ub is a small protein that participates in myriad intracellular signalling processes as a post-translational modification (PTM) of target proteins. Its 76-amino-acid sequence is highly conserved, with human and *Drosophila* Ub sequences being identical, while the yeast sequence differs by only three residues. It folds tightly into a compact structure with a flexible 6-residue tail at the C-terminus, resulting in a highly stable protein that is resistant to acid and heat (Figure 1.1A) [299, 215]. Canonical ubiquitination involves the conjugation of the Ub C-terminus to the amino-ε group of substrate lysine residues, forming a covalent isopeptide (amide) bond. More recently, non-canonical ubiquitination of serine, threonine and cysteine residues has been described; these modifications are more labile than lysine ubiquitination, and have therefore not been as well-studied [161]. Ubiquitination of proteins involves a three-step ATP-dependent process involving E1 activating, E2 conjugating, and E3 ligase enzymes (Figure 1.1B). The human genome encodes two E1 enzymes, approximately 40 E2s, and over 600 E3s [144]. There are two main categories of E3 enzymes, Really Interesting New Gene (RING) and Homologous to E6AP C-Terminus (HECT) [238, 126]. RING ligases function as E2 activators, stimulating Ub transfer directly from the E2 to the substrate (Figure 1.1B, left). In comparison, HECT ligases transfer the Ub from the E2 onto a catalytic C residue on the E3, before transferring the Ub to the substrate lysine (Figure 1.1B, right) [238]. A third class of E3 ligases, RING-in-between-RING (IBR) -RING ligases (RBR ligases), structurally resemble RING ligases but function similarly to HECT ligases in that Ub is transferred to the substrate via a catalytic C on the E3 [311].

1.2.1 Structure-function relationships in the Ub system

Ubiquitination is a highly complex PTM, due to the fact that Ub, itself a protein, can be further modified by PTMs. Ub contains 7 lysines, which alongside its N-terminus are all solvent exposed, allowing further ubiquitination to form chains (Figure 1.1A). Ub chains may consist of a single linkage type (homotypic), different linkages (heterotypic), and may contain multiple Ub linkages on a single moiety (branched chains); the vast combination of potential modifications of Ub is termed the Ubiquitin Code (Figure 1.1C) [126]. For RING E3 ligases, the chain type specificity is predominantly determined by the E2, while for HECT and RBR E3 ligases, the chain type is determined by the E3 [325, 126]. Ub chains linked at K48 and K63, termed canonical linkages, are the most common Ub linkage type. K48 chains are thought to destine the substrate for degradation by the Ub-proteasome system (UPS), while K63 chains are generally thought to have non-degradative signalling roles [23, 48, 265].

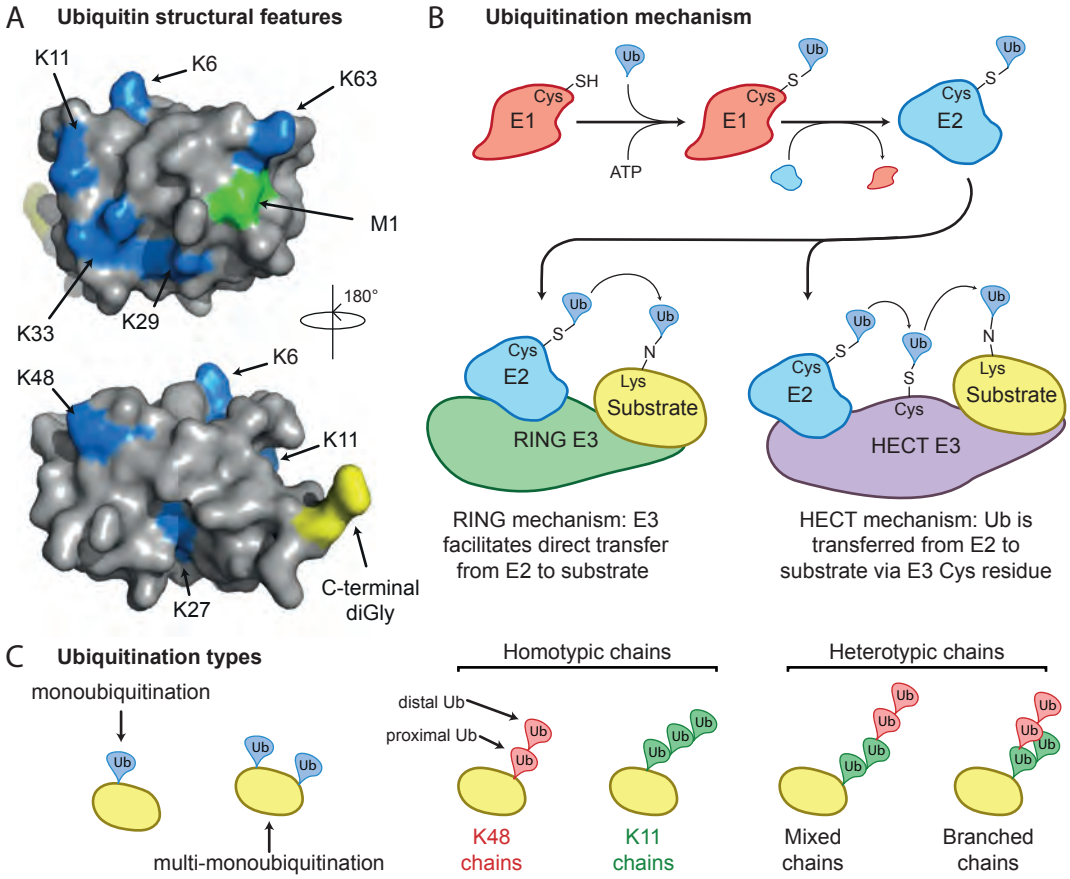

Fig. 1.1 **Ubiquitination is a versatile PTM. A.** Surface representation of Ub (PDB code 1UBQ [299]), with features relevant for conjugation indicated (lysines in blue, M1 in green, C-terminus in yellow). **B.** Mechanism of RING- and HECT-mediated substrate ubiquitination. The catalytic C residue of the E1 activating enzyme (red) is charged with the Ub C-terminal carboxy group in an ATP-dependent process. The Ub is then transfered in a transesterification process to an E2 (blue) C residue. RING E3 ligases (left) mediate the direct transfer of the Ub from the E2 to a substrate K residue, while HECT E3 ligases (right) transfer the Ub to a catalytic C residue prior to the substrate K residue. **C.** Illustration of ubiquitination types.

In addition to the canonical chains, the non-canonical M1 (linear), K6, K11, K27, K29 and K33 chains all exist in cells [305, 118, 275]. More recent work has established a role for M1-linked chains in immune signalling [254], K11 chains in cell cycle control [314], while K6 chains have been implicated in mitophagy [36, 63]. Further, Ub chains of mixed linkages occur in cells, and a function has been described for K11/K63 mixed chains in the regulation of MHC Class I receptor import into cells [12]. Chain branching has also been detected in cells [35], but the extent to which this modification is important for cellular signalling remains unclear.

Due to the location of the K residues on different surfaces of Ub (Figure 1.1A), differently linked Ub chains form distinct structures. Generally speaking, K63- and M1-linked chains form very open structures, analogous to beads on a string [127]. Conversely, K6, K11, and K48 chains form compact structures, in which the various linked Ub molecules form direct interfaces with one another [89, 15, 32]. These structural differences underlie the function of distinct chain types in diverse signalling processes, and is conferred by the preferential binding of proteins containing different Ub-binding domains (UBDs) to specific chain types. Mechanistically, UBDs may recognise a specific chain type by directly binding the Ub-Ub interface, which underlies the K48-specific binding of the Ub-associated (UBA) domain of the yeast protein Mud1 [284]. Alternatively, linkage specificity can be conferred by linkage-specific avidity, a form of cooperative binding in which binding of one domain to Ub places the second domain in an optimal conformation for binding to a specific chain type [258]. This is the case for the protein Rap80, which contains two Ub-interacting motifs (UIMs) that confer K63 linkage specificity [263]. Rather than recognising the Ub-Ub interface, linkage specificity in Rap80 is determined by an alpha-helical linker between the two UIMs that places the second UIM in a position to preferentially bind the open K63-linked conformation [258]. Substrate monoubiquitination can also be recognised by the binding to both the Ub and a domain within the substrate, as is the case for the binding of polι to monoubiquitinated PCNA during DNA damage [8]. In addition to recognition of Ub modifications by UBDs, substrate ubiquitination can cause autoinhibition by blocking a binding site; monoubiquitination of Smad4 prevents its association with phosphorylated Smad2, which regulates TGFβ signalling [43]. Ubiquitination has also been shown to control subcellular localisation of a protein, such as the monoubiquitination of p53, which controls its export from the nucleus [20].

Ubiquitination is relieved by deubiquitinases (DUBs), for which 99 genes (including some probable pseudogenes) exist in humans [29]. Ub-specific protease (USP) DUBs are generally believed to have some degree of substrate specificity but low Ub chain type preference [45]. Conversely, JAMM family DUBs such as AMSH tend to have a preference for K63 chains [162], while the OTU family DUBs OTUB1 and OTULIN are K48- and M1-specific respectively [306, 115]. USP30, a mitochondrial-resident DUB, is unusual among USP DUBs as it shows linkage specificity towards K6 chains [183, 310]. The function of USP30 is described further in Section 1.3.7.

To add further complexity to the Ub code, Ub can also be modified by other PTMs such as acetylation and phosphorylation [194, 104, 112, 129]. Acetylation at K6 and K48 was detected in higher molecular weight smears on SDS-PAGE gels, indicating that the acetylated Ub was conjugated to substrates [194]. Because acetylation, like ubiquitination, occurs on K residues, such a modification could directly antagonise ubiquitination, although the biological function of Ub acetylation is still unclear. Mass spectrometry (MS)-based proteomics datasets have revealed phosphorylation of Ub at T7 and T12 [140], T14 [335], S20 [148], T22, T55 and T66 [273], S57 [212], T59 [234], and S65 [200]. *In vitro* assays have found that phosphorylation at Ub at different sites can alter the activity and chain type specificity of both E3 ligases and DUBs, indicating that Ub phosphorylation could affect the chain type complement of a given system [92]. However, only the function of S65 phosphorylation has been determined *in vivo*, for its role in mitophagy as described further below. These PTMs greatly expand the repertoire of potential Ub modifications, which could allow for exquisite regulation of diverse protein functions. However, the interplay between different modifications on Ub itself has remained mostly unexplored.

1.2.2 Methods for studying ubiquitination in cells

Several classes of tools have been developed to study ubiquitination in cells and organisms, which in many cases utilises the biology of the Ub system. Many different antibodies have been raised against total or conjugated Ub, specific chain types, and K11/K48-linked heterotypic chains [54, 190, 324]. Similarly, UBDs, such as tandem Ub binding entities (TUBEs), which are synthetic constructs consisting of a tandem series of four UBDs [85], have been used for affinity enrichment of ubiquitinated substrates for various applications including the estimation of average Ub chain length in cells [47, 90, 289]. The varying chain type specificity of different DUBs has also been harnessed to determine the chain type

complement of a biological sample, using a technique called Ubiquitin Chain Restriction (UbiCRest) [88]. If treatment of a sample with a chain-type specific DUB liberates Ub, this indicates that the sample in question contains that particular chain type.

The function of specific Ub chain types in cells has been investigated using K-to-R Ub mutants [23]. These investigations have allowed the initial discovery that Ub K48 is important for targeting proteins to the proteasome, and is indeed the only lysine in Ub that is essential for viability in yeast [48, 23]. However, the use of Ub mutants has several important caveats. Firstly, overexpression of mutant Ubs without concurrent knockdown of the cellular Ub pool results in the mutant Ub comprising only a small fraction of the total Ub; this can be overcome by knocking down Ub in cells [318]. However, Ub is encoded in four different genes, two of which are fused to ribosomal subunits [49]. Therefore, replacement of WT Ub with a mutant form requires small hairpin (sh)RNA treatment of the four Ub-encoding genes, and reintroduction of both the mutant Ub and the ribosomal subunits [318]. Secondly, as suggested by its highly conserved amino acid sequence, cellular viability is highly sensitive to mutations in Ub, especially those that affect binding of Ub to UBDs [236]. The K-to-R mutations could also interfere in as yet unappreciated ways with other lysine modifications such as acetylation. These caveats must therefore be taken into account when analysing results obtained using Ub mutants.

Most importantly, MS approaches have enabled the unbiased analysis of the ubiquitome: ubiquitination events on both substrates and Ub at a proteome-wide scale [282]. MS analysis of ubiquitomes is enabled by the fact that, during tryptic digest, ubiquitination events can be observed by the presence of a diGly remnant on previously ubiquitinated K residues [212]. While trypsin usually cleaves C-terminally to K and R residues, ubiquitination results in a missed cleavage event at the ubiquitinated substrate K residue. Trypsin also cleaves Ub at R74, leaving the C-terminal G75 and G76 (diGly) residues still attached by an isopeptide bond to the substrate K residue. A ubiquitinated peptide is therefore characterised by a missed cleavage event, and the addition of 114 Da due to the diGly [212]. DiGly remnant analysis, combined with the development of methods for Ub- or diGly-enrichment and sample fractionation, has resulted in the detection of more than 50,000 different ubiquitination sites in cells [56]. The number and abundance of these ubiquitination events can be modulated by various cellular stressors including UPS or DUB inhibition, or mitophagy induction as described further below [305, 118, 292, 62, 237, 96]. However, due to the process of tryptic digest, which divides proteins into multiple peptides, the context of each modification with

respect to one another is lost. DiGly proteomics therefore cannot easily answer the question of whether and to what extent multi-monoubiquitination occurs, and whether combinations of Ub modifications, such as chain branching or an interplay between chain formation and phosphorylation, occur in cells.

It was recently established that Lb^{pro}, the leader protease from the Foot and mouth disease virus (FMDV), has specificity for ISG15, a Ub-like protein that is conjugated to protein K residues via its C-terminus during immune signalling [274]. Unlike typical deconjugating enzymes, which cleave the isopeptide bond between the ISG15 C-terminal glycine and the substrate lysine, Lb^{pro} cleaves ISG15 C-terminal to residue R155 [274] (Figure 1.2A). This cleavage event, when performed on an ISGylated substrate, results in the formation of a C-terminally clipped ISG15 that is unable to be recognised by the ISG15 conjugation machinery, and a diGly-modified substrate K residue that is unable to be ISGylated (Figure 1.2A). Given that ISG15 and Ub share homology, including 100% identity in the four important C-terminal residues, it was shown that Lb^{pro} could also deconjugate Ub from substrates via an identical mechanism (cleaving at R74), although with much lower activity (Figure 1.2B) [274]. However, mutation of L102 of Lb^{pro} to a bulky tryptophan allowed increased binding and activity towards Ub with a concurrent reduction in activity towards ISG15 [275]. Lb^{pro} L102W, referred to as $Lb^{pro}*$, can therefore be used for the analysis of ubiquitomes in cells, in an application termed Ub-clipping [275]. Similarly to tryptic digest, $Lb^{pro}*$ treatment leaves a diGly remant on previously ubiquitinated K residues, but unlike tryptic digest, $Lb^{pro}*$ treatment does not further digest the Ub molecule into peptides (Figure 1.2B). The benefit derived from the use of Ub-clipping is therefore two-fold. Firstly, this specificity only for R74 of Ub means that multiple modifications of Ub such as chain branching can be detected via MS by the presence of multiple diGly modifications of a single Ub moiety (Figure 1.2C). Secondly, the collapse of a complex ubiquitinated sample into diGly-modified mono-Ubs can greatly simplify sample preparation; enrichment of the diGly-modified Ub can be performed by SDS-PAGE fractionation and excision of the 8 kDa mono-Ub band [275]. Analysis of Ub-modified substrates, which would resolve at their original size on SDS-PAGE following $Lb^{pro}*$ treatment, and analysis of multi-monoubiquitination of non-Ub substrates, are further potential applications of Ub-clipping that have not yet been explored in depth [275]. One potential application of Ub-clipping is in analysing the interplay between Ub phosphorylation and chain formation by the kinase PINK1 and the E3 Ub ligase Parkin, which occurs during mitophagy, as described in the following section.

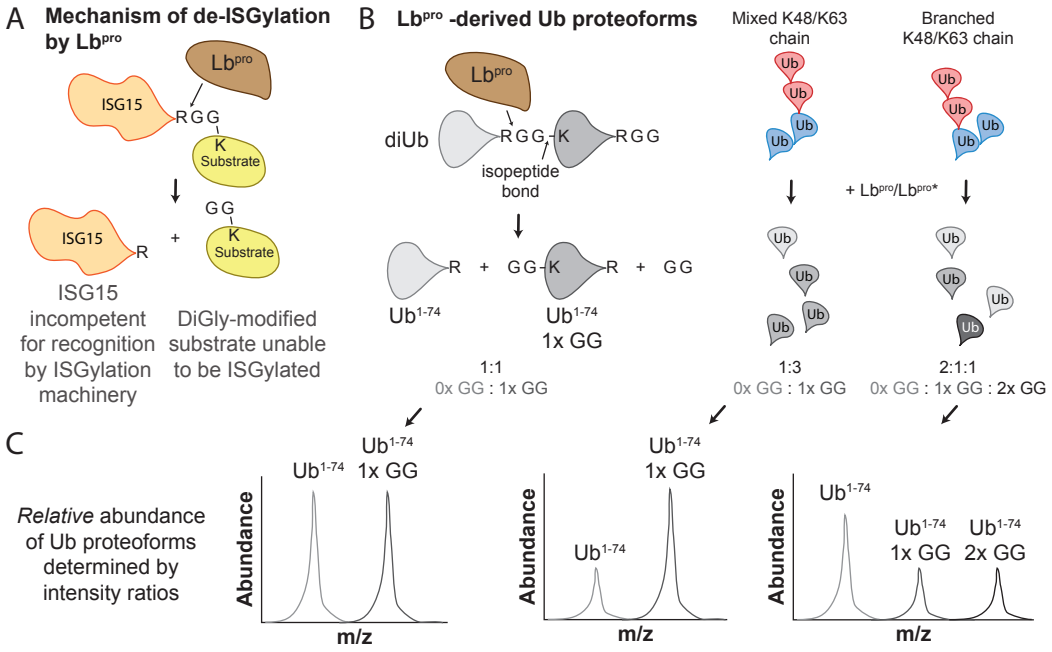

Fig. 1.2 **Lb^{pro} mechanism and use in analysis of Ub proteoforms by Ub-clipping. A.** Mechanism of action of Lb^{pro}, the leader protease of FMDV, against ISG15 [274]. Lb^{pro} cleaves ISG15 C-terminal to R155, either on free ISG15 (not shown) or on an ISGylated substrate. It is hypothesised that this would disrupt immune signalling via inactivation of ISG15 or by preventing further ISGylation of substrates. **B-C.** Mechanism of action of Lb^{pro} against Ub and its application to Ub-clipping [275]. Left, Lb^{pro} cleaves Ub C-terminal to R74, which when applied to a diUb molecule liberates two Ub proteoforms, Ub$^{1\text{-}74}$ and diGly-modified Ub$^{1\text{-}74}$, in equimolar amounts (illustrated in C; each peak is separated by a mass of 114 Da). Right, Ub-clipping can be used to distinguish between mixed and branched chains by the proteoforms produced by Lb^{pro} treatment. Note that Lb^{pro} and Lb^{pro}* have identical mechanisms of action towards Ub, but Lb^{pro}* has approximately ten-fold higher activity against Ub than Lb^{pro} [275].

1.3 PINK1, Parkin and mitophagy

1.3.1 Mitochondrial involvement in Parkinson's Disease

Parkinson's disease (PD) is the second most common age-related neurodegenerative disease, first described by James Parkinson in 1817, and has an estimated prevalence of 1.8% of people aged over 65 [233]. PD is characterised clinically by motor symptoms such as resting tremor, bradykinesia (slowing of movement), and postural instability [86], and non-motor symptoms such as olfactory and gastrointestinal dysfunction [78, 110]. The classic motor symptoms of PD are believed to be caused by loss of dopaminergic (DA) neurons of the substantia nigra pars compacta, with aggregates termed Lewy bodies, predominantly containing the protein α-synuclein, accumulating in the brains of most PD patients [13, 266]. Parkinsonism refers to a collection of diseases, of which PD is most common, that recapitulate the clinical symptoms of PD but may be caused by different genetic or environmental factors [230].

The first indication that mitochondrial dysfunction may play a role in the etiology of PD came when patients who had been exposed to 1-methyl-4-phenyl-1,2,3,6-tetrahydropyridine (MPTP), a by-product present in certain illicit drugs, exhibited symptoms of parkinsonism within days after injecting the substance [135, 38]. MPTP readily crosses the blood brain barrier, is metabolised to the toxic metabolite 1-methyl-4-phenylpyridinium (MPP^+) by non-dopaminergic cells, then is rapidly taken up by dopaminergic neurons where it inhibits Complex I of the mitochondrial respiratory chain [259, 223]. Population studies found links between PD and exposure to pesticides such as rotenone and paraquat (PQ), which both elicit mitochondrial oxidative damage through Complex I [55, 252, 278]. Further, post-mortem studies of idiopathic PD patient brains have revealed selective deficiency in Complex I [246], as well as mtDNA mutations and other mitochondrial pathologies [331, 6, 283].

Further evidence for the role of mitochondria in the etiology of PD came with studies of genetic forms of parkinsonism. While most cases of PD are idiopathic, approximately 10% of parkinsonisms have a genetic cause [270]. Two of the most prevalent causes of autosomal recessive parkinsonsim are mutations in *PRKN* (*PARK2*), encoding the E3 ligase Parkin, and *PINK1* (*PARK6*), encoding the protein kinase PTEN-induced putative kinase 1 (PINK1) [122, 295, 294]. Early studies in *Drosophila* indicated that PINK1 and Parkin function in a common pathway that serves to maintain mitochondrial integrity [210, 30]. Since then, myriad studies in cell culture systems have shown that these proteins are able to induce mitophagy, and have determined the precise activation sequence of the pathway in exquisite

molecular detail. A description of the known mechanisms of PINK1 and Parkin activation and the turnover of damaged mitochondria is presented below.

1.3.2 PINK1 activation

PINK1 localises to mitochondria and is phylogenetically the most divergent human kinase [151, 294]. Its structure consists of the N-terminal region, a kinase domain, and a C-terminal region (CTR; Figure 1.3A). The N-terminal region, consisting of a mitochondrial targeting sequence (MTS), an OMM localisation sequence (OMS), and a transmembrane sequence (TMS), is important for the regulation of PINK1's stability and mitochondrial localisation, as discussed further below. Its kinase domain, like other kinases, consists of an N-lobe and a C-lobe. Unique to PINK1, the kinase domain contains three large insertions that protrude from the N-lobe [132, 249]. The CTR forms extensive contacts with the C-lobe, and is likely important for its structure [132, 249]. The mechanism by which PINK1 is activated upon mitochondrial damage is illustrated in Figure 1.3B. Under basal conditions, PINK1 protein levels in the cell are very low, due to constitutive degradation in a proteasome-dependent manner [145]. This occurs by the $\Delta\Psi$m-dependent import of the PINK1 MTS via the TOM and TIM23 complexes [145, 59, 185, 160]. The partially imported PINK1 is cleaved first within the MTS by MPP, then within the TMS by presenilin-associated rhomboid-like protein (PARL; Rhomboid-7 in *Drosophila*) to form a 52 kDa product [145, 101, 312, 39, 169, 70]. The 52 kDa protein is retrotranslocated into the cytosol where it is degraded by the proteasome according to the N-end rule pathway [323]. Upon loss of mitochondrial membrane potential, MTS-dependent import and subsequent PARL-mediated cleavage of PINK1 is inhibited [145, 101, 39, 169, 70]. The OMS then directs PINK1 to the OMM [195], in a manner dependent on TOMM7 [77], where it is stabilised [145, 160, 185]. PINK1 incorporates into a subset of TOM complexes [136], and this interaction may involve PINK1 dimerisation [198]. Once stabilised on the OMM, PINK1's kinase function is activated, which requires autophosphorylation in trans [197, 132, 249]. The autophosphorylation events stabilise insertions 2 and 3 respectively in the N-lobe, and insertion 3 in particular is important for Ub binding [132, 249]. PINK1 phosphorylates Ub at S65 [112, 104, 129], as well as the S65 residue on Parkin's Ubl domain [128, 253]. Both of these phosphorylation events are required for full Parkin activation by PINK1, as either S65A Parkin [204, 166] or S65A Ub [201], mutants that disallow phosphorylation-dependent regulation, greatly reduce Parkin-dependent mitochondrial ubiquitination. Interestingly, S65 phosphorylation of Ub changes the protein's conformation, resulting in an equilibrium between the "common" Ub conformation and a

C-terminally retracted form (Ub-CR) [310, 41, 65]. PINK1 prefers to phosphorylate Ub that is locked in the Ub-CR conformation, and structural studies indicate that unphosphorylated Ub needs to be in the Ub-CR conformation to be phosphorylated [65, 249]. Upon regaining of $\Delta\Psi$m, PINK1 is rapidly re-imported into mitochondria and degraded as above, thereby allowing an "off" switch for the pathway [136].

1.3.3 Parkin activation

Parkin is an RBR ligase, with a domain structure consisting of an N-terminal ubiquitin-like (Ubl) domain, a unique Parkin domain (UPD, sometimes referred to as RING0), RING1 (important for E2 binding), IBR, and catalytic RING2 domains (Figure 1.4A) [255, 91, 311]. The known mechanism of Parkin activation by PINK1 is illustrated in Figure 1.4B. Prior to activation by PINK1, Parkin exists in the cytosol in an autoinhibited state, in which a UPD-RING2 interface occludes access to the catalytic C431 residue, and the IBR-RING2 linker interacts with the RING1 domain to prevent E2~Ub binding [308, 235, 285]. Parkin activation therefore requires significant rearrangement of its domain structure. Inactive Parkin typically localises diffusely in the cytosol, but redistributes rapidly to mitochondria upon mitochondrial depolarisation in a PINK1-dependent manner [184, 160]. This is achieved first by phosphorylation of pre-existing mitochondrial Ub by PINK1 [196, 202, 166], which may be seeded on mitochondrial proteins by the E3 ligase MARCH5 [130]. Parkin binds pS65-Ub, which induces a conformational change that displaces the Ubl from its interaction with the RING1 domain [104, 112, 129, 309, 131, 244]. PINK1 then phosphorylates Parkin's Ubl at the equivalent S65 residue [128, 253]. Full Parkin activation is achieved when the phosphorylated Ubl (pUbl) domain binds to the UPD, displacing the RING2 [64, 245]. Further, a conserved linker region between the Ubl and UPD, termed the ACT element, binds to a hydrophobic pocket on UPD that is vacated by the released RING2 [64]. The catalytic RING2 domain in active Parkin is highly mobile [64, 245], and Parkin is able to catalyse the ubiquitination of diverse mitochondrial substrates and produce multiple Ub chain types *in vitro* and *in vivo* [204, 36, 237]. Parkin-catalysed ubiquitination of mitochondrial proteins provides further substrate for phosphorylation by PINK1, which further recruits Parkin, and cycles of Ub phosphorylation and chain formation by PINK1 and Parkin on mitochondria results in robust ubiquitination of mitochondrial substrates [204, 201]. The retention of Parkin at mitochondria is dependent on its catalytic activity, as C431S Parkin is partially activated through phosphorylation by PINK1 but is not retained on mitochondria [138]. The S65-phosphorylated Ub produced on mitochondrial proteins by PINK1 and Parkin

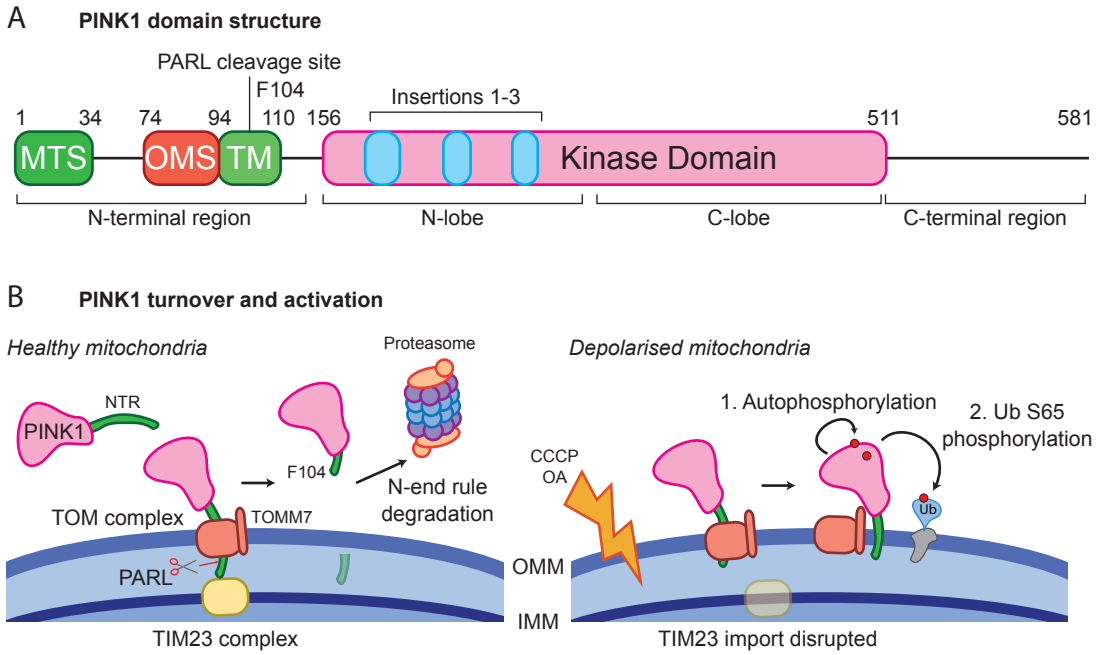

Fig. 1.3 **PINK1 domain structure and activation on mitochondria. A.** Domain structure of PINK1, consisting of the mitochondrial targeting sequence (MTS), outer membrane targeting sequence (OMS), transmembrane (TM) region, kinase domain, and C-terminal region. **B.** PINK1 activation on mitochondria. In healthy mitochondria (left), the $\Delta\Psi$m is intact, and PINK1 is constitutively imported via the TIM23/presequence pathway. PARL cleaves PINK1 N-terminal to F104, and PINK1 is released into the cytosol. The exposed N-terminal F104 leads to N-end rule degradation of PINK1 by the proteasome. When mitochondria are damaged with agents that disrupt $\Delta\Psi$m (right), TIM23-mediated import is blocked. The OMS signals for PINK1 localisation in the OMM, where it interacts with the TOM complex. PINK1 is activated by autophosphorylation in trans, then active PINK1 phosphorylates Ub on S65. The downstream phosphorylation and activation of Parkin is shown in Figure 1.4. NTR: N-terminal region, OMM/IMM: outer/inner mitochondrial membrane.

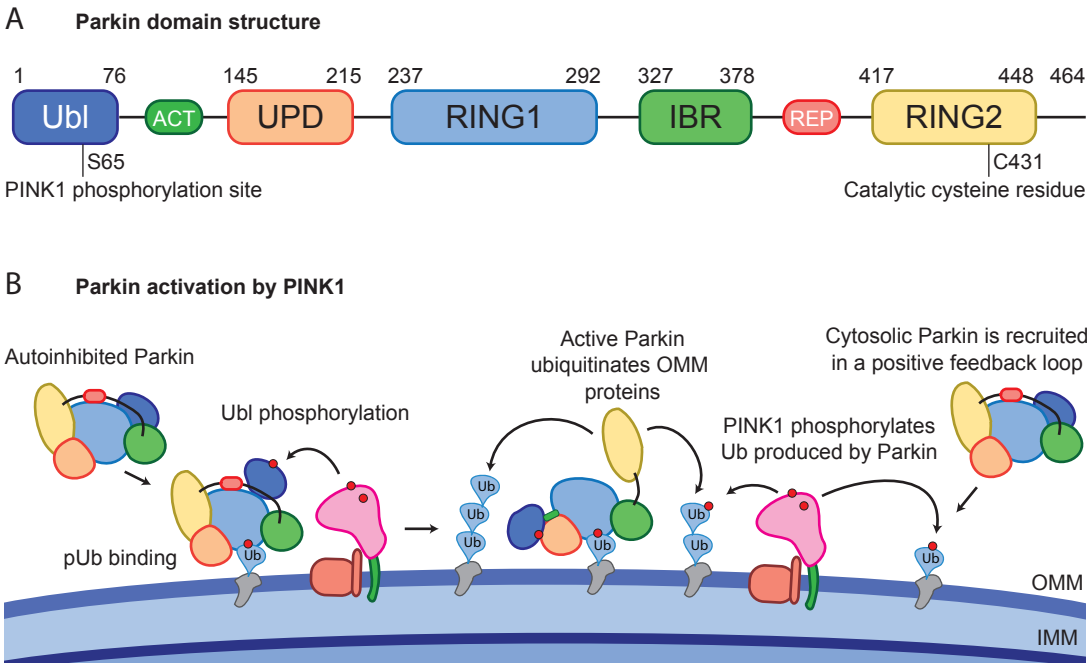

Fig. 1.4 **Parkin domain structure and activation on mitochondria. A.** Domain structure of Parkin, consisting of the Ub-like (Ubl) domain, activating element (ACT), unique Parkin domain (UPD), RING1, IBR, repressor element (REP), and RING2 domain. **B.** Parkin activation by PINK1, following PINK1 activation in Figure 1.3B. Parkin exists in the cytosol in an autoinhibited state. It binds pS65-Ub, which displaces the Ubl domain and promotes its phosphorylation at S65 by PINK1. The Ubl and ACT bind to the UPD, displacing the catalytic RING2 domain and activating Parkin's E3 ligase activity. Parkin ubiquitinates OMM proteins, which provide substrate for PINK1 phosphorylation. More Parkin protein is recruited, resulting in a positive feedback loop of pS65-Ub production by PINK1 and Parkin. OMM/IMM: outer/inner mitochondrial membrane.

is recognised in HeLa cells primarily by the autophagy receptors optineurin (OPTN) and nuclear dot protein 52 (NDP52), which results in the recruitment of the autophagy machinery to the damaged mitochondria [139].

1.3.4 Parkin substrates and chain types

Initial targeted investigations into the substrates of Parkin-mediated ubiquitination found the mitofusin proteins [57, 277, 337, 221], the mitochondrial motility-associated protein Miro [307], as well as Voltage-dependent anion channel 1 (VDAC1) [59] to be Parkin substrates. Later MS-based studies have followed, showing numerous mitochondrial and non-mitochondrial substrates [242, 204, 36, 202, 203]. In particular, one recent study used absolute quantification (AQUA)-based MS techniques to investigate the absolute abundance

of diGly-modified mitochondrial substrates upon depolarisation [202]. This study identified the three VDAC proteins as the most heavily ubiquitinated mitochondrial substrates, followed by a collection of other proteins including Mfn2, CISD1 and TOMM20. The authors were able to establish the kinetics of substrate ubiquitination and Ub phosphorylation, both of which correlate positively with Parkin levels [202]. In terms of Ub chain types produced by Parkin, early cellular studies using Ub K-to-R mutants found that Parkin produces K27 and K63 chains in response to depolarisation [59]. However, more systematic MS-based studies found Parkin-dependent production primarily of K6, K11, K48 and K63 chains on mitochondria, and Parkin has also been shown to assemble predominantly those chain types *in vitro* [204, 275]. pS65-Ub is a poor substrate for Parkin-mediated ubiquitination, so it is likely that chains are phosphorylated downstream of ubiquitination by Parkin [310, 204]. While the substrate and chain type repertoire of Parkin has now been established in great detail, the broader Ub chain architecture, such as the interplay between chain formation and phosphorylation of Ub, or the presence of chain branching, remains mostly unexplored.

Several observations indicate that Parkin in fact has low substrate selectivity. Firstly, the structure of active Parkin, in which the catalytic RING2 domain is relieved of contacts with the rest of the protein, indicates that the catalytic domain potentially has a large amount of mobility, which could allow ubiquitination of a broad range of substrates [64, 245]. Secondly, the abundance of diGly modifications in different tissues correlates well with the total abundance of those substrates in the mitochondrial proteome of that tissue; indeed, the VDAC proteins are both the most abundant and most heavily ubiquitinated proteins on the OMM [202]. Finally, ectopic targeting of several non-mitochondrial proteins to the OMM enables their ubiquitination by Parkin, indicating that Parkin ubiquitinates proteins in close proximity rather than proteins with a particular sequence or structural element [130]. This low specificity underscores the need for tight regulation of Parkin activation to prevent aberrant ubiquitination of other cellular substrates. These observations also suggest that the abundance, rather than the precise nature, of Parkin-mediated ubiquitination underlies the protein's function.

1.3.5 Mitophagosome formation and delivery to the lysosome

The incorporation of ubiquitinated mitochondria into autophagosomes first occurs by binding of autophagy receptors, primarily NDP52 and OPTN in HeLa cells, to ubiquitinated mitochondrial proteins [139]. OPTN recruitment to mitochondria results in the activation of the

kinase TBK1, which phosphorylates OPTN and improves its binding to Ub chains [83, 232]. Therefore, OPTN and TBK1 function in a second positive feedback loop to promote focal recruitment of autophagy receptors to the site of mitochondrial damage [83]. The autophagy receptors recruit the kinase ULK1, and the proteins DFCP1 and WIPI1, while Atg9A is also recruited, resulting in the initiation of autophagosome formation at the site of the damaged mitochondrion [139, 99]. The Atg8 family of proteins, which in humans consist of six members with partially redundant functions (LC3A, LC3B, LC3C, GABARAP, GABARAPL1, and GABARAPL2), are Ub-like proteins that are required for the efficient expansion of the autophagosomal membrane [288, 192, 206]. The Atg8 proteins are first processed by Atg4 to reveal a C-terminal G residue [120]. Next, the processed Atg8 is conjugated via its C terminus to phosphatidylethanolamine (PE) in a ubiquitination-like process requiring the E1-like Atg7, the E2-like Atg3, and the E3-like Atg5/Atg12/Atg16 complex [95, 272, 178, 176]. The Atg5/Atg12/Atg16 complex is itself produced by another ubiquitination-like process involving Atg7 and the E2-like Atg10 to conjugate the C-terminus of Atg12 to Atg5, which then assembles noncovalently with Atg16L1 [177, 176]. After recruitment of Atg8 proteins to the growing phagophore, the Atg8s recruit further autophagy receptors, including p62, resulting in a third positive feedback loop of Atg8-driven receptor recruitment [206]. The Atg8 proteins are also essential for downstream delivery of the autophagsome to the lysosome, either through autophagosome-lysosome fusion or degradation of the inner leaflet after fusion [192, 288]. Hence, loss of either Atg5 or Atg8 greatly diminishes autophagy [288, 192, 117]. Following fusion of the autophagosome with the lysosome, the mitochondrial contents are degraded by lysosomal hydrolases. Therefore, mitophagy is considered to be a protective mechanism that removes dysfunctional mitochondria from the network to prevent oxidative damage or apoptotic signalling caused by lost mitochondrial integrity.

1.3.6 Involvement of p97 and the proteasome

While it is understood that the primary means of depolarisation-induced mitochondrial turnover in cultured cells is mitophagy, proteasomal processes appear to also be involved in PINK1/Parkin-dependent mitophagy. OMM proteins can be turned over under steady-state levels via ubiquitination, extraction from the membrane by the AAA ATPase p97, and degradation by the proteasome, in a process termed OMM-associated degradation (OMMAD) [189, 319]. Early experiments found that inhibition of p97, or the proteasome, resticted depolarisation-induced mitophagy [277, 21], while more recently it has been shown that p97 is recruited to depolarised mitochondria in a manner that is dependent on Parkin and the p97

cofactor UBXD1, and that this recruitment enhances the rate of mitophagy [7]. Degradation of the mitofusin proteins (required for fusion of the OMM) appears to be an early event in mitophagy and occurs via this pathway [189, 337, 319]. This finding led to the hypothesis that rapid degradation of mitofusins by Parkin prevents the damaged mitochondrion from fusing with the network, which in turn aids its turnover by mitophagy [277]. Indeed, later studies found that Mfn2 is the most rapidly ubiquitinated substrate in response to depolarisation, and that p97-mediated Mfn2 degradation is necessary for destruction of ER-mitochondria contact sites, which then promotes further substrate ubiquitination by Parkin [164]. However, more recent studies into the process, using more physiological levels of Parkin, have found that p97 inhibition did not dramatically affect Parkin-dependent ubiquitination of mitochondrial proteins or the turnover of the majority of OMM proteins upon mitophagy induction [203].

1.3.7 USP30 is a negative regulator of PINK1/Parkin mitophagy

USP30 is the only DUB that is localised to mitochondria, with an N-terminal OMM localisation sequence and its catalytic USP domain facing the cytosol (Figure 1.5A) [183]. The first evidence for the involvement of USP30 in the PINK1/Parkin pathway came from a screen for DUBs that could counteract Parkin-mediated mitophagy in cultured cells [10]. Studies in flies also showed that Usp30 knockdown could partially rescue the phenotypes of *Pink1* and *park* mutants (encoding Pink1 and parkin), as well as PQ-induced neuronal toxicity [10]. Early cellular studies found that USP30 could cleave K6, K11, and K48 linkages in cells, while other studies *in vitro* showed that USP30 preferentially cleaves K6-linked di-Ub [36, 310, 63, 243]. This apparent chain type specificity is unusual among USP DUBs, which are typically pan-specific for all Ub chain types [45]. Crystal structures of USP30 in complex with K6-linked diUb have established the molecular explanation for this preference, wherein contacts between the USP domain and both the distal and proximal Ub moieties restricts the possible orientation of the Ub moieties with respect to each other, preferring the K6-linked configuration (Figure 1.5B) [243, 63]. Indeed, the K6 linkage preference is conferred solely by binding, as K11 and K48 linkages are more efficiently hydrolysed once bound to USP30 [243]. The residues in USP30 that mediate the contacts that confer K6 specificity are well conserved across species, but are not conserved among other USP family members [243]. In addition to cleaving K6 chains, USP30 is clearly able to counteract substrate monoubiquitination, as it can regulate the abundance of diGly-modified mitochondrial substrates as measured by MS [36, 203]. One potentially important USP30 substrate is TOMM20, whose ubiquitination has been described as essential for mitophagy [10], while

K6-linked ubiquitination specifically of TOMM20 has been shown to be regulated by USP30 [63]. Further, while some sites on TOMM20 are regulated both by USP30 and Parkin, others are regulated by USP30 in a Parkin-independent manner [203]. Consistent with a Parkin-independent role for USP30, the DUB has been shown to regulate basal mitophagy, while Parkin appears to function only in damage-induced mitophagy [10, 152]. USP30 has also been found to be involved in pexophagy (autophagy of peroxisomes), due to the presence of a peroxisome localisation sequence [36, 152]. This finding indicates that pexophagy might also be mediated by ubiquitination, which is corroborated by evidence that PINK1 targeted to peroxisomes can induce their autophagic degradation [136].

The currently accepted model for the involvement of USP30 in PINK1 and Parkin-mediated mitophagy is that USP30 activity under basal conditions regulates the amount of ubiquitination of mitochondrial substrates prior to PINK1 activation, which potentially sets the threshold for activation of PINK1/Parkin (Figure 1.5C, left) [36]. Activation of PINK1 and Parkin results in deactivation of USP30, allowing robust production of Ub chains on mitochondrial proteins, leading to autophagic clearance of the damaged organelle. Three mechanisms for the inactivation of USP30 upon activation of PINK1 and Parkin have been proposed (Figure 1.5C, right). Firstly, Parkin is able to ubiquitinate USP30 directly, which could result in turnover of the protein by the proteasome [10]. However, USP30 degradation was observed only at longer timepoints, and monoubiquitination of USP30 appears not to affect its DUB activity [10, 63]. Secondly, pS65-Ub is a poor USP30 substrate, so phosphorylation of Ub chains by PINK1 is likely to prevent their hydrolysis by USP30 [310]. Finally, USP30 is an exo-DUB, meaning that it can only cleave Ub chains one moiety at a time, starting from the most distal [63, 243]. Therefore, it has been proposed that long Ub chains may hinder USP30-mediated cleavage [243]. However, whether USP30 does indeed function in physiological conditions to counteract PINK1/Parkin mitophagy remains to be determined, as most studies have been cell-based, relying on USP30 overexpression. USP30 has also been described as a regulator of mitochondrial protein import, by deubiquitinating proteins as they are imported through the TOM complex [214, 203]. Therefore USP30's primary function, be it in regulating mitochondrial protein import or in counteracting mitophagy, remains to be established.

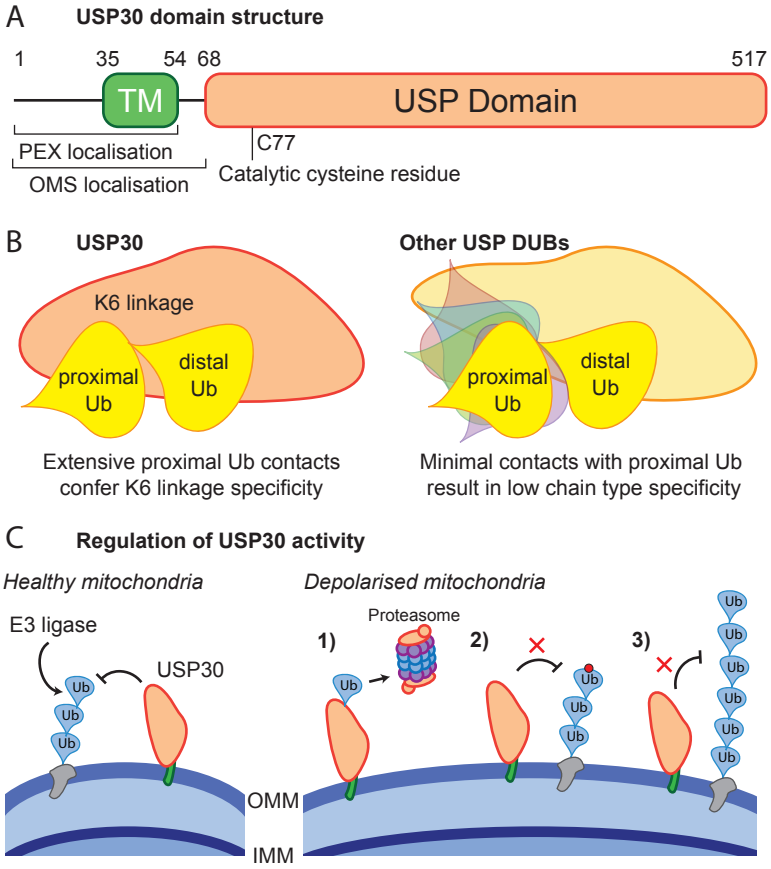

Fig. 1.5 **USP30 domain structure, mechanism of K6 linkage specificity, and regulation on mitochondria. A.** Domain structure of human USP30, consisting of a transmembrane (TM) region, localisation sequences for mitochondria (OMS) and peroxisomes (PEX), and USP domain. **B.** Mechanism of USP30 K6 linkage specificity. USP30 (left) contacts both the distal and proximal moiety, restricting its substrate preference to K6-linked Ub. Conversely, most other USP DUBs (right) form most of their contacts with the distal Ub moiety, which does not restrict the orientation of the proximal Ub. Therefore, USP DUBs typically have low Ub linkage specificity. **C.** USP30 activity on mitochondria. Under basal conditions (left), USP30 deubiquitinates mitochondrial proteins, thereby reducing initial substrate for phosphorylation by PINK1. Upon mitochondrial damage and PINK1/Parkin activation (right), USP30 activity is reduced. This may occur by 1) ubiquitination and proteasomal degradation of USP30, 2) phosphorylation of Ub chains, thereby preventing USP30-mediated hydrolysis, and/or 3) increased Ub chain length, which would hinder USP30's obligate exo-DUB activity.

1.3.8 PINK1/Parkin-independent mitophagy

Additional to its role in response to damage, mitophagy is important in several physiological processes during development, including elimination of paternal mitochondria during egg fertilization, and in the elimination of mitochondria during the differentiation of red blood cells [271, 1, 250, 241]. Patients with homozygous loss-of-function alleles of *PINK1* and *PRKN* do not display developmental abnormalities [122, 295], which suggests that PINK1- and Parkin-mediated mitophagy either does not occur during these processes, or operates redundantly with other pathways. Further, PINK1 and Parkin have been shown to be dispensable for basal mitophagy in mice and flies [168, 142]. Indeed, several other mitochondrial-resident E3 ligases have been identified, which conceivably could induce autophagy receptor recruitment by ubiquitinating mitochondrial substrates independently of or cooperatively with PINK1 and Parkin [189, 144, 326]. MUL1 (Mitochondrial Ub E3 ligase 1, also known as MULAN, MAPL, GIDE, and HADES) is a RING E3 ligase that is localised to the OMM with its RING domain facing the cytosol [144]. It has been shown to be involved in numerous cellular pathways, including NF-κB signalling, apoptosis, and mitochondrial dynamics [159, 103, 329, 222]. Further, an LC3-interacting region (LIR) has been described in the MUL1 RING domain that enables binding to GABARAP, an Atg8 family protein, which implicates MUL1 in mitophagy [3], although the functional relevance of this interaction is unclear. Overexpression of MUL1 in flies rescues *Pink1* and *park* mutant phenotypes, and Mfn2 has been shown to be a substrate of MUL1-mediated ubiquitination [329]. MUL1-mediated SUMOylation of Drp1 has also been described as a means of regulating mitochondrial fission [222]. It is likely, given that manipulations that increase mitochondrial fission tend to rescue *Pink1* and *park* mutant phenotypes in flies [220], that MUL1's protective effect on PINK1 and Parkin phenotypes is due to its role in regulating mitochondrial dynamics [329, 222]. MARCH5 (also known as MITOL) is another OMM-spanning E3 ligase and has similarly been proposed to regulate a wide variety of functions, including innate immune signalling, apoptosis, mitochondrial dynamics and, most recently, mitochondrial protein import [327, 268, 326, 214]. MARCH5 has been shown to ubiquitinate sites that are deubiquitinated by USP30, and to ubiquitinate the autophagy receptor FUNDC1, which is discussed further below [214, 25].

The F-box family protein FBXO7 is another E3 ligase that has been implicated in PINK1- and Parkin-dependent mitophagy [16]. Interestingly, autosomal recessive forms of parkinsonism, similar to those described in patients with *PINK1* or *PRKN* mutations, have been described due to mutations in *PARK15*, the gene encoding FBXO7 [52, 209]. While FBXO7

is not exclusively resident at mitochondria, it partially redistributes to mitochondria in a PINK1-dependent manner upon depolarisation [16]. Further, FBXO7 interacts directly with both PINK1 and Parkin through distinct binding sites, and loss of FBXO7 expression reduces Parkin translocation to mitochondria upon depolarisation [16]. Overexpression of human FBXO7 in *Drosophila* is able to rescue *park* mutant phenotypes [16]. However, while FBXO7 was shown to genetically interact with Pink1, its ectopic expression was unable to rescue *Pink1* or *Pink1, park* double mutants. This suggests that FBXO7 acts downstream of PINK1, but, unlike parkin [210, 30], its function is totally dependent on Pink1 activity in flies. However, FBXO7 has been shown not to be a substrate of PINK1 [128], indicating that this activation is indirect. While the fly data indicated that FBXO7 and parkin may interact redundantly in flies, FBXO7 was unable to rescue mitophagy in HeLa cells, which lack endogenous Parkin expression [16]. These results could indicate either that FBXO7 and parkin can operate redundantly to induce mitophagy only in flies, or that the rescue conferred by FBXO7 is not through mitophagy. Further work is needed to determine the precise role of FBXO7 in mitochondrial quality control.

Ub-independent mitophagy has also been described. During erythrocyte differentiation, the mitochondria of red blood cells are removed by mitophagy via a mechanism that requires the protein NIX (also known as BNIP3L) [250, 241]. FUNDC1, an intregal OMM protein, has also been described as a Ub-independent mitophagy receptor that directly associates with the core autophagy machinery through its LIR [146]. FUNDC1-mediated mitophagy occurs in cells in response to hypoxia but not depolarisation with FCCP, highlighting the diversity of mitophagic pathways in different circumstances [146]. Interestingly, cross-talk has been observed between FUNDC1- and MARCH5-mediated mitophagy, whereby MARCH5 ubiquitinates FUNDC1, resulting in its proteasomal degradation, which may act as a fine-tuning mechanism to prevent over-induction of mitophagy in response to stress [25]. Externalisation of cardiolipin, normally resident in the inner leaflet of the IMM, to the outer leaflet of the OMM, has also been described as a signal for various forms of mitochondrial damage-induced mitophagy [28]. Further, PINK1- and Parkin-independent mitophagy in response to iron chelation has also been described [2].

1.3.9 Mitophagy-independent mitochondrial quality control

In addition to PINK1/Parkin-independent forms of mitophagy, there are alternative mitochondrial quality control pathways, some of which appear to involve PINK1 and Parkin. These

quality control pathways maintain mitochondrial integrity at different levels, in different sub-compartments or in response to different stimuli. OMM-associated degradation (OMMAD) is a Ub-dependent quality control pathway for membrane-spanning OMM proteins [189, 319]. Proteins destined for degradation are ubiquitinated, extracted from the membrane by p97 and delivered to the proteasome where they are deubiquitinated, unfolded, and hydrolysed into peptides [189, 337, 319]. As discussed in Section 1.3.6, an interplay between OMMAD and mitophagy is believed to improve the efficiency of mitochondrial turnover. The mitochondrial unfolded protein response (UPR^{mt}) is a broad transcriptional response in nuclear-encoded genes that was first described in mammalian cells but is best characterised in *C. elegans* [156, 332, 186]. In worms, the UPR^{mt} is initiated by the redistribution of the transcription factor ATFS-1 from mitochondria to the nucleus [79, 186]. ATFS-1 contains both an MTS and a nuclear localisation sequence (NLS), and under steady-state levels is imported into the mitochondria and degraded by the Lon protease [186]. When mitochondrial protein import is disrupted, for example by deletion of the Tim23 protein or treatment with PQ, the mitochondrial import of ATFS-1 is inhibited and the protein localises in the nucleus via its NLS, where it activates a broad transcriptional response including expression of chaperone proteins and a switch from oxidative to glycolytic metabolism [186]. The mechanism of UPR^{mt} activation in mammals is less clear, although it has been found to be stimulated by exogenous expression of the ΔOTC protein, a form of the ornithine transcarbamylase enzyme that is prone to misfolding in the mitochondrial matrix [332, 170]. Three potential paralogs of ATFS-1 (ATF4, ATF5, and CHOP) exist in mammals, but it is likely that UPR^{mt} activation in mammals occurs via a different mechanism from that of ATFS-1 in *C. elegans* [332, 334, 279, 50, 224, 170]. It is also yet to be firmly established to what extent UPR^{mt} and mitophagy are coordinated, or under which circumstances or cell types each pathway is preferentially activated [170].

More recently, an alternative vesicular quality control pathway for mitochondria has been described, termed mitochondria-derived vesicles (MDVs) [188]. MDVs are defined as cargo-selective vesicles with a diameter of 80 to 100 nm, formed independently of Drp1, and were first described in the trafficking of mitochondrial contents to peroxisomes [188]. Later, delivery of MDVs to the lysosome for destructuion of oxidised cargo was described, in a process independent of the core autophagy component Atg5 [264]. The vesicles can be comprised of IMM only (containing matrix), OMM only (containing IMS), or both membranes, but there appears to be further selectivity of cargo contained within a given MDV, as evidenced by the discovery of OMM-containing MDVs that lack TOMM20

[188, 165]. Interestingly, a role for PINK1 and Parkin has been described in the formation of matrix-only MDVs [163]. The MDVs were formed in response to oxidative damage such as Antimycin A treatment, while treatments that dissipated $\Delta\Psi$m, such as CCCP or Oligomycin/Antimycin A (OA) led to mitophagy [163]. It has been proposed that MDV formation and delivery to the lysosome operates upstream of mitophagy, prior to complete loss of $\Delta\Psi$m, to allow the piecemeal delivery of damaged mitochondrial fragments to the lysosome [163]. This is because the timescale of MDV formation (1 to 4 hours) was observed to be faster than that of mitophagy (4 to 24 hours) upon damage induction [163]. Further, VPS35, encoded by a PD-associated gene [336, 301], has been suggested to partake in the shuttling of OMM-containing MDVs to peroxisomes, and has been shown in flies to interact genetically with parkin [14, 150]. It is therefore possible that MDVs are a mitochondrial quality control pathway that are highly relevant in the pathogenesis of PD.

1.3.10 Methods for measuring mitophagy

Several methods have been descirbed for measuring mitophagy in cells and organisms. Two reporters, mtKeima and mito-QC, take advantage of the acidic nature of the lysosome and the varying pH-sensitivity of different fluorophores to allow detection of mitochondrial delivery to the lysosome by microscopic techniques, and have been successfully applied in whole-animal models [269, 167, 142]. The mtKeima probe consists of the Keima protein, a protease-resistant fluorophore whose emission spectrum is dependent on pH, fused to an N-terminal mitochondrial matrix-targeting sequence [107]. The fluorophore can emit at two different wavelengths upon excitation, in a manner dependent on pH, so the intensity ratio of the emission spectra is used to determine whether mitochondria have been delivered to an acidified lysosome [107]. In comparison, mito-QC consists of an mCherry-GFP fusion protein fused to the FIS1 OMM targeting sequence [2, 167]. GFP fluorescence is readily quenched by the acidic lysosome while mCherry fluorescence is resistant, meaning that targeting of mitochondria to lysosomes can be detected by the formation of "red-only puncta" [2]. However, given the mito-QC reporter's OMM localisation, the possibility for degradation of OMM-localised proteins independently of mitophagy [192] can complicate the use of this reporter for the analysis of mitophagy. In contrast, while mtKeima is matrix targeted and therefore protected from OMM-associated degradation, it is incompatible with fixation, which dissipates the lysosomal pH [107]. More recently, a new pH-sensitive mitophagy reporter, termed mito-SRAI, has been described [106]. This reporter is targeted to the mitochondrial matrix, and its fluorescence is retained upon fixation [106]. However, all

of the above reporter methods analyse late-stage mitophagy, relying on the delivery of an autophagosome to a correctly acidified lysosome. Lysosome acidification can be disrupted upon treatment with depolarising agents used to induce mitochondrial damage, such as CCCP [207], which could hinder the utility of the reporters. These late-stage readouts are also unable to distinguish between different modes of mitophagy activation upstream of lysosomal delivery, such as whether the induction is PINK1- or Parkin-dependent.

Generation of pS65-Ub appears to be dependent on PINK1 and amplified by Parkin [139]. Therefore, pS65-Ub has been proposed as a biomarker for PINK1 activity [216]. Given the specificity of the signal for PINK1 and Parkin activation, the formation of pS65-Ub could be used as an early-stage readout for mitophagy induction, although it should be noted that pS65-Ub formation alone does not indicate that mitophagy is occurring. Combining the readouts of pS65-Ub generation with the delivery of mitochondria to lysosomes could help to specify whether the turnover of mitochondria is both PINK1- and Parkin-dependent, and occurs by autophagy. However, monitoring of pS65-Ub formation in response to different inducers of mitochondrial damage has not been widely employed, unlike the use of mito-QC [2]. A complementary analysis could help to answer the question of whether PINK1- and Parkin-dependent mitochondrial turnover occurs primarily by mitophagy or by other means such as MDV formation.

1.4 Animal models of PINK1 and Parkin deficiency

To date, numerous genetic models of PINK1 and Parkin have been described, mostly in rodents and *Drosophila*. While *Drosophila* models have recapitulated many aspects of mitochondrial pathology common to AR-JP patients, mouse models have shown much milder phenotypes, which hinders their use in understanding the etiology of PD and in designing potential diagnoses or treatments. A description of the known animal models of PINK1 and Parkin follows.

1.4.1 *Drosophila* models

Drosophila melanogaster is a commonly used model organism, and is ideal for studying neurodegeneration due to its straightforward genetic manipulations, short lifespan, high numbers of progeny, and the fact that approximately 75% of human disease-related genes are conserved [239, 231, 9]. There are fly homologs of PINK1 (*Pink1* gene, Pink1 protein),

Parkin (*park* gene, parkin protein), USP30 (*Usp30* gene, Usp30 protein), and Atg5 (*Atg5* gene, Atg5 protein), and analyses of fly mutants of these genes have been invaluable in determining the molecular events underlying disease [71, 210, 30, 117, 10]. Treatment of flies with rotenone or PQ, which both induce mitochondrial dysfunction at Complex I, result in selective loss of dopaminergic neurons in flies [34, 10]. Surprisingly, PQ treatment did not appear to alter mitochondrial morphology [10]. The locomotor defects, but not neuronal survival, in both models can be rescued by treatment with L-dopa, indicating that these are faithful models of parkinsonism [34, 10]. Unfortunately, of the five Ub-binding autophagy receptors described in mammals, only p62 has a known *Drosophila* homolog, Ref(2)P [191]. This complicates our understanding of the molecular events downstream of Pink1/parkin activation in this model, given that p62 has been described as not important for mitophagy initiation in HeLa cells [139].

Loss-of-function mutants in the *park* gene result in reduced lifespan, locomotor defects and male sterility [71]. Surprisingly, it appears that degeneration of the indirect flight muscles, rather than neurodegeneration, underlies the locomotor phenotype [71]. However, later studies found that *park* mutant flies exhibit selective loss of DA neurons from the PPL1 cluster [313]. This selective neuronal loss and lack of Lewy pathology provide striking parallels to the clinical manifestation of familial parkinsonism in humans [313, 276]. *Pink1* mutant flies, like the *park* mutants, display reduced longevity, male sterility, and mitochondrial dysfunction leading to degeneration of the indirect flight muscle, accompanied by climbing and flight defects, as well as modest degeneration of dopaminergic neurons [210, 30]. Both *Pink1* and *park* mutants display an abnormal wing phenotype and thoracic indentations [71, 313, 210]. Studies of genetic interaction between the two genes found that the phenotype of *Pink1* and *park* double mutants was no more severe than each single mutant, which provided the first evidence that the two gene products operate in the same pathway [210, 30]; indeed, these studies provided the first unequivocal link between two PD-associated genes in a common pathway. The *Pink1* mutant could be rescued by parkin overexpression, but not vice versa, indicating that parkin operates downstream of Pink1 [210, 30]. This finding in particular is surprising, given that *in vitro* and cell-based work has suggested that, in mammals, PINK1 is required to activate Parkin through relief of Parkin's autoinhibited state [64, 245, 139, 204]. *Drosophila* parkin contains an N-terminal region not present in the well-studied mammalian forms, which combined with the apparent lack of requirement for Pink1 for its activity suggests that *Drosophila* parkin may have an alternative mode of activation.

Proteomics approaches have been used in flies to determine the effect of the loss of *Pink1* and *park* on mitochondrial protein turnover [302]. While loss of *park* resulted in the accumulation of mitochondrial substrates that overlapped well with loss of the core autophagy gene *Atg7*, there was also a subset of mitochondrial proteins that appeared to be regulated by parkin independently of autophagy. Surprisingly, the proteins affected by loss of *Pink1* had very little overlap with the *Atg7* mutant, but some overlap with the *park* mutant, indicating that Pink1 and parkin may regulate turnover of specific mitochondrial proteins in a manner that is independent of autophagy [302]. Whether Pink1 and parkin induce mitophagy in flies has been further questioned by the finding that basal mitophagy, as measured by the mito-QC reporter, is unaffected by loss of *Pink1* or *park* [142]. However, a more recent study using the mtKeima reporter found that loss of *Pink1* or *park* negatively affected mitophagy in aged flies [33], so there may indeed be a role for mitophagy mediated by Pink1 and parkin in specific contexts.

Drosophila has been an excellent model for identifying other factors that interact with the PINK1/Parkin pathway. Knockdown of *Usp30* was found to partially rescue *Pink1* and *park* mutant phenotypes, as well as PQ-induced neuronal toxicity, which enabled the establishment of the protein as a regulator of mitophagy [10]. Genetic manipulations that increase mitochondrial fission rescued *Pink1* and *park* mutant phenotypes, while fusion-increasing manipulations worsened the phenotypes [220]. While it has since been established that PINK1 and Parkin do not directly mediate mitochondrial dynamics, later studies have confirmed that increased mitochondrial fission improves the efficiency of mitophagy, either by allowing segregation of the damaged mitochondrion or by improving distillation of damaged and undamaged proteins in the mitochondrial network [277, 125]. Studies in *Drosophila* have also found strong genetic interactions between parkin and the PD-related proteins FBXO7 [16] and VPS35 [150], further implicating mitochondrial maintenance in PD etiology. Interestingly, while double heterozygous mutants for *park* and *vps35* showed neurodegenerative phenotypes and increased PQ sensitivity, the authors did not find a genetic interaction between *vps35* and *Pink1*, suggesting that parkin can operate in Pink1-independent pathways [150].

1.4.2 Mouse models

Similarly to fly models, mouse models are genetically tractable and offer an insight into the phenotypic outcomes of various genetic or pharmacological manipulations at an organismal

level. Complex behavioural outcomes, such as memory or fine motor skills, can be more easily measured in mice with sensitive assays [51, 166]. As mammals, mouse genes are more highly conserved to humans than flies; only 1% of human genes have no mouse homolog and vice versa [27]. One of the earliest PD animal models involved injection of MPTP into mice [81]. Parenteral administration of MPTP resulted in selective degeneration of nigrostriatal neurons and reduction in dopamine content, with no effect on serotonin levels [81]. Indeed, mouse models were used to classify MPTP as a Complex I inhibitor, and in the discovery that rotenone, another Complex I inhibitor, causes neurodegeneration [82].

Unfortunately, mice deficient in PINK1 or Parkin do not display phenotypes consistent with parkinsonism, which has somewhat limited their use as a model for the disease [66, 213, 123]. Further, loss of PINK1 does not appear to affect basal mitophagy in mice [168]. Regardless, some important insights into the function of PINK1 and Parkin have been gleaned from mouse models. A Parkin S65A mutant knock-in mouse displayed modest locomotor deficits, similar to full Parkin knockout, indicating that this PINK1 phosphosite is important for Parkin function *in vivo* [166]. Further, combining the Parkin knockout mouse with the mutator mouse, in which the mice express a proofreading-deficient mitochondrial DNA polymerase (polγ) that increases mtDNA mutation load [286], results in neurodegenerative phenotypes without Lewy pathology [216]. Similarly, having the mice perform exhaustive exercise resulted in neurodegenerative phenotypes reminiscent of PD, which could be rescued by inhibiting the STING innate immune pathway [261]. This finding provided further evidence for the growing connection between PD and immune dysfunction [261, 61]. The finding that a double-hit of mitochondrial damage in addition to loss of PINK1 or Parkin is necessary to observe PD-like phenotypes in mice is consistent with the proposal that the PINK1/Parkin pathway occurs under circumstances of mitochondrial stress, and not basally. However, it is unclear if this proposal is consistent with the near-complete penetrance of disease observed in patients with homozygous recessive (or compound heterozygous) mutations in *PINK1* or *PRKN*. Further, the *park* loss-of-function phenotypes in *Drosophila* could not be rescued by inhibiting the equivalent immune pathways, which suggests that immune dysfunction does not cause the degenerative phenotypes observed in flies [141].

1.5 Aims

Although many of the molecular details surrounding PINK1- and Parkin-mediated mitophagy have been elucidated in recent years, several questions remain to be addressed. Firstly,

what is the architecture of the mitochondrial ubiquitome in cells? To what extent does chain branching occur, and what is the relationship between Ub phosphorylation and chain formation on mitochondria? This thesis aims to develop and apply new methods to the study of mitochondrial ubiquitination events. This includes the novel application of established methods, such as sodium carbonate extraction and affimer protection assays described in Chapter 3, and establishment of new methods using Ub-clipping for the analysis of Ub modifications by MS in Chapter 4. These experiments aim to establish the architecture of the mitochondrial ubiquitome. To what extent branched Ub chains occur, and the relationship between Ub phosphorylation and chain formation *in vivo* will be explored. While it is clear that alternative E3 ligases and modes of mitophagy exist, the focus of this thesis will be on the role of Parkin-dependent ubiquitination of mitochondrial substrates. The precise identity of Parkin's mitochondrial substrates will not be explored, given this has received ample prior attention in previous studies.

Secondly, what is the role of PINK1 and Parkin *in vivo*, in an organism? An important question that remains in the field is the extent to which the feedforward production of pS65-Ub by PINK1 and Parkin occurs in physiological contexts, as most studies have explored this phenomenon in the artificial context of overexpression and chemical depolarisation in cell culture. To answer this question, methods to determine the mitochondrial ubiquitome of *Drosophila* models were established, taking into account the much lower mitochondrial Ub content in fly tissues compared with cultured cells. The effects of modulation of the levels of Pink1, parkin, and Atg5 on the fly mitochondrial ubiquitome will also be determined. These experiments establish the Ub chain type complement of fly mitochondria, investigate whether flies produce pS65-Ub in a Pink1-dependent manner, and determine whether manipulations in mitophagy-related genes affect the fly mitochondrial ubiquitome. Further, the role of ageing and PQ treatment of flies on the makeup of the fly mitochondrial ubiquitome were investigated, to determine whether these known risk factors for parkinsonism in humans also affect pS65-Ub production in flies.

Two key principles were followed during the development of the Ub-clipping method for the study of the mitochondrial ubiquitome, where practical. Firstly, the use of low-cost techniques and reagents was prioritised to enable the use of the technology as widely as possible. Secondly, the use of affinity enrichment of Ub was avoided as far as possible. This is because it is impossible to determine whether affinity enrichment biases against as yet undefined Ub modifications, so there is always the possibility that affinity enrichment

methods systematically deplete rare Ub forms. The methods developed therefore aimed to present a systematic description of the mitochondrial ubiquitome with minimal bias from purification techniques.

Chapter 2

Materials and Methods

2.1 Expression of recombinant proteins in *Escherichia coli*

2.1.1 Bacterial transformation and culture

In preparation for recombinant protein expression, plasmids (Table 2.1) were transformed into BL21 pLysE cells (Sigma). Following a 30 second heat shock at 42 °C, 2x TY medium was added, and recovery was initiated in a shaking incubator at 37 °C for 1 h. The cells were plated onto agar plates containing the relevant antibiotic (Table 2.1), and grown overnight at 37 °C. Single colonies were picked and grown overnight in 2x TY at 37 °C to form a starter culture, from which 10 mL was inoculated into 1 L flasks containing 2x TY. Cells were grown at 37 °C to an OD_{600} between 0.6 and 0.8, then expression was induced using IPTG (Table 2.1). The cultures were grown overnight at 18 °C, then harvested by centrifugation at 4,000 rpm, 4 °C (Beckman rotor JLA 8.1).

Table 2.1 **Plasmids and growth conditions used for protein expression.**

Plasmid	**Antibiotics used**	**[IPTG] for induction**
pET11d-Lb^{pro}	Ampicillin, Chloramphenicol	0.4 mM
pET11d-Lb^{pro}* (L74W)	Ampicillin, Chloramphenicol	0.4 mM
pGEX-6P-GST-4xUBA-6xHis	Ampicillin	0.2 mM

2.1.2 Affinity purification of TUBEs using Ni-NTA resin

In order to enrich Ub chains, tandem Ub binding entities (TUBEs) were employed, with the construct used consisting of an N-terminal GST tag, a series of four UBA domains from human ubiquilin-1 (residues 536-589) and a C-terminal hexahistidine tag [85]. For the purification of this construct, Ni-NTA affinity purification was employed as previously described [47, 90], with modifications. Cell pellets were resuspended gently in lysis buffer (50 mM Tris-HCl pH 7.4, 150 mM NaCl, 2 mM BME, 40 mM imidazole), then frozen at -80 °C. Upon thawing, 1 mg/mL lysozyme (Sigma) and 0.1 mg/mL DNase (Sigma) were added, and lysis was performed by sonication (Sonics VC750 750 W sonicator, 70% amplitude, 10 seconds on, 10 seconds off, 3 minutes total time). Lysates were centrifuged at 19,000 rpm, 4 °C (Beckman rotor JA25.50). Ni-NTA beads (Qiagen, 1 mL slurry per 10 mg expected yield) were washed with 20 column volumes (CVs) of lysis buffer, then incubated with the clarified lysate for 15 minutes, 4 °C with gentle rolling. The flowthrough was discarded and the beads were washed with 400 CVs of lysis buffer. The purified protein was eluted using lysis buffer supplemented with 300 mM imidazole, and dialysed overnight into storage buffer (PBS containing 10% (w/v) glycerol, 1 mM DTT). The protein concentration was measured using a NanoDrop spectrophotometer (Thermo Fisher Scientific), and the sample was concentrated using an Amicon Ultra 10K MWCO centrifugation device (Merck Millipore) to a final concentration of 10 mg/mL. The resulting protein was aliquotted into thin-walled tubes, snap-frozen in liquid nitrogen, and stored at -80 °C prior to use.

2.1.3 Expression and purification of Lb^{pro}

Expression and purification of Lb^{pro} (FMDV, residues 29-195) was performed according to [119], with modifications. Lb^{pro}* denotes the Lb^{pro} L102W point mutant (L74W in the construct used), which has 10-fold increased activity towards Ub compared with WT Lb^{pro} [275]. Both constructs were purified in the same manner and used in subsequent experiments as indicated throughout the text. Following transformation of the plasmid and induction of protein expression according to Section 2.1.1 and Table 2.1, the bacterial cell pellets were resuspended in Buffer A (50 mM Tris-HCl pH 8.0, 50 mM NaCl, 1 mM EDTA, 5 mM DTT, 5% (w/v) glycerol) and stored at -80 °C. Upon thawing, 1 mg/mL lysozyme (Sigma) and 0.1 mg/mL DNase (Sigma) were added and the mixture was incubated on ice for 10 minutes. The cells were then lysed by sonication (Sonics VC750 750 W sonicator, 60% amplitude, 10 seconds on, 10 seconds off, 3 minutes total time), and the lysate was cleared by centrifugation at 19,000 rpm, 4 °C (Beckman rotor JA25.50). The cleared lysate was transferred to a beaker

Table 2.2 **ResourceQ settings for the purification of Lb^{pro}**

Column pre-wash	3 CVs, 100% Buffer A, 6 mL/min
Column pre-wash	5 CVs, 100% Buffer B, 6 mL/min
Column pre-wash	3 CVs, 100% Buffer A, 6 mL/min
Sample application	3 mL/min
Column wash	5 CVs, 100% Buffer A, 6 mL/min
Elution	20 CVs, linear gradient 0-100% Buffer B, 6 mL/min
Column wash	5 CVs, 100% Buffer B, 6 mL/min
Column wash	5 CVs, 100% Buffer A, 6 mL/min

containing a stirrer bar, and saturated ammonium sulfate was added dropwise to a final concentration of 30% (v/v). The mixture was incubated 2 h at 4 °C with gentle stirring, then centrifuged as above. The supernatant was transferred to a fresh beaker with stirrer bar, and saturated ammonium sulfate was added to a final concentration of 60% (v/v). The mixture was incubated at 4 °C with gentle stirring for a further 2 h, then centrifuged as above. The supernatant was discarded and the pellet was gently resuspended in Buffer A. The resuspended pellet was dialysed overnight into Buffer A in 10K MWCO SnakeSkin^{TM} dialysis tubing (Thermo Fisher Scientific). Following dialysis, the lysate was clarified by centrifugation, diluted 1:10 in Buffer A, then loaded onto a ResourceQ anion exchange column using a sample pump (GE Healthcare). The conditions used for the ResourceQ run are outlined in Table 2.2. Elution from the column was performed using Buffer B (50 mM Tris-HCl pH 8.0, 500 mM NaCl, 1 mM EDTA, 5 mM DTT, 5% (w/v) glycerol). The fractions were analysed by SDS-PAGE and those containing Lb^{pro} were pooled and concentrated to 1.5 mL using an Amicon Ultra 10K MWCO centrifugation device (Merck Millipore). The concentrated sample was then run on a size exclusion column (HiLoad 26/60 Superdex 75 pg), and the Lb^{pro}-containing fractions were determined by SDS-PAGE. Those fractions with minimal contamination from other proteins were concentrated as above to a final concentration of 1 mM, as measured using a NanoDrop spectrophotometer (Thermo Fisher Scientific). The resulting protein was aliquotted into thin-walled tubes, snap-frozen in liquid nitrogen and stored at -80 °C until needed.

2.2 Mammalian cell biology techniques

2.2.1 Cell culture and mitophagy induction

Doxycycline-inducible HeLa Flp-In Trex cells expressing Parkin (WT or C431S, and *PINK1*$^{-/-}$ cells expressing WT Parkin; a gift from A. Ordureau and J.W. Harper, Harvard) were cultured in DMEM plus GlutaMAX (Gibco) containing Penicillin/Streptomycin (P/S; Sigma-Aldrich), and 10% (v/v) Fetal Bovine Serum (FBS; Gibco). For mitophagy induction, 4 million cells were plated onto 15 cm dishes and grown at 37 °C, 5% (v/v) CO_2 for two days. Parkin expression was induced with 0.5 μM doxycycline (Sigma) for 16 h, then mitochondrial damage was induced with OA (10 μM Oligomycin (Merck) and 4 μM Antimycin A (Sigma)), or CCCP (10 μM Carbonyl cyanide m-chlorophenyl hydrazone, Sigma). Unless otherwise stated, cells were incubated a further 2 h at 37 °C, 5% (v/v) CO_2 prior to harvesting.

2.2.2 Transfection of HeLa cells using FuGENE HD reagent

For the transfection of HeLa Flp-In Trex cells with pcDNA3.1-HA-Ub, the FuGENE HD reagent (Promega) was used. For each 10 cm dish at approximately 70% confluency, 19 μg plasmid DNA was added to 879 μL sterile MilliQ water. 56 μL FuGENE HD transfection reagent was added, then the mixture was briefly vortexed and incubated at room temperature for 5 minutes. 850 μL of the mixture was then added dropwise to cells containing 15 mL DMEM with P/S and 10% (v/v) FBS. The cells were incubated at 37 °C, 5% CO_2 for 24 h prior to harvest. Additional treatments, such as CCCP treatment, were performed as indicated by addition of the drug to the culture medium.

2.2.3 Preparation of mitochondrial extracts

Mammalian cells

Mitochondrial enrichment was performed as per [137], with minor modifications. All steps were performed on ice or at 4 °C, unless otherwise noted. After aspirating the media, the cells were washed twice with PBS containing 200 mM chloroacetamide (PBS + CAA; Sigma). Cells were removed from plates by scraping, resuspsended in PBS + CAA and centrifuged 5 minutes at 1,000 x g. The pellet was washed again in PBS and centrifuged as above, prior to storage at -80 °C. Frozen pellets were thawed on ice then resuspended in Solution A (20 mM HEPES-KOH pH 7.6, 220 mM mannitol, 70 mM sucrose, 1 mM EDTA) containing 1x PhosSTOP phosphatase inhibitor cocktail (Roche) and 1x cOmplete^{TM} protease inhibitor

cocktail (Roche). After a 20 minute incubation, the lysate was homogenised in a dounce homogeniser with 35 strokes of a drill-fitted pestle at 1,900 rpm. The homogenate was transferred to a Falcon tube then centrifuged 5 minutes at 1,000 x g. The supernatant (containing mitochondria) was transferred to fresh microcentrifuge tubes, while the pellet (containing nuclei and unbroken cells) was resuspended in Solution A and the homogenisation and 1,000 x g centrifugation steps were repeated as above to increase the yield. The supernatants from the two steps were pooled and centrifuged 10 minutes at 10,000 x g. The supernatant from this step (post-mitochondrial supernatant) was removed, and the pellet (containing mitochondria) was resuspended in Solution A. This homogenate was cleared by centrifugation for 5 minutes at 800 x g. The supernatant was transferred to a fresh microcentrifuge tube and centrifuged 10 minutes at 10,000 x g. The supernatant was removed and the pellet was washed in Solution A, centrifuged 10 minutes at 10,000 x g, and the supernatant removed again. This wash step was performed three times in total, then the pellet was resuspended in Sucrose Storage Buffer (500 mM sucrose, 10 mM HEPES-KOH pH 7.6). Protein concentration was determined using a Pierce^{TM} BCA Protein Assay Kit (Thermo Fisher Scientific), and the mitochondria were stored at -80 °C until needed.

Mouse brain

Mitochondrial extraction from mouse brain was performed as above with minor modifications. Freshly isolated brains from 3-month-old CD1 mice (obtained by scavenging) were dissected into 4 mm^3 cubes prior to homogenisation. All subsequent steps were performed as above.

Drosophila whole flies

Purification of mitochondria from whole flies was performed similarly to mammalian cells, with the following modifications to ensure no contamination from the fly cuticle. Whole flies were placed in a dounce homogeniser, Solution A containing protease and phosphatase inhibitors was added (approximately 10 μL per fly), and the flies were homogenised with 35 strokes of a drill-fitted pestle as above. The homogenate was transferred to a Falcon tube and incubated 30 minutes, then centrifuged for 5 minutes at 1,000 x g. The supernatant (containing mitochondria) was transferred to microcentrifuge tubes and centrifuged 15 minutes at 10,000 x g. The post-mitochondrial supernatant was removed and the pellet (containing mitochondria) was resuspended in Solution A. The homogenate was then clarified by centrifugation for 5 minutes at 800 x g, and the supernatant transferred to a fresh tube. This clarification step was repeated once more to ensure all cuticle was removed from the sample.

The supernatant was then centrifuged 10 minutes at 10,000 x g, the post-mitochondrial supernatant discarded, and the pellet washed three times in Solution A as above. The washed pellet was resuspended in Sucrose Storage Buffer and stored at -80 °C until needed.

2.2.4 Swelling and Proteinase K protection assay

All steps were performed on ice or at 4 °C. Using mitochondrial extracts prepared in Section 2.2.3, 50 μg aliquots were resuspended in either Solution A or Swelling Buffer (20 mM HEPES pH 7.6, 150 mM NaCl). The mitochondria were incubated 30 minutes, then 5 mg/mL Proteinase K was added to tubes as indicated, and incubated a further 10 minutes. 1 mM PMSF was then added to all tubes, followed by a further 10 minute incubation, then the samples were centrifuged 30 minutes at 21,000 x g. The supernatant and pellet fractions were separated and analysed by western blotting as per Section 2.2.9.

2.2.5 Sodium carbonate extraction of mitochondria

Mitochondria produced in Section 2.2.3 were resuspended in 100 mM Na_2CO_3 (1 μL per μg mitochondrial protein). The mixture was incubated 30 minutes on ice with occasional vortexing, then centrifuged 30 minutes, 21,000 x g, 4 °C. The supernatant, containing soluble and peripheral membrane proteins, was separated and discarded or retained for analysis by western blotting. The pellet, containing integral membrane proteins, was then used for downstream applications including Lb^{pro} treatment.

2.2.6 TUBE-mediated Ub pulldown assay

All steps were performed on ice or at 4 °C. For the enrichment of mitochondrial Ub chains, mitochondria produced in Section 2.2.3 were pelleted at 16,000 x g, 10 minutes, and resuspended in TUBE lysis buffer (PBS containing 1% (v/v) NP-40, 2 mM EDTA, 1 mM DTT, 10 mM CAA, 1x cOmplete^{TM} protease inhibitor cocktail (Roche)) supplemented with 8 μg/mL TUBE (produced in Section 2.1.2). The mixture was incubated 20 minutes, then centrifuged 15 minutes at 21,000 xg. Glutathione Sepharose 4B resin (GE Healthcare; 5 μL slurry per 100 μg mitochondrial protein) was washed 3 times in 500 μL TUBE lysis buffer. The cleared lysate was incubated with the beads on a rotating wheel for 2 h. The lysate was then removed and the beads were washed three times with 500 μL PBST, then once with PBS, prior to use in downstream applications as indicated.

2.2.7 UbiCRest analysis of mitochondrial Ub

UbiCRest analysis was performed as previously described [88] with modifications. DUB constructs used included USP21 (human, residues 196-565), vOTU (Crimean-Congo hemorrhagic fever virus, residues 1-183), Cezanne (human, residues 53-446) and OTULIN (human, residues 1-352) [88]. Additionally, OTUB1*, consisting of residues 1-147 of human UBE2D2 followed by a 10-residue GGSS linker, followed by residues 16-271 of OTUB1 was also used as it conferred increased activity [172]. Similarly, AMSH*, consisting of residues 5-188 of STAM2 followed by a 6-residue GGSSGG linker, followed by residues 243-424 of human AMSH, improves efficiency of the enzyme [172]. The above purified DUBs (gifts of Paul Elliott, Komander lab) were made to a 2x stock in DUB dilution buffer (25 mM Tris pH 7.4, 150 mM NaCl, 10 mM DTT) and incubated 15 minutes at room temperature. Mitochondria treated as per Section 2.2.5 were resuspended in 2x DUB reaction buffer (100 mM Tris pH 7.4, 100 mM NaCl, 10 mM DTT) and mixed 1:1 with each 2x DUB stock. Samples were incubated 45 minutes at 37 °C, then centrifuged 30 minutes at 21,000 x g, 4 °C. The supernatant and pellet fractions were kept for western blotting analysis.

2.2.8 Affimer protection assays

Using mitochondrial extracts prepared in Section 2.2.3, thawed mitochondria were incubated with the indicated amounts of biotin-linked affimer proteins (a gift of Martin Michel, Komander Lab [173]) in Solution A on ice for 10 minutes. The samples were then centrifuged 10 minutes at 10,000 x g, 4 °C (Step 1). 1 μM USP21 was added, and the mixture was incubated 1 h at 37 °C. This mixture was returned to ice and pelleted at 10,000 x g, 10 minutes, 4 °C (Step 2). The pellet was sodium carbonate-extracted as per Section 2.2.5 (Step 3). The pellet from this next step was resuspended in Solution A containing 1 μM USP21, incubated 45 minutes at 37 °C, and centrifuged as above (Step 4). At each of the four steps noted above, an aliquot was taken for analysis by western blot.

2.2.9 SDS-PAGE and western blotting techniques

Samples to be analysed by SDS-PAGE were resuspended in 1x LDS loading dye (Life Technologies) containing 25 mM DTT, and loaded onto NuPAGE 4-12% Bis-Tris gels (Life Technologies). Samples were run in 1x MES SDS-PAGE buffer (50 mM MES, 50 mM Tris Base, 0.1% (w/v) SDS, 1 mM EDTA pH 7.3) for 25 minutes at 100 V, then the voltage was increased to 200 V and run for a further 35 minutes. Coomassie staining was performed

where indicated using InstantBlue Coomassie Protein Stain (Expedeon) with gentle rocking overnight, followed by destaining in MilliQ water. western transfer was performed where indicated using the BioRad Trans-Blot Turbo^{TM} transfer system onto pre-cut Immun-Blot 0.2 μm PVDF membranes (BioRad). All incubation and wash steps were performed with gentle rocking, and three washes were performed between each incubation step. During each wash step, membranes were incubated in PBS containing 0.1% (v/v) Tween 20 (PBST) for 5 minutes. Blocking was performed in PBST containing 5% (w/v) skim milk powder for 30 minutes at room temperature. Primary antibody incubation was performed overnight at 4 °C at the concentrations listed in Table 2.3, while secondary antibody incubation was performed for 1 hour at room temperature in PBST containing 5% (w/v) skim milk at the concentrations listed in Table 2.3. After the final wash, membranes were incubated in PBS for 5 minutes, then incubated for 5 minutes in ECL reagent (Clarity, BioRad), and imaged on a BioRad MP Chemidoc system.

2.3 Lb^{pro} treatment and Mass Spectrometry techniques

2.3.1 Lb^{pro} treatment of mitochondrial extracts

Sodium carbonate-extracted mitochondria

Sodium carbonate-extracted mitochondria (produced in Section 2.2.5) were resuspended in Lb^{pro} reaction buffer (50 mM NaCl, 50 mM Tris pH 7.4, plus 10 mM DTT unless otherwise indicated) containing 10 μM Lb^{pro}* and incubated overnight at 37 °C. The samples were centrifuged 30 minutes, 21,000 x g, 4 °C, and the supernatant containing liberated Ub proteoforms was retained for further analysis.

TUBE-enriched mitochondrial Ub

Enriched Ub chains produced in Section 2.2.6 were digested on-bead in Lb^{pro} reaction buffer containing 20 μM Lb^{pro}* for 16 h at 37 °C. The supernatant was removed and the beads were washed once with Lb^{pro} reaction buffer. The supernatants, containing Ub proteoforms, were pooled and retained for further analysis.

Table 2.3 **Primary antibodies used for western Blotting.**

Antibody	**Supplier**	**Catalog ID**	**Secondary**	**Dilution**
Primary				
Biotin	Sigma	B7653	Mouse	1:1,000
Cytochrome *c*	Abcam	AB110325	Mouse	1:1,000
GAPDH	Ambion	AM4300	Mouse	1:10,000
HA	Novus Biologicals	NB600-362	Goat	1:10,000
K6-linked Ub affimer	M. Michel [173]		Biotin-conjugated	1:500
K11-/33-linked Ub affimer	M. Michel [173]		Biotin-conjugated	1:1,000
K48-linked Ub (Apu2)	Merck Millipore	05-1307	Rabbit	1:1,000
K63-linked Ub (Apu3)	Merck Millipore	05-1308	Mouse	1:1,000
Lamin A	Santa Cruz Biotech	Sc-20680	Rabbit	1:200
Phospho-Ser65-Ub	Merck Millipore	ABS1513-I	Rabbit	1:1,000
TOMM20	Santa Cruz Biotech	Sc-11415	Rabbit	1:200
Ubiquitin	Novus Biologicals	Ubi-1	Mouse	1:1,000
Secondary (HRP-conjugated)				
Anti-goat	Santa Cruz Biotech	Sc-2020		1:10,000
Anti-mouse	GE Healthcare	NXA931V		1:10,000
Anti-rabbit	GE Healthcare	NA934V		1:10,000

2.3.2 Perchloric acid precipitation

Without dialysis

In order to remove excess Lb^{pro} and unwanted mitochondrial proteins after Lb^{pro} treatment, samples were mixed 1:1 with 1% (v/v) perchloric acid, incubated on ice for 15 minutes, then centrifuged 20 minutes at 21,000 x g, 4 °C. The supernatant was transferred to a new tube, then lyophilised, resuspended in 0.1% (v/v) FA and desalted using C_4 ZipTips (Merck Millipore) according to the manufacturer's instructions. The desalted sample was lyophilised and resuspended in 0.1% (v/v) FA for analysis by mass spectrometry.

With dialysis

Following the perchloric acid treatment and centrifugation steps above, the Ub proteoforms were transferred to a pre-equilibrated Slide-a-Lyzer MINI Dialysis unit (Thermo Fisher Scientific) and dialysed 5 h into 50 mM Tris pH 7.4, then overnight into MilliQ water. Following dialysis, the sample was lyophilised prior to analysis by mass spectrometry.

2.3.3 Ub purification using StageTips

Mitochondrial Ub proteoforms generated in Section 2.3.1 were further purified using StageTips [228]. StageTips were assembled using 4 plugs that were cut using a gauge 16 needle (Hamilton) from C_4 substrate (AffiniSEP) and assembled into a P200 pipette tip using a plunger (Hamilton). The matrix was activated by the addition of 20 μL methanol and the tip was centrifuged inside a 2 mL eppendorf tube at 800 x g for 30 seconds at room temperature to allow the liquid to pass through. The tip was then equilibrated by passing through 20 μL 80% (v/v) ACN, 0.1% (v/v) FA, followed by 20 μL 0.1% (v/v) FA. The sample to be applied to the StageTip was acidified to a pH less than 4 using FA, then loaded and centrifuged as above until almost all the liquid had passed through. The tip was then desalted by passing through 25 μL 0.1% (v/v) FA, twice. In some experiments as indicated, a pre-elution step was included: 10-25% (v/v) ACN, 0.1% (v/v) FA was passed through twice prior to elution. For elution of the Ub, the tip was transferred to a fresh Lo-Bind Eppendorf tube, and 25 μL 40-80% (v/v) ACN, 0.1% (v/v) FA was added to elute the protein from the matrix. A further 25 μL elution buffer was added to ensure full elution, and the sample was lyophilised.

Table 2.4 **AQUA peptides used in this study and their stock concentrations.** Underlined residues are heavy-labelled (^{13}C, ^{15}N), while [pS] indicates a phosphorylated residue. K(GG) indicates that the K residue is diGly-modified. All peptides were supplied by Cell Signaling Technologies except the pS65 peptide, which was supplied by Cambridge Research Biochemicals. The K63/pS65 peptide was used in initial AQUA experiments only and was not included in the stock.

Peptide	Sequence and modifications	Stock concentration (fmol/μL)
K6	MQIFVK(GG)T<u>L</u>TGK	20
K11	TLTGK(GG)TITLEVEPSDTIEN<u>V</u>K	20
TITLE	TITLEVEPSDTIEN<u>V</u>K	900
K48	LIFAGK(GG)Q<u>L</u>EDGR	150
K63	TLSDYNIQK(GG)ESTLHLV<u>L</u>R	150
pS65	E[pS]<u>L</u>HLVLR	3.3205
K63/pS65	TLSDYNIQK(GG)E[pS]TLHLV<u>L</u>R	NA

For AQUA analysis, the sample was resuspended in Trypsin Resuspension Buffer (Promega) supplemented with Tris pH 8.0 to ensure a final pH above 6. Trypsin (Promega) was added at a concentration of 1 μg per 50 μg initial mitochondrial protein, and the samples were incubated 8-16 h at 37 °C. For StageTip purification after trypsin treatment, the sample was acidified to pH less than 4 using FA. For initial experiments using HeLa mitochondria, an AQUA stock containing equimolar amounts of all the peptides listed in Table 2.4 was added. For subsequent experiments, 0.5-2 μL AQUA peptide stock (concentrations listed in Table 2.4) was added, then the sample was loaded into a StageTip containing 4 plugs of C_{18} substrate (AffiniSEP) that had been assembled, activated and pre-equilibrated as above. The tip was washed 3 times in 0.1% (v/v) FA, then elution was performed twice with 25 μL 80% (v/v) ACN, 0.1% (v/v) FA. The samples were lyophilised prior to mass spectrometry analysis.

2.3.4 TiO_2 enrichment of phosphorylated Ub

Where indicated, enrichment of phosphorylated peptides was performed using the High-Select^{TM} TiO_2 Phosphopeptide Enrichment kit (Thermo Fisher Scientific). Following C_4 StageTip fractionation and trypsin treatment of Lb^{pro}*-treated Ub from 4 mg sodium carbonate-extracted mitochondria, the sample was divided between two TiO_2 columns and

prepared according to the manufacturer's instructions. The eluates were pooled, lyophilised and analysed by LC-MS as using the AQUA mass spectromtry parameters in Section 2.3.7.

2.3.5 Identifying the source of R-clipping

To identify the cause of the production of Ub^{1-73}, Ub^{1-74} was generated *in vitro* by incubation of 10 μg recombinant Ub with 20 μM Lb^{pro} for 2.5 hours at 37 °C. The Lb^{pro} was removed by perchloric acid precipitation and dialysis as per Section 2.3.2. The Ub^{1-74} was incubated with isolated mitochondria, with or without sodium carbonate extraction as indicated, overnight at 37 °C. The samples were then centrifuged 30 minutes, 21,000 x g, 4 °C, and the supernatant desalted using C_4 ZipTips (Merck Millipore). The resulting samples were analysed by intact mass spectrometry as per Section 2.3.7.

2.3.6 Lb^{pro}* treatment of UBE2L3

To assess multi-ubiquitination of a Parkin substrate, an *in vitro* Ub assembly assay was performed by C. Gladkova [275]. In brief, 0.2 μM human E1, 4 μM UBE2L3, 4 μM phosphorylated Parkin, 15 μM Ub, and 1.5 μM pS65-Ub were incubated 2 h at 37 °C in reaction buffer (50 mM Tris pH 8.5, 200 mM NaCl, 10 mM $MgCl_2$, 10 mM ATP, 10 mM DTT). The assembly reaction was terminated by the addition of 2 mU of apyrase (Sigma) for 1 h at 37 °C, then the assembly was incubated 5 h with 10 μM Lb^{pro}* in Lb^{pro} reaction buffer (Section 2.3.1) at 37 °C. The mixture was dialysed in a pre-equilibrated Slide-a-Lyzer MINI Dialysis unit (Thermo Fisher Scientific) in 50 mM Tris pH 7.4 for 5 h, then overnight in MilliQ water. The sample was then lyophilised prior to analysis by intact mass spectrometry.

2.3.7 LC-MS parameters

Intact MS

For the analysis of intact Ub proteoforms by mass spectrometry, samples were resuspended in 5% (v/v) ACN, 0.1% (v/v) FA, and 10 μL was injected onto a Dionex Ultimate 3000 HPLC system (Thermo Fisher Scientific). The sample was first loaded onto a C4 PepMap300 precolumn trap (Thermo Fisher Scientific) at a flow rate of 30 μL min^{-1}. Elution from the trap was performed with an acetonitrile gradient (5-40%) over 45 minutes at a flow rate of 0.3 μL min^{-1}. Immediately prior to electrospray ionisation, the sample was passed through an EASY-Spray Accucore C_4 reverse-phase column (2.6 μm, 150 Å, 75 μm x 25 cm; Thermo Fisher Scientific). Mass spectrometry was performed with a Q Exactive mass spectrometer

(Thermo Fisher Scientific) using the following settings: resolution, 140,000; AGC target, 3E6; maximum injection time, 200 ms; scan range, 150-2,000 m/z.

AQUA MS

For the analysis of tryptic digests containing heavy-labelled AQUA reference peptides by mass spectrometry, samples were first resuspended in 0.1% (v/v) FA. 10 μL was injected onto a Dionex Ultimate 3000 HPLC system (Thermo Fisher Scientific), and trapped on a C18 Acclaim PepMap100 (5 μm, 100 μm x 20 mm nanoViper; Thermo Scientific). Peptides were eluted with a 60 minute acetonitrile gradient (2-40%) at a flow rate of 0.3 μL min^{-1}. The analytical column outlet was directly interfaced via an EASY-Spray electrospray ionisation source to a Q Exactive mass spectrometer (Thermo Fisher Scientific). The following settings were used: resolution, 140,000; AGC target, 3E6; maximum injection time, 200 ms; scan range, 150-2,000 m/z.

2.3.8 Higher-energy collisional dissociation analysis of R-clipped Ub

For the identification of Ub^{1-73}, a PRM assay was conducted. The LC-MS conditions were identical to those used for intact MS of Ub above, with minor modifications. The PRM assay was conducted with an isolation window of 5 m/z around the +12 charge state of the suspected Ub^{1-73} peak (m/z = 692.1322), with a higher-energy collisional dissociation (HCD) collision energy of 30 eV. The MS2 peaks were annotated using Expert System [187], and cross-checked using Thermo Xcalibur Qual Browser version 2.2 (Thermo Fisher Scientific) to ensure correct assignment with regard to charge state.

2.3.9 Quantification of mass spectrometry results

Relative quantification of Ub proteoforms by extracted ion chromatogram

Raw files were analysed in Thermo Xcalibur Qual Browser version 2.2 (Thermo Fisher Scientific) and layouts were applied according to Table 2.5, focusing on the +12 charge state, which had been established as the most common charge state for all intact Ub proteoforms analysed [275], aside from Ub^{1-73} for which the +11 charge state was most highly abundant. Peaks were manually inspected for charge state and chromatography trends for validation. The summed peak intensities for each species were quantified and the data inputted into Microsoft Excel for analysis. The relative abundance of each species was calculated according

to the following equation, using $Ub^{1\text{-}74}$ as an example:

$$\%\ Abundance\ (Ub^{1\text{-}74}) = \frac{Intensity\ (Ub^{1\text{-}74})}{Summed\ intensities\ of\ all\ Ub\ species} \times 100$$

Relative quantification of Ub proteoforms by peak deconvolution

In the Xcalibur Qual Browser, using the known retention times determined from the extracted ion chromatogram method above, an averaged mass spectrum was produced across the retention times for all Ub species being analysed. Using this averaged mass spectrum, a deconvoluted mass spectrum was generated using the default settings. After deconvolution, the mass list was imported into Excel, and the intensity of the nominal mass for each Ub species was extracted. The relative abundance of each species was determined using the above equation.

AQUA analysis by extracted ion chromatogram

Raw files were opened in the Xcalibur Qual Browser and layouts were applied according to Table 2.5. MS1 peaks were validated manually by observing the charge state and retention times as compared with the heavy labelled reference peptides. The peak area for each peptide was quantified, and the absolute abundance calculated in Microsoft Excel by the following equation, using the heavy peptide amounts from Table 2.4:

$$Amount\ (light\ (fmol)) = \frac{Area\ (light)}{Area\ (heavy)} \times Amount\ (heavy\ (fmol))$$

In the case of the K63-modified peptide, in which the +3 and +4 charge state are both abundant, the following equation was used:

$$Amount\ (light\ (fmol)) = \frac{Area\ (light^{+3}) + Area\ (light^{+4})}{Area\ (heavy^{+3}) + Area\ (heavy^{+4})} \times Amount\ (heavy\ (fmol))$$

The abundance of total Ub was determined by quantification of the TITLE locus, and was calculated by addition of the abundances calculated for the TITLE peptide and the K11-GG peptide, which also contains the TITLE sequence (Table 2.4).

Table 2.5 **m/z values used for quantification of Ub species.** H and L refer to the heavy and light peptides respectively.

	Ub species	**Expected m/z**	**z**	**Lower bound**	**Upper bound**
Intact MS	Ub^{1-74}	705.2273	12	705.21321	705.24141
	Ub^{1-74} 1x GG	714.7309	12	714.71660	714.74518
	Ub^{1-74} 2x GG	724.2345	12	724.21998	724.24894
	pUb^{1-74}	711.8923	12	711.87806	711.90654
	pUb^{1-74} 1x GG	721.4009	12	721.38642	721.41528
	pUb^{1-74} 2x GG	730.9094	12	730.89478	730.92402
	Ub^{1-73}	755.0486	11	755.03349	755.06369
	Ub^{1-73} 1x GG	765.4161	11	765.40082	765.43144
AQUA MS	K6-GG H	462.9347	3	462.91	462.95
	K6-GG L	460.5915	3	460.57	460.61
	K11-GG H	803.4315	3	803.41	803.45
	K11-GG L	801.4269	3	801.41	801.45
	TITLE H	897.4742	2	897.45	897.49
	TITLE L	894.4673	2	894.45	894.49
	K48-GG H	489.9391	3	489.92	489.96
	K48-GG L	487.6001	3	487.58	487.62
	K63-GG H (+3)	751.0767	3	751.06	751.10
	K63-GG H (+4)	563.5593	4	563.54	563.58
	K63-GG L (+3)	748.7376	3	748.72	748.76
	K63-GG L (+4)	561.8050	4	561.79	561.83
	S65-p H	385.5396	3	385.52	385.56
	S65-p L	383.2006	3	383.18	383.22

2.3.10 Data presentation and statistical analysis

Pie charts of single replicate results were produced in Microsoft Excel. All other graphs were produced using GraphPad Prism 7. Statistical tests, such as linear regression analyses, were performed as indicated using GraphPad Prism 7.

2.4 *Drosophila melanogaster* techniques and treatments

2.4.1 *Drosophila* maintenance and husbandry

Flies were maintained on food containing cornmeal, agar, molasses, yeast, and propionic acid, and incubated in a 12 h/ 12 h light/dark cycle in incubators (MIR-254, Sanyo) at 25 °C. Male flies only were harvested from crosses, and flies were harvested two to five days post-eclosion unless otherwise indicated. For ageing experiments, flies were separated into males and females and flipped onto fresh food every two to three days, with anaesthesia avoided where practicable. For harvest, flies were immobilized by CO_2-induced anaesthesia, and maintained on ice for at least 20 minutes prior to performing mitochondrial enrichment. Table 2.6 lists the *Drosophila* lines used in this study.

2.4.2 Paraquat treatment

To induce mitochondrial damage, w^{1118} flies (both males and females) were transferred to bottles containing filter paper saturated with 5 mM paraquat (Sigma), 5% (w/v) sucrose. The flies were incubated at 25 °C for 3 days prior to harvest.

Table 2.6 **Fly lines used in this study and their source.**

Name	Genotype	Source	Identifier
$Atg5^{5cc5}$	$Atg5^{5cc5}$/FM7.GFP	G. Juhasz	Kim et al. 2016 [117]
$Atg5^{5cc5}$; *da*-GAL4	w^{1118} $Atg5^{5cc5}$/FM7.GFP; *da*-GAL4	A.J. Whitworth	N/A
da-GAL4	w^{*}; $Kr^{If\text{-}1}$/CyO; P{$w^{+mW.hs}$ = GAL4-*da*.G32}UH1	BDSC	RRID: BDSC_55850
$park_{C2}$	*w*; P{UAS-*park*}C2 II	A.J. Whitworth	Greene et al. 2003 [71]
$Pink1^{B9}$	*w* $Pink1^{B9}$/FM7.GFP	J.K. Chung	FlyBase: FBal0193144
$Pink1^{B9}$; *da*-GAL4	*w* $Pink1^{B9}$/FM6; P{*da*-GAL4}	A.J. Whitworth	N/A
TcPink1	*w*; P{UAS-*Tc-Pink1*}2A/CyO	A.J. Whitworth	N/A
w^{1118}	w^{1118}	BDSC	RRID: BDSC_6326

Chapter 3

Biochemical investigations of the Parkin-dependent mitochondrial ubiquitome

3.1 Introduction

PINK1 and Parkin function in a form of mitophagy that can be stimulated using agents that induce mitochondrial damage [184]. Dissipation of the mitochondrial membrane potential results in accumulation of PINK1 on the OMM, where its kinase function is activated and it phosphorylates both Ub and the Ubl domain of Parkin at S65 [136, 112, 104, 129, 128]. pS65-Ub binding and Ubl phosphorylation of Parkin cause significant structural rearrangements that activate its E3 ligase activity [64, 245], resulting in the ubiquitination of mitochondrial proteins [204, 36]. These ubiquitination events lead to destruction of the damaged mitochondria by autophagy through recognition of the ubiquitinated proteins by the autophagy machinery [184, 139]. To date, studies from the Harper group and others have used MS techniques to derive insights into the Ub chain linkages present on mitochondria, and the stoichiometry of ubiquitination on mitochondrial substrates [242, 204, 36, 201, 237, 202]. However, an understanding of the mitochondrial Ub chain architecture, including the interplay between phosphorylation and chain formation, has so far been lacking. This chapter provides further insight into the architecture of the Parkin-dependent ubiquitome using biochemical methods.

To deeply probe the role of Ub architecture in PINK1/Parkin mitophagy, first a method for the enrichment of mitochondrial ubiquitin was developed using sodium carbonate extraction, to ensure the absence of contaminating DUB activity and unconjugated mono-Ub in the mitochondrial sample. The potential presence of intra-mitochondrial Ub was also explored. Finally, the mitochondrial Ub architecture in depolarised HeLa cells expressing exogenous Parkin was investigated using a variety of biochemical techniques developed in the Komander lab. These techniques include UbiCRest, which uses a panel of chain type-specific DUBs to probe the Ub chain types present on a given substrate [88]; antibodies and affimer reagents specific for distinct Ub chain types [190, 173]; and the development of an affimer protection assay to probe the abundance of K6 and K11/33 chains on mitochondria. The following chapter will then explore the use of Ub-clipping in MS.

3.2 Optimisation of mitochondrial Ub enrichment

3.2.1 Mitochondrial enrichment by differential centrifugation

Using conditions described previously [204], HeLa Flp-In Trex cells expressing doxycycline-inducible Parkin (wild-type (WT) or catalytic dead C431S mutant) were depolarised to induce mitophagy. Depolarisation of the mitochondrial membrane potential, $\Delta\Psi$m, is a robust trigger for PINK1/Parkin pathway activation [184], and was achieved using either carbonyl cyanide m-chlorophenyl hydrazone (CCCP) or a combination of oligomycin and antimycin A (OA) as indicated. CCCP is a protonophore that rapidly dissipates $\Delta\Psi$m by allowing diffusion of protons across the IMM [105, 84]. However, while CCCP is often used for the induction of mitophagy [184, 204, 173], it is not specific to mitochondria, and has been shown to interfere with lysosomal pH [207]. Antimycin A inhibits Complex III of the respiratory chain [260], while oligomycin inhibits Complex V [211]. Use of the two drugs in combination (OA) depletes mitochondrial respiration and prevents Complex V from operating in reverse to maintain the $\Delta\Psi$m, resulting in depolarisation [303, 163]. While OA results in slower depolarisation of $\Delta\Psi$m than CCCP [163], CCCP's effects on lysosomes mean that this drug is not ideal for investigating autophagy [207]. Therefore, where practical, OA was preferably used for induction of mitochondrial dysfunction. Crude mitochondrial fractions were obtained by differential centrifugation, with enrichment of mitochondria measured by western blotting of TOMM20 (Figure 3.1A). Addition of a sucrose cushion step resulted in modest further mitochondrial enrichment as indicated by reduction of cytosolic GAPDH signal (Figure 3.1A, compare lanes 3 and 4), but significantly reduced the yield, and

was therefore not incorporated into the enrichment method. With chemical depolarisation, Parkin was enriched in the mitochondrial fraction (Figure 3.1B), and expression levels of WT and C431S Parkin in whole cell lysates were comparable upon doxycycline induction (Figure 3.1C).

When comparing recruitment of WT and C431S Parkin to mitochondria, WT Parkin displayed a strong signal in the mitochondrial fraction relative to the post-mitochondrial supernatant (PMS), indicating mitochondrial recruitment (Figure 3.1D). In contrast, C431S Parkin showed modest mitochondrial recruitment, with a doublet band that represents oxyester bond formation between S431 and the Ub C terminus, that is dependent on PINK1 [97, 138, 333]. This doublet band was also present in the PMS, indicating that C431S Parkin is recruited to but not retained at mitochondria upon depolarisation. Examination of the Ub signal in the mitochondrial fractions obtained through differential centrifugation raised two issues (Figure 3.1E). Firstly, a significant amount of unconjugated mono-Ub was present in the mitochondrial fraction (Figure 3.1E, first lane). Secondly, when incubated at 37 °C, a large amount of Ub was released into the supernatant, presumably due to collapse of chains by a contaminating protease (Figure 3.1E, second lane). The contaminating protease activity occurred with similar kinetics to digestion with Lb^{pro} (Figure 3.1E, compare lanes 2 and 4), which would be problematic for downstream applications using Lb^{pro}. Both the contaminating mono-Ub and the residual protease activity therefore needed to be eliminated in order to perform analyses of the mitochondrial Ub.

3.2.2 Investigating the sub-mitochondrial localisation of Ub

In order to choose the best approach to separate the conjugated Ub from the contaminating unconjugated mono-Ub present in the mitochondrial fractions, it was first necessary to determine whether the mono-Ub was inside the mitochondria, and would therefore co-enrich with any further mitochondrial purification steps. To test this, a swelling and Proteinase K (PK) protection assay was performed, as described in Figure 3.2. Upon treatment with PK, proteins that are on the outside of mitochondria are exposed and therefore degraded by PK, while proteins that are inside the mitochondria are protected. Incubation of mitochondria in a hypotonic buffer causes swelling of the IMM, which results in disruption of the OMM, and release of soluble IMS proteins into the supernatant. Combining swelling and PK treatments can therefore indicate the sub-mitochondrial localisation of a protein of interest (Figure 3.2A). Sodium carbonate (Na_2CO_3) extraction at high pH disrupts peripheral membrane

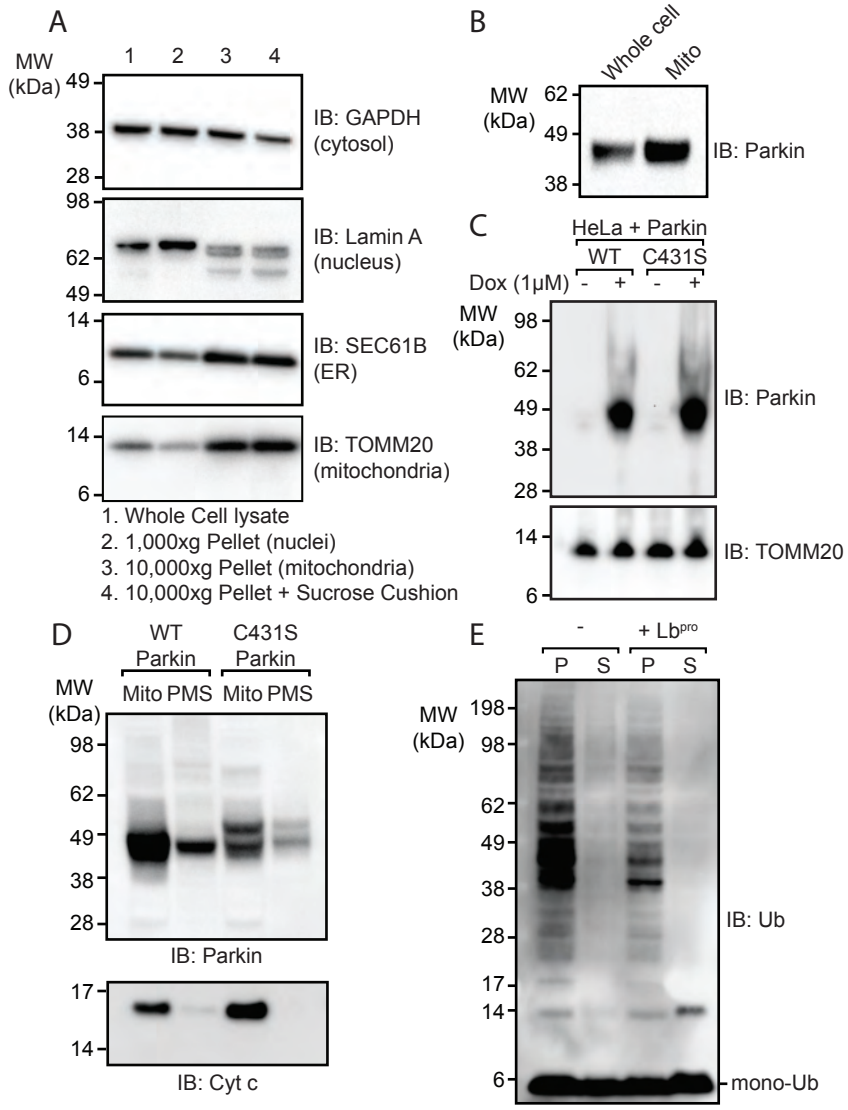

Fig. 3.1 **Parkin expression and mitochondrial enrichment. A.** HeLa cells were subjected to differential centrifugation, and mitochondrial enrichment was investigated using organelle-specific antibodies as indicated. **B.** HeLa Flp-In Trex (WT Parkin) cells were induced with doxycycline for 16 h, then depolarised with CCCP for 1 h. Differential centrifugation was performed to confirm Parkin enrichment at mitochondria. **C.** HeLa Flp-In Trex (WT or C431S Parkin) cells were incubated in the presence or absence of doxycycline for 16 h, then whole cell lysates were immunostained for Parkin to measure induction of expression. **D.** HeLa Flp-In Trex cells were induced with doxycycline for 16 h then depolarised with OA for 4 h. The mitochondrial fraction was obtained through differential centrifugation. The post-mitochondrial supernatant (PMS) was the supernatant from the 10,000 x g centrifugation step. **E.** Following mitophagy induction, mitochondria were incubated for 90 minutes at 37 °C in the presence or absence of 100 μM Lb^{pro}. The resulting mixture was centrifuged at 10,000 x g, and the pellet (P) and supernatant (S) fractions analysed for Ub content by western blotting. IB: immunoblot.

protein associations, and therefore separates integral membrane proteins from soluble and peripheral membrane proteins upon high-speed centrifugation [53] (Figure 3.2B). Upon PK treatment of CCCP-treated mitochondrial fractions, the OMM-exposed proteins Parkin and TOMM20 were degraded, while the IMS-localised Cytochrome *c* (Cyt *c*) remained protected (Figure 3.3, compare lanes 1 and 3). Swelling resulted in release of the IMS-localised Cyt *c* (Figure 3.3, compare lanes 1 and 2 with lanes 5 and 6). Sodium carbonate extraction resulted in retention of the integral OMM protein TOMM20 and lipidated LC3B-II in the pellet, while the peripheral membrane-associated Parkin and Cyt *c* proteins were present in the supernatant (Figure 3.3, lanes 9 and 10). PK treatment appeared to increase the amount of mono-Ub detected (Figure 3.3, lane 4), likely due to collapse of poly-Ub chains into Ub monomers, coupled with a failure of PK to degrade the tightly folded Ub protein. While there appeared to be a slight increase in mono-Ub release into the supernatant upon swelling (Figure 3.3, compare lanes 2 and 6), the apparent resistance of mono-Ub to PK treatment precluded a clear interpretation of this result. Mono-Ub was found in the soluble fraction upon sodium carbonate extraction, indicating that it is either soluble or peripherally associated with the membrane (Figure 3.3, lanes 9 and 10). PK treatment resulted in a collapsing of the poly-pS65-Ub chains into mono-pS65-Ub moieties (Figure 3.3, lanes 3 and 4). Interestingly, there appeared to be no unconjugated mono-pS65-Ub present prior to PK treatment (Figure 3.3, lanes 1 and 2). This indicated that ubiquitinated substrates, rather than free Ub, are phosphorylated by PINK1. Sodium carbonate extraction resulted in the retention of pS65-Ub signal in the pellet, indicating that the pS65-Ub is conjugated mostly to integral membrane proteins (Figure 3.3, lanes 9 and 10).

To circumvent the apparent resistance of mono-Ub to degradation by PK, N-terminally tagged HA-Ub was transfected into cells and the experiment was repeated, this time probing for the loss of signal from the PK-sensitive HA tag by western blot. Unlike when probing directly for mono-Ub, PK treatment did not result in increased mono-HA-Ub (Figure 3.4, lanes 3 and 4), indicating that the effect seen in Figure 3.3 was indeed a result of collapse of Ub chains to PK-resistant mono-Ub. HA-Ub behaved most similarly to Cyt *c* across the assay as it was resistant to PK (lane 3) and was released from mitochondria during swelling (lane 6), indicating that the unconjugated HA-mono-Ub may exist in the IMS. To test the dependency of the apparent HA-mono-Ub protection upon PK treatment on depolarisation, the experiment was repeated both with and without CCCP (Figure 3.5). Parkin localisation at mitochondria was clearly CCCP-dependent as expected, with the majority of Parkin present in the PMS in the absence of CCCP (Figure 3.5, lane 11), while it was mostly present in

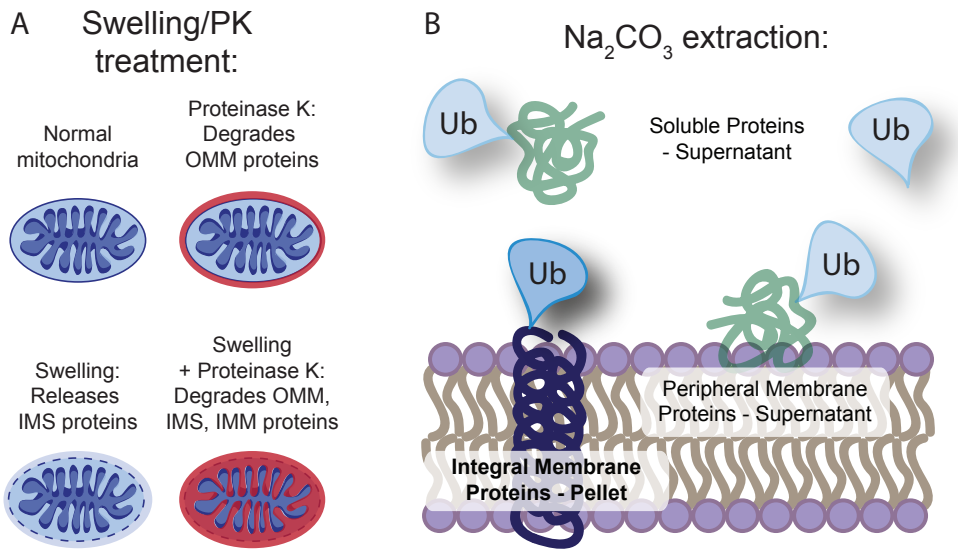

Fig. 3.2 **Swelling, Proteinase K treatment, and sodium carbonate extraction. A.** An explanation of swelling and PK treatment to determine a protein's sub-mitochondrial localisation. Red denotes protease sensitivity, while the dotted lines indicate disruption of the OMM during swelling. **B.** An explanation of sodium carbonate (Na_2CO_3) extraction. High-pH sodium carbonate solution disrupts ionic interactions between peripheral membrane proteins and phospholipid head groups in the membrane bilayer, thereby solubilising peripheral membrane proteins [53]. After centrifugation the peripheral membrane proteins and soluble, non-membrane-associated proteins will be present in the supernatant, while integral membrane proteins are retained in the pellet. In the case of Ub, only Ub that is conjugated to integral membrane proteins will be retained in the pellet fraction.

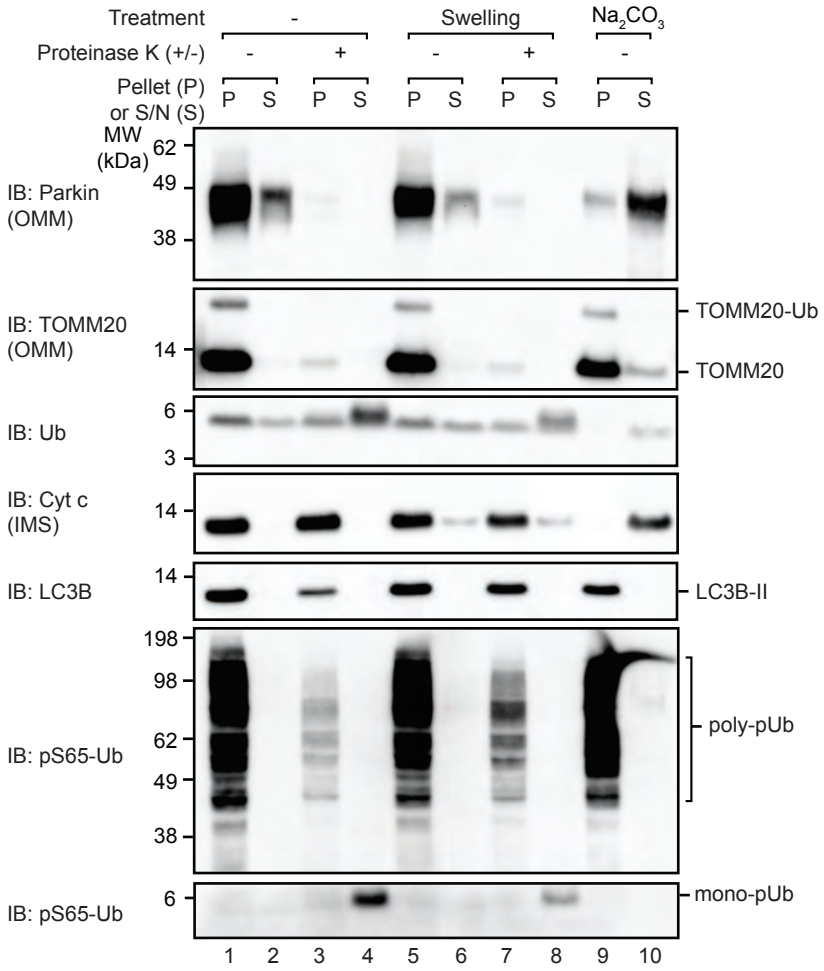

Fig. 3.3 **Assessment of the sub-mitochondrial localisation of mono-Ub using swelling, PK and sodium carbonate extraction assays.** HeLa Flp-In Trex cells expressing WT Parkin were induced 16 h with doxycycline, then depolarised 1 h with CCCP. Swelling, PK treatment and sodium carbonate extraction were performed on mitochondrial fractions to assess the sub-mitochondrial localisation of Ub. IB: immunoblot. IMS: intermembrane space. OMM: outer mitochondrial membrane. S/N: supernatant.

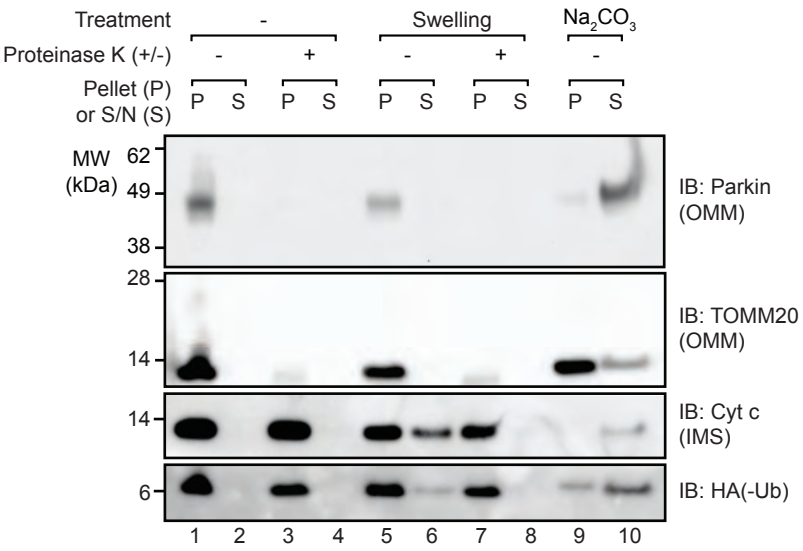

Fig. 3.4 **Assessment of the sub-mitochondrial localisation of HA-Ub.** HeLa Flp-In Trex cells expressing WT Parkin were transfected with HA-Ub, induced 16 h with doxycycline, then depolarised 1 h with CCCP. Swelling, PK treatment and sodium carbonate extraction were performed on mitochondrial fractions to assess the sub-mitochondrial localisation of HA-Ub. IB: immunoblot. IMS: intermembrane space. OMM: outer mitochondrial membrane. S/N: supernatant.

the mitochondrial fraction in CCCP-treated cells (Figure 3.5, lane 13). Similarly, while TOMM20's mitochondrial localisation was unaffected by CCCP treatment as expected, mono-ubiquitination of TOMM20 was observed only in the presence of CCCP (Figure 3.5, compare lanes 1 and 13). Cyt *c*'s behaviour in the assay was unaffected by depolarisation. In contrast, HA-mono-Ub was less efficiently protected from PK treatment in the absence of CCCP (Figure 3.5, compare lanes 3 and 15). The release of HA-Ub into the supernatant was also greatly reduced in the absence of CCCP (Figure 3.5, compare lanes 5 and 6 with lanes 17 and 18). The protection of HA-mono-Ub is therefore mostly CCCP-dependent, although the mechanism of protection remains unclear. The mitochondrial fraction appeared to contain autophagosomal membranes as evidenced by the presence of lipidated LC3B (Figure 3.3). Therefore, the PK protection and release of mono-HA-Ub into the supernatant during swelling could be due to release of mono-Ub from mitophagosomes rather than from within mitochondria. These observations are further discussed in Section 3.4.2.

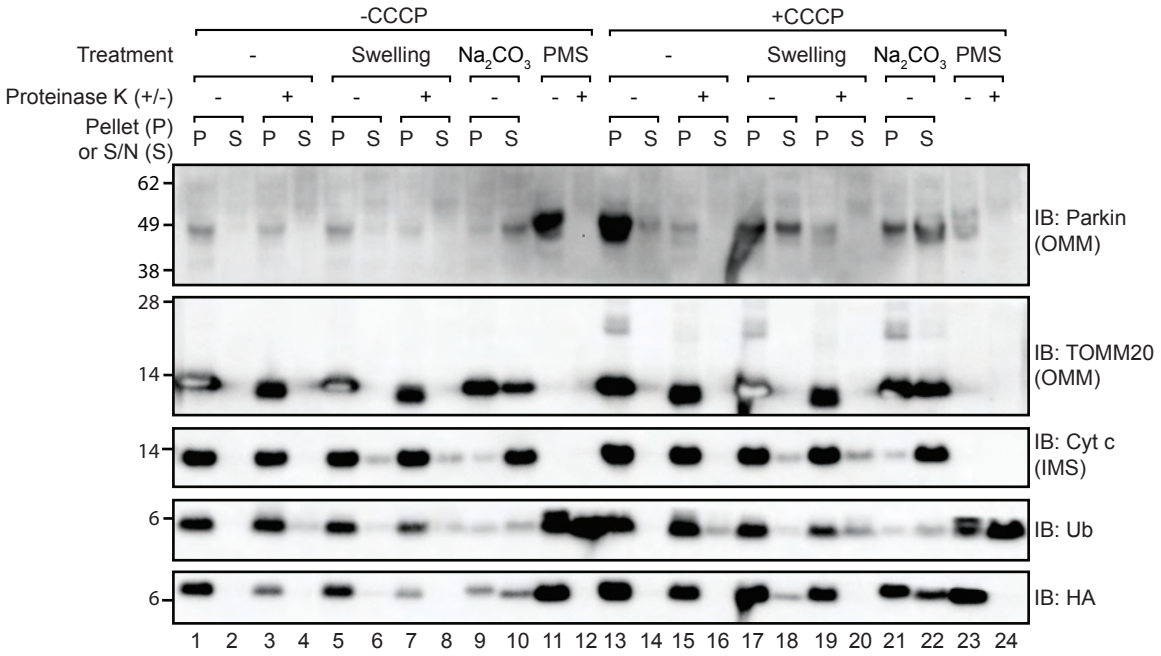

Fig. 3.5 **The sub-mitochondrial localisation of HA-Ub is CCCP-dependent.** HeLa Flp-In Trex cells expressing WT Parkin were transfected with HA-Ub, induced 16 h with doxycycline, then left untreated or depolarised 1 h with CCCP. Swelling, PK treatment and sodium carbonate extraction were performed on mitochondrial fractions to assess the sub-mitochondrial localisation of HA-Ub. IB: immunoblot. IMS: intermembrane space. OMM: outer mitochondrial membrane. PMS: post-mitochondrial supernatant. S/N: supernatant.

3.2.3 Enrichment of conjugated mitochondrial Ub using sodium carbonate extraction

While assessing the sub-mitochondrial localisation of unconjugated mono-Ub, it was found that sodium carbonate extraction efficiently separated Ub chains from unconjugated mono-Ub (Figure 3.3, lanes 9 and 10). Therefore, sodium carbonate extraction was trialled as a method for further purification of mitochondrial polyubiquitin, downstream of differential centrifugation. Figure 3.6A shows the effect of sodium carbonate extraction on both the presence of unconjugated mono-Ub and the contaminating protease activity. Following mitochondrial enrichment by differential centrifugation, a large amount of unconjugated mono-Ub was present in the mitochondrial fraction (Figure 3.6A, lane 1). Brief (2.5 h) incubation at 37 °C resulted in the release of a substantial amount of mono-Ub into the supernatant (Figure 3.6A, lanes 2 and 3). No reduction in the mono-Ub signal in the pellet was observed during the 37 °C treatment, indicating that the Ub present in the supernatant was due to collapse of poly-Ub chains by a protease rather than a release of the mitochondrially associated mono-Ub into the supernatant. This protease activity occurred in a similar timescale to incubation with Lb^{pro} (Figure 3.6A, lanes 4 and 5). In contrast, sodium carbonate extraction (Figure 3.6A, lane 6) severely depleted the unconjugated mono-Ub, while conjugated Ub appeared to increase in intensity, possibly due to an increase in antigenicity caused by the removal of soluble and peripheral membrane proteins from the sample. Incubation at 37 °C following sodium carbonate extraction did not cause release of mitochondrial Ub to the supernatant, indicating that the protease was either removed or inactivated by the sodium carbonate extraction (Figure 3.6A, lanes 7 and 8). Lb^{pro} treatment collapsed the conjugated Ub into mono-Ub (Figure 3.6A, lanes 9 and 10), indicating that sodium carbonate extraction is compatible with downstream applications using Lb^{pro} and other DUBs.

Sodium carbonate extraction efficiently separated unconjugated mono-Ub from conjugated mitochondrial (phospho-)Ub in samples expressing both WT Parkin and the catalytic inactive C431S mutant (Figure 3.6B). Therefore, sodium carbonate extraction can be employed for the enrichment of conjugated ubiquitin from mitochondria. Enrichment of ubiquitinated proteins can also be achieved using Tandem Ub Binding Entities (TUBEs) [85]. Previous studies have used Ub-binding domains to enrich for ubiquitinated mitochondrial proteins [204, 202, 203]. The TUBE construct used in this thesis consisted of four human ubiquilin-1 UBA domains fused C-terminal to a GST tag, allowing affinity purification of Ub chains as described previously [85]. When comparing the Ub smear observed by western blotting

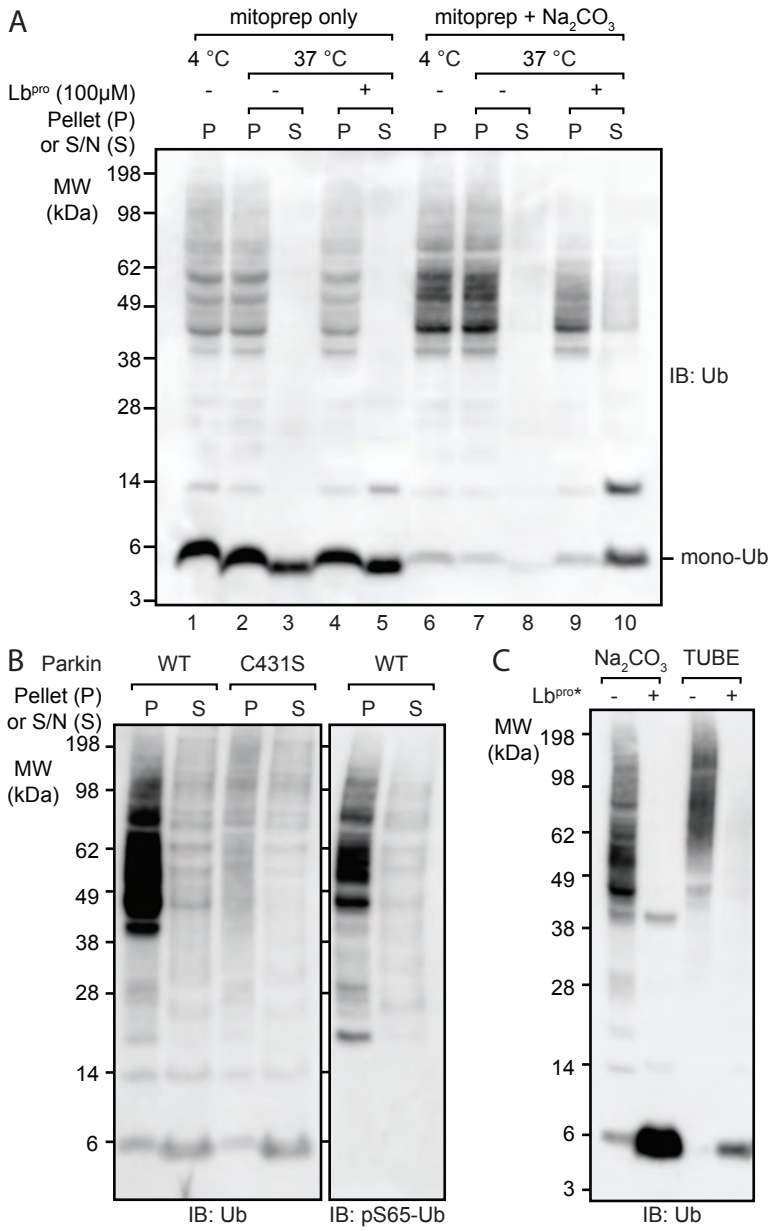

Fig. 3.6 **Sodium carbonate extraction enriches conjugated mitochondrial Ub. A.** Following depolarisation with OA and mitochondrial enrichment by differential centrifugation (mitoprep), mitochondria were either sodium carbonate-extracted and the pellet retained (lanes 6 to 10) or analysed without sodium carbonate treatment (lanes 1 to 5). Samples were incubated 2.5 hours, either at 4 °C or 37 °C, with or without Lb^{pro}. The pellet and supernatant fractions after centrifugation were retained for analysis. **B.** Mitochondria from 2 h OA-depolarised cells expressing either WT or C431S Parkin as indicated were sodium carbonate-extracted, and the pellet and supernatant fractions retained for analysis. **C.** Mitochondria from 2 h OA-treated cells expressing WT Parkin were treated by either sodium carbonate extraction or TUBE pulldown. Enriched Ub chains were then treated overnight at 37 °C with 20 μM Lb^{pro}*. IB: immunoblot. S/N: supernatant.

of Ub upon enrichment by sodium carbonate extraction or TUBE pulldown, the majority of the observed Ub signal for sodium carbonate enrichment was in a mass range between approximately 40 and 150 kDa (Figure 3.6C, left lane), which was comparable to the 40 to 100 kDa region observed upon crude mitochondrial enrichment (Figure 3.6A, left lane). In contrast, TUBE pulldown enriched Ub conjugates predominantly between 60 to >200 kDa (Figure 3.6C, third lane). Therefore, TUBE pulldown appears to bias towards longer Ub chains or larger Ub-substrate conjugates than sodium carbonate extraction. Further, TUBE pulldown resulted in a much lower yield of Ub, as evidenced by the abundance of mono-Ub after treatment with Lb^{pro}* (Figure 3.6C, compare the mono-Ub abundance in the second and fourth lanes). Given the TUBE's bias towards longer chains, these results indicate that the majority of ubiquitination events on mitochondria are mono-ubiquitination of integral membrane substrates. Given that sodium carbonate extraction better preserved the abundance and distribution of mitochondrial Ub conjugates than TUBE pulldown, this method was used wherever possible for the analysis of the mitochondrial ubiquitome. The following section details several experiments performed using a combination of mitochondrial enrichment, sodium carbonate extraction, and treatment with reagents that enable an elucidation of the Ub chain types and complex architectures present on mitochondria.

3.3 Biochemical evaluation of the Parkin-dependent ubiquitome in cultured cells

3.3.1 Linkage-specific antibodies and affimers reveal a broad increase in Ub chain types

In order to probe the Ub linkage composition of purified mitochondria, western blots using linkage-specific antibodies and affimers were employed [190, 173]. Commercial linkage-specific antibodies for K48-Ub and K63-Ub and a commercial pS65-Ub antibody could all detect WT Parkin-dependent signal accumulation in sodium carbonate-extracted mitochondria, although the relative increase in pS65-Ub was greater than that of K48 or K63 chains (Figure 3.7A). An antibody specific for M1-linked chains was also tested but no signal could be detected (data not shown), consistent with the reported absence of M1-linked chains on mitochondria [204, 202]. The specificity of the pS65-Ub antibody for phosphorylated Ub was also validated by treating mitochondrial extracts with Lambda phosphatase (λPP). λPP treatment completely abolished pS65-Ub signal, confirming the antibody's specificity (Figure

3.7D).

Linkage-specific affimer reagents were also employed. One affimer is specific for K6 chains, while the other detects both K11- and K33-linked chains with a slightly higher affinity for K33-linked Ub [88]. In brief, the affimers, based on a cystatin fold, were created by screening a large library of sequence combinations against K6- and K33-linked di-Ub. Chain type specificity is conferred by the affimers' orientation with respect to one another in the dimeric form, and the affimers are expressed as tandem repeats to aid dimerisation. Given that K11- and K33-linked Ub dimers have similar conformations, the affimer reagent is able to recognise both. In contrast, the K6 affimer is highly specific for K6 chains due to K6-linked Ub's distinct compact topology [89]. The western blotting method employed for affimer detection required the use of an anti-Biotin antibody to detect the biotinylated affimer reagent. Sodium carbonate-extracted mitochondria showed a molecular weight distribution of K6 affimer signal that was comparable to the anti-total Ub signal (Figure 3.7D). Several discrete bands, that were removed by sodium carbonate extraction, were detected at similar abundances in WT and C431S Parkin samples. These bands are likely to be biotinylated carboxylase enzymes such as pyruvate carboxylase (129 kDa) and acetyl CoA carboxylase (265 kDa) [193, 5]. Both affimer reagents showed a large WT Parkin-dependent increase in western blotting signal in the presence of OA (Figure 3.7B). Under high exposures, K6 chains but not K11 or K33 chains could be detected by this method in mitochondria from C431S Parkin-expressing cells (Figure 3.7C). This is consistent with previous reports that other E3 enzymes, such as HUWE1, produce K6 linkages on mitochondrial substrates [173].

The use of linkage-specifc reagents in western blotting has several limitations. Firstly, differing levels of sensitivity between reagents precludes quantitative comparisons of different chain types. Secondly, analyses are limited to the chain types for which reagents are available, thus preventing analysis of K27 or K29 chains, or delineating the relative presence and role of K11 and K33 chains. Analyses of mitochondrial substrates using linkage-specific antibodies are therefore restricted to qualitative assessments of chain distribution and relative quantification of a particular chain type between treatments, which are nonetheless useful to a degree in determining the architecture of the mitochondrial ubiquitome.

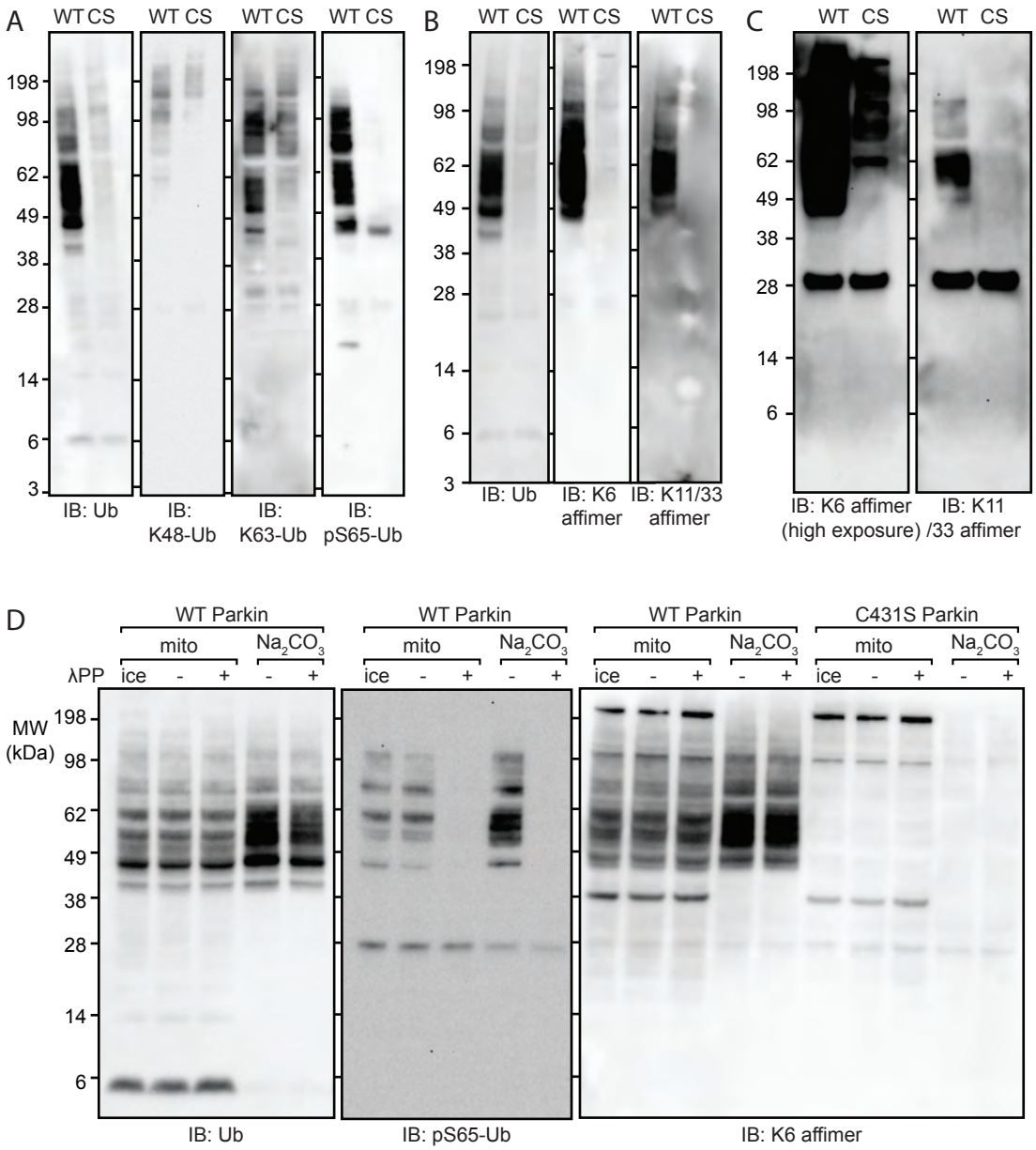

Fig. 3.7 **Linkage-specific antibodies reveal a broad range of Ub modifications on depolarised mitochondria. A.** Ub linkage-specific western blots of sodium carbonate-extracted mitochondria from 2 h OA-treated cells expressing WT or catalytic inactive C431S (CS) Parkin. **B.** Cells treated as in A, analysed by western blotting with linkage-specific affimer reagents. **C.** Sodium carbonate-extracted mitochondria from Parkin-expressing cells were depolarised 4 h with OA and subjected to western blotting with linkage-specific affimers. **D.** Mitochondrial fractions (mito) and sodium carbonate-extracted mitochondrial fractions (Na_2CO_3) were left untreated (ice), or incubated 45 minutes at 37 °C in the presence or absence of Lambda phosphatase (λPP). The resulting samples were subjected to western blotting with the indicated antibodies and affimers. IB: immunoblot.

3.3.2 UbiCRest analysis shows an abundance of K63 chains

Ubiquitin Chain Restriction (UbiCRest) utilises a panel of chain type-specifc DUBs to elucidate the Ub chain types present on a substrate of interest [88]. Unlike western blotting using linkage-specific reagents, the UbiCRest assay allows a more direct comparison of the relative abundance of specific chain types within a sample. This assay employed the DUBs OTUB1 (K48-specific), OTULIN (highly M1-specific), AMSH (K63-specific), Cezanne (K11-specific at low concentrations, some K63- and to a lesser extent K48-specificity at higher concentrations), and the pan-specific USP21 and vOTU enzymes [88] (Figure 3.8A). Collapse of a Ub chain with a particular DUB indicates that its preferred chain type is present in the sample. Figure 3.8B shows sodium carbonate-extracted mitochondria from depolarised Parkin-expressing cells after treatment with the aforementioned panel of DUBs. OTULIN treatment resulted in no difference in the chain distribution on mitochondria compared to the untreated control, consistent with the absence of M1-linked Ub on mitochondria [204, 202]. OTUB1 and low concentrations of Cezanne had little effect on the mitochondrial Ub smear, indicating that K48 and K11 chains do not constitute a large proportion of the mitochondrial Ub. In comparison, AMSH and high Cezanne concentrations did result in a large reduction in the Ub smear, indicating that K63 chains do constitute a large proportion of the mitochondrial Ub. Interestingly, several treatments resulted in the formation of di-Ub moieties, indicating the presence of heterotypic (mixed) chains. A di-Ub doublet was particularly visible upon AMSH treatment. K6-linked Ub dimers migrate more slowly than other chain types on SDS-PAGE [89], so the higher di-Ub band may correspond to K6-linked di-Ub. The release of this dimer into the supernatant upon AMSH treatment indicates that some K6 chains may exist distal to K63 chains on mitochondria.

The UbiCRest assay was expanded to include a comparative analysis of depolarised mitochondria from WT and C431S Parkin-expressing cells. Compared with mitochondria from WT Parkin-expressing cells, the C431S Parkin condition contained less total Ub and very little pS65-Ub (Figure 3.9, compare lanes 1 and 3). Mitochondria from the C431S Parkin condition displayed similar relative sensitivities to all of the DUBs tested, indicating that Parkin has no specific preference for any of the tested chain types (K11, K48 and K63), but produces a global increase in all analysed chain types. The pS65-Ub signal from WT Parkin was most sensitive to Cezanne treatment, which may indicate that K11 chains are preferentially phosphorylated. The pS65-Ub and total Ub abundances correlated well between OTUB1 and AMSH treatment, indicating no strong preference for phosphorylation of one of K48 or K63 chains over the other.

A

DUB	Specificity
USP21	All chain types and substrate ubiquitination
vOTU	All chain types except M1 and some substrate ubiquitination
Cezanne	K11 > K63 > K48
OTUB1*	K48
AMSH*	K63
OTULIN	M1

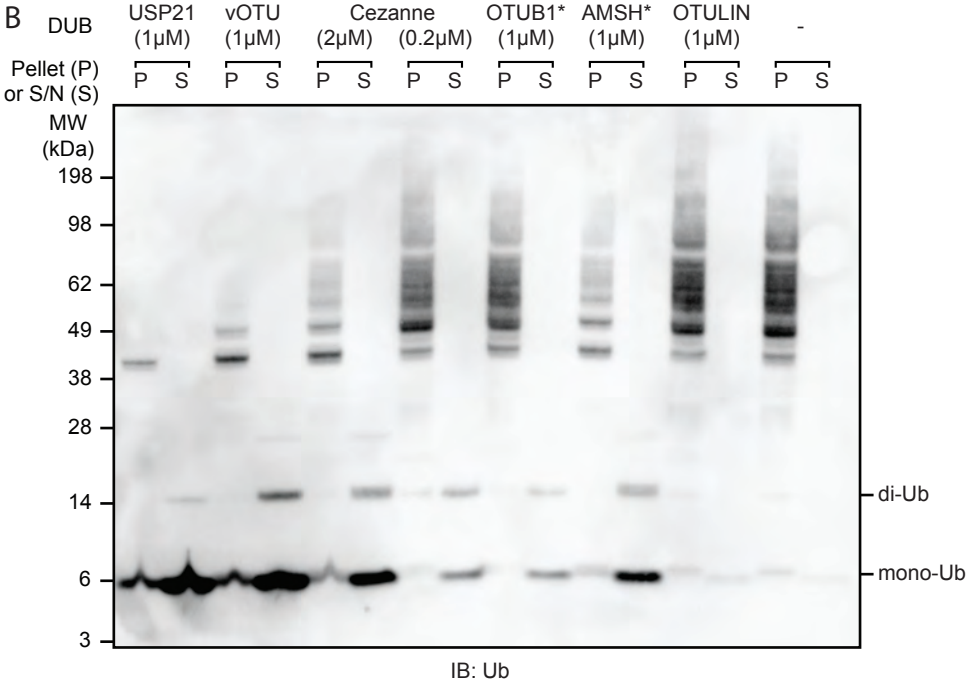

Fig. 3.8 **UbiCRest analysis of mitochondrial Ub reveals an abundance of K63 chains. A.** Ub chain specificity of the selected deubiquitinases (DUBs), as modified from [88]. Asterisks indicate that these enzymes are optimised for efficient activity. **B.** Sodium carbonate-extracted mitochondria from WT Parkin-expressing HeLa cells depolarised 2 h with OA were subjected to UbiCRest analysis. Following incubation with the indicated DUBs, samples were centrifuged and the pellet (P) and supernatant (S) fractions analysed by western blotting. IB: immunoblot.

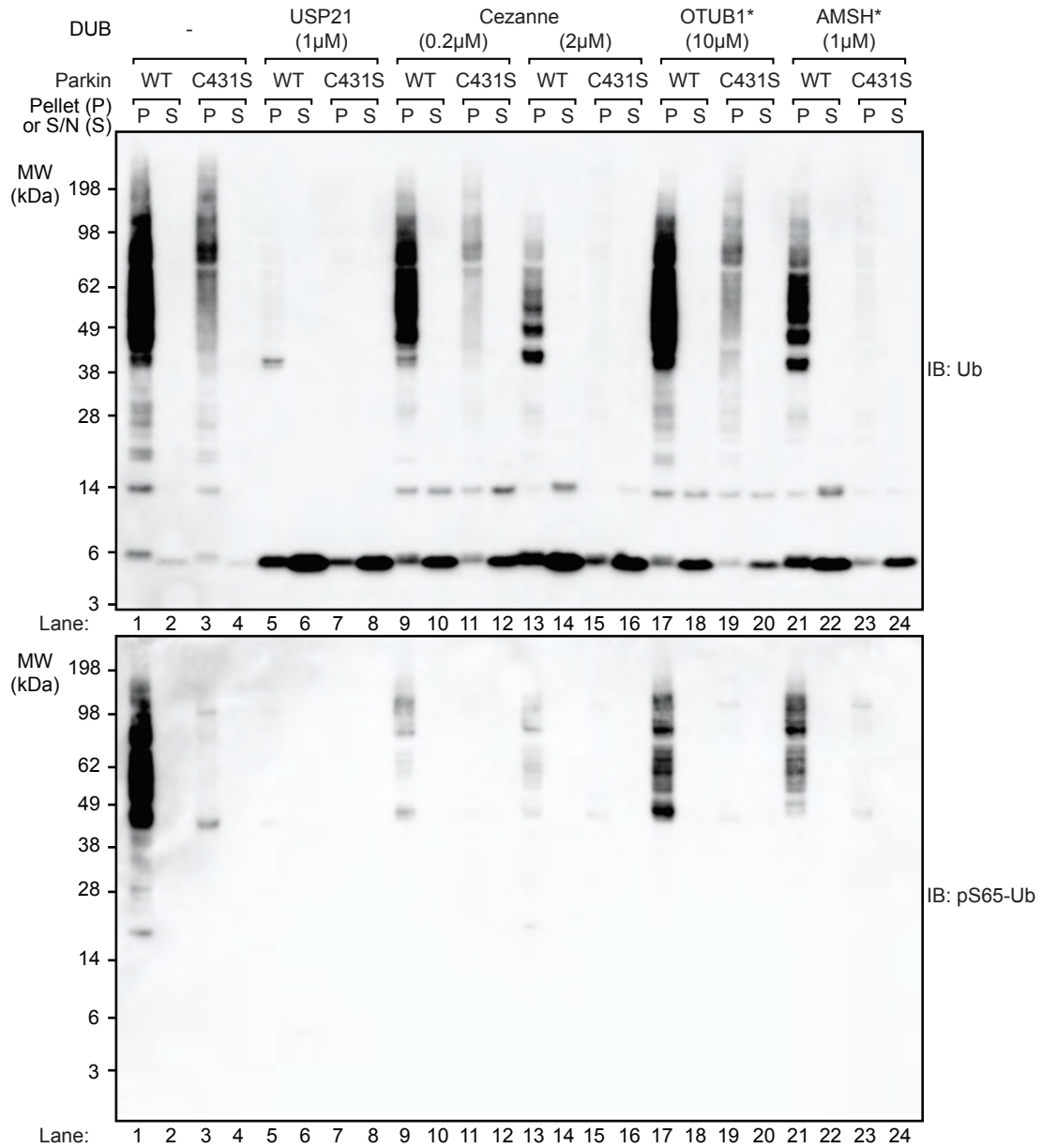

Fig. 3.9 **Comparison of WT- and C431S Parkin-dependent mitochondrial Ub using UbiCRest.** Sodium carbonate-extracted mitochondria from WT or C431S Parkin-expressing cells depolarised 2 h with OA were treated 45 minutes with the indicated deubiquitinases (DUBs). The resulting samples were centrifuged, and the pellet (P) and supernatant (S) fractions analysed by western blotting. IB: immunoblot.

3.3.3 Affimer protection assay shows modest K6-ubiquitination

In order to better understand the relative amounts of K6 and K11/33 chains in mitochondrial extracts, an affimer protection assay was developed. As explained in Figure 3.10A, the process begins with the incubation of mitochondrial fractions with the affimer reagent. The mitochondria were then treated with USP21 to liberate any mitochondrial Ub that was not protected by the affimer. Next, sodium carbonate extraction was performed to remove the affimer, then the sample was again treated with USP21 to liberate the newly exposed Ub chains. 5 ng affimer per microgram of mitochondrial protein was sufficient to provide maximal K6 affimer protection (Figure 3.10B). Both the K6 and K11/K33 affimers conferred some protection against USP21 treatment relative to the no affimer control (Figure 3.11, Step 2). The K6 affimer conferred more protection than the K11/K33 affimer to the mitochondrial smear, consistent with reports that K6 chains are more abundant than K11 or K33 chains on depolarised mitochondria in this system [204]. Interestingly, the K11/K33 affimer but not the K6 affimer resulted in the formation of a poly-Ub ladder that was liberated into the supernatant upon USP21 treatment (Figure 3.11, compare lanes 12 and 20). This suggests that K11 or K33 chains on mitochondria may be quite long. No discernible protection was conferred by either affimer against Mfn2 or TOMM20, indicating that the majority of Ub chain formation on these substrates is not K6-, K11- or K33-linked (Figure 3.10C). This result contrasts with, but does not contradict, previous reports of K6 chains specifically modifying Mfn2 and TOMM20 [173, 63], as discussed further below.

3.4 Discussion and conclusions

In this chapter, a new method for the purification of mitochondrial Ub is presented. Simple mitochondrial enrichment resulted in the retention of substantial amounts of unconjugated Ub (Figure 3.1E), which would hinder downstream analysis of the abundance and distribution of Ub chain types. Additionally, crude mitochondrial fractions harboured a contaminating protease activity that would also complicate downstream analysis (Figure 3.1E). Sodium carbonate extraction, a method typically used to determine whether a membrane protein associates peripherally with the membrane or is an integral membrane protein [53], successfully separated Ub conjugated to substrates from the unconjugated Ub. The method also either inactivated or removed the contaminating protease activity, rendering the resultant product competent for downstream biochemical analyses to probe the mitochondrial ubiquitome (Figure 3.6A). In contrast, TUBE pulldown of mitochondrial extracts produced low Ub

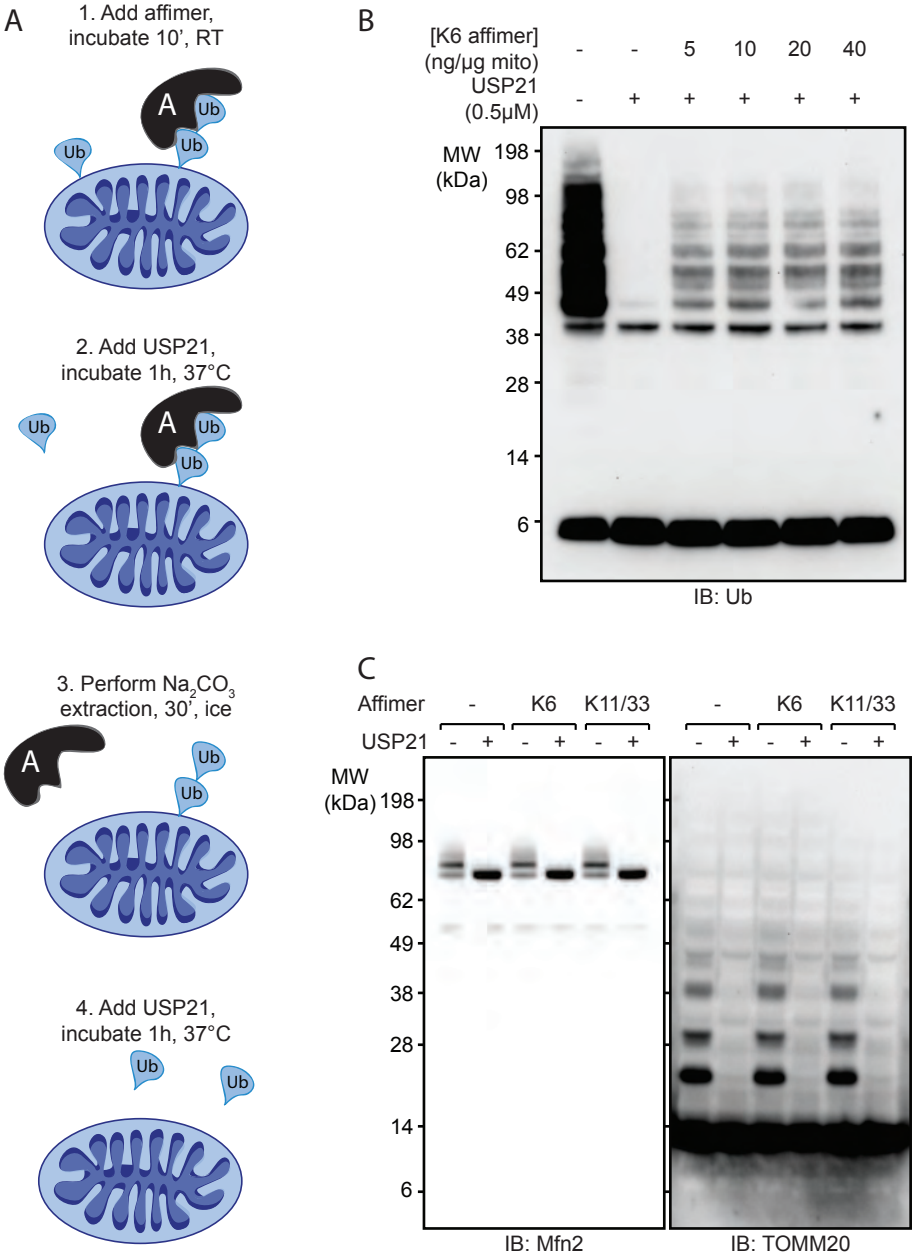

Fig. 3.10 **Mitochondrial affimer protection assay setup and validation. A.** Diagram explaining the four steps of the affimer protection assay: 1. Incubation of the affimer with the mitochondrial sample, 2. USP21 treatment to liberate unprotected Ub, 3. Sodium carbonate extraction to remove the affimer from its bound Ub, and 4. USP21 treatment to deplete the now-unprotected Ub. **B.** Titration of the K6 affimer. Increasing affimer amounts as indicated were incubated with mitochondria, and steps 1 and 2 from A were performed, followed by immunoblotting for Ub. **C.** The indicated affimer reagents were incubated with mitochondria (1 μg affimer with 120 μg mitochondria) then incubated with or without USP21 as per steps 1 and 2 in A, and immunoblotted for the mitochondrial substrates Mfn2 and TOMM20. IB: immunoblot. RT: room temperature.

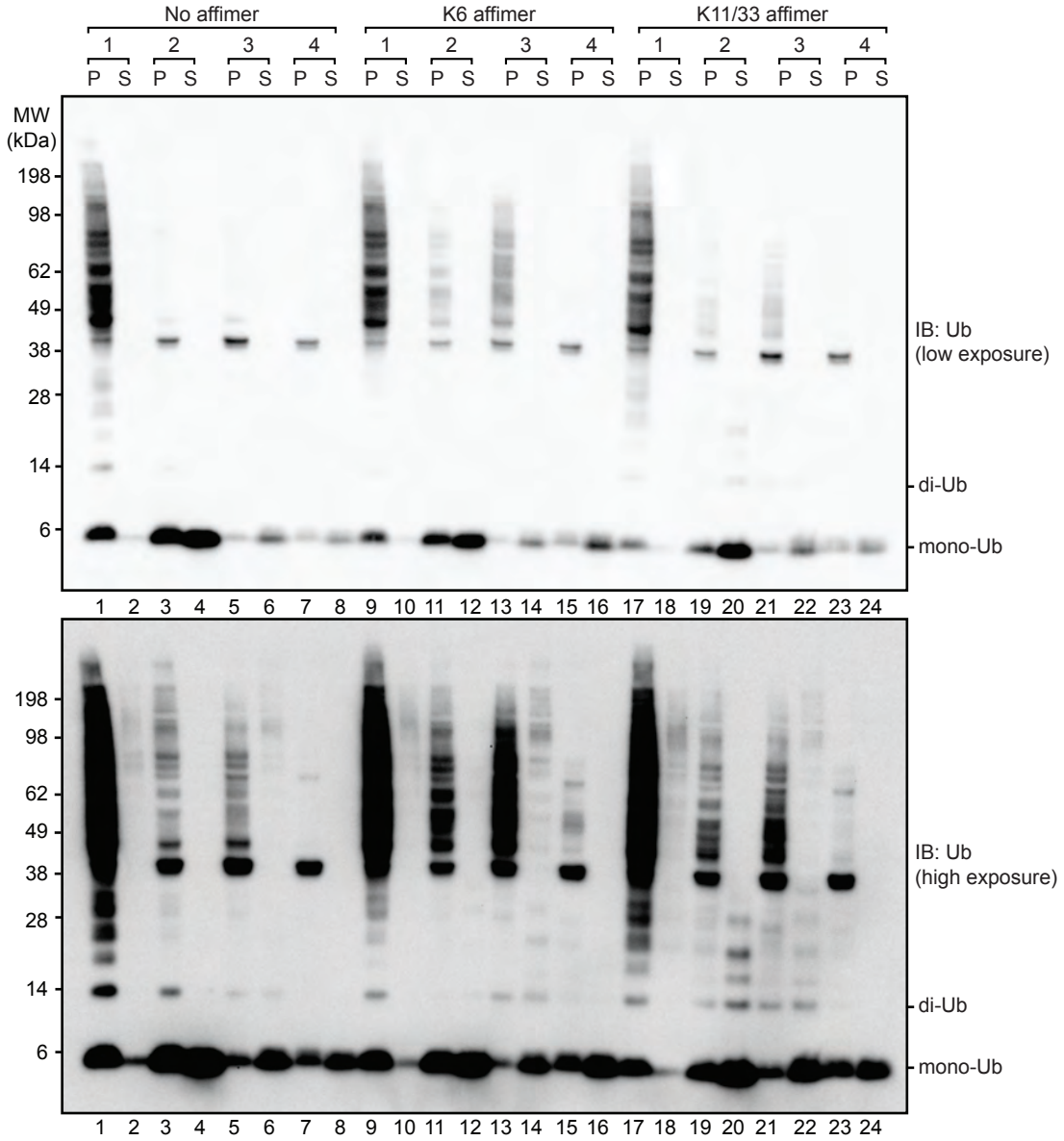

Fig. 3.11 **Mitochondrial affimer protection assay shows K6 chains on mitochondria.** Mitochondria from OA-depolarised WT Parkin-expressing cells were incubated with affimer proteins as indicated at a ratio of 40 ng affimer per μg mitochondria. The assay was performed in four steps as per Figure 3.10A. Following each step an aliquot was taken, centrifuged, and the pellet (P) and supernatant (S) separated and retained for western blot analysis. IB: immunoblot.

yield, with a bias towards longer chains (Figure 3.6C). Further, the low Ub yield observed using TUBE pulldown, which biases towards longer chains, indicated that the majority of mitochondrial ubiquitination is likely to be mono-ubiquitination (Figure 3.6C).

3.4.1 Sodium carbonate extraction reveals most Parkin substrates are integral membrane proteins

The swelling and PK assay, in addition to determining the sub-mitochondrial localisation of the unconjugated mitochondrial Ub, revealed that most conjugated mitochondrial Ub is present on integral membrane proteins (Figures 3.3, 3.6B). While auto-ubiquitination of the peripherally associated Parkin protein has been described, many of these studies involve *in vitro* assembly reactions [308, 112, 309, 64] or overexpression of Parkin, sometimes with a bulky fluorescent tag, in cell culture systems [160, 225, 129, 44], and are therefore likely to be artefactual. Conversely, the most abundant Parkin substrates in HeLa cells as determined by AQUA MS (VDACs 1-3, CISD1, TOMM70A, and TOMM20 [202]) are all embedded in the OMM [5]. Interestingly, none of the unconjugated mono-Ub appeared to be phosphorylated (Figure 3.3), indicating that PINK1 prefers to phosphorylate conjugated Ub. This observation does not appear to be due to a failure of the anti-pS65-Ub antibody to recognise mono-pS65-Ub, as PK-digested chains could be observed as mono-pS65-Ub within the same experiment. While there may be a small amount of phosphorylated, unconjugated Ub produced by PINK1 that is below the antibody's detection limit, the vast majority of pS65-Ub is conjugated to substrates. This observation was also made independently recently using alternative methods [202]. PINK1 has been shown to phosphorylate unconjugated mono-Ub, dimers and tetramers of all eight linkage types, and mono-ubiquitinated proteins, all with similar kinetics [113]. The phosphorylation of conjugated Ub by PINK1 is therefore most likely due to availability of substrate rather than an intrinsic preference for conjugated Ub. This observation therefore lends weight to the hypothesis that there must be conjugated Ub present on mitochondria prior to PINK1 activation that is produced by another E3 ligase [104, 204, 196, 130]. It also suggests that the unconjugated mitochondrial Ub observed herein is not located in close proximity to PINK1. In terms of signalling for mitophagy, phosphorylation of Ub that is conjugated to an integral membrane protein would ensure that the signal for Parkin recruitment is restricted to the damaged mitochondrion, thereby providing strong spatial regulation of Parkin activity.

3.4.2 Is there Ub inside mitochondria?

In Section 3.2.2, a mostly CCCP-dependent PK protection of HA-tagged Ub was observed, raising the possibility that Ub can exist inside the mitochondria, specifically in the intermembrane space. This is an unusual observation, given that protein import through the TOM complex has long been known to require the protein to be either unfolded or in a single alpha helical loop [76]. A recent cryo-EM structure of the *Saccharomyces cerevisiae* TOM complex showed that the TOM40 pore was only 19Å by 13Å wide at its narrowest point, which would not be large enough for folded Ub [290]. Ub's resistance to PK degradation shown in Figure 3.3 is evidence of its tightly folded nature, thus precluding it from being unfolded at the TOM complex and then imported. Import of Ub into mitochondria through the TOM complex would therefore need to be co-translational. CCCP treatment depolarises the IMM, therefore hampering the import of amphipathic presequence-containing mitochondrial proteins that travel via the TIM23 complex [154, 287]. In contrast, the effect of disrupted membrane potential on the import of IMS proteins is unclear, as IMS proteins are imported via a separate pathway involving a distinct subset of TOM complexes [134]. The main pathway for import of IMS proteins involves a disulfide relay system [68]. Ub lacks cysteine residues, making participation in this specific pathway impossible. A mechanism for Ub import into mitochondria is therefore not immediately apparent.

Another explanation for the increased PK protection of Ub upon CCCP treatment is that the Ub is contained within mitophagosomes that are present in crude mitochondrial fractions. Figure 3.3 shows that LC3B is present in the mitochondrial fraction, while the sodium carbonate extraction shows that it is lipidated and therefore marks autophagosomal membranes. Previous studies in similar albeit not identical HeLa cell culture systems have shown autophagosome formation within one hour of depolarisation [192, 206]. It is therefore possible that the swelling reaction, when performed on mitophagosomes, disrupts both the OMM and the autophagosomal membrane, thus releasing both IMS proteins and soluble proteins outside the mitochondria into the supernatant. A soluble protein outside the mitochondria but contained within the mitophagosome would therefore behave identically to an IMS protein in the swelling and PK assay. Further work to dissect this could involve enrichment or separation of mitochondria from mitophagosomes, or *in vitro* import assays to assess whether Ub can be imported into mitochondria, exists inside mitophagosomes, or is bound noncovalently to proteins on the OMM. Ubiquitination of IMS-exposed proteins has been observed during Parkin-dependent mitophagy [242, 237, 203], possibly occuring due to proteasome-dependent OMM rupture resulting in the exposure of IMS and IMM proteins

to the cytosol [328]. This explanation for IMS protein ubiquitination is more parsimonious than one involving Ub import into mitochondria, as Ub import would further require the import of the E1/E2/E3 machinery to allow Ub conjugation to substrates. However, the exact mechanism for IMS protein ubiquitination has not yet been established, and therefore import of the ubiquitination machinery into mitochondria remains a possibility.

3.4.3 The likely Parkin-dependent mitochondrial ubiquitome

The conclusions regarding the makeup of the mitochondrial ubiquitome upon induction of mitochondrial depolarisation in the presence of Parkin are summarised in Table 3.1. The comparison of sodium carbonate extraction with TUBE pulldown, which biases towards longer chains, indicated that a large amount of the mitochondrial Ub is mono-ubiquitination of mitochondrial substrates. Across the different assays, a relative Ub chain type abundance was determined: K63 > K48 > K6 > K11 > M1. This corresponds well with previous MS studies [204, 202]. While K33 chains are recognised by the K11/K33 affimer, the relative contribution of K33 chains is not easily established by this method alone, and no corroborating evidence is available in the UbiCRest data. K27 and K29 chains were not studied due to a lack of suitable tools, but previous studies have shown that these linkages, alongside M1, are not particularly abundant in this system [204, 202]. Most importantly, the evidence presented herein begins to give an indication of the broader architecture of mitochondrial Ub. A model for some of the more complex architectures (excluding substrate monoubiquitination) of the Parkin-dependent mitochondrial ubiquitome, based on the conclusions presented in Table 3.1, is shown in Figure 3.12. This model takes into account the relative abundances of the different chain types, their relative length, the presence of heterotypic chains, and phosphorylation of specific chain types. However, several unknowns remain: the precise amounts of each chain type; the location of the pS65-Ub within the chain; and the average chain length could not be established using these methods. Indeed, the examples of complex architectures presented in Figure 3.12 are likely to represent only a small fraction of the Parkin-dependent mitochondrial ubiquitome.

In contrast with the reported literature [173, 63], the affimer protection assay indicated that the detectable majority of Mfn2 and TOMM20 ubiquitination by Parkin is not K6 chains (Figure 3.10C). The difference in results can be easily explained by a difference in methods used. Michel et al. used a K6 affimer pulldown followed by western blotting against Mfn2 to show that Mfn2 is modified with K6 Ub chains, which decrease in abundance upon

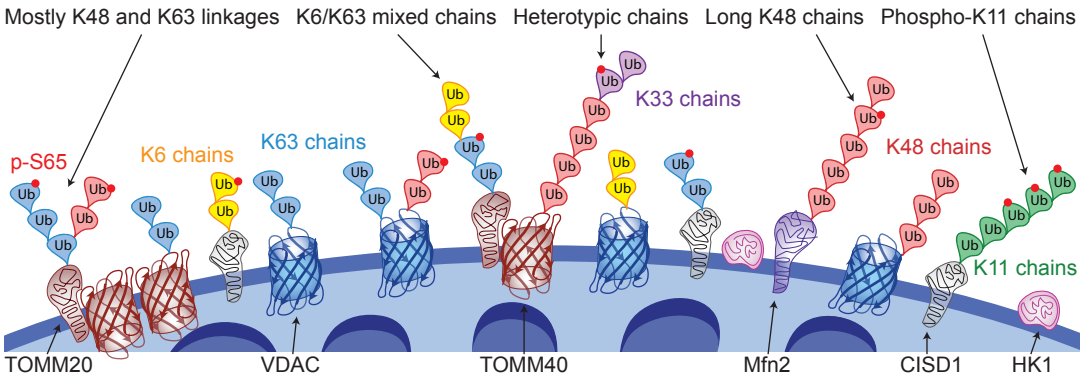

Fig. 3.12 **Model for the mitochondrial ubiquitome based on biochemical evidence.** Using the conclusions presented in Table 3.1 and derived from the literature [202], a reconstruction of some Ub chain architectures on OMM proteins is presented. This model excludes the contribution of mono-ubiquitination, which is highly abundant, and the specific placement of pS65-Ub within the chain, which was not investigated in depth in this chapter.

knockdown of the K6-generating E3 ligase HUWE1 [173]. Similarly, Gersch et al. used the same affimer pulldown to describe significant K6-ubiquitination of TOMM20, Mfn2, VDAC1 and Miro1, with K6-ubiquitination of TOMM20 alone increasing upon knockdown of USP30 [63]. In contrast, Figure 3.10C shows the total mitochondrial pool of Mfn2 and TOMM20, of which K6-modified Mfn2 constitutes only a small fraction. Therefore, while K6-modified forms of Mfn2 and TOMM20 do exist, they are very lowly abundant, and therefore the functional relevance of K6 chains on these mitochondrial substrates remains unclear.

3.4.4 Conclusions and future directions

In this chapter, a new method for the enrichment of ubiquitinated mitochondrial proteins using sodium carbonate extraction is described. Combined with other biochemical assays, they give an indication of the broader architecture of the Parkin-dependent mitochondrial ubiquitome, as summarised in Table 3.1 and illustrated in Figure 3.12. However, the methods described herein are limited by the availability of reagents to investigate specific Ub modifications, the sensitivity of western blotting, and the fact that they give mostly qualitative results. Therefore, an investigation using MS is needed to give a more quantitative understanding of the mitochondrial ubiquitome. Importantly, the sodium carbonate extraction method is compatible with downstream Lb^{pro} treatment and MS analysis, thus allowing more in-depth and quantitative analysis. The application of these methods to the MS context to further probe the Parkin-dependent mitochondrial ubiquitome is presented in Chapter 4.

Table 3.1 **Summary of the biochemical findings on the Parkin-dependent mitochondrial ubiquitome.**

Method	Findings
Sodium carbonate extraction	• Most Parkin substrates are integral membrane proteins • Most pS65-Ub is conjugated to substrates • A large amount of conjugated mitochondrial Ub is mono-Ub or short chains
Linkage-specific antibodies and affimers	• Large WT Parkin-dependent increase in total Ub, pS65-Ub, K6 and K11/33 chains • Modest WT Parkin-dependent increase in K48 and K63 chains • K48 chains tend to be longer or decorate larger substrates • pS65-Ub and total Ub have similar overall molecular weight distributions
UbiCRest	• M1 $<<$ K11, K48 $<$ K63 linkages • Heterotypic Ub chains are present on mitochondria • K6/K63 mixed chains with K6 distal to K63 • Parkin-dependent increase in all chain types tested • K11 chains may be preferentially phosphorylated • Neither K48 or K63 chains are preferentially phosphorylated
Affimer protection assay	• K11/K33 $<$ K6 linkages • Some long K11/K33-linked chains present • The majority of Ub on Mfn2 and TOMM20 is not K6-, K11- or K33-linked

Chapter 4

Mass spectrometry investigations of the mitochondrial ubiquitome

4.1 Introduction

Following the qualitative analysis of the mitochondrial Ub chain architecture presented in Chapter 3, this chapter details the development of methods to analyse Lb^{pro}*-generated mitochondrial Ub proteoforms by MS [275]. Compared with western blotting-based methods, MS provides a more quantitative platform with higher sensitivity, which enables a more accurate estimate of the abundance of Ub modifications. Substrate ubiquitination can be evaluated by diGly analysis; tryptic digest results in the retention of a characteristic diGly remnant from the Ub C-terminus on the lysine of a previously ubiquitinated substrate [212]. Hence, analysis of diGly modifications on Ub gives an indication of the chain types present in a given sample. Previous studies of the mitochondrial ubiquitome have indicated that there is an abundance primarily of K6, K11, K48 and K63 Ub chains and S65-Ub phosphorylation produced by Parkin [204, 36]. However, the interplay between these modifications has thus far been unexplored without significant manipulation of the cellular Ub pool [201], and very little investigation into the mitochondrial Ub architecture has been performed. For example, it is unknown whether branched chains, in which one Ub is further ubiquitinated on two lysines, exist on mitochondria. While PINK1 preferentially phosphorylates the distal moiety of a K6 di-Ub *in vitro* [63], it is unclear whether this preference is maintained in the complex cellular milieu. Additionally, very little work has been done to establish the composition of the mitochondrial ubiquitome under more physiological conditions, outside of depolarised cultured cells. *Drosophila* are an excellent animal model of neurodegeneration, especially given that mutations in fly *Pink1* and *park*, homologs of human PINK1 and Parkin, both reca-

pitulate many aspects of PD [71, 210, 30]. Understanding the effect of genetic manipulations in flies on the makeup of the mitochondrial ubiquitome could aid our understanding of the role of PINK1- and Parkin-dependent mitochondrial ubiquitination in the etiology of PD, in a more physiologically relevant context than previous studies.

This chapter details the development of MS methods in conjunction with Ub-clipping to analyse the mitochondrial ubiquitome. Ub-clipping uses an enzyme, Lb^{pro}, or its improved form, Lb^{pro}*, to collapse Ub chains into mono-Ub moieties [275]. However, unlike conventional DUBs, the site of Lb^{pro}* cleavage is two residues upstream of the Ub C-terminus at R74, and therefore a diGly remnant is retained on previously ubiquitinated substrate K residues (Figure 1.2A). Therefore, Ub-clipping generates an intact mono-$Ub^{1\text{-}74}$ that is decorated with diGly modifications that are indicative of prior chain formation (Figure 1.2B). However, while significant work had been done previously in the Komander lab to engineer Lb^{pro}* and establish a basic pipeline for whole-cell digests and MS analysis, little targeted work had been done with a specific biological question in mind. Given that PINK1 and Parkin generate pS65-Ub and Ub chains respectively, the use of Ub-clipping should reveal interactions between these two activities in a way previously inaccessible by other MS-based techniques; an in-depth analysis of the interplay between Ub chain formation and phosphorylation in the context of a single Ub moiety. Further, the simplified sample preparation afforded by Ub-clipping could be applied to more physiological contexts in which the abundance of mitochondrial Ub is lower than in previously characterised cell-based studies, without the need for expensive diGly enrichment strategies.

Two applications, termed intact MS and AQUA MS, were used and specific protocols established for each. Intact MS, which detects mono-Ub decorated with any combination of phosphorylation and diGly modifications on the same Ub moiety, provides an indication of the chain architecture [275]. Several permutations in sample preparation were performed, as indicated throughout Section 4.2 and outlined in Figure 4.1. Optimisation of this process required the identification and removal of chemical artefacts introduced during sample preparation, as outlined in Sections 4.2.1 and 4.2.2. In contrast, AQUA MS involves tryptic digest of the Ub molecule into peptides. Heavy isotope-labelled reference peptides are spiked into the mixture, allowing quantification of the absolute abundance of a particular peptide in a sample based on its signal intensity relative to the intensity of the heavy reference peptide [121]. While the architectural information is lost upon tryptic digest, combining Ub-clipping with AQUA MS can greatly simplify sample preparation [275]. For example, a complex

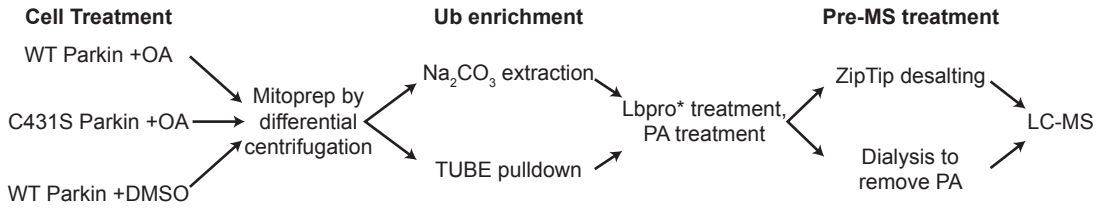

Fig. 4.1 **Experimental setup for analysing the Parkin-dependent ubiquitome by intact MS.** Flp-In HeLa Trex cells expressing WT or C431S Parkin were treated 2 h with OA or DMSO, then harvested, and mitochondria were enriched by differential centrifugation. Ub enrichment was then performed either by sodium carbonate extraction of integral membrane proteins or TUBE pulldown of Ub chains. The samples were treated with Lb^{pro}* to generate diGly-modified Ub proteoforms, then treated with perchloric acid (PA) to precipitate non-Ub contaminants. The sample was then either desalted using ZipTips, or dialysed to remove the PA prior to LC-MS.

mixture of ubiquitinated proteins can be treated with Lb^{pro}, separated by SDS-PAGE, and the band corresponding to mono-Ub can be excised and treated by in-gel tryptic digest, allowing quantification of Ub chain types without diGly or Ub chain enrichment [275]. In this thesis, an alternative purification pipeline is presented using StageTips, which obviates the need for SDS-PAGE separation for the enrichment of mono-Ub. In this chapter, the AQUA MS method was developed and optimised using a previously described HeLa cell model [204], then applied to the study of the mitochondrial ubiquitome of *Drosophila* and brain homogenates from mice to better understand the *in vivo* mitochondrial ubiquitome.

4.2 Intact MS analysis of mitochondrial Ub proteoforms

4.2.1 Identification and removal of perchloric acid artefacts

Given the known interplay between ubiquitination and phosphorylation in the PINK1/Parkin pathway, Ub-clipping was combined with intact MS to investigate the architecture of mitochondrial ubiquitination upon activation of the pathway by chemical depolarisation. Lb^{pro}*-generated Ub proteoforms were derived from sodium carbonate-extracted mitochondria from HeLa Flp-In Trex cells expressing WT Parkin, depolarised 2 h with OA (Figure 4.1). To obtain sufficient signal, 2 mg mitochondrial protein was used per replicate, corresponding to ten 15 cm dishes of initial cell material. In order to purify the $Ub^{1\text{-}74}$ from the Lb^{pro}* and mitochondrial contaminants present, the sample was treated with perchloric acid (PA; Figure 4.1). PA is typically used during the purification of recombinant Ub, as Ub remains soluble at high PA concentrations while most other proteins precipitate [215]. Surprisingly,

the initial batches of samples contained many peaks corresponding to Ub proteoforms additional to those expected for phosphorylated and diGly-modified Ub^{1-74} (Figure 4.2A). The unidentified peaks occurred in multiples of 74 Da, and the modification occurred on diGly-modified and phosphorylated Ub^{1-74} in addition to unmodified Ub^{1-74}, indicating that a 74 Da artefact was indiscriminately modifying Ub molecules. The precise chemical nature of the artefact was not determined, so the modification was termed PA artefact (PAA). Unfortunately, both Ub^{1-74} with two diGly modifications (branched Ub), and phosphorylated Ub^{1-74} modified with two PAAs, carried the same mass and charge state distribution (m/z = 724.05, z = 12; m = 8678.62 Da). It was therefore important to ensure that the two species could be distinguished by a means unrelated to their mass, in order to ensure that methods used to remove the artefact did so without removing the bona fide branched Ub species. Given that the two species represent different chemical modifications, they could be expected to exhibit different chromatographic properties during LC-MS. The retention time distribution of PAA-modified Ub proteoforms was therefore analysed (Figure 4.2B). Each PAA modification resulted in a striking leftward shift in the chromatography pattern relative to unmodified Ub^{1-74}, while phosphorylation resulted in a modest rightward shift (Figure 4.2B). DiGly modification resulted in a very slight rightward shift (Figure 4.2D, compare the grey and red peaks in the top panel). Therefore, the identity of the 8678.62 Da peak could be determined by its behaviour during liquid chromatography relative to unmodified Ub^{1-74}. In order to prevent the formation of PAAs on Ub^{1-74} moieties, the PA was dialysed away from Lb^{pro}*-treated mitochondrial Ub prior to lyophilisation (Figure 4.1). Dialysis prior to lyophilisation abolished the formation of the PAAs on all Ub species (Figure 4.2C). The relative amount of branched Ub was reduced compared with previous experiments, but its retention time distribution relative to unmodified Ub^{1-74} was consistent with the species indeed being a doubly diGly-modified Ub (Figure 4.2D, compare the grey and green peaks in each treatment). Therefore, the removal of PA using dialysis was sufficient to remove the PAAs, enabling the robust identification and quantification of branched Ub moieties.

4.2.2 Identification and prevention of Ub R-clipping

After removing the PAAs it became apparent that another unwanted modification of the Ub proteoforms was occurring, resulting in a very high apparent relative abundance of pUb that was on occasion as high as 80% of the total Ub (data not shown). The mass spectra were therefore searched for other artefacts, and a highly abundant peak of a mass 156 Da less than Ub^{1-74} was found, with a strong rightward shift in retention time relative to Ub^{1-74} (Figure

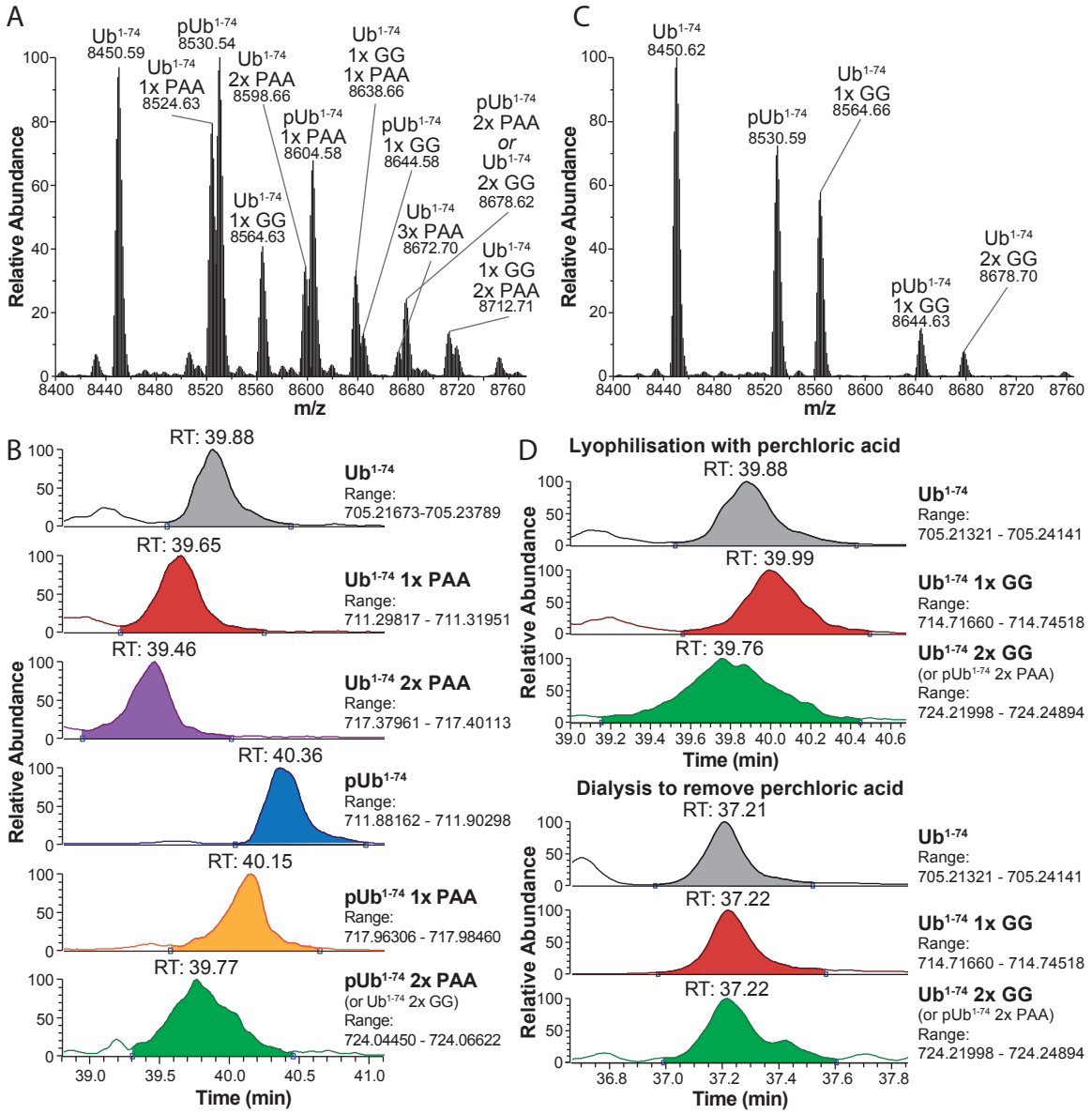

Fig. 4.2 **Lyophilisation in perchloric acid modifies Ub with a 74 Da artefact. A.** Deconvoluted mass spectrum of Ub proteoforms from OA-treated Flp-In Trex cells expressing WT Parkin, after purification without dialysis to remove perchloric acid (PA) as per Section 2.3.2. **B.** Extracted ion chromatogram of samples treated as in A, showing $Ub^{1\text{-}74}$ and $pUb^{1\text{-}74}$, with up to two 74 Da PA artefact (PAA) modifications per Ub. Note that $pUb^{1\text{-}74}$ 2x PAA and $Ub^{1\text{-}74}$ 2x GG have overlapping m/z ratios. **C.** Deconvoluted mass spectrum of Ub treated as in A, but with a dialysis step to remove the PA prior to lyophilisation. **D.** Extracted ion chromatogram of Ub proteoforms from samples treated as in A (top) and C (bottom). Note the difference in relative retention times (RT) of the $Ub^{1\text{-}74}$ (grey) and $Ub^{1\text{-}74}$ 2x GG peak (green) between the two samples.

4.3A, and 4.4E, purple peak). The change in mass was equivalent to the loss of an R residue, so it was hypothesised that this peak may correspond to Ub lacking its C-terminal RGG residues (Ub^{1-73}) in an event hereafter referred to as R-clipping. Interestingly, R-clipping only occurred on non-phosphorylated Ub, thus explaining the implausibly high pUb abundances initially observed when quantifying only Ub^{1-74} (Figure 4.3A, note the absence of a pUb^{1-73} peak at 8375.6 Da). To determine whether the peak observed did indeed correspond to Ub^{1-73}, an MS/MS experiment was performed in which the suspected Ub^{1-73} peak was isolated and fragmented (Figure 4.3B). The experiment yielded good y-ion coverage, with ions mapping unambiguously to the C-terminus of Ub lacking the C-terminal RGG. The identity of the fragment ions, alongside the mass of the parent ion, confirmed that the species observed was indeed Ub^{1-73}. While the most abundant charge state of Ub^{1-74} is +12, the charge state distribution of Ub^{1-73} was significantly altered due to the loss of a positively charged R residue, such that its most abundant charge state was +11. This charge state disruption meant that quantification of Ub could not be performed by simple addition of the measured intensities of Ub^{1-74} and Ub^{1-73}, and therefore the artefact needed to be removed in order to reliably quantify the amount of Ub proteoforms in the sample.

The structure and known mechanism of Lb^{pro}-mediated ISG15 cleavage, which is almost identical to that of Lb^{pro}* for Ub, shows that Lb^{pro} has high specificity for cleaving the R-G peptide bond towards the C-terminus of Ub and ISG15 [274]. This suggested that it is unlikely that Lb^{pro}* was responsible for hydrolysing the peptide bond N-terminal to R74. Therefore, it was hypothesised that a mitochondrial peptidase activity may cleave the exposed R that is generated by Lb^{pro}*-mediated Ub cleavage. This hypothesis was tested by monitoring the conversion of Ub^{1-74} to Ub^{1-73} in mitochondrial extracts in the absence of Lb^{pro}*. To do this, Ub^{1-74} was generated *in vitro* by treating recombinant Ub with Lb^{pro}*. The Lb^{pro}* was removed by PA precipitation, then the Ub^{1-74} was dialysed and incubated with mitochondrial extracts. The samples were then centrifuged and the supernatants prepared for LC-MS. Incubation of Ub^{1-74}, but not Ub^{1-76}, with mitochondrial extracts resulted in the formation of Ub^{1-73}, in the absence of Lb^{pro}* (Figure 4.4, compare A and B with D). Note that Ub^{1-76} and pUb^{1-76} were detected upon incubation of mitochondria with Ub^{1-74} (Figure 4.4A and B); these species correspond to deconjugated mitochondrial Ub due to residual DUB activity in the mitochondrial extracts, as such species were not observed in the initial Ub^{1-74} sample (Figure 4.4C). These Ub^{1-76} and pUb^{1-76} species were also more abundant in crude mitochondrial extracts than sodium carbonate-extracted mitochondria, consistent with the removal of contaminating DUBs upon sodium carbonate extraction (Figure 3.6A).

The R-clipping phenomenon was observed in both crude and sodium carbonate-extracted mitochondrial extracts, but the $Ub^{1\text{-}73}$:$Ub^{1\text{-}74}$ ratio was much higher in crude mitochondria (Figure 4.4A and B). This suggests that the R-clipping activity is weaker in sodium carbonate-extracted mitochondria, indicating that the enzyme is likely to be soluble or peripherally associated with the mitochondrial membrane (Figure 3.2B). As anticipated, incubation of Lb^{pro}* and Ub in the absence of mitochondria resulted in the formation of $Ub^{1\text{-}74}$ but not $Ub^{1\text{-}73}$ (Figure 4.4C). The R-clipping enzyme is therefore likely to be a mitochondrial peptidase, although its precise identity is unclear. It was found that inclusion of 10 mM DTT during the incubation of sodium carbonate-extracted mitochondria with Lb^{pro}* was sufficient to abolish the observed R-clipping activity (Figure 4.4E and F). DTT was therefore included in the Lb^{pro} reaction buffer in all subsequent experiments, and intact MS data were regularly monitored by peak integration analysis to ensure that no $Ub^{1\text{-}73}$ was produced.

4.2.3 Analysis of mitochondrial Ub proteoforms in HeLa cells

With the removal of the PA and R-clipping artefacts, the amount of mitochondria required per replicate was reduced from 2 mg to 200 μg, therefore enabling a more practical analysis of the mitochondrial ubiquitome under multiple conditions. In order to investigate the architecture of the mitochondrial ubiquitome in a quantitative manner, several initial parameters were tested. As a label-free method with no reliable internal standards against which to normalise the data, quantification of intact Ub proteoforms could only be determined relative to the abundance of all Ub proteoforms in a sample, and between samples that were analysed under comparable conditions in adjacent MS experiments. Two different quantification methods were therefore performed and compared. Peak integration of the Ub proteoforms in the +12 charge state, followed by measurement of the area under the curve, yielded 23.7% phosphorylated Ub in samples from OA-treated cells expressing WT Parkin when purified by sodium carbonate extraction (Figure 4.5A). In comparison, deconvolution of the raw MS spectrum and subsequent quantification of the relative Ub and pUb abundances revealed 33.1% pUb (Figure 4.5B). While the difference in relative pUb abundance was quite large, the results were consistent across replicates within a single quantification method (Figure 4.5, note that the relative pUb amount is higher across both sodium carbonate extraction and TUBE-enriched samples in B compared with A). Therefore, combined with previous reports that pUb comprises approximately 20% of mitochondrial Ub in this system upon depolarisation in the presence of Parkin [204, 201], peak integration was used for the relative quantification of Ub proteoforms in subsequent experiments. Quantification by deconvolution

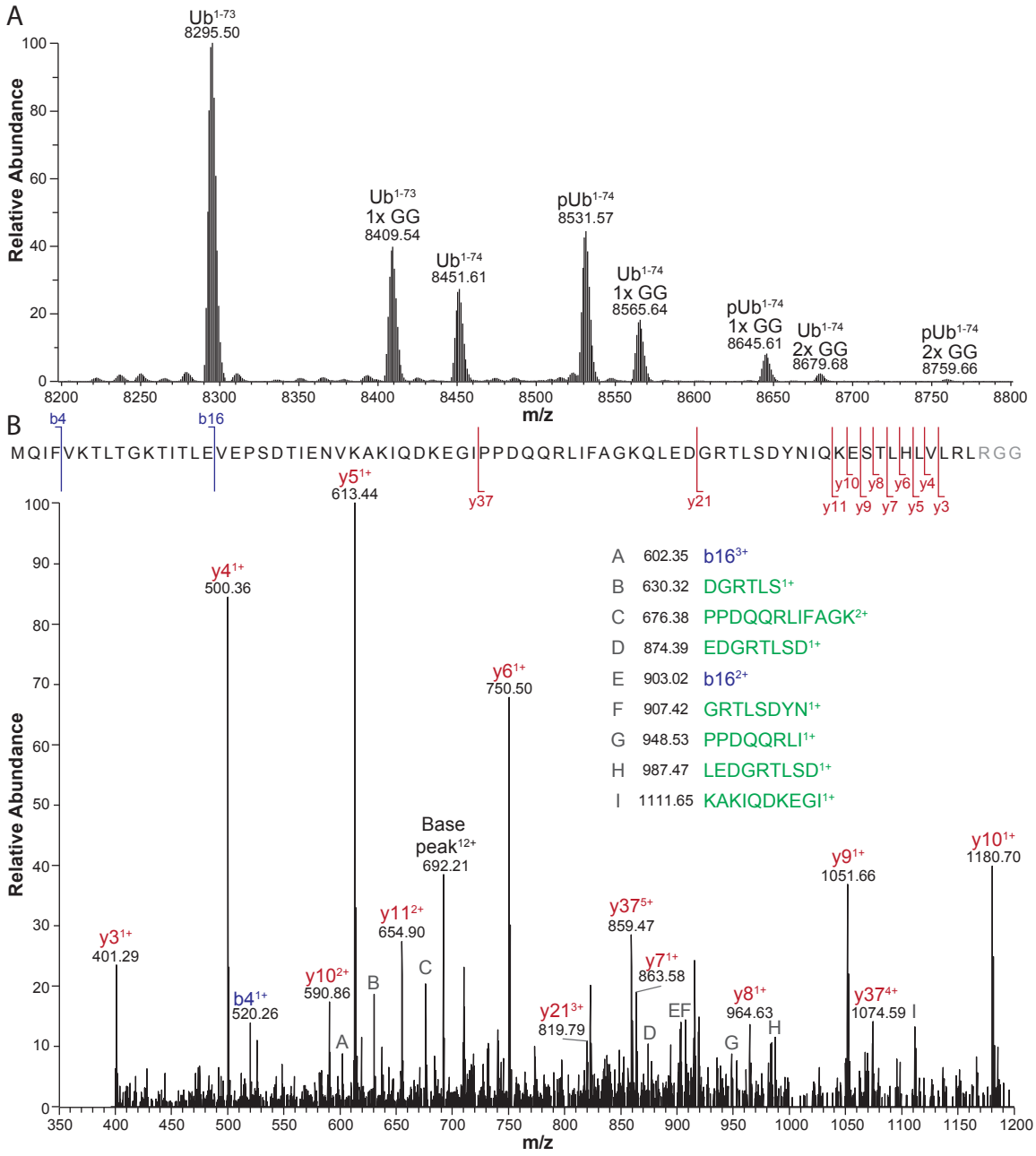

Fig. 4.3 **Incubation of Lb^{pro}* with mitochondrial Ub produces "R-clipped" Ub. A.** Deconvoluted mass spectrum of sodium carbonate-extracted mitochondrial Ub incubated with Lb^{pro}* in the absence of DTT shows the presence of "R-clipped" Ub (Ub$^{1-73}$). **B.** Annotated MS2 spectrum from an isolation window corresponding to Ub$^{1-73}$ (m/z = 692.1322, Higher-energy collisional dissociation, collision energy = 30 eV). Peaks were annotated using Expert System and manually validated for charge state congruity. Red = y-ions, blue = b-ions, green = internal ions.

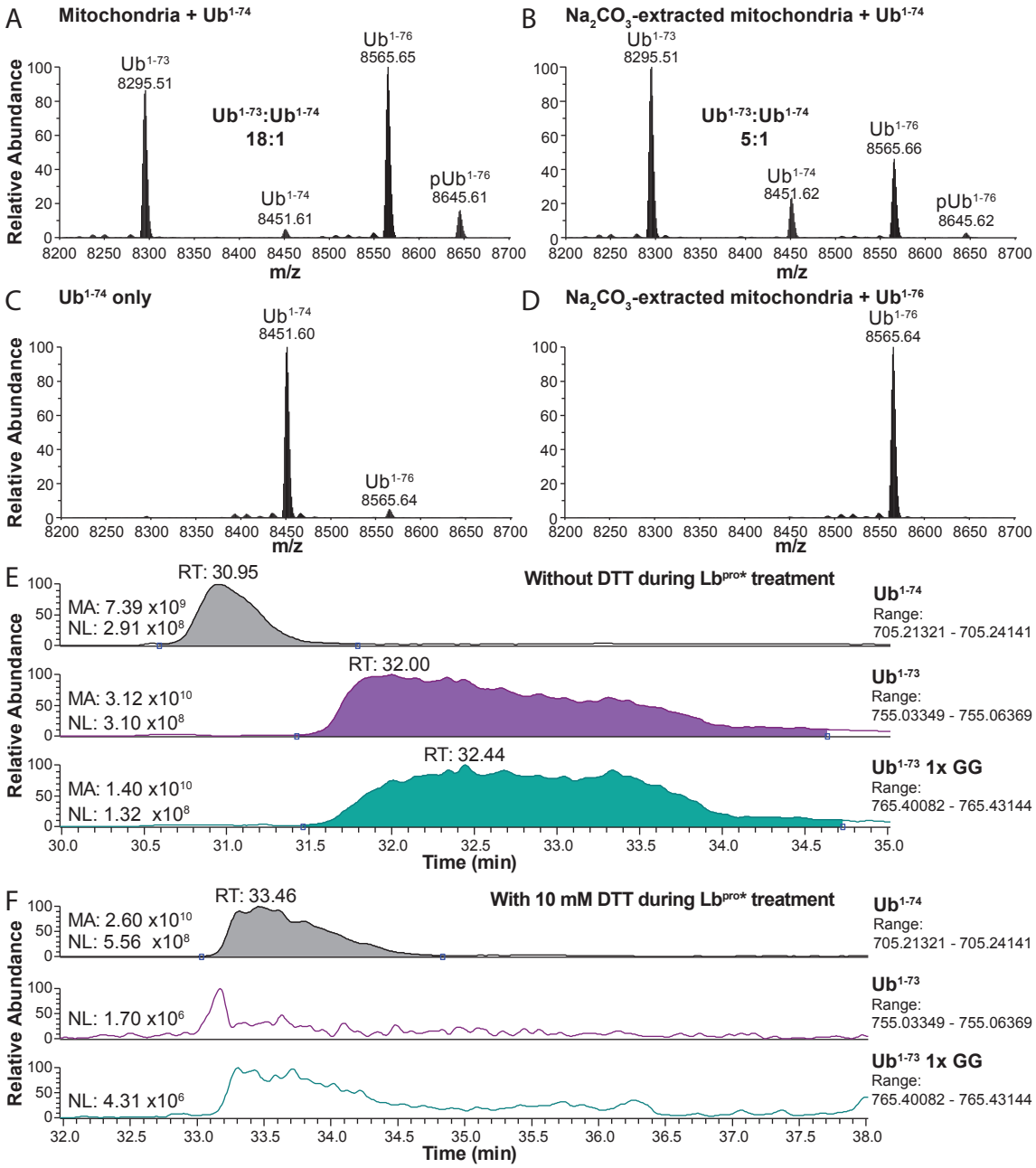

Fig. 4.4 **R-clipping is caused by a mitochondrial enzyme and can be inhibited with DTT. A-B.** Deconvoluted mass spectra showing incubation of mitochondria (**A**) and sodium carbonate-extracted mitochondria (**B**) with Ub^{1-74} that was generated *in vitro*, resulting in the formation of Ub^{1-73}. **C.** Deconvoluted mass spectrum of Lb^{pro}*-treated Ub used as the Ub^{1-74} substrate in A and B. **D.** Deconvoluted mass spectrum of recombinant Ub^{1-76} incubated with sodium carbonate-extracted mitochondria. **E-F.** Extracted ion chromatogram of the indicated Ub proteoforms, generated by Lb^{pro}* treatment in the absence (**E**) or presence (**F**) of 10 mM DTT. RT: retention time. MA: measured area under the curve (filled colour). NL: normalised levels of ion current detected within the indicated mass range.

was also performed in all subsequent experiments, and the trends in relative abundances were consistent across both methods. For this reason, only the peak integration results are presented herein.

Next, enrichment of conjugated Ub from mitochondria using sodium carbonate extraction was compared with TUBE-mediated enrichment of Ub chains. Sodium carbonate extraction, which does not involve affinity purification of Ub, results in enrichment of Ub attached to integral membrane proteins, while TUBEs pull down ubiquitinated proteins, with a bias for longer Ub chains over substrate monoubiquitination (Figure 3.6C). When comparing the two methods in OA-treated cells expressing WT Parkin, the relative amount of pUb obtained from sodium carbonate extraction was modestly higher than in the TUBE-enriched samples (Figure 4.5A). The increase in total mitochondrial Ub upon OA treatment, shown as a fold increase in the abundance of all Ub proteoforms compared with DMSO-treated cells, was higher for sodium carbonate extraction than for TUBE pulldown of mitochondrial extracts (Figure 4.5C). Given that TUBEs bias towards longer chains, this result indicates that a large amount of Parkin-dependent ubiquitination is shorter chains or monoubiquitination. Next, the presence of diGly modifications on unphosphorylated and phosphorylated Ub was compared, thereby giving an indication of where pUb lies within a chain. Figure 4.5D depicts the fraction of Ub and pUb that is diGly-modified. The proportion of singly and doubly diGly-modified pUb was much lower than that of unphosphorylated Ub; when sodium carbonate extraction was performed, 19.3% of pUb was singly or doubly diGly-modified, while 40.9% of unphosphorylated Ub contained diGly modifications. Similary, TUBE pulldown revealed 25.7% of pUb to be diGly-modified, compared with 51.3% of unphosphorylated Ub. Therefore, pUb is preferentially located either on mono-Ub or at the distal end of Ub chains. Taken together, these results indicate that the mitochondrial Ub deposited by Parkin upon chemical depolarisation consists mostly of monoubiquitination, while mono-Ub or the distal end of chains are preferentially phosphorylated.

While Parkin has been shown to be directly activated by PINK1 upon depolarisation in HeLa cells, several other mitochondrial-resident E3 ligases are known to exist and could have an effect on the mitochondrial ubiquitome [189, 144, 326]. To disambiguate the role of Parkin activity in OA-stimulated mitochondrial ubiquitination, WT Parkin expression was compared with C431S Parkin under identical conditions of OA treatment. WT Parkin expression resulted in a higher fold increase in total Ub proteoforms (5.30, SEM = 1.05) than C431S Parkin (1.44, SEM = 0.19) relative to DMSO-treated cells (Figure 4.6A), consistent

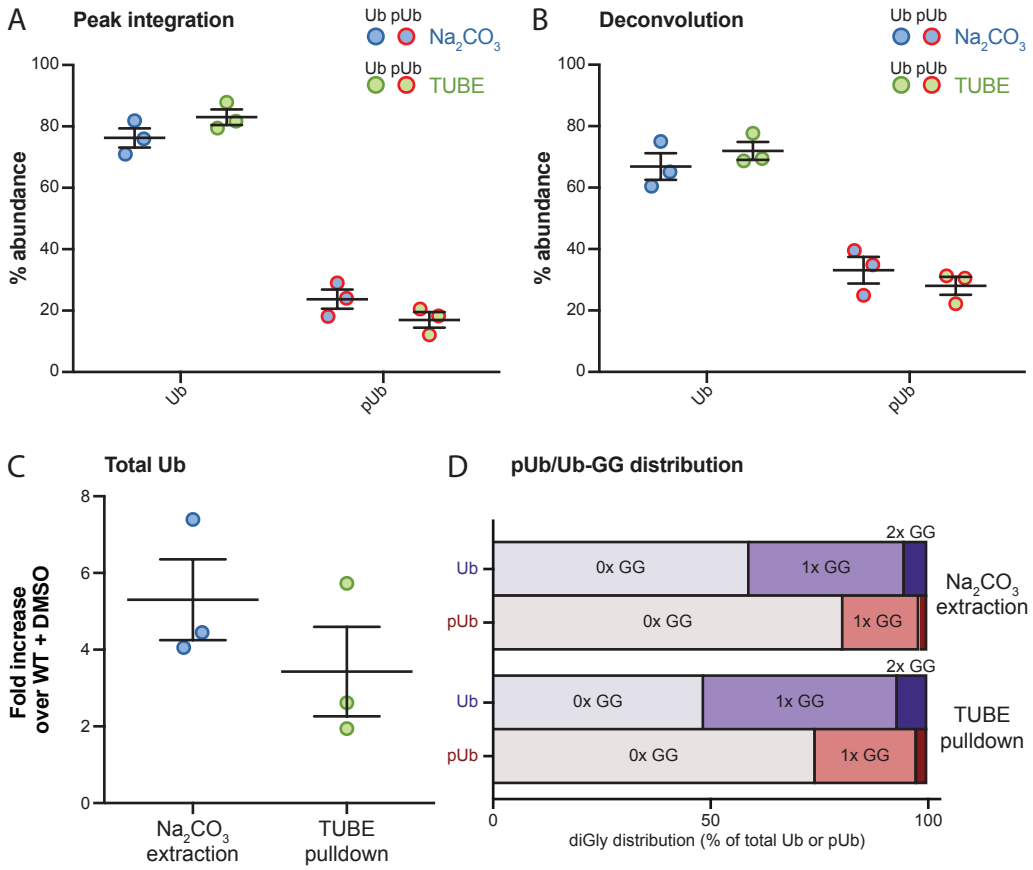

Fig. 4.5 **Comparison of methods for capture and quantification of mitochondrial ubiquitination events. A-B.** Relative abundance of unphosphorylated and phosphorylated Ub^{1-74}, quantified by peak integration (**A**) and deconvolution (**B**) for mitochondria enriched by sodium carbonate extraction (blue) and TUBE pulldown (green), from 2h OA-treated cells expressing WT Parkin. **C.** Total Ub^{1-74} from samples treated and quantified as in A, shown as a fold increase over DMSO-treated cells expressing WT Parkin. **D.** Samples treated and quantified as in A, displayed as the distribution of diGly modifications for both unphosphorylated (purple) and phosphorylated (red) Ub. Error bars: mean +/- SEM (n = 3 independent biological replicates).

with the known role of Parkin E3 ligase activity in amplifying the mitophagy signal in a positive feedback loop [104, 204]. However, it should be noted that OA-treated C431S Parkin samples displayed a nearly 50% increase in mitochondrial Ub relative to DMSO-treated cells, which is consistent with reports of PINK1-dependent, Parkin-independent mitophagy driven by phosphorylation of Ub on mitochondrial proteins [139]. DMSO-treated samples lacked detectable pUb (Figure 4.6B). In contrast, pUb was detected in OA-treated C431S Parkin samples (Figure 4.6B), which contradicts previous findings that WT Parkin is required for Ub phosphorylation by PINK1 [204, 201]. However, even with a higher ratio of PINK1 to total mitochondrial Ub in the C431S Parkin condition, the relative proportion of pUb was lower than for the OA-treated WT Parkin condition (Figure 4.6B). This result indicates that active Parkin stimulates PINK1 activity in some way, perhaps by providing Ub substrate in close proximity to PINK1. The relative proportion of all six detected Ub proteoforms across the three treatments was quantified (Figure 4.6C and D). In all three samples, the relative amounts of unphosphorylated 0x GG- and 1x GG- $Ub^{1\text{-}74}$ were noticeably different when comparing sodium carbonate extraction with TUBE pulldown of mitochondrial extracts. This is consistent with the different biases of the two extraction methods observed by western blotting, whereby TUBE pulldown preferentially enriches longer Ub chains (Figure 3.6C). TUBE enrichment also resulted in a lower relative amount of pUb compared with sodium carbonate extraction, both for WT and C431S Parkin (Figure 4.6C and D). Interestingly, OA treatment in the presence of WT or C431S Parkin did not substantially affect the relative proportion of diGly-modified Ub proteoforms relative to DMSO-treated controls, indicating that the average chain length across all samples is not changed (Figure 4.6C and D). It therefore appears that Parkin amplifies the abundance of mitochondrial Ub without drastically changing its chain length.

The observation that Ub is preferentially phosphorylated at distal moieties or on monoubiquitinated substrates gives rise to the question: does PINK1 prefer to phosphorylate distal and mono-Ub, or does Parkin prefer not to build chains onto phosphorylated Ub? PINK1 has been shown to preferentially phosphorylate the distal moiety of K6 di-Ub *in vitro* [63], but whether this occurs in a mitochondrial context has not been determined. Further, while previous work has established that pS65-Ub is a poor substrate for building chains by Parkin [310, 204], it is less clear whether or not pS65-Ub is an ideal substrate on which to build Ub chains. The diGly distribution for unphosphorylated and phosphorylated mitochondrial Ub was therefore calculated, as in Figure 4.5D, for both WT and C431S Parkin samples (Figure 4.7). If the effect is dependent on Parkin activity, then C431S Parkin mitochondria

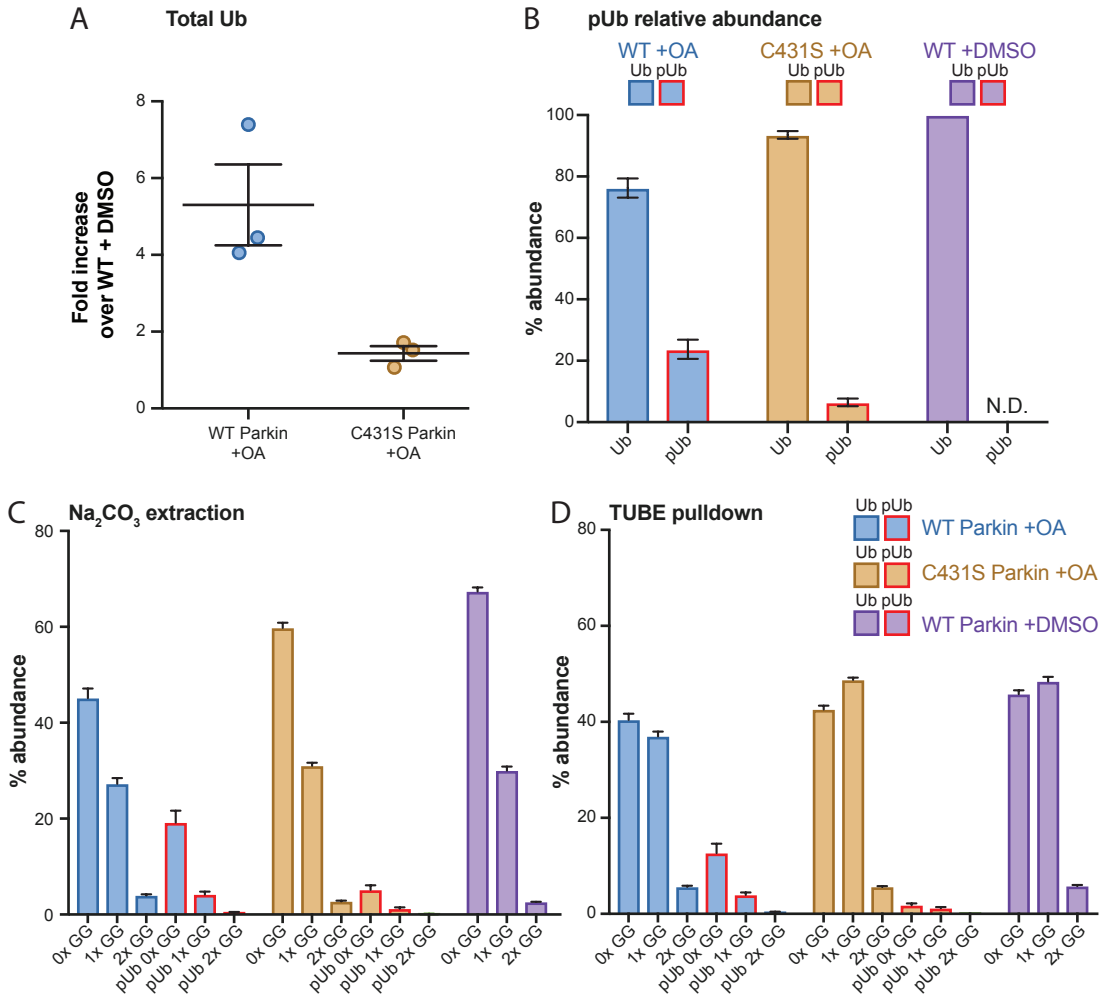

Fig. 4.6 **WT Parkin amplifies the OA-dependent mitochondrial pUb signal. A.** Total Ub, quantified by peak integration and shown as a fold increase over DMSO-treated cells expressing WT Parkin, for 2h OA-treated cells expressing WT Parkin (blue) or C431S Parkin (brown). Mitochondrial Ub enrichment was performed by sodium carbonate extraction. **B.** Samples treated and quantified as in A, shown as abundance of unphosphorylated and phosphorylated Ub, relative to the total Ub for that sample. N.D: not detected. **C-D.** Abundances of six Ub proteoforms, relative to the total Ub for that sample, quantified by peak integration, for sodium carbonate-extracted (**C**) and TUBE-enriched (**D**) mitochondrial extracts. Error bars: mean +/- SEM (n = 3 independent biological replicates).

should have a similar distribution of diGly modifications on pUb and Ub. However, as with WT Parkin, pUb from C431S Parkin mitochondria was preferentially not diGly-modified, with an almost identical profile compared with WT Parkin when the Ub was purified by sodium carbonate extraction (Figure 4.7, top). This indicates that the preference for distal or mono-Ub phosphorylation is Parkin-independent. In contrast, the pUb from TUBE-enriched C431S Parkin mitochondria appeared to have a much weaker preference for distal phosphorylation (Figure 4.7, bottom). The distinction in results observed between sodium carbonate extraction and TUBE pulldown of mitochondrial extracts may be because most Ub phosphorylation occurs on monoubiquitinated substrates, which are better enriched by sodium carbonate extraction compared with TUBE-mediated Ub pulldown. Taken together, these results indicate that Parkin primarily deposits mono-Ub on mitochondrial substrates, and these moieties are preferentially phosphorylated by PINK1. A further discussion of this phenomenon is presented in Section 4.4.1.

4.2.4 Identification of multi-site ubiquitination of intact UBE2L3

While the focus of this thesis has been on the architecture of Ub chains on mitochondria, it should be noted that Lb^{pro}-mediated Ub-clipping also leaves a diGly remnant on previously ubiquitinated substrates [275]. To test whether multi-monoubiquitination of a substrate protein could be observed by MS, an *in vitro* Ub assembly assay was conducted using Parkin as the E3 enzyme and UBE2L3, also known as UbcH7, as the E2. Parkin and UBE2L3 can function together to ubiquitinate substrates *in vitro*, and UBE2L3 has been shown to function in Parkin-dependent mitophagy *in vivo* in cellular assays [311, 129, 60, 46, 245]. UBE2L3 was an ideal target for studying multi-monoubiquitination by Ub-clipping and MS as it is a relatively small protein that contains a large number of K residues (18 out of 154 amino acids), and it is ubiquitinated during *in vitro* Ub assembly assays [64]. The *in vitro* assembly assay was performed by C. Gladkova, using a higher relative proportion of UBE2L3 than typical assays to further encourage its ubiquitination [275]. This assembly mixture was treated with Lb^{pro}* and the formation of diGly-modified UBE2L3 was monitored by intact MS (Figure 4.8). The inset shows the most abundant charge state, +21, with peaks corresponding to five proteoforms of UBE2L3 (unmodified and up to four diGly modifications). Such an experiment could not be so easily performed and interpreted by standard tryptic digest methods, because trypsin would digest the protein internally and therefore the context of each diGly modification with respect to the rest of the protein would

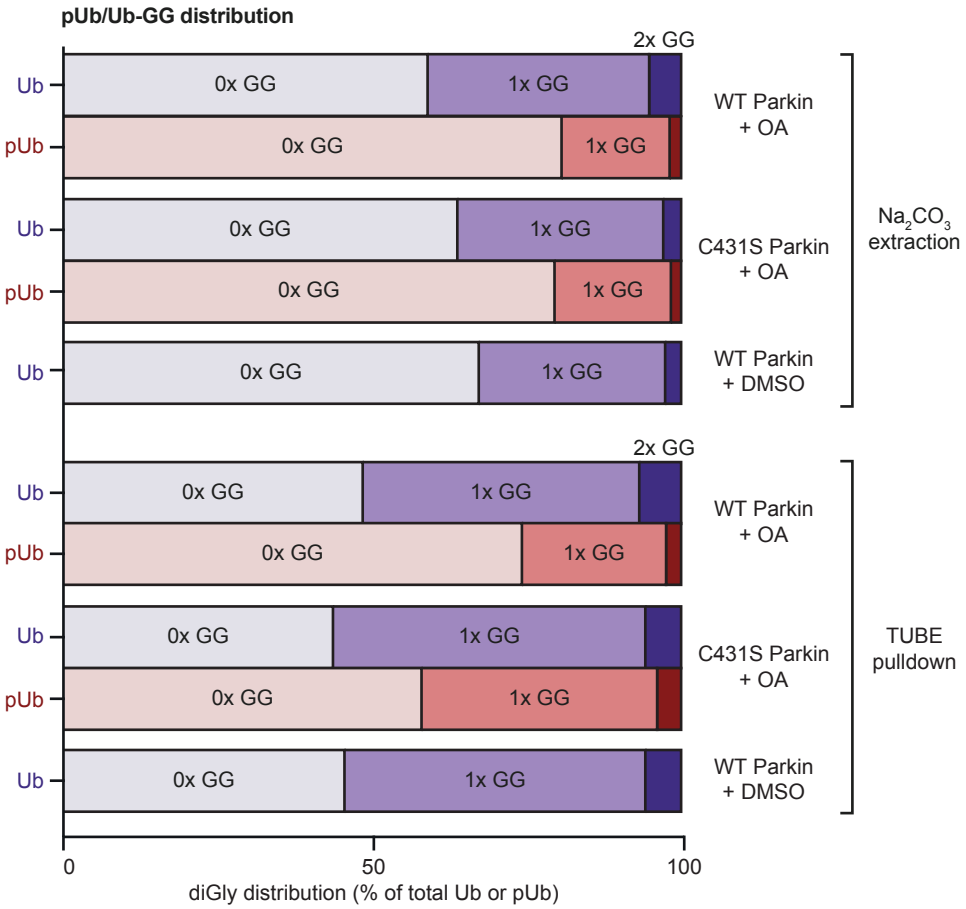

Fig. 4.7 **Distal or mono-Ub moieties are preferentially phosphorylated independent of Parkin activity.** Comparison of the diGly distribution of phosphorylated (red) and unphosphorylated (purple) Ub, for mitochondrial Ub from DMSO- or OA-treated cells expressing WT or C431S Parkin, enriched by sodium carbonate extraction (top) or TUBE pulldown (bottom), quantified by peak integration. 3 independent biological replicates were performed.

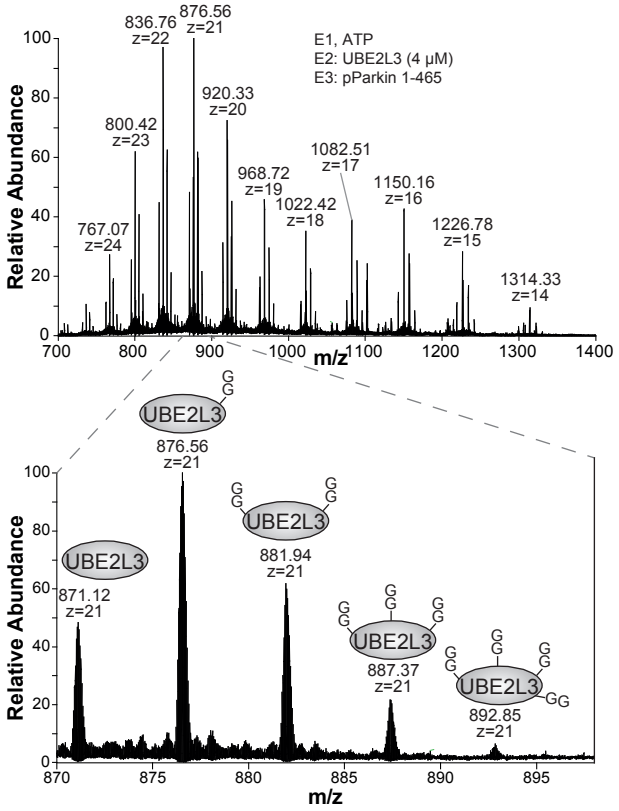

Fig. 4.8 **UBE2L3 is ubiquitinated on up to four sites per molecule.** An *in vitro* Ub assembly conducted with human E1, UBE2L3 and Parkin was treated with Lb^{pro}* and analysed by intact MS. The raw mass spectrum for UBE2L3 is shown. Inset: a zoomed-in image of the +21 charge state, showing up to four diGly modifications on a single UBE2L3 molecule. The assembly and digest was performed in triplicate, with one representative experiment shown.

be lost. Therefore, investigation of multi-monoubiquitination of substrates is a potentially powerful novel application of Ub-clipping.

4.2.5 Analysis of Ub proteoforms from *Drosophila* mitochondria

Ub-clipping and intact MS analysis of mitochondrial Ub proteoforms was performed on *Drosophila* whole fly samples. Fly models of *Pink1* and *park* deficiency are one of the few animal models that show mitochondrial dysfunction and age-related tissue degeneration, and are therefore an ideal model to investigate the molecular events underpinning these events [71, 210, 30]. Compared with cell culture models, *Drosophila* models have the advantage that a correlation can be drawn between the molecular events caused by a specific manipulation and the behavioural phenotype, such as flight or climbing, that manifests in the fly. Analysis

of the mitochondrial ubiquitome in *Drosophila* models of mitochondrial dysfunction and manipulation of autophagy can therefore be married with the known effects of the intervention on survivial and locomotor abilities to give an insight into the physiological relevance of changes in the mitochondrial ubiquitome. Unfortunately, the Ub present on WT (w^{1118}) mitochondria was barely detectable by western blot, and incubation with an anti-pS65-Ub antibody failed to generate a signal (data not shown). While the low Ub abundance presented challenges in detection, it is likely to represent a more physiological abundance of mitochondrial Ub than the HeLa system, so the sample preparation method was adapted accordingly. For initial experiments, a fly model expressing *Tribolium castaneum* Pink1 (*Tc*Pink1) under the control of a *da*-GAL4 driver was used in order to boost the pS65-Ub signal above the threshold for detection by MS. *TcPink1* was used because *Drosophila Pink1* overexpression is poorly tolerated by the fly [220], and *Tc*Pink1 protein has been shown to be active *in vitro* and well-tolerated in flies [316]. Whole flies were lysed and mitochondria enriched by differential centrifugation, then 500 μg mitochondrial protein (approximately 50 to 100 flies) was sodium carbonate-extracted, Lb^{pro}*-treated, and purified by PA treatment and dialysis to obtain the mitochondrial Ub proteoforms. These samples were analysed by intact MS, and three Ub proteoforms (unmodified, diGly-modified and phosphorylated $Ub^{1\text{-}74}$) were observed (Figure 4.9A, B). The signal corresponding to $pUb^{1\text{-}74}$ constituted approximately 9% of the total Ub signal in *da>TcPink1* mitochondria and could be removed by lambda phosphatase (λPP) treatment, thus confirming that the species was indeed phosphorylated Ub (Figure 4.9C, D). Note that combinations of modifications, such as chain branching or diGly-modified $pUb^{1\text{-}74}$, were not observed (Figure 4.9B). This may be because combinatorial Ub modifications do not exist on fly mitochondria, or because the amount of total mitochondrial Ub signal was dramatically less than in the previously studied HeLa context, meaning that these very lowly abundant proteoforms exist below the level of detection by MS.

With the establishment of a method for studying mitochondrial Ub proteoforms in flies, the presence of phosphorylated Ub in w^{1118} flies was investigated. Given that autophagic turnover decreases with age [257], mitochondria from young (2 to 5 days post-eclosion) and old (60 days post-eclosion) flies were compared, in an attempt to boost the pUb signal detection independently of Pink1 overexpression. Notably, the combined raw signal intensities measured by peak integration for all mitochondrial Ub proteoforms was much higher in old flies (3.20×10^9) compared with young flies (4.07×10^8; Figure 4.10A, B). pUb was observed in samples from both young and old flies (Figure 4.10C, D). The relative composition of the three observed Ub proteoforms was broadly similar between the two conditions (Figure

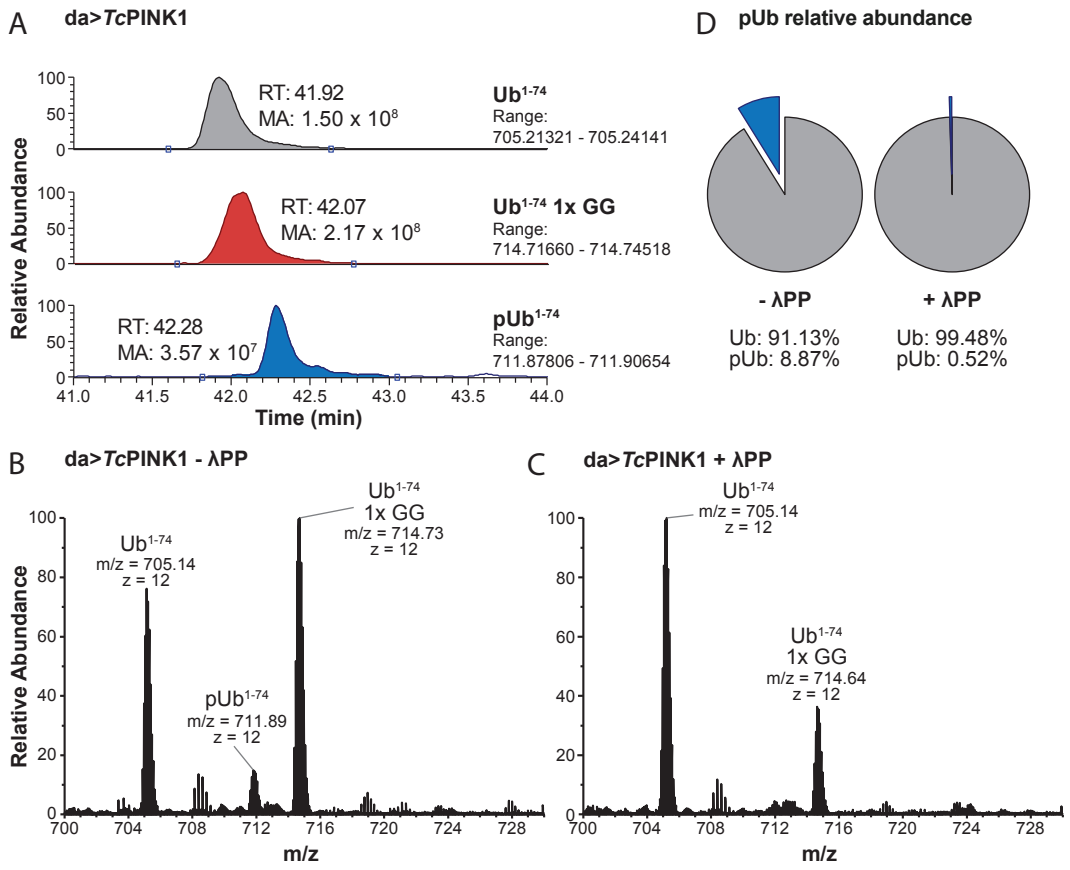

Fig. 4.9 **Identification of phosphorylated Ub by intact MS in flies expressing *Tc*Pink1.** **A.** Extracted ion chromatogram of the indicated Ub proteoforms from intact MS analysis of *da>TcPink1* flies after sodium carbonate extraction of mitochondria, Lb^{pro}* treatment and purification by perchloric acid extraction and dialysis. **B.** Raw mass spectrum of samples from A, showing the indicated Ub proteoforms. **C.** Raw mass spectrum showing Ub proteoforms from flies treated as in B, but with Lambda phosphatase (λPP) treatment performed after incubation with Lb^{pro}*. **D.** Quantification by peak integration of the relative abundance of $pUb^{1\text{-}74}$ and unphosphorylated $Ub^{1\text{-}74}$ in samples B and C. A single replicate was performed. RT: retention time. MA: measured area (shaded region).

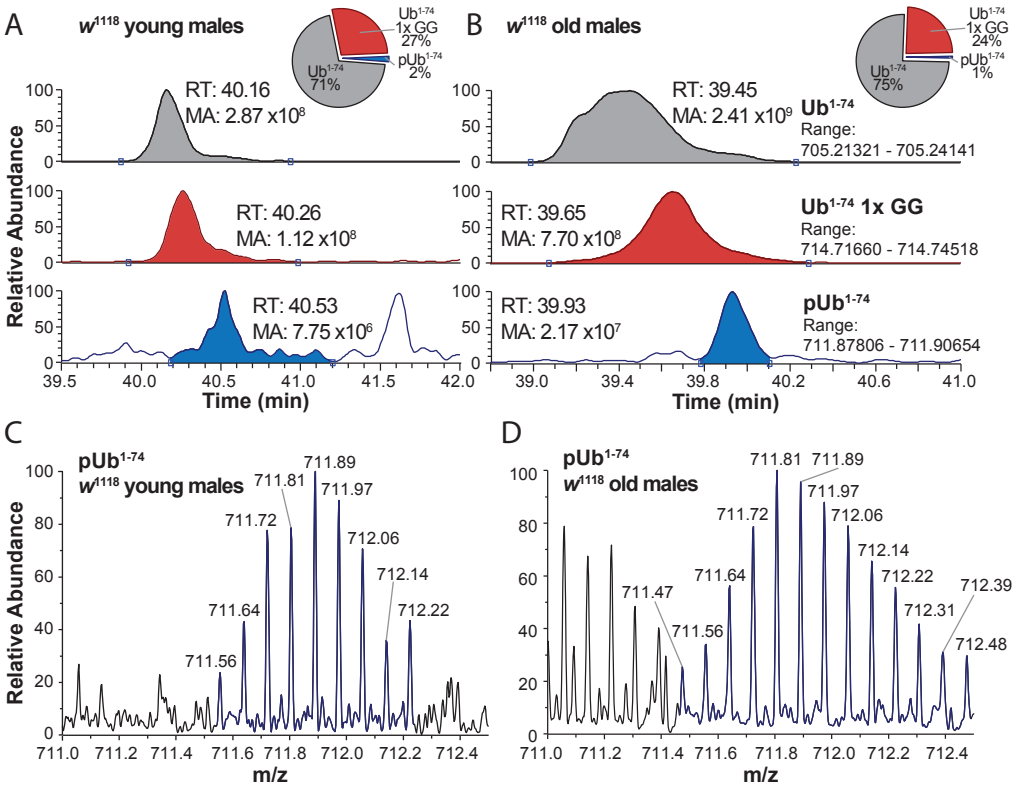

Fig. 4.10 **Ub phosphorylation occurs in w^{1118} flies. A-B.** Extracted ion chromatogram of Ub proteoforms from 2-5-day-old (**A**) and 60-day-old (**B**) w^{1118} flies, after sodium carbonate extraction and Lb^{pro}* treatment of mitochondria, then perchloric acid treatment and dialysis. Inset: pie charts quantifying the relative abundances of the three proteoforms by peak integration. A single replicate was performed. **C-D.** Raw mass spectrum showing pUb^{1-74} (m/z = 711.89, z = 12) from samples A and B. The blue coloured region corresponds to isotopes of pUb^{1-74}. RT: retention time. MA: measured area (shaded region).

4.10A, B), and similar results were observed in female flies (not shown). However, large sample amounts were required, thus precluding the analysis of multiple replicates, and the pUb signal in particular was very low, meaning that a reliable quantification of Ub proteoforms could not be performed. This, alongside the fact that combinatorial modifications were again not observed, and the limited scope for normalisation of results between replicates, indicated that intact MS was not the best method for determining the makeup of the mitochondrial ubiquitome in flies. Further method development and investigation using AQUA MS was therefore performed, as outlined in the following section.

4.3 AQUA analysis of mitochondrial Ub

AQUA-based MS methods are a targeted approach to quantify the absolute abundance of a particular peptide in a complex mixture [121]. Known amounts of specific reference peptides containing stable heavy isotopes of Carbon and Nitrogen are spiked into the mixture after tryptic digest. The heavy and light peptides exhibit identical chemical and chromatographic properties, and are therefore analysed simultaneously during LC-MS. The heavy labelling results in a mass shift of the reference peptide that is detected by MS, and the abundance of the light peptide in the sample is quantified based on its signal intensity relative to that of the heavy peptide. The AQUA method has been used in previous studies of Parkin-dependent ubiquitination, *in vitro* and in depolarised cells [204, 310, 201–203, 275]. Tryptic digest removes the contextual information of multiple modifications on a single Ub moiety, so the AQUA MS approach is not ideal for the study of Ub architecture. However, the addition of Lb^{pro} treatment to the sample preparation pipeline can improve enrichment of Ub, by generating diGly-modified mono-Ub that can be further enriched by other methods prior to tryptic digest. Early applications of this method used SDS-PAGE followed by Coomassie staining, excision of the mono-Ub band, and in-gel tryptic digest to great effect [275]. However, in-gel digest is not as easily scalable as in-solution methods and is prone to high levels of sample loss [124]. This section describes an alternative mode of mono-Ub enrichment using Stop-and-go extraction Tip (StageTip) fractionation [227, 228], which removed the need for SDS-PAGE fractionation and allowed for in-solution tryptic digest. The method was developed and validated using mitochondria from HeLa cells, then applied to *Drosophila* and brain homogenates from mice.

4.3.1 Enrichment of Ub proteoforms using StageTip fractionation

In order to accurately determine the fly mitochondrial ubiquitome, in which the mitochondrial Ub content was much lower than in depolarised cells, Ub enrichment after Lb^{pro}* treatment of sodium carbonate- or TUBE-enriched mitochondrial Ub was required. While PA treatment and dialysis had been used previously, concerns about the oxidising nature of the acid and its potential for forming artefacts beyond those described in Section 4.2.1 led to development of alternative forms of Ub enrichment after Lb^{pro}* treatment. Therefore, an ACN fractionation method using StageTips was trialled, to enrich the Lb^{pro}*-treated Ub proteoforms prior to tryptic digest. StageTips are pipette tips that contain a small amount of hydrophobic substrate, to which peptides and proteins bind [227, 228]. After priming and sample application to the tip, impurities can be removed by passing buffer through the tip, while high concentrations of

ACN allow elution of the peptides or proteins from the substrate [228]. It was hypothesised that Ub, Lb^{pro}*, and other mitochondrial contaminants may elute from the StageTips at different ACN concentrations, and the method could therefore be used to enrich mono-Ub by depleting other contaminants. Using Lb^{pro}*-treated Ub generated *in vitro*, the two proteins were effectively separated using stepwise fractionation (Figure 4.11A). Almost all of the Ub eluted with 30% ACN, while Lb^{pro}* eluted with 50% ACN. Next, the effectiveness of StageTip fractionation at removing contaminants from a complex sample was tested, using mitochondria from OA-treated HeLa Flp-In Trex cells expressing C431S Parkin (Figure 4.11B). Elution of the sample from the StageTip was performed in three fractions (15%, 40%, and 80% ACN), and the total ion chromatogram from the intact LC-MS analysis of each fraction is shown. The 15-40% ACN fraction (middle panel) contained the majority of the Ub signal, while lacking the contaminants present in the panels above and below that would have been present if a single elution had been performed (Figure 4.11B). Importantly, the relative abundance of the measured Ub proteoforms was comparable between the 40% and 80% ACN elutions, indicating that the fractionation method did not bias towards or against enrichment of specific Ub proteoforms (Figure 4.11C). A two-step fractionation method was therefore developed, incorporating a pre-elution step with 20% ACN, followed by elution with 45% ACN (Figure 4.11D). This allowed improvement in the enrichment of Ub from Lb^{pro}*-treated fly mitochondria, as measured by intact MS (Figure 4.11E). As shown, this step was directly compatible with analysis by intact MS, but the eluted sample could also be digested with trypsin and analysed by AQUA MS. The following sections detail the application of this method to the analysis of Ub modifications in the HeLa system, in fly models of various genotypes and environmental permutations, and in mouse brain sections.

4.3.2 AQUA MS analysis of the mitochondrial ubiquitome in HeLa cells

To demonstrate the utility of the Ub-clipping AQUA MS method in an establised system, depolarised HeLa cells expressing Parkin (WT or C431S), with or without genetic disruption of *PINK1*, were prepared and analysed by AQUA MS (Figure 4.12A). 20 μg mitochondria was used per replicate, representing a 10-fold reduction in the initial sample requirement compared with the intact MS analyses presented in the previous section. The Ub was enriched by sodium carbonate extraction due to its higher yield and reduced bias towards longer chains compared with TUBE pulldown (Figure 3.6C). Analysis of the total mitochondrial Ub content showed a five-fold increase in cells expressing WT Parkin (1.6 pmol) compared

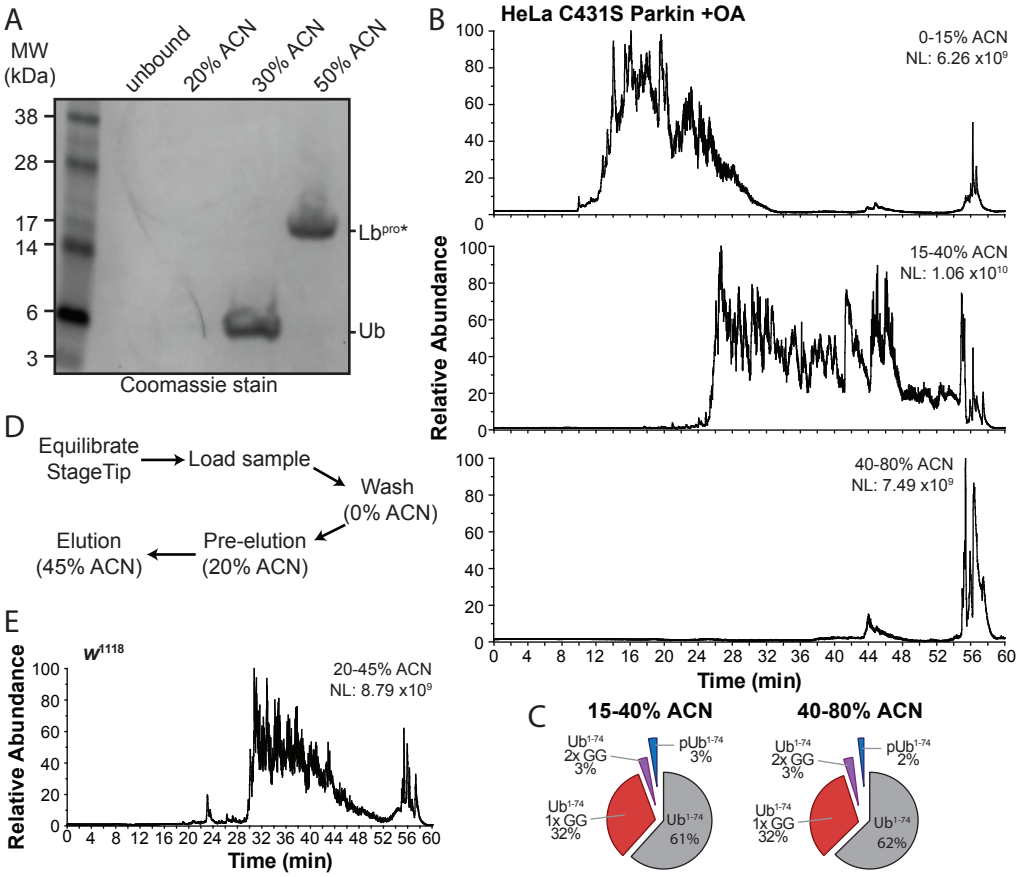

Fig. 4.11 **Fractionation of Lb^{pro}*-treated Ub using StageTips. A.** Separation of Ub and Lb^{pro}* *in vitro* using StageTips. 5 μM Ub was incubated 2 h with 10 μM Lb^{pro}*, then desalted and fractionated using a StageTip (C_4 matrix, 2 plugs of substrate) at the indicated ACN concentrations. The eluted fractions were loaded onto an SDS-PAGE gel and visualised by Coomassie staining. A representative image is shown from two replicate experiments. **B.** Lb^{pro}*-treated mitochondrial Ub from HeLa Flp-In Trex C431S Parkin cells was applied to a StageTip (C_4 matrix, 4 plugs of substrate), desalted and eluted with 15% ACN (top), then 40% ACN (middle), followed by 80% ACN (bottom). The eluate from each step was analysed by intact LC-MS. The total ion chromatogram and the normalised levels (NL) for each fraction is shown. A single replicate experiment was performed. **C.** Quantification by peak integration of the relative abundance of the indicated Ub proteoforms in B (left, 40% ACN elution; right, 80% ACN elution). **D.** Flowchart for the enrichment of Ub (after Lb^{pro}* treatment) by StageTip fractionation, used in subsequent experiments. **E.** Total ion chromatogram for Ub proteoforms from w^{1118} mitochondria, prepared as in D. A representative image from three replicate experiments is shown.

with either C431S Parkin (300 fmol) or *PINK1*$^{-/-}$ cells expressing WT Parkin (400 fmol). This result agrees with the theory that both Parkin and PINK1 activity are required for robust mitochondrial ubiquitination upon chemical depolarisation [204]. For the quantitative analysis of Ub chain types and phosphorylation, the data were normalised against total Ub to control for the substantial variation in total Ub between replicates (Figure 4.12C). The abundance of four chain types (K6, K11, K48 and K63) and S65 phosphorylation (both total and in the context of K63 chain formation) were quantified. M1-, K27-, K29-, and K33-linked Ub were not analysed due to a combination of technical issues with detecting and quantifying their respective diGly peptides, and because these modifications, in particular M1, K27 and K29, have been shown to be not highly abundant in this system [204]. K6-linked Ub was detected when WT Parkin was present, while it did not reach the limit of detection in C431S Parkin or *PINK1*$^{-/-}$ cells, even with depolarisation (Figure 4.12C). This result indicates that Parkin is responsible for the majority of K6-linked Ub on mitochondria in the context of depolarisation in this system. Similarly, K11-linked Ub increased approximately two-fold in abundance in the WT Parkin condition compared with either control, with C431S Parkin expression resulting in only a very modest increase in K11 chains compared with the *PINK1*$^{-/-}$ control (Figure 4.12C). K48-linked Ub showed a similar trend to K11-linked Ub, with a modest difference between the C431S Parkin and *PINK1*$^{-/-}$ conditions, and a more substantial increase in the presence of WT Parkin (Figure 4.12C). Surprisingly, the relative abundance of K63 chains was reduced in the WT Parkin condition (Figure 4.12C), although it should be noted that the absolute abundance of K63 chains was still higher in this condition owing to the approximately five-fold increase in total mitochondrial Ub (Figure 4.12B). Ub S65 phosphorylation was not detected in the *PINK1*$^{-/-}$ condition, consistent with PINK1 being the sole Ub kinase (Figure 4.12C). Conversely, Ub S65 phosphorylation was detected in both WT and C431S Parkin conditions in the presence of OA and endogenous PINK1. Notably, the relative pUb abundace in the C431S condition (3.5%) was lower than for WT Parkin (11.5%), despite a lower total Ub content and therefore a higher PINK1:Ub ratio, as was observed with intact MS analysis. While the calculated abundance of pUb in mitochondrial extracts from cells expressing WT Parkin differed between intact MS and AQUA MS, the relative difference in pS65-Ub abundance between WT and C431S Parkin conditions measured by AQUA MS was in agreement with the previous intact MS results, supporting a role for Parkin in increasing PINK1 activity. When analysing the interplay between phosphorylation and ubiquitination at the K63 locus when WT Parkin was expressed in the presence of endogenous PINK1, 12.5% of diGly-modified K63 was phosphorylated, which is comparable to the 11.5% of total Ub that was phosphorylated. Similarly, the

proportion of phosphorylated, diGly-modified K63 in the C431S sample (5.9%), was slightly higher than the relative amount of total pS65-Ub in those conditions (3.5%). Therefore, the preference observed by intact MS against phosphorylation and chain formation on the same Ub molecule was not consistent in this AQUA analysis of the K63 locus. It has been shown *in vitro* that PINK1 can easily phosphorylate both the proximal and distal moieties of a K63-linked chain [63], and these results suggest that K63 chains are also readily phosphorylated *in vivo*. A further discussion of the Parkin-dependent mitochondrial ubiquitome in the HeLa system is provided in Section 4.4.1. The AQUA MS results generally agreed well with the reported literature [204, 36], so the method was applied to fly and mouse brain models as shown in the following sections.

4.3.3 Ageing and paraquat treatment increase mitochondrial Ub phosphorylation in *Drosophila*

Following the optimisation of a method for the analysis of mitochondrial ubiquitomes by AQUA MS in the HeLa cell model, the method was then applied to the study of the *Drosophila* mitochondrial ubiquitome. Due to the low abundance of Ub on *Drosophila* mitochondria, several alterations were made to the method. Each replicate required 500 μg mitochondria, and a TUBE pulldown was used to enrich Ub from mitochondria (Figure 4.13A) as it resulted in less contamination from hydrophobic integral membrane proteins than sodium carbonate extraction, despite producing lower yield (data not shown and Figure 3.6C). Autophagy is known to decline with age in flies [257]. Therefore, it was hypothesised that ageing the flies may increase the amount of pUb signal observed, due to a reduction in autophagic turnover of pUb-labelled mitochondria. w^{1118} flies were aged to between 50 and 60 days, with males and females separated during the ageing process to control for lifespan effects of mating and stochastic differences that may arise from unequal loss of one sex. Paraquat (PQ), an oxidant that induces ROS generation by receiving electrons, predominantly from Complex I, to produce superoxide anions [18, 55], was also used to stimulate mitochondrial damage. It was hypothesised that PQ treatment of flies may result in activation of the PINK1/Parkin pathway, as has been shown in cells [184], thus increasing the abundance of pUb. Flies were treated 3 days with 5 mM PQ, which resulted in the death of less than 1% of flies prior to harvesting (data not shown).

Young, aged, and PQ-treated w^{1118} flies were analysed by AQUA MS. The flies were harvested and prepared as per Figure 4.13A, and the absolute abundances of diGly-modified

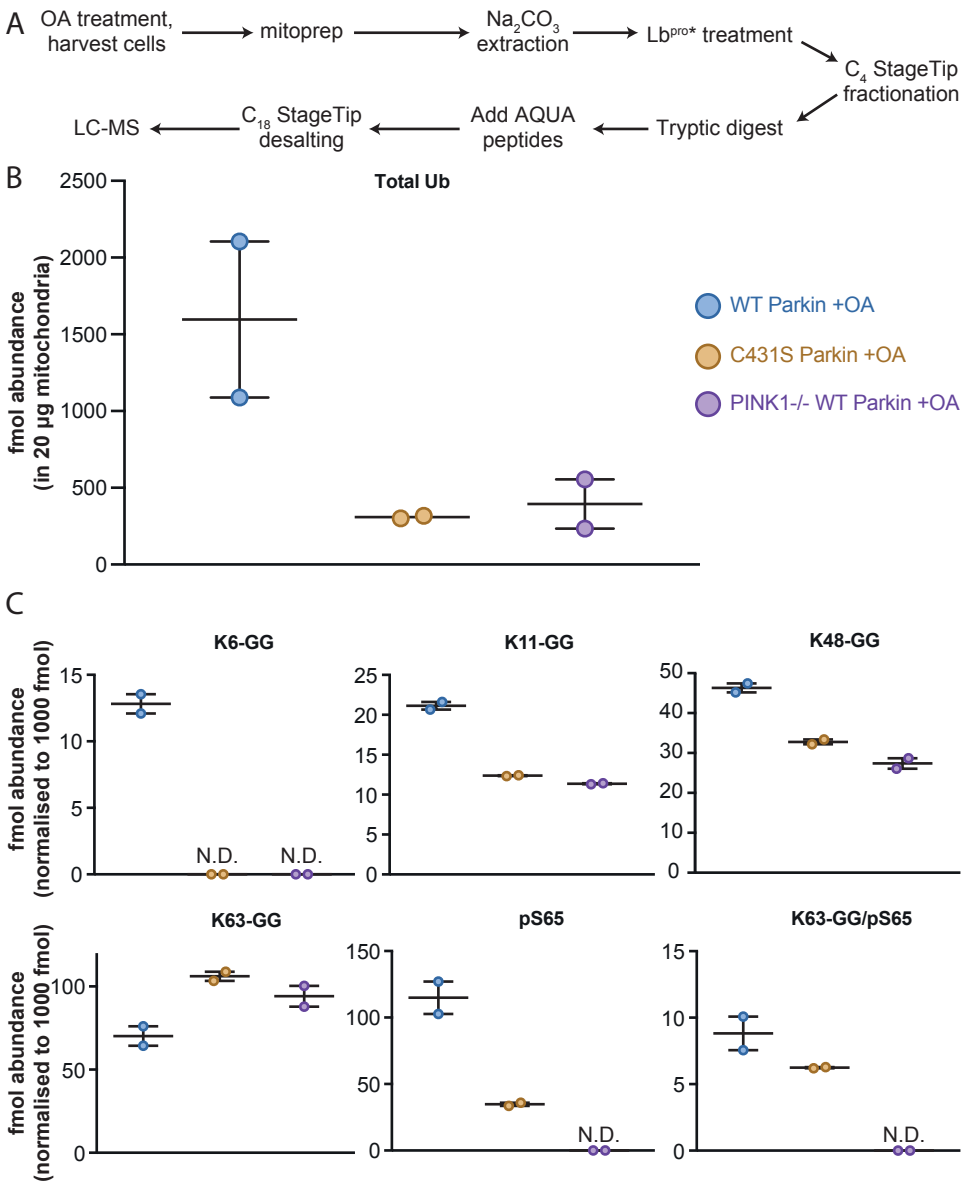

Fig. 4.12 **Parkin activity increases K6 chains and Ub phosphorylation on depolarised mitochondria.** **A.** Flow chart describing the preparation of samples for analysis of Ub modifications by LC-MS. **B.** Abundance of Ub on mitochondria from the indicated samples treated as per A, based on quantification of the TITLE locus, from 20 μg mitochondrial starting material. **C.** Abundance of the indicated Ub modifications for each sample as in B, displayed as fmol abundance relative to 1000 fmol Ub. N.D.: not detected.

K6, K11, K48 and K63 Ub peptides were quantified, alongside the abundance of total Ub and pS65-Ub. The total amount of mitochondrial Ub in 500 μg w^{1118} mitochondria without stimulation was 170 fmol. Note that this number is lower than the amount of total Ub observed in only 20 μg sodium carbonate-extracted HeLa mitochondria in the absence of PINK1 activity (Figure 4.12B). The total Ub abundance in aged flies was highly variable across both males and females, but was consistent among flies that were aged and harvested in parallel. Across both males and females, the average fold increase in total mitochondrial Ub abundance between young and aged flies was 3.5. In comparison, the PQ-treated flies displayed a 5.8-fold increase in total Ub abundance relative to untreated w^{1118} mitochondria, with less variability among biological replicates than the aged flies. Mitochondria from untreated w^{1118} flies lacked detectable S65-Ub phosphorylation under the sample preparation conditions used (Figure 4.13C). In contrast, aged males and females contained 5.5 fmol and 3.4 fmol pS65-Ub respectively per 1000 fmol total Ub, while PQ-treated flies had a much higher pS65-Ub level of 58 fmol per 1000 fmol Ub, which corresponds to 5.8% of the total mitochondrial Ub. The increase in both total Ub and pUb in the aged and PQ-treated samples indicated that the Pink1/parkin pathway may indeed be activated by these manipulations, and that PQ treatment is a much more potent activator of Pink1 activation than ageing.

Next, the Ub chain type complement of w^{1118} mitochondria was examined. As expected, the canonical K48- and K63-modified Ub were the most abundant diGly modifications, at 82 fmol and 110 fmol per 1000 fmol Ub respectively, while K6- and K11-modified Ub could be detected at lower abundance (2.2 fmol and 25 fmol respectively; Figure 4.13D-G). Preliminary experiments did not detect M1-, K27-, K29-, or K33-linked Ub, which may be due either to technical issues with the peptides or genuine low abundance of these modifications (data not shown). Aged w^{1118} mitochondria had a 2.8-fold increased abundance of K6 chains across both sexes relative to young flies (Figure 4.13D). In comparison, PQ treatment did not result in increased K6 chain abundance relative to untreated flies (Figure 4.13D). Ageing and PQ treatment resulted in only modest increases in K11-linked Ub abundance relative to control flies (Figure 4.13E). The abundance of K48-linked Ub appeared similarly reduced across both aged and PQ-treated flies relative to untreated controls, although the data across biological replicates for untreated flies were highly variable (Figure 4.13F). The relative abundance of K63-linked Ub was also lower in both aged and PQ-treated flies relative to controls (Figure 4.13G). It should be noted that a K63-GG/pS65 doubly modified heavy-labelled reference peptide was not included in the AQUA analysis of fly samples because initial characterisation experiments using overexpression of *Tc*Pink1 did not result in

detectable K63-GG/pS65 (data not shown). Given that PQ treatment induced a large amount of pS65-Ub production, it is possible that some K63-GG/pS65 may have been produced in this context. The true abundance of K63-GG Ub in the PQ-treated sample could therefore be higher than displayed in Figure 4.13G. However, this confounding effect would not solely account for the observed four-fold difference in K63-GG abundance between PQ-treated and untreated flies. Taken together, both ageing and PQ treatment resulted in increased mitochondrial bulk ubiquitination and pS65-Ub production, and both manipulations resulted in a modest increase in K11 chains. The relative amounts of K63 chains were reduced and K48-modified Ub remained relatively unchanged for both treatments, while ageing alone resulted in modestly increased K6 chains. The low fmol increase in K6 and K11 chains did not counteract the large reduction in the proportion of K63 chains, indicating that monoubiquitination of mitochondrial proteins also increased upon ageing and PQ treatment.

Unfortunately, the conditions trialled in Figure 4.13A did not result in the detection of pS65-modified Ub in unstimulated w^{1118} mitochondria (Figure 4.13C). Therefore, phosphopeptide enrichment was trialled as a method to enrich the pS65-Ub signal in w^{1118} mitochondria above the limit of detection. 4 mg w^{1118} mitochondria (approximately 1,000 flies) per replicate was prepared according to Figure 4.13H. Sodium carbonate extraction was chosen for enrichment of ubiquitinated substrates due to its higher pUb yield as observed by intact MS in the HeLa system (Figure 4.5A). Approximately 22 fmol pS65-Ub was identified in 4 mg sodium carbonate-extracted mitochondria (Figure 4.13I). Unfortunately, due to the phosphopeptide enrichment step, which depletes unphosphorylated peptides, the total Ub abundance could not be quantified within the experiment, so normalisation across replicates to total Ub content could not be performed. Regardless, it is clear that the abundance of pS65-Ub in young, healthy flies is very low, but can be increased upon ageing or treatment with mitochondrial toxins. This result is congruous with the observation that Pink1 and parkin do not play a significant role in basal mitophagy in young flies [142].

4.3.4 Genetic manipulations predominantly affect Ub phosphorylation

The effect of various mitophagy-modulating genetic manipulations on the makeup of the mitochondrial ubiquitome was examined by AQUA MS. These included overexpression of *Tc*Pink1 and parkin, to induce mitochondrial ubiquitination; genetic ablation of *Atg5*, a core autophagy machinery component (with and without concurrent parkin overexpression), to prevent turnover of ubiquitinated organelles; genetic ablation of *Pink1*, to evaluate whether

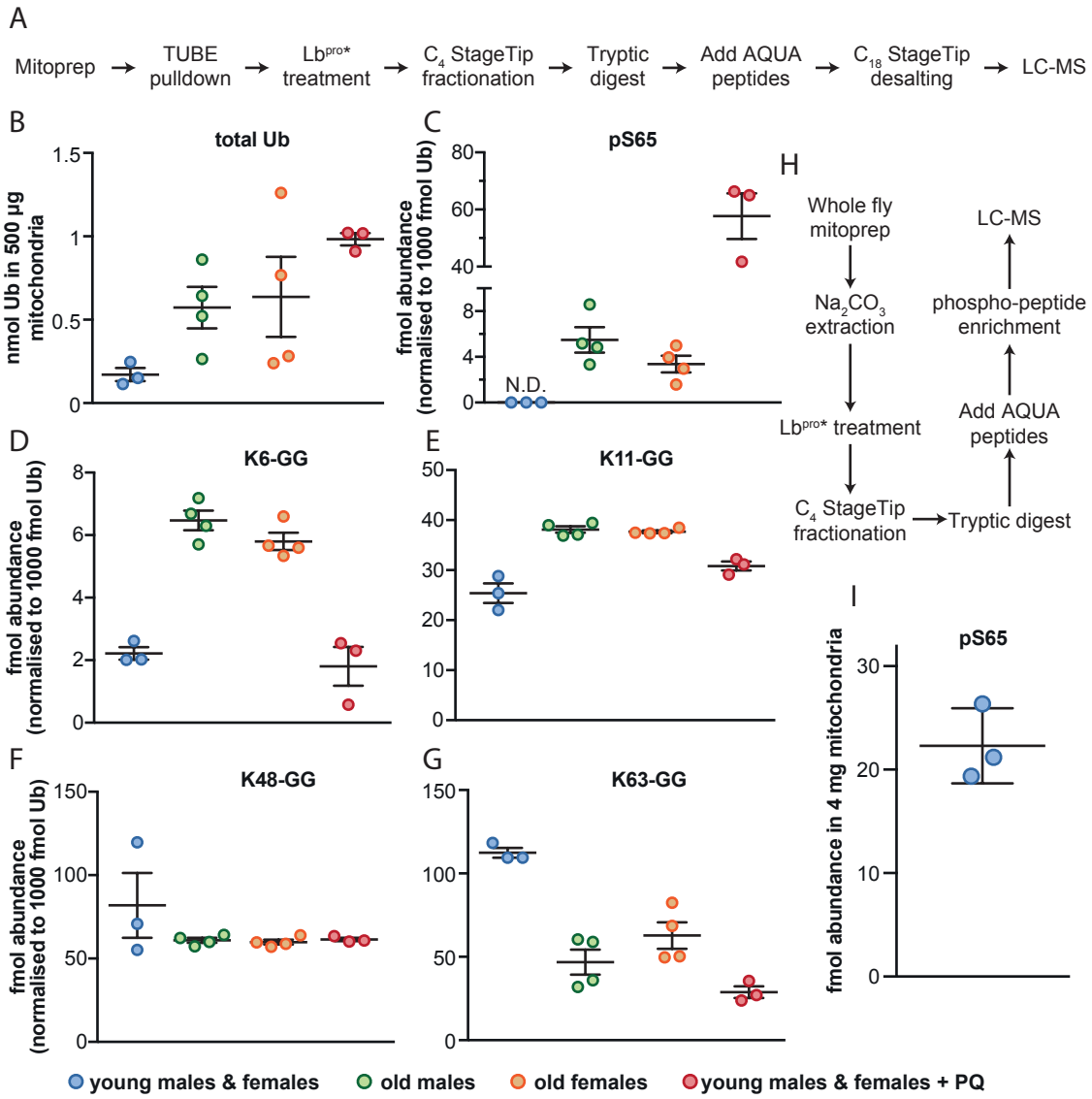

Fig. 4.13 **Ageing and paraquat treatment have different effects on the w^{1118} mitochondrial ubiquitome. A.** Flowchart illustrating the preparation of fly samples for AQUA MS analysis. **B.** Total mitochondrial Ub abundance for young flies (blue; males and females; three independent replicates), 50-60 day old males (green; four independent replicates), 50-60 day old females (blue; four independent replicates), and young flies treated 3 days with 5 mM paraquat (PQ; red; males and females; three independent replicates). **C-G.** fmol abundance of pS65 (**C**), K6-GG (**D**), K11-GG (**E**), K48-GG (**F**) and K63-GG (**G**), normalised to 1000 fmol Ub for samples treated as in B. **H.** Flow chart depicting the method used to determine the endogenous amount of pS65-Ub in young w^{1118} mitochondria using sodium carbonate extraction and TiO_2 enrichment of phosphopeptides. **I.** fmol abundance of pS65-Ub in 4 mg mitochondria from young w^{1118} flies, prepared according to H. Three independent replicates were performed. Error bars represent mean +/- SEM. N.D.: not detected.

production of pS65-Ub is dependent on Pink1 in flies; and *Pink1* null flies overexpressing parkin, to determine whether the rescue conferred in this line [30, 210] derives from an effect on ubiquitination of mitochondrial proteins. For all overexpression studies, the indicated UAS lines were crossed with *da*-GAL4 to induce whole-body expression of the protein. In the case of the $Atg5^{5cc5}$ line, to overcome issues with poor fitness of the line, heterozygous virgin females were crossed with w^{1118} males, and males hemizygous for the $Atg5^{5cc5}$ allele were analysed. $Pink1^{B9}$ males were collected from balanced stocks, and due to poor fitness of the line and amount of material required for analysis, only one replicate was analysed. The $Atg5^{5cc5}$; *da>park* and $Pink1^{B9}$; *da>park* lines were generated by crossing the $Atg5^{5cc5}$; *da*-GAL4 and $Pink1^{B9}$; *da*-GAL4 lines respectively with UAS-$park_{C2}$ to generate males of the desired genotype. The preparation of mitochondrial Ub from all lines was performed with whole male flies according to Figure 4.13A. The total Ub abundance in each 500 μg mitochondrial sample is shown in Figure 4.14A. Only modest differences among genotypes and biological replicates were observed, with the exception of a single data point from the $Atg5^{5cc5}$; *da>park* line, and the single data point available from $Pink1^{B9}$, which are likely to be outliers. Therefore, the various genetic manipulations performed did not substantially affect the total mitochondrial Ub abundance. A large degree of variation in the abundance of K6-modified Ub was observed, most likely because the abundance of this modification was very low and prone to fluctuations in signal-to-noise ratio (Figure 4.14B). Both the $Atg5^{5cc5}$ and $Atg5^{5cc5}$; *da>park* lines had increased K6 chain abundance compared with w^{1118} controls, as did the $Pink1^{B9}$; *da>park* line. Whether these increases represent a true increased abundance of K6 chains or a clearer signal of the lowly abundant peptide due to higher total Ub in these samples remains unclear (Figure 4.14A and B). Neither *TcPink1* or *park* overexpression alone resulted in increased K6 chain abundance compared with w^{1118}, which is surprising given the PINK1/Parkin pathway is known to produce K6 chains on mitochondria in cell culture models [204]. The fact that an increase in K6 chains was observed in the $Atg5^{5cc5}$ mutant could mean that the chains may be produced but turned over rapidly in the presence of functioning autophagy machinery. However, $Atg5^{5cc5}$; *da>park* did not have a substantially higher K6 abundance than $Atg5^{5cc5}$ alone, although significant variability across replicates was observed for this condition, which could mask true differences between the genotypes (Figure 4.14B). All genotypes tested had modestly higher K11 abundance than the w^{1118} control (Figure 4.14C). As with K6 chains, the two lines with genetic loss of *Atg5* had the highest abundance of K11-linked Ub, while parkin overexpression alone did not starkly increase K11 chains. K48-linked Ub did not dramatically change in abundance for most genotypes tested (Figure 4.14D). However, there was a slight increase in K48-linked

Ub in both *Pink1*^{B9}-containing lines relative to the other genotypes tested. In comparison, K63-linked Ub was universally more lowly abundant in all genotypes tested relative to the w^{1118} control (Figure 4.14E). Of all the Ub modifications that were quantified, S65 phosphorylation showed the most stark pattern among the genotypes tested, consistent with Ub phosphorylation being central to Pink1/parkin signalling (Figure 4.14F). As expected, overexpression of *Tc*Pink1 led to robust formation of pS65-Ub on mitochondria, while the *Pink1*^{B9} mutant mitochondria lacked detectable pS65 signal, which was not rescued by parkin overexpression in the *Pink1*^{B9}; *da>park* line. pS65-Ub could be detected in only a single replicate in the *da>park* line. These results indicate that the rescue that parkin overexpression confers upon loss of *Pink1* [210, 30] is not likely to be through the production of phosphorylated Ub. In contrast, the *Atg5*^{5cc5} mutant, both alone and in combination with *park* overexpression, led to detectable production of pS65-Ub (Figure 4.14F). This result indicates that pS65 Ub is likely to be produced on mitochondria *in vivo*, but the signal is lost due to rapid turnover of the pS65-Ub-labelled mitochondria by the autophagy machinery. *da*-GAL4-driven parkin overexpression did not lead to increased pUb in the context of the *Atg5*^{5cc5} mutant, further indicating that parkin's ability to rescue *Pink1* mutant phenotypes in *Drosophila* [210, 30] is not by production of pS65-Ub.

4.3.5 Atg5 mutants show increased Ub phosphorylation with age

To further probe the effect of ageing on the *Drosophila* mitochondrial ubiquitome, *Atg5*^{5cc5} flies were aged up to 25 days, harvested and their mitochondrial Ub content evaluated by AQUA MS. *Atg5*^{5cc5} flies survive to adulthood but exhibit severe mobility defects that can be rescued by expression of human Atg5, thereby demonstrating that the protein's function is conserved from flies to humans [117]. This model was chosen due to the higher baseline pS65-Ub levels observed in *Atg5*^{5cc5} flies compared with w^{1118} flies (Figure 4.14F) and because loss of *Atg5* would be expected to reduce turnover of damaged mitochondria due to a reduction in autophagy [117, 288]. Therefore, any Ub modification that accumulates with ageing upon loss of Atg5 may indicate that this modification is produced during age-related mitochondrial damage and specifically turned over by autophagy. As shown in Figure 4.15, the total Ub content and normalised amounts of pS65, K6, K11, K48 and K63 Ub modifications were plotted against the average age of the flies at the time of harvest. Linear regressions were performed to determine whether a relationship between age and Ub modification abundance existed, with the p-value for a test of non-zero linearity displayed on each graph. Total Ub abundance and pS65-Ub showed an upward trend with increasing

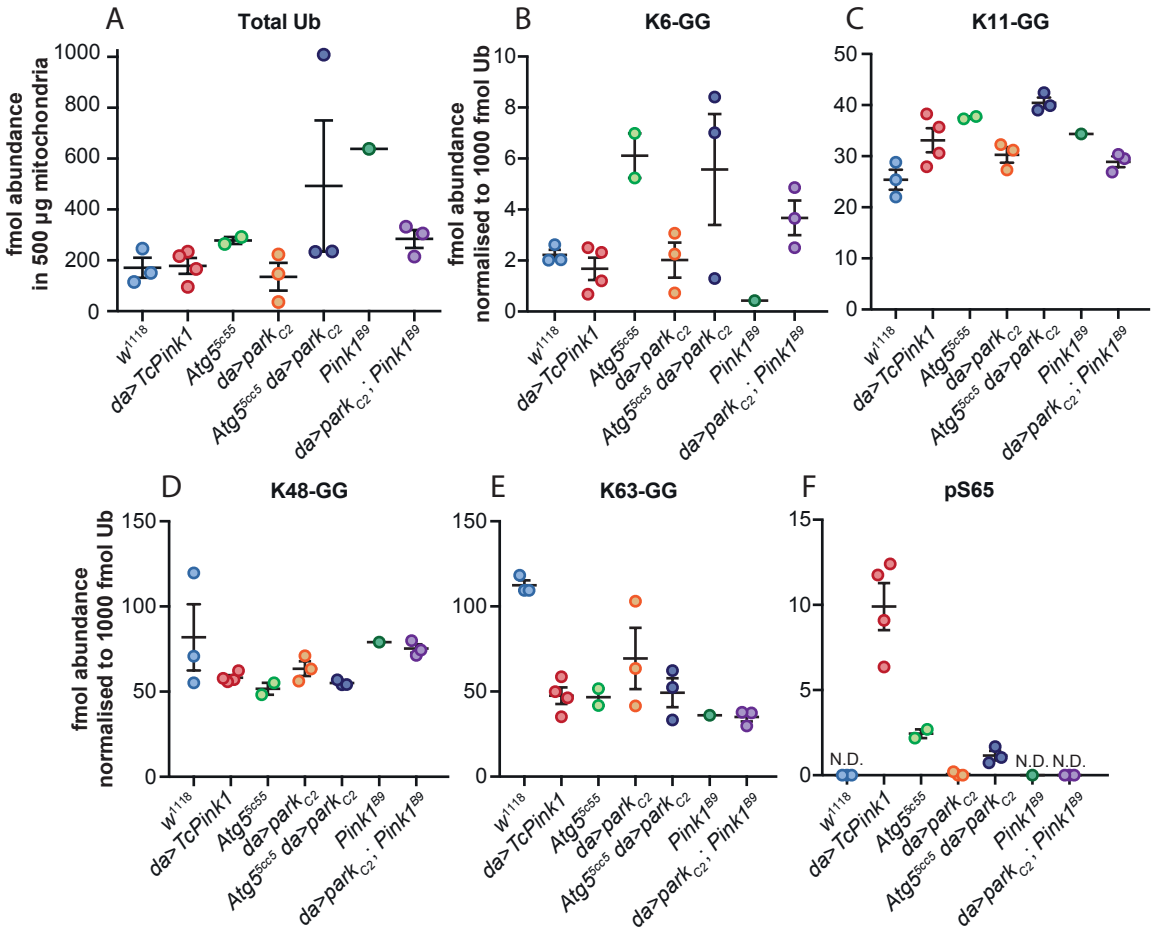

Fig. 4.14 **Genetic manipulations of *Pink1*, *park* and *Atg5* have modest effects on the mitochondrial ubiquitome. A.** Total mitochondrial Ub abundance in flies of the indicated genotypes after sample preparation according to Figure 4.13A. Each data point represents an independent biological replicate. **B-F.** fmol abundance of the indicated Ub modifications, normalised to 1000 fmol Ub for each sample. Error bars represent mean +/- SEM. N.D.: not detected.

age, although only pS65-Ub met the threshold for statistical significance (Figure 4.15A and F). K6-GG and K63-GG both trended downward with age, although the data were scattered and the association therefore did not reach statistical significance (Figure 4.15B and E). In comparison, K11-GG and K48-GG remained mostly unchanged regardless of the age of the flies at harvest (Figure 4.15C and D). These results indicate that pS65-Ub, but not any specific Ub linkage type, accumulates on mitochondria in an age-dependent manner when autophagy is defective. This may indicate that K11 and K48 chains on mitochondria can be removed by an autophagy-independent process such as p97-dependent extraction and delivery of the ubiquitinated substrates to the proteasome [277, 203], while pS65-Ub may be resistant to this process. These age-dependent trends agree reasonably well with the ageing of w^{1118} flies, with the exception of a marked increase in K6 chains in the w^{1118} mitochondria (Figure 4.13). However, it should be noted that young $Atg5^{5cc5}$ flies have increased K6 chains relative to w^{1118} controls (Figure 4.14C). These results indicate that increased K6 abundance is an early event in the $Atg5^{5cc5}$ flies, while accumulation of pS65-Ub occurs gradually over time. Further work will be required to dissect whether pS65-Ub, K6 chains, K63 chains or bulk mitochondrial Ub is the bona fide mitophagy signal, as discussed further in Chapter 5.

4.3.6 The mitochondrial ubiquitome of mouse brain determined using Ub-clipping

Given the association of PINK1 and Parkin with early-onset parkinsonism that causes degeneration specifically in the brain [122, 295], AQUA MS analysis of the mitochondrial ubiquitome was next applied to mouse brains. The CD1 mice were harvested at the age of 3 months and mitochondria were extracted from whole brains. Like in flies, the Ub content on mouse brain mitochondria was very low, and therefore the samples were prepared and analysed as in Figure 4.13A. The total Ub abundance on 500 μg mouse brain mitochondria was 1.3 pmol (Figure 4.16A), which was approximately five-fold more than was present on w^{1118} mitochondria. Of the four Ub chain types tested, K48-GG was the most highly abundant, followed by K63 and K11 chains (Figure 4.16B). In contrast, K6-linked Ub was very lowly abundant, and pS65-Ub was not detected under the conditions used (Figure 4.16B). A previous study in cortical neurons showed a pS65-Ub abundance of approximately 5 fmol per 1000 fmol Ub in whole cell lysates [216]. Assuming co-enrichment of the pS65-Ub in mitochondrial extracts, the abundance of pS65-Ub per 1000 fmol total Ub would be expected to be higher than 5 fmol in the context of mitochondrial enrichment presented herein, which would be above the limit of detection. The results presented in this study used whole brains

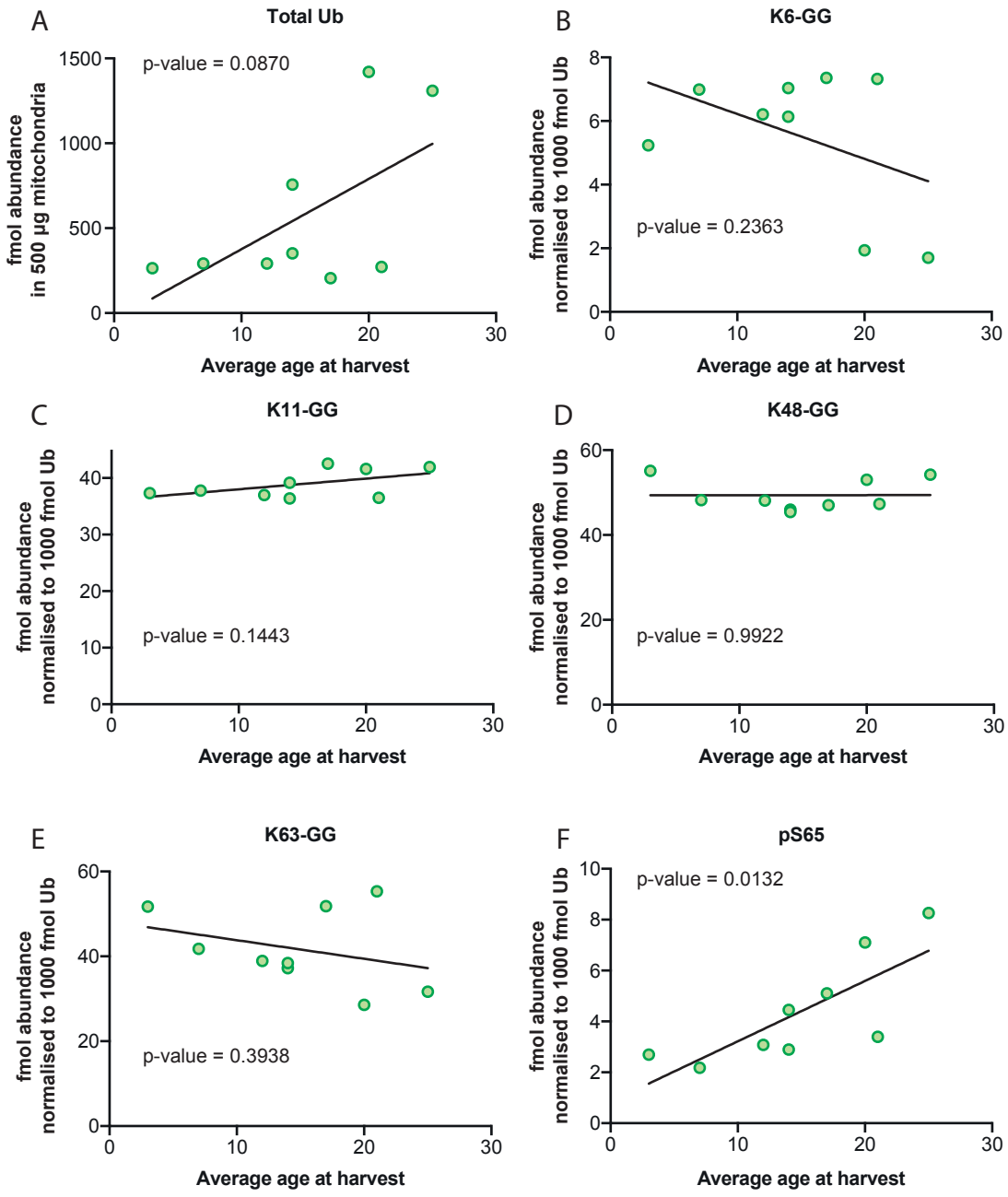

Fig. 4.15 ***Atg5*^{5cc5} flies display increased pS65-Ub with age. A.** fmol abundance of total Ub in 500 μg mitochondria from *Atg5*^{5cc5} flies harvested at the indicated ages, and prepared as per Figure 4.13A. A linear regression was performed, with the trendline and p-value for non-zero linearity displayed on the graph. **B-F.** fmol abundance, normalised to 1000 fmol Ub, of the indicated Ub modifications for flies treated as in A. Note that only pS65-Ub reaches the threshold for statistical significance ($p < 0.05$).

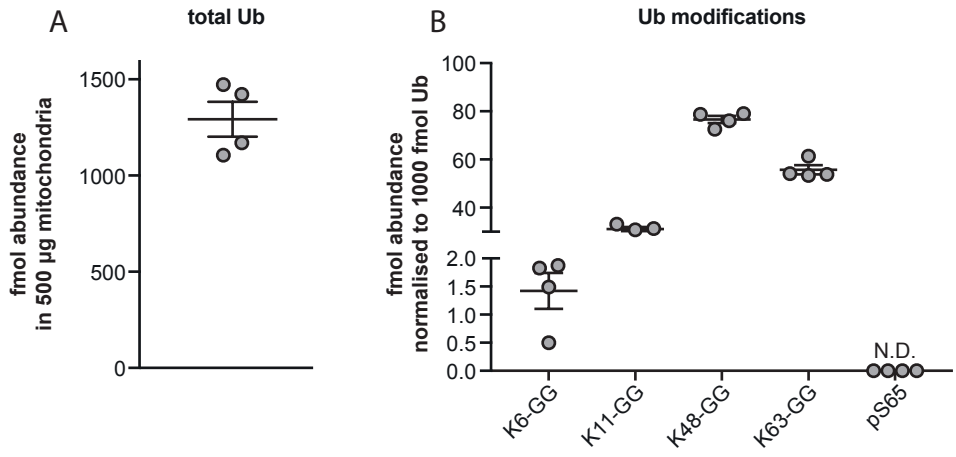

Fig. 4.16 **The mouse brain mitochondrial ubiquitome determined using AQUA MS. A-B.** Whole brains from CD1 mice were enriched for mitochondria, then the mitochondrial ubiquitome determined as in Figure 4.13A. The total Ub in 500 μg mitochondria (**A**) and the normalised abundance of the indicated Ub modifications (**B**) is shown. The data points (+/- SEM) represent data from four different mouse brains. N.D.: not detected.

rather than cortical sections that may be enriched for pS65-Ub, which may explain why pS65-Ub was not detected in this study. Interestingly, while other studies have shown no change in pS65-Ub levels in cortical sections from Parkin null mice compared with WT controls [216], later studies found an approximately five-fold increase in pS65-Ub levels in heart sections of Parkin null mice compared with WT controls, when normalised to total cell protein content [261]. Therefore, the exact quantification of pS65-Ub levels may depend on the precise tissue type being examined. These data support the notion that pS65-Ub is generated in response to mitochondrial damage, and is not highly abundant in young, healthy mice [216, 261].

4.4 Discussion and conclusions

4.4.1 What is the Parkin-dependent mitochondrial ubiquitome in cultured cells?

This chapter combined Ub-clipping and MS to investigate the architecture of the mitochondrial ubiquitome in HeLa cells. A summary of the findings from these investigations using intact MS and AQUA MS is shown in Table 4.1. The increase in total Ub and pS65-Ub in the presence of both endogenous PINK1 and exogenous WT Parkin in the context of depolarisation confirms previously reported findings in support of a positive feedback loop

of pUb production, in which PINK1 acts upstream of Parkin [204, 201]. The chain type and pS65-Ub content on mitochondria agreed reasonably well with previous *in vitro* Parkin chain assembly assays, and with results obtained under chemical depolarisation in other cell models [204, 310, 36]. However, in contrast to the reported literature, the abundance of K63 chains relative to the total Ub content, was reduced in the present study in depolarised cells expressing WT Parkin (Figure 4.12C). This difference in results is likely to reflect subtle differences in data presentation; given that K63 chains are abundant without PINK1/Parkin activation, a modest fold-increase in their abundance would represent a large change when measured as an absolute fmol increase over unstimulated cells [204]. Another finding that has not been emphasised by previous studies is the degree of substrate monoubiquitination observed in comparison to chain formation. It has been previously described *in vitro* [111], and further established in this study (Figures 4.6 and 4.12), that Parkin is predominantly a monoubiquitin ligase. The makeup of the mitochondrial ubiquitome, both in stimulated and unstimulated conditions, is important for determining the precise signal that is recognised by the downstream autophagy machinery; the possible identity of the bona fide mitophagy signal is discussed further in the following chapter.

Interestingly, across both the intact and AQUA MS methods, an increased stoichiometry of Ub phosphorylation was observed when WT Parkin was present, compared with C431S Parkin in otherwise identical conditions of OA treatment in the presence of endogenous PINK1 (Figures 4.6B and 4.12C). This is in contrast to a previous study that found that WT Parkin was required for the production of pS65-Ub [204]. These observed differences may be due to the use of a longer incubation with OA in the present study, and also support the previously reported findings that PINK1 can stimulate mitophagy, albeit more slowly, in the absence of WT Parkin [139]. Given that the ratio of PINK1 to mitochondrial Ub is higher in the absence of WT Parkin, this finding indicates that Parkin activity increases the activity of PINK1 towards Ub. Two explanations for this are possible: either the Ub chain types and monoubiquitination produced by Parkin are more ideal substrates for phosphorylation by PINK1 than the Ub conjugated by other E3 ligases, or Parkin produces ubiquitinated substrates in close proximity to PINK1. It has been shown that efficient Ub phosphorylation by PINK1 requires a strand slippage event in Ub (termed Ub-CR) to provide PINK1 with the necessary access to S65, which is buried in the "common" Ub conformation [310, 41, 65]. The dynamics of this slippage event may depend on how much dynamic flexibility is present in the Ub C-terminus, which could in turn depend on the substrate to which the Ub is conjugated. However, there is little evidence that PINK1 has significantly increased preference

for phosphorylation of specific Ub chain types, at least *in vitro* [204, 310, 63]. In fact, PINK1 appears to phosphorylate the proximal moiety of K6 chains, which are produced by Parkin, less efficiently than it does for K48 or K63 chains [63]. Indeed, the results presented herein support the notion that K63 chains on mitochondria are readily phosphorylated by PINK1 (Figure 4.12). It is possible that certain specific mitochondrial substrate lysines, when ubiquitinated, may provide better conditions for Ub strand slippage to occur. A finding to this effect would help to explain how PINK1 is able to phosphorylate Ub *in vivo*, which in the unphosphorylated form has only very low proportions of Ub-CR [65]. However, PINK1 is able to phosphorylate Ub *in vitro* with no other protein factors present [104, 112, 129], so induction of the strand slippage event by external factors is not a requirement for phosphorylation. An alternative explanation for Parkin E3 ligase activity increasing the stoichiometry of Ub phosphorylation is that binding to pS65-Ub, which occurs during Parkin's activation sequence, causes Parkin to be spatially restricted in close proximity to PINK1 on the OMM [204, 309]. In turn, the production of Ub chains by Parkin on the OMM would be spatially restricted to within close proximity of PINK1. Tethering of Parkin to the OMM would avoid aberrant ubiquitination of undamaged mitochondrial or cellular substrates by Parkin, which appears to have low substrate specificity due to its highly flexible catalytic RING2 domain when fully active [64, 245]. Therefore, it is likely that Ub phosphorylation by PINK1 results in both recruitment and retention of Parkin at the OMM in close proximity to PINK1.

Ub-clipping enabled further investigation into the mitochondrial ubiquitome beyond its composition, to establish the Ub chain architecture. The intact MS analyses revealed that the majority of mitochondrial ubiquitination events are likely to be monoubiquitination or short chains, with very little chain branching. Further, it was found that Ub is preferentially phosphorylated on mono-Ub moieties or the distal end of chains. These findings were recently confirmed independently using the same Ub-clipping technology, although different purification methods were used [203]. It has been found that, *in vitro*, PINK1 preferentially phosphorylates the distal moiety of K6 di-Ub, while USP30 has reduced DUB activity towards distally phosphorylated Ub chains of any linkage type [63]. The preference for distal Ub phosphorylation was not observed when analysing the K63 locus by AQUA MS (Figure 4.12C). This is likely to be because K63 chains exhibit a relatively open conformation [127], which would better allow access by PINK1. Indeed, the preference for distal Ub phosphorylation by PINK1 was not observed when analysing K63 chains *in vitro* [63]. It would be interesting to determine whether modulation of USP30 levels would affect the apparent preference for distal or mono-Ub phosphorylation, to disambiguate the relative roles

of PINK1 and USP30 in this process. A model for PINK1- and Parkin-dependent production of pS65-Ub on mitochondrial substrates in the context of chemical depolarisation is presented in the following chapter, based on the findings in this thesis and from the scientific literature.

4.4.2 What is the *in vivo* mitochondrial ubiquitome?

While much work has been done to establish the role of Parkin in mitophagy induced by chemical depolarisation in cultured cells, very little work has been done to investigate this process at the organismal level. Therefore, Ub-clipping was applied to the study of the mitochondrial ubiquitome of *Drosophila*, to determine whether the positive feedback loop of Pink1 and parkin activity that is well-established in cell models occurs in this more physiological context. These analyses required significant optimisation of the sample preparation method, to enable enrichment of the lowly abundant mitochondrial Ub present in flies. K6, K11, K48, and K63 chains were all detected in mitochondrial extracts from w^{1118} flies, while pS65-Ub could be detected when very large sample amounts and further enrichment steps were included (Figure 4.13). Both ageing and PQ treatment induced changes in the mitochondrial ubiquitome, as did various genetic manipulations of the mitophagy machinery (Figures 4.13 and 4.14). The effect of these manipulations on the fly mitochondrial ubiquitome, relative to untreated w^{1118} flies, is summarised in Figure 4.17. Transgenic expression of *TcPink1* increased pS65-Ub abundance while *park* did not, which is consistent with parkin functioning downstream of Pink1. Genetic manipulations of *park* and *Pink1* had only modest effects on the total Ub and abundance of most chain types (Figure 4.17). These results indicate that, in flies, overexpression of Pink1 or parkin alone does not induce feedforward ubiquitination of mitochondria. While overexpression of parkin has been shown to rescue *Pink1* mutant phenotypes [210, 30], the effect on mitochondrial ubiquitination was modest (Figures 4.14 and 4.17). No pS65-Ub was detected in these flies, which confirms that Pink1 is the sole Ub kinase and that parkin's ability to rescue *Pink1* mutant phenotypes is pS65-Ub independent. The modest effect on mitochondrial ubiquitination in these flies suggests that parkin's ability to rescue *Pink1* mutant phenotypes could be independent of its role in ubiquitinating mitochondrial proteins. Indeed, Parkin has been shown to ubiquitinate non-mitochondrial targets in cell culture models [242], which could indicate a role for the enzyme in other pathways. Alternatively, the effect of parkin expression on mitochondrial Ub may be lost in the context of constant autophagic turnover of ubiquitinated mitochondria. However, transgenic parkin expression in the context of genetic ablation of *Atg5*, which should significantly reduce autophagic flux, did not result in large differences compared with

Table 4.1 **Summary of the mass spectrometry findings on the Parkin-dependent mitochondrial ubiquitome in HeLa cells.**

Method	Findings
Intact MS	• Detectable pS65-Ub production is dependent on OA treatment but not on the presence of WT Parkin • WT Parkin increases the stoichiometry of Ub phosphorylation when compared with C431S Parkin • WT Parkin increases total mitochondrial ubiquitination in the presence of depolarisation, with no apparent increase in average chain length • Distal or mono-Ub is preferentially phosphorylated in a WT Parkin-independent manner • UBE2L3 is multi-monoubiquitinated by WT Parkin *in vitro*
AQUA MS	• WT Parkin increases bulk ubiquitination and the relative abundance of K6, K11, K48 and pS65 modifications in the presence of OA and endogenous PINK1 • WT Parkin increases the stoichiometry of S65-Ub phosphorylation when compared with C431S Parkin • K63 chains are reduced relative to total Ub (but absolute K63 levels are higher) upon OA treatment when WT Parkin is present • K48 and K63 chains increase modestly in the presence of C431S Parkin and endogenous PINK1 compared with *PINK1*$^{-/-}$ cells • There is no apparent preference for or against phosphorylation of K63 chains

the *Atg5* mutant alone (Figure 4.14, Figure 4.17). A further discussion of the role of parkin *in vivo* is provided in Chapter 5.

In contrast, ageing, PQ treatment, and genetic ablation of *Atg5* all resulted in increased total Ub and pS65-Ub, while ageing and *Atg5* mutants showed increased K6 and K11-linked Ub (Figure 4.13, 4.14, Figure 4.17). PQ treatment of WT flies resulted in the strongest induction of pS65-Ub production, which indicates that mitochondrial oxidant-induced PINK1 activation can occur robustly within an animal in the presence of endogenous levels of Pink1 and parkin. Further studies using PQ in combination with genetic modulation of *park* levels could reveal whether parkin participates in a feedforward mechanism of pUb production in *Drosophila*, as it does in cultured cells. The evidence of increased mitochondrial pUb with ageing, in the absence of chemical stimulation, supports the notion that mitochondrial damage accumulates as the fly ages due to a reduction in autophagy [257]. Further, the accumulation of pS65-Ub during ageing of $Atg5^{5cc5}$ flies suggests that pS65-Ub is a biomarker for the initial induction of mitophagy, upstream of Atg5.

4.4.3 Utility of Ub-clipping for studying mitophagy

The use of Ub-clipping in the analysis of PINK1/Parkin mitophagy enabled the identification of preferential phosphorylation of distal or monoubiquitinated substrates, and multi-monoubiquitination of UBE2L3 by Parkin *in vitro* - findings that would not have been possible with MS approaches that use tryptic digest. While limited trypsinolysis has been used to some effect to generate diGly-modified $Ub^{1\text{-}74}$ for the analysis of Ub chain branching, such approaches require fine-tuning of the ratio of trypsin to substrate to ensure that Ub is cleaved exclusively at R74 [296, 35]. In comparison, Lb^{pro}*'s specificity for R74 means that no further digestion of Ub occurs, even at extended timepoints [275], although the R-clipping observed herein underscores the need to ensure that endogenous enzymes are inhibited during digestion. It will be interesting in future to use Ub-clipping to investigate mitochondrial multi-monoubiquitination events *in vivo*, as described further in the following chapter.

The combination of Lb^{pro}* treatment with AQUA MS produced comparable results to other methods [204, 202], allowing the use of low sample amounts while obviating the need for diGly enrichment or any affinity-based Ub enrichment in cultured cells. One significant limitation that was encountered during optimisation of the Ub-clipping method in mitochondrial extracts from more physiological samples was the requirement for very

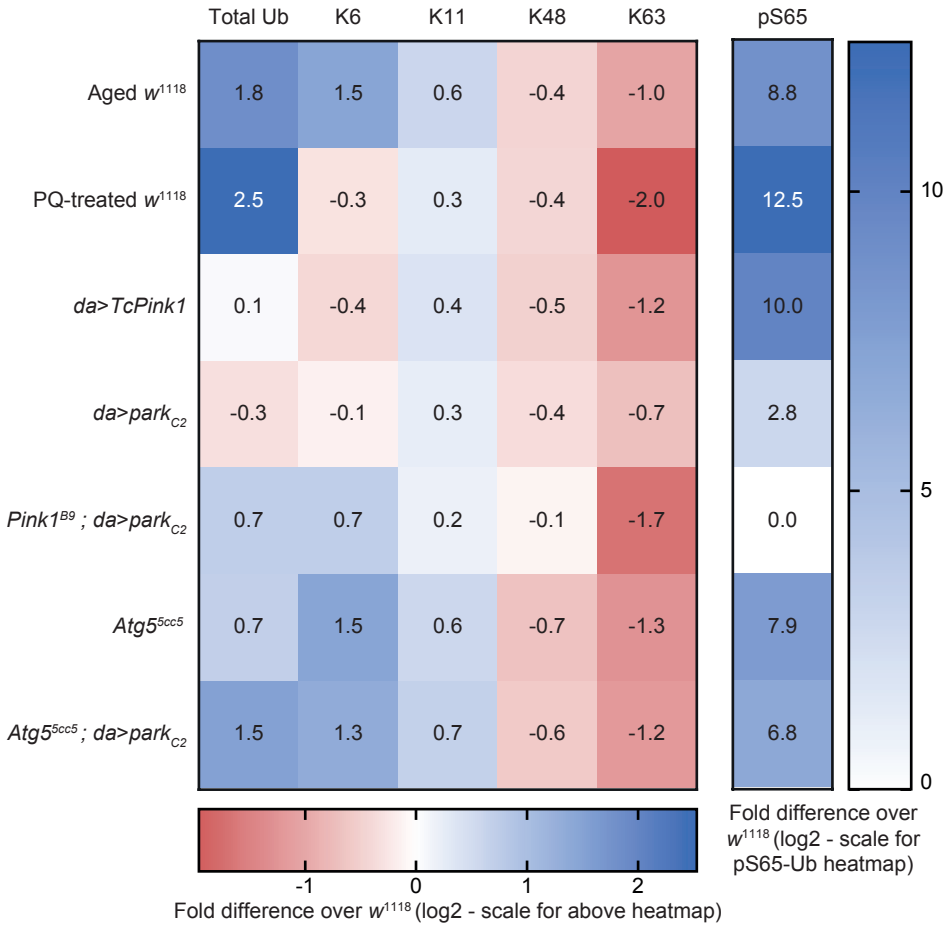

Fig. 4.17 **Effect of various manipulations of *Drosophila* on the abundance of mitochondrial Ub.** Heatmap summary of the relative change compared with young w^{1118} flies in the abundance of total Ub and Ub modifications when normalised to total Ub abundance for the indicated genetic and environmental manipulations. Note that for pS65-Ub, in order to calculate a fold change a non-zero value needed to be imputed for w^{1118} - a normalised value of 0.01 fmol per 1000 fmol Ub was chosen as this would be expected to be just below the limit of detection.

large sample amounts. This was especially difficult when analysing animal tissues, which contained much less mitochondrial Ub than even the untreated HeLa samples. Each replicate analysis of fly mitochondria, as shown in Figures 4.13-4.15, required approximately 50 to 100 flies. This requirement meant that any variation between animals could not be determined, and limited the analysis of difficult-to-aquire genotypes. Further, analysis of specific fly tissues was impractical when such large amounts were required, so the specific effects of the described manipulations on the fly brain or muscle mitochondrial ubiquitome could not be determined. Future studies using side-by-side comparisons of different methods for enrichment and analysis of diGly-modified peptides by MS could determine which method is most useful for samples in which the total Ub abundance is low.

4.4.4 Conclusion

This chapter presents the application of a new method, Ub-clipping, to the study of the mitochondrial ubiquitome in cultured cells, *Drosophila*, and mouse brain. The method confirmed previous findings into the chain composition and stoichiometry of pS65-Ub formation on mitochondria, while further identifying that Ub phosphorylation occurs *in vivo* on Ub moieties that are not further ubiquitinated. However, the role of PINK1 and Parkin outside the context of chemical depolarisation is unclear, as evidenced by very little change in the makeup of the mitochondrial ubiquitome in flies overexpressing parkin in combination with loss of Pink1 or Atg5. Importantly, it is unclear whether bulk ubiquitination, pUb, or a particular Ub chain type is the signal that is recognised by the downstream autophagy machinery. A discussion of the identity of the bona fide mitophagy signal, and the extent to which PINK1/Parkin mitophagy occurs in physiological contexts, is presented in the following chapter.

Chapter 5

Discussion

5.1 The mitochondrial ubiquitome

5.1.1 Summary of the Parkin-dependent mitochondrial ubiquitome in depolarised cells

The primary aim of this thesis was to apply the Ub-clipping method to better our understanding of the mitochondrial ubiquitome, in particular the Ub chain architecture. While the main mitochondrial substrates and Ub chain types produced by Parkin have been investigated in detail [204, 201, 36, 202], the relationship between S65 phosphorylation and chain formation had not been elucidated, and the relative contribution of chain formation versus monoubiquitination of substrates had not been explored in depth. From the intact MS results presented in Figure 4.6C, the relative abundances of the different Ub proteoforms can be applied to a pool of 20 Ub moieties; this yields 13 Ub moieties that are not further ubiquitinated (4 of which are phosphorylated), 6 that are singly diGly-modified (one of which is phosphorylated), and one that is doubly diGly-modified (Figure 5.1A). Therefore, a pool of 20 Ub moieties contains eight Ub linkage points (six singly modified and one branched Ub). The relative abundances of the different chain types determined by AQUA MS in Figure 4.12C (K6, K11, K48 and K63 at a ratio of 0.69 : 1.12 : 2.45 : 3.7, rounded to 1 : 1 : 2 : 4) can then also be applied to the pool of 8 linkage points (Figure 5.1A). This information can be combined with the information gleaned from biochemical studies presented in Chapter 3 (summarised in Table 3.1), the known mitochondrial substrates of Parkin (the most abundant of which are VDAC1 and VDAC3 [202]), and the presumed K48-linked ubiquitination of Mfn2 to facilitate its rapid degradation by the proteasome [21, 277], to provide a summary model (Figure 5.1A). In general, the mitochondrial ubiquitome consists predominantly of substrate

monoubiquitination and short chains, with phosphorylation mainly on mono-Ub moieties and the distal ends of chains. It is important to note how the composition of the mitochondrial ubiquitome changes depending on the activation of the PINK1/Parkin pathway; while K48 and K63 chains are the most abundant Ub chain type in the presence of WT PINK1 and Parkin, they are also present to an appreciable extent in the absence of Parkin and PINK1 activity (Figures 3.7A and 4.12C). Further, while the total abundance of mitochondrial Ub increased in response to depolarisation in the presence of WT Parkin, the abundance of diGly-modified Ub relative to total Ub did not drastically change relative to the untreated condition (Figure 4.6C), indicating that the chain length of the mitochondrial ubiquitome in the absence of PINK1/Parkin activation is similar to that presented in Figure 5.1A. This information is important to consider when evaluating the precise nature of the mitophagy signal produced by PINK1 and Parkin, as discussed further in Section 5.2.

The combined observations regarding pS65-Ub formation and K63 chain formation from the biochemical and MS analyses presented in Chapters 3 and 4 respectively allow insights into the co-occurence of these modifications. S65-Ub phosphorylation was unaffected by K63 chain formation, as measured by AQUA MS (Section 4.3.2), while measurements by intact MS, which incorporate the effect of all Ub chain types, showed a bias against phosphorylation and ubiquitination on a single moiety (Figure 4.5D). These results, taken together, suggest that K63 chains are overrepresented in S65-phosphorylated Ub. However, the UbiCRest analysis did not detect a preference towards phosphorylation of K63 chains, at least compared with K48 chains (Figure 3.9). Future work to determine the extent to which phosphorylation may occur on specific Ub chain types, and determining the precise identity of branched Ub moieties, could be performed using MS/MS of the doubly modified Ub species, as discussed further in Section 5.4.1.

Several apparent inconsistencies were observed when analysing the mitochondrial ubiquitome by different methods; many of these can be attributed to limitations of the methods themselves, and underscore the advantage of using multiple approaches to evaluate this complex biological system. Firstly, the affimer protection assay appeared to show a higher abundance of K6 chains in HeLa cell mitochondria than K11 and K33 chains (Figure 3.11), while the AQUA analysis showed that K11 chains were more abundant (Figure 4.12C). The AQUA results are much more likely to be accurate, given the highly quantitative nature of the method, while the extra protection apparently conferred by the K6 affimer could be from extra protection of other chain types present proximal to the K6 chain (such as K63 chains),

which may have been protected from USP21 activity by the affimer. Another discrepancy is apparent in the abundance of Ub chain types determined by intact MS compared with AQUA MS. According to the intact MS results, over 30% of the mitochondrial Ub was further diGly-modified (Figure 4.6C), compared with an apparent combined diGly composition of approximately 15% when analysed by AQUA MS (Figure 4.12C). Similarly, the proportion of pUb was apparently higher when measured by intact MS compared with AQUA MS. Several factors combined are likely to explain this observation. Firstly, the four other Ub linkage types not analysed in this study (M1, K27, K29 and K33) are likely to account for a proportion of this missing signal, although given their known low abundance from other studies [204], this will likely account only minimally for this difference. Secondly, given that branched Ub accounted for approximately 3% of the total mitochondrial Ub (or 10% of the diGly-modified Ub), if the two branchpoints were located close together in the primary sequence (such as K6/K11), the complex peptide produced during tryptic digest would not be accounted for in the targeted AQUA MS workflow. Thirdly, the lower apparent chain type abundance determined by AQUA MS could be partly due to limited efficiency of tryptic digest of the highly stable Ub moiety, and tryptic digest could be negatively affected by Ub phosphorylation. Previous studies found that S65-phosphorylated Ub produced a missed cleavage event at K63 [104, 112], although it should be noted that this peptide was not observed to an appreciable extent in the current study, presumably due to the use of relatively high trypsin concentrations (data not shown). Finally, It is possible that the intact MS quantification, which unlike AQUA only allows relative quantification, may over- or underestimate the abundance of particular proteoforms. However, Lb^{pro}-mediated digestion of *in vitro*-assembled di-Ub moieties resulted in equal proportions of unmodified and diGly-modified Ub as measured by intact MS, as expected, indicating that the intact MS method can accurately determine the relative abundance of different Ub proteoforms within a given sample [275].

5.1.2 VDAC monoubiquitination is likely a major Parkin signal

One of the most abundant mitochondrial ubiquitination events in HeLa cells in response to depolarisation in the presence of Parkin is ubiquitination of the highly abundant VDAC proteins, in particular VDAC1 and VDAC3 [202]. Given that two separate sites are highly ubiquitinated (K53 and K274 of VDAC1 each show 15% fractional occupancy in response to depolarisation [202]), and that the architecture of mitochondrial ubiquitination is predominantly mono-Ub and short chains (Figure 5.1A), this suggests that a large amount of the

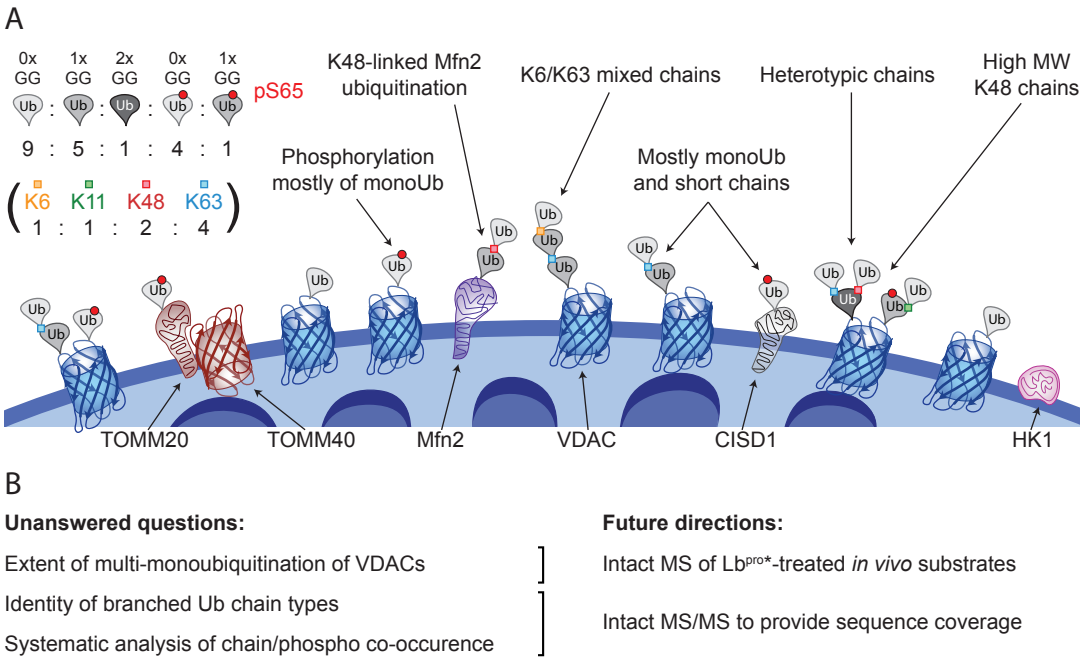

Fig. 5.1 **Model of the Parkin-dependent mitochondrial ubiquitome in response to depolarisation. A.** Using the ratio of Ub proteoforms determined in Figure 4.6C, the relative proportion of Ub chain types from Figure 4.12C, the broader architectural features determined in Chapter 3, and the most abundant Parkin substrates previously reported in HeLa cells [202], an estimation of the mitochondrial ubiquitome upon OA treatment in the presence of WT Parkin is presented. The relative abundances were applied to a pool of 20 Ub moieties to illustrate the general architecture. **B.** Three main questions regarding the makeup of the mitochondrial ubiquitome in this context remain unanswered; future method development using Ub-clipping could reveal further detail.

mitochondrial ubiquitome could consist of either mono- or multimono-ubiquitination of the VDAC proteins. While the VDAC proteins' primary function is in facilitating the transport of metabolites across the OMM [31], the VDACs have also been described as important in modulating apoptosis [26, 256] and release of mtDNA into the cytosol in response to mitochondrial damage [116]. Further, it has been recently described that ubiquitination of different VDAC K residues by Parkin can form a switch between autophagy and apoptosis [74]. The VDAC proteins have been shown to oligomerise [330], and this oligomerisation may allow the release of mtDNA into the cytosol [116]. It would be interesting to determine whether VDAC ubiquitination affects its oligomerisation, and indeed whether mono- versus multimono-ubiquitination forms a switch between different fates. In this thesis, Ub-clipping was applied to determine the extent of multi-monoubiquitination of an *in vitro* substrate, UBE2L3 (Figure 4.8). The method could be applied to determine the extent of mono- versus multimono-ubiquitination of the VDAC proteins (Figure 5.1B), although optimisation of protein enrichment and solubilisation of these integral membrane proteins are two notable technical hurdles to be overcome.

5.1.3 Is the mitochondrial ubiquitome maintained across different tissues and species?

The mitochondrial proteome differs between different tissues within a particular organism, with mitochondria from any two mouse tissues sharing approximately 75% of their mitochondrial proteomes [208]. This presumably enables mitochondria to perform specific functions according to the needs of the particular cell type. It could therefore be expected that the makeup of the mitochondrial ubiquitome, including the chain type complement, could differ between different tissues. Within this study, AQUA analyses were performed both on HeLa cells, a human cell line originally derived from a cervical carcinoma [248], and on mouse brain homogenates. Unfortunately, given the difference in species and treatment prior to tissue collection, there are a number of caveats with directly comparing the mitochondrial ubiquitomes of the two samples. Nonetheless, there was a noticable difference in the relative amount of K48 and K63 chains in the two tissues, with the mouse brain having a higher K48 chain content (Figures 4.12C and 4.16B). Interestingly, an independent study of both primary and stem cell-derived neurons similarly found that these cells contained a higher relative K48 chain complement than HeLa cells, with and without depolarisation [202]. It was also observed in this study (Figure 4.16B), and independently [202], that neuronal tissues do not appear to have a large amount of K6-linked Ub. A number of differences were also observed

between the mitochondrial ubiquitomes of HeLa cells and *Drosophila* whole flies, although, again, it is difficult to directly compare samples that have been subjected to different stimuli. Regardless, mitochondrial damage induced by depolarisation in HeLa cells expressing WT Parkin led to a robust increase in K6 chains (Figure 4.12C), while mitochondrial damage induced by PQ did not similarly lead to an increase in K6 chains in flies (Figure 4.13D). It is possible that differences in the makeup of the mitochondrial ubiquitome could result in different fates for mitochondria of specific tissues in response to otherwise identical stressors; further work is needed to explore this hypothesis.

5.2 What is the bona fide mitophagy signal?

During Ub-dependent mitophagy, the Ub-binding mitophagy receptors (OPTN, NDP52 and to a lesser extent TAX1BP1 in HeLa cells) are recruited to damaged mitochondria, resulting in autophagy initiation [139]. The vast array of different ubiquitination events produced by Parkin, and the presence of S65-phosphorylated Ub on damaged mitochondria, means that a wide variety of Ub signals are present on mitochondria. Is a particular Ub species responsible for inducing mitophagy, and if so, which one? Such a signal would need to be highly specific for damaged mitochondria, and presumably would increase in abundance on mitochondria upon activation of the PINK1/Parkin pathway, or upon a reduction of autophagic turnover, which is known to decline with age [257]. A discussion of the candidate binding partner for the autophagy receptors follows, based on the results of this thesis and the scientific literature.

5.2.1 K63 chains

One early MS-based study of mitochondrial ubiquitination produced by PINK1 and Parkin proposed that K63 chains may be the "eat me" signal for mitophagy [201]. Several lines of evidence supported this: firstly, upon chemical depolarisation in HeLa cells, a large amount of K63-linked Ub was produced in a Parkin-dependent manner, when measured as a fmol increase in chains upon depolarisation compared with an unstimulated control [204]. Secondly, replacing the cellular Ub pool with a Ub K63R mutant, so that K63 chains could not be formed, resulted in reduced clearance of damaged mitochondria [201]. Finally, several studies found more favourable binding of the autophagy receptors OPTN, NDP52 and p62 to K63 chains compared to K48 chains [201, 83, 232]. In contrast, several lines of evidence, including work presented herein, suggest that K63 chains may not be the bona fide mitophagy

signal. Firstly, it is evident that K63 chains are present on mitochondria prior to stimulation [204], and in the absence of PINK1 activity (Figure 4.12C). The baseline abundance of K63 chains in more physiologically relevant mouse brain tissue (Figure 4.16B) and neuronal cells [202] is lower than in HeLa cells; however, K63 chains did not increase substantially upon depolarisation in neuronal cells [202]. Indeed, neither ageing nor PQ treatment of flies increased the proportion of K63 chains relative to the total Ub (Figure 4.13G), indicating that this is not the major signal produced on damaged mitochondria *in vivo*. Likewise, every genetic manipulation of *Drosophila* trialled in this study led to a reduction in the proportion of K63 chains relative to the total Ub, compared with w^{1118} (Figure 4.14E), and ageing of *Atg5*-deficient flies similarly did not lead to increased mitochondrial K63 chains (Figure 4.15E). Further, more in-depth qualitative analyses of (phosphorylated) OPTN binding to all possible Ub linkage types revealed that OPTN binds M1, K6, K27, K29, and K33 chains as well or better than K63 chains [232]. Phosphorylated OPTN bound poorly to K48-linked Ub, which explained the apparent preference for K63 chains observed in previous studies [232, 201, 83]. The fact that K63 chains are present at reasonably high abundances in the absence of mitophagy induction, do not change dramatically in abundance upon stimulation, and that the autophagy receptors bind favourably to other Ub chain types, together suggest that K63 chains are not the bona fide mitophagy signal.

5.2.2 K6 chains

K6 chains are an attractive candidate as a mitophagy signal; they are an atypical linkage type produced by Parkin [204] and hydrolysed by USP30 [36, 310, 63, 243], providing a tunable signal that could be specific to mitophagy. K6 chains are very lowly abundant in cells in the absence of chemical depolarisation [204], or PINK1 or Parkin activity (Figure 4.12C), and show a large fold increase in abundance upon depolarisation [204, 36]. Further, when the cellular Ub pool was replaced with K6R Ub, depolarisation-induced mitophagy was impaired [201], although it should be noted that mutations near either terminus of Ub may not be well-tolerated in cells [236]. K6-linked ubiquitination of TOMM20 has been described as being regulated by USP30 [63], while TOMM20 ubiquitination has been described as important for the induction of mitophagy [10], leading to the proposal that K6-ubiquitinated TOMM20 is a mitophagy signal [63]. However, only a small fraction of TOMM20 appears to be modified with K6-linked Ub (Figure 3.10C), while targeting of PINK1 to peroxisomes is sufficient to induce pexophagy [136], which suggests that PINK1 is the sole mitochondria-specific factor that is required for damage-induced mitophagy. Also,

while K6 chains exhibit a large fold increase in abundance in response to depolarisation, their absolute abundance on mitochondria is still low (Figure 4.12C). This caveat could be overcome if K6 chains were bound with much higher affinity by the autophagy receptors than other chain types, but this does not appear to be the case, at least for OPTN [232]. Further, PQ treatment of flies did not substantially increase the mitochondrial K6 chain abundance, and K6 chains did not increase upon ageing of $Atg5^{5cc5}$ flies, which suggests that K6 chains do not participate in mitophagy, at least in *Drosophila*, although young $Atg5^{5cc5}$ flies and aged w^{1118} flies did display a slight increase in K6 and K11 chains (Figure 4.17). It has also been observed that depolarisation of embryonic stem cell-derived neuronal cells or DA neurons, unlike HeLa cells, failed to induce an increase in the abundance of K6 chains [202]. However, the contribution of USP30 in these scenarios was not established, and the lack of K6 chains may simply reflect their rapid removal from mitochondria by USP30. It would be interesting to investigate whether the lack of K6 chains in these systems is due to USP30 activity and, if so, whether modulating USP30 activity affects the downstream fate of the damaged mitochondria in a K6 chain-dependent manner. It should also be noted that while USP30 has a well-conserved specificity for hydrolysing K6 chains, this specificity is conferred solely by preferential binding to K6 chains; USP30 has higher activity towards K11 and K48 chains once bound, which influences USP30's apparent chain type specificity depending on the concentration of Ub chain types present [63, 243]. The functional relevance of K6 chains on mitochondria therefore remains unclear.

5.2.3 pS65-Ub

One candidate mitophagy receptor is pS65-Ub itself, given that it is genuinely unique to and exquisitely dependent on PINK1 activity. Indeed, upon overexpression of PINK1 in the absence of Parkin, it was shown that depolarisation could result in the recruitment of autophagy receptors to mitochondria and the initiation of mitophagy, presumably solely through the production of pS65-Ub [139]. Further, endogenous mitophagy receptors were found to preferentially bind to S65D mutant Ub over WT or S65A [139]. Several lines of evidence presented herein also support this hypothesis, although it should be noted that processes downstream of mitochondrial ubiquitination were not studied. Firstly, pS65-Ub was very lowly abundant in the absence of depolarisation in cells (Figure 4.12C) and young, healthy flies (Figure 4.13I), consistent with a signal that is switched on only when required. Further, unlike any specific chain type, pS65-Ub increased with age upon genetic loss of *Atg5* (Figure 4.15), and was the only Ub modification to appreciably increase in abundance

upon PQ treatment of flies (Figure 4.13). However, *in vitro* binding assays using pS65-Ub (as opposed to S65D mutants) have found that the autophagy receptors OPTN, NDP52 and TAX1BP1 bind less efficiently to pS65-Ub than unphosphorylated Ub [201, 83]. Indeed, it has been shown that neither S65D or S65E Ub mutants recapitulate the function of pS65-Ub, presenting a further caveat to the use of Ub mutants [201]. Further, increasing the stoichiometry of Ub S65 phosphorylation by overexpression of PINK1 was shown to be inhibitory towards autophagy receptor recruitment in cells [202]. Another recent study using ectopic targeting of Ub constructs to the OMM showed initiation of autophagy in the absence of PINK1, and therefore presumably pS65-Ub [321]. It is therefore likely that the function of Ub S65 phosphorylation is in the recruitment of Parkin to drive a positive feedback loop of Parkin recruitment and ubiquitination of mitochondrial proteins to enable amplification of the mitophagy signal [204, 202]. Secondary to this, pS65-Ub may protect chains from hydrolysis by USP30 [310], which could explain why PINK1 overexpression resulted in autophagy receptor recruitment in the absence of Parkin [139].

5.2.4 Bulk ubiquitination

Another potential signal for recruitment of autophagy receptors is simply a large abundance of ubiquitinated mitochondrial proteins. Indeed, the results presented herein suggest that the vast majority of Parkin-dependent Ub signal in HeLa cells is monoubiquitination of OMM substrates (Figures 4.6C-D and 4.12). Further, the abundance of total mitochondrial Ub increased upon PQ treatment and ageing of w^{1118} and $Atg5^{5cc5}$ flies (Figures 4.13B and 4.15A). However, the techniques used in this thesis relied on normalisation of the abundance of each Ub modification against the total Ub abundance. This approach therefore prevented normalisation of the total Ub abundance, meaning that the total Ub measurements were prone to large amounts of variation. A recent, independent application of Ub-clipping to the analysis of mitochondrial Ub proteoforms produced by Parkin showed an even higher abundance of Ub that was not further modified by ubquitination or phosphorylation than shown in this thesis (more than 90% unmodified $Ub^{1\text{-}74}$ even after 6 h OA treatment in the presence of WT Parkin [203]). However, the authors did not attempt to deplete the highly abundant unconjugated Ub that is clearly associated with isolated mitochondria (Figure 3.1E), thus precluding a clear interpretation of the abundance of substrate monoubiquitination in that study. Nevertheless, it is clear from this thesis and, for example, from the high stoichiometry of primary site ubiquitination in particular of the highly abundant VDAC1 (approximately 15% at two different sites [202]) that substrate monoubiquitination is the

major Parkin-dependent ubiquitination event. Further, an *in vitro* screen found a wide range of Ub chain types were bound by OPTN [232], so it could be possible that OPTN also recognises monoubiquitination of (specific) substrates. It has been observed that OPTN binds preferentially to longer K63-linked chains [83], which could indicate that longer chain length on mitochondria may result in recruitment of autophagy receptors. However, while it is difficult to directly measure chain length, the relative abundance of diGly-modified Ub did not change appreciably upon depolarisation or in the presence of WT Parkin (Figure 4.6C). This result suggests that chain length was minimally affected. Indeed, a recent study found that targeting of a linear di-Ub construct to the OMM was sufficient to recruit OPTN to otherwise healthy mitochondria [321]. The di-Ub was not simply a substrate for further ubiquitination, as a Ub K0 construct (in which all lysines are mutated to arginine) strongly induced mitophagy initiation [321]. It therefore appears that long chain length is not a requirement for autophagy receptor binding. However, an important caveat of the study was the use of a linear di-Ub construct, which binds OPTN well regardless of chain length [232] but is not present to an appreciable extent on mitochondria, even after depolarisation (Figure 3.8B) [204, 36, 202, 275]. The recruitment of OPTN to linear di-Ub-decorated mitochondria may therefore represent an artefact of the experimental setup [321].

5.2.5 Combinatorial modifications

The fact that Parkin produces a range of Ub chain types on mitochondria suggests that a more complex ubiquitination event may constitute the mitophagy signal. *In vitro* binding assays have revealed that OPTN binds M1-linked chains most efficiently, out of the eight possible Ub linkage types [232]. However, neither this work nor other reports have found evidence of M1-linked chains on mitochondria (Figure 3.8B) [204, 36, 202, 275]. Given that OPTN has been shown to be important for the induction of mitophagy [139], why does it bind most effectively to a Ub chain type not present on mitochondria? One possibility is that OPTN's most preferable binding partner is in fact a more complex type of Ub modification. Given that Parkin produces a number of chain types, it is possible that the mitophagy signal is in fact a heterotypic chain. The UbiCRest analysis revealed a di-Ub doublet released from mitochondria upon treatment with the K63-specific DUB AMSH, indicating the presence of K63-containing heterotypic chains (Figure 3.8B). The higher-migrating species could represent slow-migrating K6 chains, while the lower band likely represents another non-K63 chain type. This result suggests that heterotypic chains, a subset of which contain K6 linkages existing distal to K63 chains, may exist on mitochondria. The MS data indicated that the

degree of chain branching was low (Figure 4.6C), so this most likely represents a mixed chain. It would be interesting to determine whether any of the autophagy receptors have increased binding to K63 linkage-containing mixed chains. A recent study using ectopic targeting of di-Ub constructs to mitochondria found that a Ub K0 construct more effectively induced mitophagy induction than a construct in which Ub chains could be formed, leading the authors to conclude that chain branching may occur basally and be inhibitory to autophagy receptor recruitment [321]. However, the results presented herein do not show substantial Ub chain branching (Figure 4.6C), so this is unlikely to explain the increased receptor binding to the K0 mutant. Another candidate combinatorial modification is S65-phosphorylated K6 chains. Unfortunately it was not possible to determine whether phosphorylated K6 chains are present on mitochondria, as attempts at sequencing diGly-modified $pUb^{1\text{-}74}$ revealed poor coverage in the N-terminal region (data not shown; Figure 4.3B shows poor b-ion coverage). Further, given that the distal moiety of a K6-linked di-Ub is preferentially phosphorylated by PINK1 *in vitro* [63], and this preference appears to maintained *in vivo* (Figure 4.7), the context of the two modifications would be lost upon digestion with $Lb^{pro}*$ as they would exist on separate moieties. Several reports have found that the autophagy adaptors bind less well to phosphorylated Ub chains [201, 83], but these studies did not test phosphorylated K6 chains. A vast array of potentially complex Ub signals could therefore signal for the selective recruitment of the autophagy receptors to damaged mitochondria.

An alternative function of different chain types in mitophagy could be in the recruitment of different factors to mitochondria. While it has been shown that OPTN, NDP52, and TAX1BP1 can operate reduntantly to induce mitophagy [139], a recent study found differential recruitment of OPTN and NDP52 to mitochondria upon ectopic targeting of Ub constructs to the OMM, which may indicate that the receptors recognise different Ub signals [321]. While this discussion has centred on the role of the mammalian mitophagy adaptors, and primarily OPTN, NDP52, and TAX1BP1, it has also been observed that the Rab proteins are recruited to mitochondria in a Ub-dependent manner [322]. The authors found that RABGEF1, which contains two UBDs, is recruited to damaged mitochondria in a Parkin-dependent manner, where it recruits Rab5, then Rab7A. Rab7A in turn was important for assembly of Atg9A vesicles. This pathway was previously found to be important for autophagic degradation of damaged mitochondria by appropriately positioning the growing phagophore around the damaged mitochondria [320]. RABGEF1 was found to bind mono-Ub, pS65-Ub, K48 di-Ub and K63 di-Ub with similar affinity [322]. It would be interesting to explore whether RABGEF1 has a more complex Ub chain type preference, and

whether altering the mitochondrial Ub chain type complement has differential effects on the recruitment of the autophagy adaptors and the Rab proteins. It is also important to note that no clear homologs of OPTN, NDP52 or TAX1BP1 are known to exist in *Drosophila*, and it is unclear whether mitophagy initiation occurs in flies in a manner that is similar to that of mammalian cells.

5.2.6 Is ubiquitination sufficient to induce mitophagy?

The preceding discussion has centred on the role of Ub-dependent signalling for mitophagy, in the assumption that there are no mitochondria-specific factors – other than PINK1 – that are necessary for mitophagy signalling. Several observations support that the mitophagy signal derives solely from Ub. Firstly, artificial targeting of PINK1 to peroxisomes is able to cause autophagy of that organelle, which suggests that specific factors on the OMM (aside from PINK1) are not important [136]. Secondly, in the absence of the five Ub-binding autophagy receptors, mitophagy initiation does not occur in response to depolarisation, and cannot be rescued by reintroduction of receptor constructs that are unable to bind Ub [139]. Similarly, it is possible to bypass the Ub-binding function of autophagy receptors, and artificial targeting of NDP52 to mitochondria or peroxisomes can also initiate mitophagy or pexophagy respectively [297]. Thirdly, ectopic targeting of a linear di-Ub construct was sufficient to induce mitophagy initiation by OPTN in the absence of mitochondrial damage or PINK1 activity [321]. However, several observations suggest that other local factors may be involved in mitophagy initiation, perhaps through improving the efficiency of autophagosome formation. Firstly, while targeting of PINK1 to either mitochondria or peroxisomes can induce their autophagy, the pexophagy occurs less efficiently, and targeting PINK1 to lysosomes did not result in their autophagy [136]. Further, while artifical targeting of NDP52 to mitochondria can induce mitophagy, this occurs much less efficiently than occurs during depolarisation [297]. Given that there is some overlap between the proteomes of mitochondria and peroxisomes, including USP30, Fis1 and MUL1 [320, 188, 152], this suggests that there may indeed be other local factors that facilitate mitophagy. Further, it has been reported that cardiolipin, typically considered a mitochondrial-specific lipid, also exists in peroxisomes [317]. Given the known role for cardiolipin in mitophagy [28], this could be one such factor. Further work is required to determine the degree of conservation, both of Ub-dependent signalling and organelle-specific factors, in the autophagy of mitochondria, peroxisomes, and other cellular components, in order to better understand the process of mitophagy initiation. It also remains to be fully elucidated whether Ub-independent mitophagy, such as that mediated

by NIX or FUNDC1, occurs independently to or cooperatively with Ub-dependent mitophagy in physiological settings.

5.3 Does Parkin-dependent mitophagy occur *in vivo*?

Since the discovery that treating mitochondria with depolarising agents led to a robust induction of mitophagy in a Parkin- and PINK1-dependent manner [184, 185, 160], it has been proposed that a defect in mitophagy likely underlies the parkinsonism experienced by patients with homozygous recessive mutations in *PARK2* or *PARK6*. However, several lines of evidence suggest that mitophagy may not be the sole, or even main, pathway by which PINK1 and Parkin preserve mitochondrial integrity *in vivo*. It has been found that loss of PINK1 does not affect basal mitophagy in mice [168], and loss of either Pink1 or parkin in flies similarly does not affect basal mitophagy [142]. While this thesis did not focus on the molecular events downstream of mitochondrial ubiquitination, it was interesting to note that many of the genetic manipulations of the mitophagy machinery had only modest effects on the makeup of the mitochondrial ubiquitome. Further, while PQ treatment of flies resulted in robust formation of pS65-Ub, how can one reconcile the apparent double-hit hypothesis of PINK1/Parkin loss and exogenous mitochondrial damage with the near-complete penetrance of parkinsonism in humans with *PARK2* or *PARK6* mutations? An early indication that PINK1 and Parkin may regulate mitochondrial quality control independently of mitophagy came from a study of protein half-lives in *Pink1*-, *park*-, and *Atg7*- deficient flies [302]. Turnover of mitochondrial proteins was affected in all three lines, with some overlap between the targets of parkin and Atg7. However, a subset of mitochondrial proteins, including several encoded by the mitochondrial genome, were turned over by Pink1 and parkin independently of the core autophagy machinery. Therefore, it is possible that multiple mitochondrial quality control pathways are influenced by PINK1 and Parkin, and depolarisation-induced mitophagy may indeed be an extreme event with limited physiological relevance.

5.3.1 Mitophagy or MDVs?

A compelling candidate for the physiological role of PINK1 and Parkin is in the formation of MDVs to allow the piecemeal delivery of selected dysfunctional mitochondrial components to the lysosome. Multiple studies have identified apparent cargo-selective turnover of mitochondrial components, including the study by Vincow et al. mentioned above [302]. Additionally, PINK1 and Parkin have been observed to be specifically associated with mitochondrial frag-

ments enriched for Complex I components in a cell model with deleterious mtDNA mutations [93]. Further, overexpression of a misfolding-prone matrix-targeted protein, ΔOTC, in cells also leads to the association of PINK1 and Parkin with punctate mitochondrial-associated structures, allowing turnover of damaged components while sparing the remainder of the mitochondrial network [17]. These studies, combined with the characterisation of MDVs as vehicles for cargo-selective mitochondrial turnover (discussed in Section 1.3.9), are all consistent with a model in which the primary function of PINK1 and Parkin *in vivo* is in the delivery of damaged mitochondrial components to the lysosome via MDVs. The hypothesis is also supported by the finding that treatment of cells with Antimycin A alone primarily induces MDV formation while OA stimulated mitophagy, and that the timeline of MDV formation is more rapid than that of mitophagy [163]. Unfortunately, given the small size of MDVs, imaging them is challenging, especially within the context of an organism. It is therefore not yet known whether MDVs are formed in complex tissues such as neurons. Further, given the small size and low abundance of these vesicles, it would be difficult to analyse their Ub content as has been described for whole mitochondrial fractions in this thesis; indeed, MDVs that have budded off from mitochondria were likely to have been lost during sample preparation, which used differential centrifugation to enrich membranes of a particular density. It would therefore be useful to develop methods to enrich MDVs biochemically to determine their cargo, trafficking factors and potential ubiquitination events using unbiased approaches such as MS. Another outstanding question is how mitophagy and MDV formation are regulated with respect to one another. Do PINK1 and Parkin operate a switch between mitophagy and MDV formation? Determining the ubiquitination profile of mitochondria undergoing mitophagy, compared with that of MDVs, could determine whether the extent or type of ubiquitination determines the downstream fate of damaged mitochondrial cargo.

5.3.2 Immune regulatory roles for PINK1 and Parkin

An increasingly apparent consequence of the loss of PINK1 and Parkin activity is dysregulation of immune signalling. Indeed, large-scale association studies have found a link between PD and autoimmune diseases such as type 1 diabetes and rheumatoid arthritis [315]. PINK1 and Parkin have been described as important in suppressing the presentation of mitochondrial antigens on cell-surface major histocompatibility complex (MHC) Class I receptors, in a process that relies on the formation of MDVs [158]. This process could be triggered by lipopolysaccharide (LPS) treatment [158], and intestinal infection with a

Gram-negative bacterium was sufficient to cause PD-like phenotypes in *PINK1*$^{-/-}$ mice [157]. Innate immune activation was also observed in *PRKN*$^{-/-}$ and *PINK1*$^{-/-}$ mice that had been subjected to exhaustive exercise [261]. The immune response, and associated neurodegeneration, could be rescued by concurrent loss of STING – an immune regulator that responds to the presence of cytosolic DNA – leading the authors to hypothesise that PINK1 and Parkin function to prevent mtDNA release into the cytosol [261]. However, genetic disruption of the STING pathway in *Drosophila* was insufficient to rescue the defects caused by loss of *park* in this model, suggesting that immune suppression, through the STING pathway, is not a conserved parkin function [141]. Regardless, the implication of PINK1 and Parkin in preventing aberrant immune activation [158, 261], combined with the observation that PD-like symptoms are triggered by intestinal infection in mice [157], and the emerging role of the gut microbiota-brain axis in the etiology of PD [247], mean that this is an important avenue for future research.

5.3.3 The PINK1-Complex I connection

Defects in the Complex I of the mitochondrial OXPHOS machinery have been implicated in the etiology of PD. A specific defect in Complex I activity was observed in brain tissue from sporadic PD patients [246], PINK1 and Parkin were observed specifically associated with Complex I-positive structures in a model of mtDNA heteroplasmy [93], and an association was found between exposure to toxins that directly affect Complex I activity and onset of PD [135, 38, 278]. Several lines of evidence also point to an involvement of PINK1 in maintaining Complex I activity. Firstly, several tissues in both mice and *Drosophila* with genetic ablation of *PINK1* show a specific reduction in Complex I activity [180], and expression of the yeast enzyme Ndi1p, to bypass Complex I, is able to rescue *Drosophila Pink1*-null phenotypes [300]. Further, two separate studies independently found an interaction between PINK1 and the Complex I subunit NDUFA10 (ND42 in *Drosophila*) [219, 179]. Morais et al. [179] investigated the phosphorylation status of Complex I in mouse tissues and found that loss of PINK1 was associated with reduced phosphorylation of NDUFA10. Reintroduction of WT or phosphomimetic NDUFA10 (or ND42) was able to rescue the Complex I defect in *PINK1*-deficient cell lines or flies respectively, suggesting a role for PINK1 in the phospho-regulation of Complex I. In contrast, Pogson et al. [219] performed a screen of phenocopiers and suppressors of *Drosophila Pink1* null phenotypes and found that overexpression of ND42 was able to rescue the *Pink1* Complex I defect. However, the authors did not observe a requirement for phosphorylation of ND42, and neither study demonstrated

that PINK1 directly phosphorylates NDUFA10 or ND42 [219, 179]. Interestingly, no Complex I defect was observed in *park*-null flies, and accordingly, overexpression of Complex I-related genes ND42 and Ndi1p did not rescue the phenotypes of *park*-deficient flies [300, 219]. These studies suggest that PINK1, but not Parkin, operates in some way in ensuring the proper functioning of Complex I. In contrast, another study found that Vitamin K_2, which may act as an electron carrier to overcome OXPHOS defects, was able to rescue both *Pink1* and *park* null phenotypes in flies [304]. Further work is needed to determine precisely the mechanism by which PINK1 ensures the proper functioning of Complex I, for example whether this is in regulation of Complex I enzymatic activity, import of subunits or assembly factors, or turnover of damaged subunits or complexes. It also remains to be determined whether this proposed function of PINK1 is mediated in some way by the phosphorylation of Ub, or by the formation of MDVs.

5.3.4 PINK1/Parkin involvement in mitochondrial protein import regulation

The fact that the vast majority of mitochondrial proteins are translated in the cytosol and imported into mitochondria means that regulation of protein import can be a means of modulating mitochondrial function, and events deleterious to protein import could be very detrimental to mitochondrial function. Several reports have implicated PINK1, Parkin, or the ubiquitination of mitochondrial proteins in the regulation of mitochondrial protein import. Gehrke et al. [58] found that PINK1 and Parkin both have a positive effect on the mitochondrial localisation and translation of specific mRNAs that encode respiratory chain subunits. Genetic interaction studies in flies revealed that PINK1, Parkin and the translation repressor Pum operate in a pathway, with PINK1 most upstream and Parkin most downstream, and the authors observed ubiquitination of another translational regulator, Glo. More recently, Jacoupy et al. [100] developed a biosensor for mitochondrial protein import, which itself appeared to cause protein import stress. They found that import of the biosensor could be improved by overexpression of PINK1, Parkin, or S65D Ub. This rescue was unaffected by loss of Atg5 so was therefore autophagy-independent. Quantitative proteomics revealed an increase in K11-linked chains upon expression of the biosensor, compared with an increase in K63 chains upon OA treatment, which supports the intriguing possibility that different Ub chain types could denote alternative downstream fates. The effect was negatively regulated by USP30 overexpression, further suggesting that this is a Ub-dependent pathway. However, neither report can fully exclude that the beneficial effect conferred by PINK1 and

Parkin is through formation of MDVs [58, 100]. Further, more recent reports suggest that USP30 in fact positively regulates the import of specific mitochondrial proteins, and that this process is not regulated by PINK1 or Parkin [214, 203]. However, a role for disrupted mitochondrial import in the etiology of PD is possible, as certain forms of α-synuclein can bind to TOMM20 competitively with MTS-containing proteins, resulting in mitochondrial stress [40]. While TOMM20 was shown to interact with the TOM complex receptor subunit TOMM22 in non-neuronal cell lines, this interaction was not observed in neuronal tissues but could be observed upon knockdown of endogenous α-synuclein, suggesting that α-synuclein may interfere with the TOMM20-TOMM22 interaction basally. Given that some genetic forms of PD appear to be caused by increased levels of α-synuclein [22], and indeed α-synuclein is a major component of Lewy bodies [266], these findings suggest that the loss of DA neurons could occur due to mitochondrial damage caused by α-synuclein-induced import stress [40]. Indeed, overexpression of PINK1 or Parkin in *Drosophila* rescued the locomotor dysfunction of flies overexpressing α-synuclein [80, 281]. It would be interesting to further investigate whether this rescue is conferred by a direct regulation of mitochondrial import, or perhaps by mitochondrial turnover by mitophagy or MDV formation. Such a discovery could help to unravel which functions of Parkin and PINK1 are important *in vivo*.

5.3.5 Non-mitochondrial roles for Parkin

In the absence of mitochondrial damage, Parkin exists in the cytosol in an autoinhibited state [184, 308]. It is therefore possible that Parkin could have functions beyond ubiquitination of OMM proteins. While overexpression of parkin in flies rescues the locomotor defects induced by loss of Pink1 [30, 210], there was little effect on the mitochondrial ubiquitome in this genotype relative to w^{1118} or $Pink1^{B9}$ flies lacking parkin overexpression (Figures 4.14 and 4.17). Could Parkin's protective function in this scenario be conferred by a non-mitochondrial function? Parkin has been shown to regulate the ubiquitination of numerous non-mitochondrial substrates [242], and recently has been described as important for downstream trafficking of a subset of MDVs to the lysosome [240]. Our current understanding is that Parkin activation requires PINK1-dependent phosphorylation, both of Parkin and Ub [128, 104, 112, 129]. In order for Parkin's E3 ligase activity to be activated in non-mitochondrial contexts, an alternative activation mechanism would therefore be required to relieve the protein's autoinhibition. A recently published structure of active Parkin found that a previously unappreciated linker region, termed ACT, was important for allowing relief of autoinhibitory contacts between the UPD and the RING2 domain [64]. This linker

contained several annotated phosphorylation sites, which could allow PINK1-independent phosphoregulation of Parkin activity, thereby enabling activation of Parkin outside the OMM [64]. It has also been suggested that Parkin's RING1 domain can bind DNA, leading to the hypothesis that Parkin acts as a transcription factor in a manner independent of its E3 ligase activity [37, 42]. If Parkin does indeed function in alternative, non-mitochondrial pathways, the redistribution of Parkin to the mitochondria upon induction of damage may deplete the protein from alternative sites. However, the loss of *park* in flies results in clear mitochondrial dysfunction [71], and given the links between mitochondrial dysfunction and neurodegeneration [283], it is highly likely that Parkin's main function *in vivo* is in the maintenance of mitochondrial quality control.

5.4 Future directions

5.4.1 Development of methods to sequence diGly-modified intact Ub

An important remaining question regarding the makeup of the mitochondrial ubiquitome concerns the precise identity of the doubly modified Ub species observed (branched Ub and diGly-modified pUb). Preliminary experiments using higher-energy collisional dissociation (HCD) in a Q Exactive mass spectrometer yielded good y-ion (C-terminal) coverage, but failed to generate sufficient b-ions to gain sequence coverage of any lysine other than K63 (Figure 4.3B). Indeed, it appears that K63 chains can be branched in cells [275], but the identity of other lysine residues that participate in branching remains unclear. Two complementary approaches could be used to determine the site-specific identity of multiply-modified Ub species by MS. Firstly, alternative modes of fragmentation such as electron capture dissociation, during which fragmentation occurs more evenly along the peptide backbone than HCD, have been successfully used to gain high sequence coverage for intact Ub (a frequently used model substrate for intact MS method development) [338, 251]. To enable a more high-throughput analysis, specific software for the analysis of MS/MS spectra of diGly-modified Ub would need to be developed, as most software for targeted proteomics analysis (for example Skyline) relies on relatively simple spectra derived from small, trypsin-digested peptides [149]. Secondly, recent advances have been made in ion mobility spectrometry, a method that allows proteoforms of an identical mass to be separated based on their gas-phase mobility in the presence of an electric field [298]. Branched Ub with differently placed diGly modifications could be expected to exhibit different ion mobility, and could therefore be identified without the need for MS/MS-based sequencing. Such

an approach would first require characterisation of the ion mobility profiles of different multiply-modified Ub proteoforms of a known identity produced *in vitro*, prior to application to a complex *in vivo* sample.

5.4.2 Does paraquat induce mitophagy *in vivo*?

In this study, a robust generation of pS65-Ub on mitochondria was observed in response to non-lethal doses of PQ (Figure 4.13C). It would be interesting to probe the cellular responses downstream of pS65-Ub formation – whether the mitochondria are turned over, and whether this occurs by mitophagy – using a mitophagy probe such as mito-QC or mtKeima. Manipulation of the levels of Pink1 and parkin could also determine whether these factors are responsible for turnover of PQ-damaged mitochondria in the context of an organism. Further, the treatment could be used as a screen for other E3 ligases that may operate alongside or redundantly with parkin, and determine whether USP30 counteracts damage-induced mitophagy in a more physiological system. It would also be interesting to determine whether other forms of mitochondrial damage result in activation of the PINK1/Parkin pathway, and generation of pS65-Ub, in an organism. One alternative mode of mitochondrial damage is overexpression of ΔOTC, a form of the matrix-localised ornithine transcarbamylase enzyme that is prone to misfolding [332]. While initial studies of ΔOTC in mammalian cells found that it induced UPR^{mt} [332], more recently it was found that ΔOTC expression led to import arrest and activation of PINK1 [102]. Interestingly, this occurred without a loss of mitochondrial membrane potential, indicating that depolarisation is not necessary for the induction of mitophagy [102]. ΔOTC expression led to clearance of discrete mitochondrial fragments containing aggregated proteins rather than the entire mitochondrial network, and therefore may represent a more physiological trigger of mitochondrial damage than chemical depolarisation [102, 17]. ΔOTC expression in flies also resulted in disrupted mitochondrial function that could be rescued by concurrent overexpression of parkin [217]. However, the observed locomotor deficits were mild, and no neurodegeneration was observed in this model system, limiting its use as a physiological mitochondrial stressor [217]. Another potential physiological source of mitochondrial damage could arise from mtDNA mutations, as increased mtDNA mutations have been observed in a number of neurodegenerative diseases including PD [114]. Studies in the mutator mice, which express proofreading-deficient mtDNA polymerase (polγ) [286], have found that pS65-Ub is generated in this model, and that endogenous Parkin protects against mitochondrial damage in DA neurons [216]. However, expression of an equivalent mutant mitochondrial DNA polymerase construct in flies does not

result in strong degenerative phenotypes [109]. Recently, an alternative *Drosophila* mutator model was described, using the expression of a mitochondrially targeted cytidine deaminase, APOBEC1 [4]. This model produced a higher degree of non-synomynous mutations and consequently the flies displayed mitochondrial dysfunction, and reduced locomotor activity and survival [4]. It would therefore be interesting to determine whether either of these two models, ΔOTC or mito-APOBEC1, leads to the generation of pS65-Ub in flies, as occurs with PQ treatment, and whether this correlates with increased mitophagy in the context of an organism.

5.5 Conclusions

Given the association of PINK1, Parkin, and mitochondrial dysfunction with the pathogenesis of PD, it is vital to understand precisely how PINK1 and Parkin function to maintain mitochondrial integrity, to better understand disease progression and to provide therapeutic intervention for this currently incurable disease. PINK1 and Parkin, a kinase and Ub ligase respectively, operate in a pathway that generates S65-phosphorylated Ub on mitochondrial substrates. In this thesis, a new method, termed Ub-clipping, was applied to understand the architecture of the Ub signal produced on damaged mitochondria by Parkin, revealing that the majority of the signal consists of short chains and monoubiquitinated substrates, with phosphorylation predominantly on mono-Ub moieties and the distal ends of chains. Ub phosphorylation occurs independently of Parkin activity, but is increased in the presence of WT Parkin and is absolutely dependent on PINK1. Further, the mitochondrial Ub composition of *Drosophila* was determined for the first time, and it was discovered that PQ treatment robustly induces the formation of pS65-Ub in the presence of endogenous PINK1 and Parkin, thereby indicating that the feedforward process of pS65-Ub production occurs not just in cultured cells, but also in an organism.

References

[1] Al Rawi, S., Louvet-Vallée, S., Djeddi, A., Sachse, M., Culetto, E., Hajjar, C., Boyd, L., Legouis, R., and Galy, V. (2011). Postfertilization autophagy of sperm organelles prevents paternal mitochondrial DNA transmission. *Science*, 334(6059):1144–1147.

[2] Allen, G. F. G., Toth, R., James, J., and Ganley, I. G. (2013). Loss of iron triggers PINK1/Parkin-independent mitophagy. *EMBO Reports*, 14(12):1127–1135.

[3] Ambivero, C. T., Cilenti, L., Main, S., and Zervos, A. S. (2014). Mulan E3 ubiquitin ligase interacts with multiple E2 conjugating enzymes and participates in mitophagy by recruiting GABARAP. *Cellular Signalling*, 26(12):2921–2929.

[4] Andreazza, S., Samstag, C. L., Sanchez-Martinez, A., Fernandez-Vizarra, E., Gomez-Duran, A., Lee, J. J., Tufi, R., Hipp, M. J., Schmidt, E. K., Nicholls, T. J., Gammage, P. A., Chinnery, P. F., Minczuk, M., Pallanck, L. J., Kennedy, S. R., and Whitworth, A. J. (2019). Mitochondrially-targeted APOBEC1 is a potent mtDNA mutator affecting mitochondrial function and organismal fitness in Drosophila. *Nature Communications*, 10(1):3280.

[5] Bateman, A., Martin, M.-J., Orchard, S., Magrane, M., Alpi, E., Bely, B., Bingley, M., Britto, R., Bursteinas, B., Busiello, G., Bye-A-Jee, H., Silva, A. D., Giorgi, M. D., Dogan, T., Castro, L. G., Garmiri, P., Georghiou, G., Gonzales, D., Gonzales, L., Hatton-Ellis, E., Ignatchenko, A., Ishtiaq, R., Jokinen, P., Joshi, V., Jyothi, D., Lopez, R., Luo, J., Lussi, Y., MacDougall, A., Madeira, F., Mahmoudy, M., Menchi, M., Nightingale, A., Onwubiko, J., Palka, B., Pichler, K., Pundir, S., Qi, G., Raj, S., Renaux, A., Lopez, M. R., Saidi, R., Sawford, T., Shypitsyna, A., Speretta, E., Turner, E., Tyagi, N., Vasudev, P., Volynkin, V., Wardell, T., Warner, K., Watkins, X., Zaru, R., Zellner, H., Bridge, A., Xenarios, I., Poux, S., Redaschi, N., Aimo, L., Argoud-Puy, G., Auchincloss, A., Axelsen, K., Bansal, P., Baratin, D., Blatter, M.-C., Bolleman, J., Boutet, E., Breuza, L., Casals-Casas, C., Castro, E. d., Coudert, E., Cuche, B., Doche, M., Dornevil, D., Estreicher, A., Famiglietti, L., Feuermann, M., Gasteiger, E., Gehant, S., Gerritsen, V., Gos, A., Gruaz, N., Hinz, U., Hulo, C., Hyka-Nouspikel, N., Jungo, F., Keller, G., Kerhornou, A., Lara, V., Lemercier, P., Lieberherr, D., Lombardot, T., Martin, X., Masson, P., Morgat, A., Neto, T. B., Paesano, S., Pedruzzi, I., Pilbout, S., Pozzato, M., Pruess, M., Rivoire, C., Sigrist, C., Sonesson, K., Stutz, A., Sundaram, S., Tognolli, M., Verbregue, L., Wu, C. H., Arighi, C. N., Arminski, L., Chen, C., Chen, Y., Cowart, J., Garavelli, J. S., Huang, H., Laiho, K., McGarvey, P., Natale, D. A., Ross, K., Vinayaka, C. R., Wang, Q., Wang, Y., Yeh, L.-S., and Zhang, J. (2018). UniProt: a worldwide hub of protein knowledge. *Nucleic Acids Research*, 47(D1):D506–D515.

[6] Bender, A., Krishnan, K. J., Morris, C. M., Taylor, G. A., Reeve, A. K., Perry, R. H., Jaros, E., Hersheson, J. S., Betts, J., Klopstock, T., Taylor, R. W., and Turnbull, D. M.

(2006). High levels of mitochondrial DNA deletions in substantia nigra neurons in aging and Parkinson disease. *Nature Genetics*, 38(5):515–517.

[7] Bento, A. C., Bippes, C. C., Kohler, C., Hemion, C., Frank, S., and Neutzner, A. (2018). UBXD1 is a mitochondrial recruitment factor for p97/VCP and promotes mitophagy. *Scientific Reports*, 8(1):12415.

[8] Bienko, M., Green, C. M., Crosetto, N., Rudolf, F., Zapart, G., Coull, B., Kannouche, P., Wider, G., Peter, M., Lehmann, A. R., Hofmann, K., and Dikic, I. (2005). Ubiquitin-Binding Domains in Y-Family Polymerases Regulate Translesion Synthesis. *Science*, 310(5755):1821–1824.

[9] Bilen, J. and Bonini, N. M. (2005). Drosophila as a Model for Human Neurodegenerative Disease. *Annual Review of Genetics*, 39(1):153–171.

[10] Bingol, B., Tea, J. S., Phu, L., Reichelt, M., Bakalarski, C. E., Song, Q., Foreman, O., Kirkpatrick, D. S., and Sheng, M. (2014). The mitochondrial deubiquitinase USP30 opposes parkin-mediated mitophagy. *Nature*, 510(7505):370–375.

[11] Bohnert, M., Pfanner, N., and Laan, M. v. d. (2015). Mitochondrial machineries for insertion of membrane proteins. *Current Opinion in Structural Biology*, 33:92–102.

[12] Boname, J. M., Thomas, M., Stagg, H. R., Xu, P., Peng, J., and Lehner, P. J. (2009). Efficient internalization of MHC I requires lysine-11 and lysine-63 mixed linkage polyubiquitin chains. *Traffic*, 11(2):210–220.

[13] Braak, H. and Braak, E. (2000). Pathoanatomy of Parkinson's disease. *Journal of Neurology*, 247(S2):II3–II10.

[14] Braschi, E., Goyon, V., Zunino, R., Mohanty, A., Xu, L., and McBride, H. M. (2010). Vps35 Mediates Vesicle Transport between the Mitochondria and Peroxisomes. *Current Biology*, 20(14):1310–1315.

[15] Bremm, A., Freund, S. M. V., and Komander, D. (2010). Lys11-linked ubiquitin chains adopt compact conformations and are preferentially hydrolyzed by the deubiquitinase Cezanne. *Nature Structural and Molecular Biology*, 17(8):939–947.

[16] Burchell, V. S., Nelson, D. E., Sanchez-Martinez, A., Delgado-Camprubi, M., Ivatt, R. M., Pogson, J. H., Randle, S. J., Wray, S., Lewis, P. A., Houlden, H., Abramov, A. Y., Hardy, J., Wood, N. W., Whitworth, A. J., Laman, H., and Plun-Favreau, H. (2013). The Parkinson's disease-linked proteins Fbxo7 and Parkin interact to mediate mitophagy. *Nature Neuroscience*, 16(9):1257–1265.

[17] Burman, J. L., Pickles, S., Wang, C., Sekine, S., Vargas, J. N. S., Zhang, Z., Youle, A. M., Nezich, C. L., Wu, X., Hammer, J. A., and Youle, R. J. (2017). Mitochondrial fission facilitates the selective mitophagy of protein aggregates. *Journal of Cell Biology*, 216(10):3231–3247.

[18] Bus, J. S. and Gibson, J. E. (1984). Paraquat: Model for Oxidant-Initiated Toxicity. *Environmental Health Perspectives*, 55:37.

[19] Carroll, J., Fearnley, I. M., Skehel, J. M., Shannon, R. J., Hirst, J., and Walker, J. E. (2006). Bovine Complex I Is a Complex of 45 Different Subunits. *Journal of Biological Chemistry*, 281(43):32724–32727.

[20] Carter, S., Bischof, O., Dejean, A., and Vousden, K. H. (2007). C-terminal modifications regulate MDM2 dissociation and nuclear export of p53. *Nature Cell Biology*, 9(4):428–435.

[21] Chan, N. C., Salazar, A. M., Pham, A. H., Sweredoski, M. J., Kolawa, N. J., Graham, R., Hess, S., and Chan, D. C. (2011). Broad activation of the ubiquitin–proteasome system by Parkin is critical for mitophagy. *Human Molecular Genetics*, 20(9):1726–1737.

[22] Chartier-Harlin, M.-C., Kachergus, J., Roumier, C., Mouroux, V., Douay, X., Lincoln, S., Levecque, C., Larvor, L., Andrieux, J., Hulihan, M., Waucquier, N., Defebvre, L., Amouyel, P., Farrer, M., and Destée, A. (2004). α-synuclein locus duplication as a cause of familial Parkinson's disease. *The Lancet*, 364(9440):1167–1169.

[23] Chau, V., Tobias, J., Bachmair, A., Marriott, D., Ecker, D., Gonda, D., and Varshavsky, A. (1989). A multiubiquitin chain is confined to specific lysine in a targeted short-lived protein. *Science*, 243(4898):1576–1583.

[24] Chen, H., Detmer, S. A., Ewald, A. J., Griffin, E. E., Fraser, S. E., and Chan, D. C. (2003). Mitofusins Mfn1 and Mfn2 coordinately regulate mitochondrial fusion and are essential for embryonic development. *Journal of Cell Biology*, 160(2):189–200.

[25] Chen, Z., Liu, L., Cheng, Q., Li, Y., Wu, H., Zhang, W., Wang, Y., Sehgal, S. A., Siraj, S., Wang, X., Wang, J., Zhu, Y., and Chen, Q. (2017). Mitochondrial E3 ligase MARCH 5 regulates FUNDC 1 to fine-tune hypoxic mitophagy. *EMBO Reports*, 18(3):495–509.

[26] Cheng, E. H.-Y., Sheiko, T. V., Fisher, J. K., Craigen, W. J., and Korsmeyer, S. J. (2003). VDAC2 Inhibits BAK Activation and Mitochondrial Apoptosis. *Science*, 301(5632):513–517.

[27] Chinwalla, A. T., Cook, L. L., Delehaunty, K. D., Fewell, G. A., Fulton, L. A., Fulton, R. S., Graves, T. A., Hillier, L. W., Mardis, E. R., McPherson, J. D., Miner, T. L., Nash, W. E., Nelson, J. O., Nhan, M. N., Pepin, K. H., Pohl, C. S., Ponce, T. C., Schultz, B., Thompson, J., Trevaskis, E., Waterston, R. H., Wendl, M. C., Wilson, R. K., Yang, S.-P., An, P., Berry, E., Birren, B., Bloom, T., Brown, D. G., Butler, J., Daly, M., David, R., Deri, J., Dodge, S., Foley, K., Gage, D., Gnerre, S., Holzer, T., Jaffe, D. B., Kamal, M., Karlsson, E. K., Kells, C., Kirby, A., Kulbokas, E. J., Lander, E. S., Landers, T., Leger, J. P., Levine, R., Lindblad-Toh, K., Mauceli, E., Mayer, J. H., McCarthy, M., Meldrim, J., Meldrim, J., Mesirov, J. P., Nicol, R., Nusbaum, C., Seaman, S., Sharpe, T., Sheridan, A., Singer, J. B., Santos, R., Spencer, B., Stange-Thomann, N., Vinson, J. P., Wade, C. M., Wierzbowski, J., Wyman, D., Zody, M. C., Birney, E., Goldman, N., Kasprzyk, A., Mongin, E., Rust, A. G., Slater, G., Stabenau, A., Ureta-Vidal, A., Whelan, S., Ainscough, R., Attwood, J., Bailey, J., Barlow, K., Beck, S., Burton, J., Clamp, M., Clee, C., Coulson, A., Cuff, J., Curwen, V., Cutts, T., Davies, J., Eyras, E., Grafham, D., Gregory, S., Hubbard, T., Hunt, A., Jones, M., Joy, A., Leonard, S., Lloyd, C., Matthews, L., McLaren, S., McLay, K., Meredith, B., Mullikin, J. C., Ning, Z., Oliver, K., Overton-Larty, E., Plumb, R., Potter, S., Quail, M., Rogers, J., Scott, C., Searle, S., Shownkeen, R., Sims, S., Wall,

M., West, A. P., Willey, D., Williams, S., Abril, J. F., Guigó, R., Parra, G., Agarwal, P., Agarwala, R., Church, D. M., Hlavina, W., Maglott, D. R., Sapojnikov, V., Alexandersson, M., Pachter, L., Antonarakis, S. E., Dermitzakis, E. T., Reymond, A., Ucla, C., Baertsch, R., Diekhans, M., Furey, T. S., Hinrichs, A., Hsu, F., Karolchik, D., Kent, W. J., Roskin, K. M., Schwartz, M. S., Sugnet, C., Weber, R. J., Bork, P., Letunic, I., Suyama, M., Torrents, D., Zdobnov, E. M., Botcherby, M., Brown, S. D., Campbell, R. D., Jackson, I., Bray, N., Couronne, O., Dubchak, I., Poliakov, A., Rubin, E. M., Brent, M. R., Flicek, P., Keibler, E., Korf, I., Batalov, S., Bult, C., Frankel, W. N., Carninci, P., Hayashizaki, Y., Kawai, J., Okazaki, Y., Cawley, S., Kulp, D., Wheeler, R., Chiaromonte, F., Collins, F. S., Felsenfeld, A., Guyer, M., Peterson, J., Wetterstrand, K., Copley, R. R., Mott, R., Dewey, C., Dickens, N. J., Emes, R. D., Goodstadt, L., Ponting, C. P., Winter, E., Dunn, D. M., Niederhausern, A. C. v., Weiss, R. B., Eddy, S. R., Johnson, L. S., Jones, T. A., Elnitski, L., Kolbe, D. L., Eswara, P., Miller, W., O'Connor, M. J., Schwartz, S., Gibbs, R. A., Muzny, D. M., Glusman, G., Smit, A., Green, E. D., Hardison, R. C., Yang, S., Haussler, D., Hua, A., Roe, B. A., Kucherlapati, R. S., Montgomery, K. T., Li, J., Li, M., Lucas, S., Ma, B., McCombie, W. R., Morgan, M., Pevzner, P., Tesler, G., Schultz, J., Smith, D. R., Tromp, J., Worley, K. C., Lander, E. S., Abril, J. F., Agarwal, P., Alexandersson, M., Antonarakis, S. E., Baertsch, R., Berry, E., Birney, E., Bork, P., Bray, N., Brent, M. R., Brown, D. G., Butler, J., Bult, C., Chiaromonte, F., Chinwalla, A. T., Church, D. M., Clamp, M., Collins, F. S., Copley, R. R., Couronne, O., Cawley, S., Cuff, J., Curwen, V., Cutts, T., Daly, M., Dermitzakis, E. T., Dewey, C., Dickens, N. J., Diekhans, M., Dubchak, I., Eddy, S. R., Elnitski, L., Emes, R. D., Eswara, P., Eyras, E., Felsenfeld, A., Flicek, P., Frankel, W. N., Fulton, L. A., Furey, T. S., Gnerre, S., Glusman, G., Goldman, N., Goodstadt, L., Green, E. D., Gregory, S., Guigó, R., Hardison, R. C., Haussler, D., Hillier, L. W., Hinrichs, A., Hlavina, W., Hsu, F., Hubbard, T., Jaffe, D. B., Kamal, M., Karolchik, D., Karlsson, E. K., Kasprzyk, A., Keibler, E., Kent, W. J., Kirby, A., Kolbe, D. L., Korf, I., Kulbokas, E. J., Kulp, D., Lander, E. S., Letunic, I., Li, M., Lindblad-Toh, K., Ma, B., Maglott, D. R., Mauceli, E., Mesirov, J. P., Miller, W., Mott, R., Mullikin, J. C., Ning, Z., Pachter, L., Parra, G., Pevzner, P., Poliakov, A., Ponting, C. P., Potter, S., Reymond, A., Roskin, K. M., Sapojnikov, V., Schultz, J., Schwartz, M. S., Schwartz, S., Searle, S., Singer, J. B., Slater, G., Smit, A., Stabenau, A., Sugnet, C., Suyama, M., Tesler, G., Torrents, D., Tromp, J., Ucla, C., Vinson, J. P., Wade, C. M., Weber, R. J., Wheeler, R., Winter, E., Yang, S.-P., Zdobnov, E. M., Waterston, R. H., Whelan, S., Worley, K. C., and Zody, M. C. (2002). Initial sequencing and comparative analysis of the mouse genome. *Nature*, 420(6915):520–562.

[28] Chu, C. T., Ji, J., Dagda, R. K., Jiang, J., Tyurina, Y. Y., Kapralov, A. A., Tyurin, V. A., Yanamala, N., Shrivastava, I. H., Mohammadyani, D., Wang, K., Zhu, J., Klein-Seetharaman, J., Balasubramanian, K., Amoscato, A. A., Borisenko, G., Huang, Z., Gusdon, A. M., Cheikhi, A., Steer, E. K., Wang, R., Baty, C., Watkins, S., Bahar, I., Bayır, H., and Kagan, V. E. (2013). Cardiolipin externalization to the outer mitochondrial membrane acts as an elimination signal for mitophagy in neuronal cells. *Nature Cell Biology*, 15(10):1197–1205.

[29] Clague, M. J., Urbé, S., and Komander, D. (2019). Breaking the chains: deubiquitylating enzyme specificity begets function. *Nature Reviews Molecular Cell Biology*, 20(6):338–352.

[30] Clark, I. E., Dodson, M. W., Jiang, C., Cao, J. H., Huh, J. R., Seol, J., Yoo, S., Hay, B. A., and Guo, M. (2006). Drosophila pink1 is required for mitochondrial function and interacts genetically with parkin. *Nature*, 441(7097):1162–1166.

[31] Colombini, M. (2016). The VDAC channel: Molecular basis for selectivity. *Biochimica et Biophysica Acta (BBA) - Molecular Cell Research*, 1863(10):2498–2502.

[32] Cook, W. J., Jeffrey, L. C., Carson, M., Chen, Z., and Pickart, C. M. (1992). Structure of a diubiquitin conjugate and a model for interaction with ubiquitin conjugating enzyme (E2). *Journal of Biological Chemistry*, 267(23):16467–16471.

[33] Cornelissen, T., Vilain, S., Vints, K., Gounko, N., Verstreken, P., and Vandenberghe, W. (2018). Deficiency of parkin and PINK1 impairs age-dependent mitophagy in Drosophila. *eLife*, 7:e35878.

[34] Coulom, H. and Birman, S. (2004). Chronic Exposure to Rotenone Models Sporadic Parkinson's Disease in Drosophila melanogaster. *Journal of Neuroscience*, 24(48):10993–10998.

[35] Crowe, S. O., Rana, A. S. J. B., Deol, K. K., Ge, Y., and Strieter, E. R. (2017). Ubiquitin Chain Enrichment Middle-Down Mass Spectrometry Enables Characterization of Branched Ubiquitin Chains in Cellulo. *Analytical Chemistry*, 89(8):4428–4434.

[36] Cunningham, C. N., Baughman, J. M., Phu, L., Tea, J. S., Yu, C., Coons, M., Kirkpatrick, D. S., Bingol, B., and Corn, J. E. (2015). USP30 and parkin homeostatically regulate atypical ubiquitin chains on mitochondria. *Nature Cell Biology*, 17(2):160–169.

[37] Da Costa, C. A., Sunyach, C., Giaime, E., West, A., Corti, O., Brice, A., Safe, S., Abou-Sleiman, P. M., Wood, N. W., Takahashi, H., Goldberg, M. S., Shen, J., and Checler, F. (2009). Transcriptional repression of p53 by parkin and impairment by mutations associated with autosomal recessive juvenile Parkinson's disease. *Nature Cell Biology*, 11(11):1370–1375.

[38] Davis, G. C., Williams, A. C., Markey, S. P., Ebert, M. H., Caine, E. D., Reichert, C. M., and Kopin, I. J. (1979). Chronic parkinsonism secondary to intravenous injection of meperidine analogues. *Psychiatry Research*, 1(3):249–254.

[39] Deas, E., Plun-Favreau, H., Gandhi, S., Desmond, H., Kjaer, S., Loh, S. H. Y., Renton, A. E. M., Harvey, R. J., Whitworth, A. J., Martins, L. M., Abramov, A. Y., and Wood, N. W. (2011). PINK1 cleavage at position A103 by the mitochondrial protease PARL. *Human Molecular Genetics*, 20(5):867–879.

[40] Di Maio, R., Barrett, P. J., Hoffman, E. K., Barrett, C. W., Zharikov, A., Borah, A., Hu, X., McCoy, J., Chu, C. T., Burton, E. A., Hastings, T. G., and Greenamyre, J. T. (2016). α-Synuclein binds to TOM20 and inhibits mitochondrial protein import in Parkinson's disease. *Science Translational Medicine*, 8(342):342ra78.

[41] Dong, X., Gong, Z., Lu, Y.-B., Liu, K., Qin, L.-Y., Ran, M.-L., Zhang, C.-L., Liu, Z., Zhang, W.-P., and Tang, C. (2017). Ubiquitin S65 phosphorylation engenders a pH-sensitive conformational switch. *Proceedings of the National Academy of Sciences*, 114(26):6770–6775.

[42] Duplan, E., Sevalle, J., Viotti, J., Goiran, T., Bauer, C., Renbaum, P., Levy-Lahad, E., Gautier, C. A., Corti, O., Leroudier, N., Checler, F., and Costa, C. A. d. (2013). Parkin differently regulates presenilin-1 and presenilin-2 functions by direct control of their promoter transcription. *Journal of Molecular Cell Biology*, 5(2):132–142.

[43] Dupont, S., Mamidi, A., Cordenonsi, M., Montagner, M., Zacchigna, L., Adorno, M., Martello, G., Stinchfield, M. J., Soligo, S., Morsut, L., Inui, M., Moro, S., Modena, N., Argenton, F., Newfeld, S. J., and Piccolo, S. (2009). FAM/USP9x, a Deubiquitinating Enzyme Essential for TGFβ Signaling, Controls Smad4 Monoubiquitination. *Cell*, 136(1):123–135.

[44] Durcan, T. M., Tang, M. Y., Pérusse, J. R., Dashti, E. A., Aguileta, M. A., McLelland, G.-L. L., Gros, P., Shaler, T. A., Faubert, D., Coulombe, B., and Fon, E. A. (2014). USP8 regulates mitophagy by removing K6-linked ubiquitin conjugates from parkin. *The EMBO Journal*, 33(21):2473–2491.

[45] Faesen, A., Luna-Vargas, M. A., Geurink, P., Clerici, M., Merkx, R., van Dijk, W., Hameed, D., El Oualid, F., Ovaa, H., and Sixma, T. (2011). The Differential Modulation of USP Activity by Internal Regulatory Domains, Interactors and Eight Ubiquitin Chain Types. *Chemistry & Biology*, 18(12):1550–1561.

[46] Fiesel, F. C., Moussaud-Lamodière, E. L., Ando, M., and Springer, W. (2014). A specific subset of E2 ubiquitin-conjugating enzymes regulate Parkin activation and mitophagy differently. *Journal of Cell Science*, 127(16):3488–3504.

[47] Fiil, B., Damgaard, R., Wagner, S., Keusekotten, K., Fritsch, M., Bekker-Jensen, S., Mailand, N., Choudhary, C., Komander, D., and Gyrd-Hansen, M. (2013). OTULIN restricts Met1-linked ubiquitination to control innate immune signaling. *Molecular Cell*, 50(6):818–830.

[48] Finley, D., Sadis, S., Monia, B. P., Boucher, P., Ecker, D. J., Crooke, S. T., and Chau, V. (1994). Inhibition of proteolysis and cell cycle progression in a multiubiquitination-deficient yeast mutant. *Molecular and Cellular Biology*, 14(8):5501–5509.

[49] Finley, D., Özkaynak, E., and Varshavsky, A. (1987). The yeast polyubiquitin gene is essential for resistance to high temperatures, starvation, and other stresses. *Cell*, 48(6):1035–1046.

[50] Fiorese, C., Schulz, A., Lin, Y.-F., Rosin, N., Pellegrino, M., and Haynes, C. (2016). The Transcription Factor ATF5 Mediates a Mammalian Mitochondrial UPR. *Current Biology*, 26(15):2037–2043.

[51] Fisher, E. M. C. and Bannerman, D. M. (2019). Mouse models of neurodegeneration: Know your question, know your mouse. *Science Translational Medicine*, 11(493):eaaq1818.

[52] Fonzo, A. D., Dekker, M. C. J., Montagna, P., Baruzzi, A., Yonova, E. H., Guedes, L. C., Szczerbinska, A., Zhao, T., Dubbel-Hulsman, L. O. M., Wouters, C. H., Graaff, E. d., Oyen, W. J. G., Simons, E. J., Breedveld, G. J., Oostra, B. A., Horstink, M. W., and Bonifati, V. (2008). FBXO7 mutations cause autosomal recessive, early-onset parkinsonian-pyramidal syndrome. *Neurology*, 72(3):240–245.

[53] Fujiki, Y., Fowler, S., Shio, H., Hubbard, A. L., and Lazarow, P. B. (1982). Polypeptide and phospholipid composition of the membrane of rat liver peroxisomes: comparison with endoplasmic reticulum and mitochondrial membranes. *Journal of Cell Biology*, 93(1):103–110.

[54] Fujimuro, M., Sawada, H., and Yokosawa, H. (1994). Production and characterization of monoclonal antibodies specific to multi-ubiquitin chains of polyubiquitinated proteins. *FEBS Letters*, 349(2):173–180.

[55] Fukushima, T., Yamada, K., Isobe, A., Shiwaku, K., and Yamane, Y. (1993). Mechanism of cytotoxicity of paraquat. *Experimental and Toxicologic Pathology*, 45(5-6):345–349.

[56] Fulzele, A. and Bennett, E. J. (2018). Ubiquitin diGLY Proteomics as an Approach to Identify and Quantify the Ubiquitin-Modified Proteome. volume 1844 of *Methods in Molecular Biology*, pages 363–384. Clifton, N.J.

[57] Gegg, M. E., Cooper, J., Chau, K.-Y. Y., Rojo, M., Schapira, A. H., and Taanman, J.-W. W. (2010). Mitofusin 1 and mitofusin 2 are ubiquitinated in a PINK1/parkin-dependent manner upon induction of mitophagy. *Human Molecular Genetics*, 19(24):4861–4870.

[58] Gehrke, S., Wu, Z., Klinkenberg, M., Sun, Y., Auburger, G., Guo, S., and Lu, B. (2015). PINK1 and Parkin Control Localized Translation of Respiratory Chain Component mRNAs on Mitochondria Outer Membrane. *Cell Metabolism*, 21(1):95–108.

[59] Geisler, S., Holmström, K. M., Skujat, D., Fiesel, F. C., Rothfuss, O. C., Kahle, P. J., and Springer, W. (2010). PINK1/Parkin-mediated mitophagy is dependent on VDAC1 and p62/SQSTM1. *Nature Cell Biology*, 12(2):119–131.

[60] Geisler, S., Vollmer, S., Golombek, S., and Kahle, P. J. (2014). The ubiquitin-conjugating enzymes UBE2N, UBE2L3 and UBE2D2/3 are essential for Parkin-dependent mitophagy. *Journal of Cell Science*, 127(15):3280–3293.

[61] Gelders, G., Baekelandt, V., and Perren, A. V. d. (2018). Linking Neuroinflammation and Neurodegeneration in Parkinson's Disease. *Journal of Immunology Research*, 2018:4784268.

[62] Gendron, J. M., Webb, K., Yang, B., Rising, L., Zuzow, N., and Bennett, E. J. (2016). Using the Ubiquitin-modified Proteome to Monitor Distinct and Spatially Restricted Protein Homeostasis Dysfunction. *Molecular & Cellular Proteomics*, 15(8):2576–2593.

[63] Gersch, M., Gladkova, C., Schubert, A. F., Michel, M. A., Maslen, S., and Komander, D. (2017). Mechanism and regulation of the Lys6-selective deubiquitinase USP30. *Nature Structural and Molecular Biology*, 24(11):920–930.

[64] Gladkova, C., Maslen, S. L., Skehel, M. J., and Komander, D. (2018). Mechanism of parkin activation by PINK1. *Nature*, 559(7714):410–414.

[65] Gladkova, C., Schubert, A. F., Wagstaff, J. L., Pruneda, J. N., Freund, S. M., and Komander, D. (2017). An invisible ubiquitin conformation is required for efficient phosphorylation by PINK 1. *The EMBO Journal*, 36(24):3555–3572.

[66] Goldberg, M. S., Fleming, S. M., Palacino, J. J., Cepeda, C., Lam, H. A., Bhatnagar, A., Meloni, E. G., Wu, N., Ackerson, L. C., Klapstein, G. J., Gajendiran, M., Roth, B. L., Chesselet, M.-F., Maidment, N. T., Levine, M. S., and Shen, J. (2003). Parkin-deficient Mice Exhibit Nigrostriatal Deficits but Not Loss of Dopaminergic Neurons. *Journal of Biological Chemistry*, 278(44):43628–43635.

[67] Gomes, L. C., Benedetto, G. D., and Scorrano, L. (2011). During autophagy mitochondria elongate, are spared from degradation and sustain cell viability. *Nature Cell Biology*, 13(5):589–598.

[68] Gornicka, A., Bragoszewski, P., Chroscicki, P., Wenz, L.-S., Schulz, C., Rehling, P., and Chacinska, A. (2014). A discrete pathway for the transfer of intermembrane space proteins across the outer membrane of mitochondria. *Molecular Biology of the Cell*, 25(25):3999–4009.

[69] Gray, M. W., Burger, G., and Lang, B. F. (1999). Mitochondrial Evolution. *Science*, 283(5407):1476–1481.

[70] Greene, A. W., Grenier, K., Aguileta, M. A., Muise, S., Farazifard, R., Haque, M., McBride, H. M., Park, D. S., and Fon, E. A. (2012). Mitochondrial processing peptidase regulates PINK1 processing, import and Parkin recruitment. *EMBO Reports*, 13(4):378–385.

[71] Greene, J. C., Whitworth, A. J., Kuo, I., Andrews, L. A., Feany, M. B., and Pallanck, L. J. (2003). Mitochondrial pathology and apoptotic muscle degeneration in Drosophila parkin mutants. *Proceedings of the National Academy of Sciences*, 100(7):4078–4083.

[72] Griparic, L., Wel, N. N. v. d., Orozco, I. J., Peters, P. J., and Bliek, A. M. v. d. (2004). Loss of the Intermembrane Space Protein Mgm1/OPA1 Induces Swelling and Localized Constrictions along the Lengths of Mitochondria. *Journal of Biological Chemistry*, 279(18):18792–18798.

[73] Hales, K. G. and Fuller, M. T. (1997). Developmentally Regulated Mitochondrial Fusion Mediated by a Conserved, Novel, Predicted GTPase. *Cell*, 90(1):121–129.

[74] Ham, S. J., Lee, D., Yoo, H., Jun, K., Shin, H., and Chung, J. (2020). Decision between mitophagy and apoptosis by Parkin via VDAC1 ubiquitination. *Proceedings of the National Academy of Sciences*, 117(8):4281–4291.

[75] Harner, M., Neupert, W., and Deponte, M. (2011). Lateral release of proteins from the TOM complex into the outer membrane of mitochondria. *The EMBO Journal*, 30(16):3232–3241.

[76] Hartl, F.-U., Pfanner, N., Nicholson, D. W., and Neupert, W. (1989). Mitochondrial protein import. *Biochimica et Biophysica Acta (BBA) - Reviews on Biomembranes*, 988(1):1–45.

[77] Hasson, S. A., Kane, L. A., Yamano, K., Huang, C.-H., Sliter, D. A., Buehler, E., Wang, C., Heman-Ackah, S. M., Hessa, T., Guha, R., Martin, S. E., and Youle, R. J. (2013). High-content genome-wide RNAi screens identify regulators of parkin upstream of mitophagy. *Nature*, 504(7479):291–295.

[78] Hawkes, C. H., Shephard, B. C., and Daniel, S. E. (1997). Olfactory dysfunction in Parkinson's disease. *Journal of Neurology, Neurosurgery & Psychiatry*, 62(5):436–446.

[79] Haynes, C. M., Yang, Y., Blais, S. P., Neubert, T. A., and Ron, D. (2010). The Matrix Peptide Exporter HAF-1 Signals a Mitochondrial UPR by Activating the Transcription Factor ZC376.7 in C. elegans. *Molecular Cell*, 37(4):529–540.

[80] Haywood, A. F. and Staveley, B. E. (2004). parkin counteracts symptoms in a Drosophila model of Parkinson's disease. *BMC Neuroscience*, 5(1):14.

[81] Heikkila, R., Hess, A., and Duvoisin, R. (1984). Dopaminergic neurotoxicity of 1-methyl-4-phenyl-1,2,5,6-tetrahydropyridine in mice. *Science*, 224(4656):1451–1453.

[82] Heikkila, R. E., Nicklas, W. J., Vyas, I., and Duvoisin, R. C. (1985). Dopaminergic toxicity of rotenone and the 1-methyl-4-phenylpyridinium ion after their stereotaxic administration to rats: Implication for the mechanism of 1-methyl-4-phenyl-1,2,3,6-tetrahydropyridine toxicity. *Neuroscience Letters*, 62(3):389–394.

[83] Heo, J.-M., Ordureau, A., Paulo, J. A., Rinehart, J., and Harper, J. W. (2015). The PINK1-PARKIN Mitochondrial Ubiquitylation Pathway Drives a Program of OPTN/NDP52 Recruitment and TBK1 Activation to Promote Mitophagy. *Molecular Cell*, 60(1):7–20.

[84] Heytler, P. G. (1963). uncoupling of oxidative phosphorylation by carbonyl cyanide phenylhydrazones. I. Some characteristics of m-Cl-CCP action on mitochondria and chloroplasts. *Biochemistry*, 2(2):357–361.

[85] Hjerpe, R., Aillet, F., Lopitz-Otsoa, F., Lang, V., England, P., and Rodriguez, M. S. (2009). Efficient protection and isolation of ubiquitylated proteins using tandem ubiquitin-binding entities. *EMBO Reports*, 10(11):1250–1258.

[86] Hoehn, M. M. and Yahr, M. D. (1967). Parkinsonism: onset, progression, and mortality. *Neurology*, 17(5):427–427.

[87] Hoogenraad, N. J., Ward, L. A., and Ryan, M. T. (2002). Import and assembly of proteins into mitochondria of mammalian cells. *Biochimica et Biophysica Acta (BBA) - Molecular Cell Research*, 1592(1):97–105.

[88] Hospenthal, M., Mevissen, T., and Komander, D. (2015). Deubiquitinase-based analysis of ubiquitin chain architecture using Ubiquitin Chain Restriction (UbiCRest). *Nature Protocols*, 10(2):349–361.

[89] Hospenthal, M. K., Freund, S. M. V., and Komander, D. (2013). Assembly, analysis and architecture of atypical ubiquitin chains. *Nature Structural and Molecular Biology*, 20(5):555–565.

[90] Hrdinka, M., Fiil, B., Zucca, M., Leske, D., Bagola, K., Yabal, M., Elliott, P., Damgaard, R., Komander, D., Jost, P., and Gyrd-Hansen, M. (2016). CYLD limits Lys63- and Met1-linked ubiquitin at receptor complexes to regulate innate immune signaling. *Cell Reports*, 14(12):2846–2858.

[91] Hristova, V. A., Beasley, S. A., Rylett, R. J., and Shaw, G. S. (2009). Identification of a novel Zn2+-binding domain in the autosomal recessive juvenile Parkinson-related E3 ligase parkin. *Journal of Biological Chemistry*, 284(22):14978–14986.

[92] Huguenin-Dezot, N., De Cesare, V., Peltier, J., Knebel, A., Kristaryianto, Y. A., Rogerson, D. T., Kulathu, Y., Trost, M., and Chin, J. W. (2016). Synthesis of Isomeric Phosphoubiquitin Chains Reveals that Phosphorylation Controls Deubiquitinase Activity and Specificity. *Cell Reports*, 16(4):1180–1193.

[93] Hämäläinen, R. H., Manninen, T., Koivumäki, H., Kislin, M., Otonkoski, T., and Suomalainen, A. (2013). Tissue- and cell-type-specific manifestations of heteroplasmic mtDNA 3243A>G mutation in human induced pluripotent stem cell-derived disease model. *Proceedings of the National Academy of Sciences*, 110(38):E3622–E3630.

[94] Höhr, A. I. C., Straub, S. P., Warscheid, B., Becker, T., and Wiedemann, N. (2014). Assembly of β-barrel proteins in the mitochondrial outer membrane. *Biochimica et Biophysica Acta (BBA) - Molecular Cell Research*, 1853(1):74–88.

[95] Ichimura, Y., Kirisako, T., Takao, T., Satomi, Y., Shimonishi, Y., Ishihara, N., Mizushima, N., Tanida, I., Kominami, E., Ohsumi, M., Noda, T., and Ohsumi, Y. (2000). A ubiquitin-like system mediates protein lipidation. *Nature*, 408(6811):488–492.

[96] Iesmantavicius, V., Weinert, B. T., and Choudhary, C. (2014). Convergence of Ubiquitylation and Phosphorylation Signaling in Rapamycin-treated Yeast Cells. *Molecular & Cellular Proteomics*, 13(8):1979–1992.

[97] Iguchi, M., Kujuro, Y., Okatsu, K., Koyano, F., Kosako, H., Kimura, M., Suzuki, N., Uchiyama, S., Tanaka, K., and Matsuda, N. (2013). Parkin-catalyzed ubiquitin-ester transfer is triggered by PINK1-dependent phosphorylation. *Journal of Biological Chemistry*, 288(30):22019–22032.

[98] Ishihara, N., Nomura, M., Jofuku, A., Kato, H., Suzuki, S. O., Masuda, K., Otera, H., Nakanishi, Y., Nonaka, I., Goto, Y.-I., Taguchi, N., Morinaga, H., Maeda, M., Takayanagi, R., Yokota, S., and Mihara, K. (2009). Mitochondrial fission factor Drp1 is essential for embryonic development and synapse formation in mice. *Nature Cell Biology*, 11(8):958–966.

[99] Itakura, E., Kishi-Itakura, C., Koyama-Honda, I., and Mizushima, N. (2012). Structures containing Atg9A and the ULK1 complex independently target depolarized mitochondria at initial stages of Parkin-mediated mitophagy. *Journal of Cell Science*, 125(6):1488–1499.

[100] Jacoupy, M., Hamon-Keromen, E., Ordureau, A., Erpapazoglou, Z., Coge, F., Corvol, J.-C., Nosjean, O., Cour, M. C. l., Millan, M., Boutin, J., Harper, J., Brice, A., Guedin, D., Gautier, C., and Corti, O. (2019). The PINK1 kinase-driven ubiquitin ligase Parkin promotes mitochondrial protein import through the presequence pathway in living cells. *Scientific Reports*, 9(1):1–15.

[101] Jin, S., Lazarou, M., Wang, C., Kane, L. A., Narendra, D. P., and Youle, R. J. (2010). Mitochondrial membrane potential regulates PINK1 import and proteolytic destabilization by PARL. *Journal of Cell Biology*, 191(5):933–942.

[102] Jin, S. M. and Youle, R. J. (2013). The accumulation of misfolded proteins in the mitochondrial matrix is sensed by PINK1 to induce PARK2/Parkin-mediated mitophagy of polarized mitochondria. *Autophagy*, 9(11):1750–1757.

[103] Jung, J. H., Bae, S., Lee, J. Y., Woo, S. R., Cha, H. J., Yoon, Y., Suh, K.-S., Lee, S.-J., Park, I.-C., Jin, Y.-W., Lee, K.-H., An, S., and Lee, J. H. (2011). E3 ubiquitin ligase Hades negatively regulates the exonuclear function of p53. *Cell Death and Differentiation*, 18(12):1865–1875.

[104] Kane, L. A., Lazarou, M., Fogel, A. I., Li, Y., Yamano, K., Sarraf, S. A., Banerjee, S., and Youle, R. J. (2014). PINK1 phosphorylates ubiquitin to activate Parkin E3 ubiquitin ligase activity. *Journal of Cell Biology*, 205(2):143–153.

[105] Kasianowicz, J., Benz, R., and McLaughlin, S. (1984). The kinetic mechanism by which CCCP (carbonyl cyanidem-Chlorophenylhydrazone) transports protons across membranes. *The Journal of Membrane Biology*, 82(2):179–190.

[106] Katayama, H., Hama, H., Nagasawa, K., Kurokawa, H., Sugiyama, M., Ando, R., Funata, M., Yoshida, N., Homma, M., Nishimura, T., Takahashi, M., Ishida, Y., Hioki, H., Tsujihata, Y., and Miyawaki, A. (2020). Visualizing and Modulating Mitophagy for Therapeutic Studies of Neurodegeneration. *Cell*, 181(5):1176–1187.e16.

[107] Katayama, H., Kogure, T., Mizushima, N., Yoshimori, T., and Miyawaki, A. (2011). A sensitive and quantitative technique for detecting autophagic events based on lysosomal delivery. *Chemistry & Biology*, 18(8):1042–1052.

[108] Kato, H. and Mihara, K. (2008). Identification of Tom5 and Tom6 in the preprotein translocase complex of human mitochondrial outer membrane. *Biochemical and Biophysical Research Communications*, 369(3):958–963.

[109] Kauppila, T. E. S., Bratic, A., Jensen, M. B., Baggio, F., Partridge, L., Jasper, H., Grönke, S., and Larsson, N.-G. (2018). Mutations of mitochondrial DNA are not major contributors to aging of fruit flies. *Proceedings of the National Academy of Sciences*, 115(41):E9620–E9629.

[110] Kaye, J., Gage, H., Kimber, A., Storey, L., and Trend, P. (2006). Excess burden of constipation in Parkinson's disease: A pilot study. *Movement Disorders*, 21(8):1270–1273.

[111] Kazlauskaite, A., Kelly, V., Johnson, C., Baillie, C., Hastie, C. J., Peggie, M., Macartney, T., Woodroof, H. I., Alessi, D. R., Pedrioli, P. G. A., and Muqit, M. M. K. (2014a). Phosphorylation of Parkin at Serine65 is essential for activation: elaboration of a Miro1 substrate-based assay of Parkin E3 ligase activity. *Open Biology*, 4(3):130213.

[112] Kazlauskaite, A., Kondapalli, C., Gourlay, R., Campbell, D. G., Ritorto, M. S., Hofmann, K., Alessi, D. R., Knebel, A., Trost, M., and Muqit, M. M. (2014b). Parkin is activated by PINK1-dependent phosphorylation of ubiquitin at Ser65. *The Biochemical Journal*, 460(1):127–139.

[113] Kazlauskaite, A., Martínez-Torres, J. R., Wilkie, S., Kumar, A., Peltier, J., Gonzalez, A., Johnson, C., Zhang, J., Hope, A. G., Peggie, M., Trost, M., Aalten, D. M., Alessi, D. R., Prescott, A. R., Knebel, A., Walden, H., and Muqit, M. M. (2015). Binding to serine

65-phosphorylated ubiquitin primes Parkin for optimal PINK1-dependent phosphorylation and activation. *EMBO Reports*, 16(8):939–954.

[114] Keogh, M. J. and Chinnery, P. F. (2015). Mitochondrial DNA mutations in neurodegeneration. *Biochimica et Biophysica Acta (BBA) - Bioenergetics*, 1847(11):1401–1411.

[115] Keusekotten, K., Elliott, P. R., Glockner, L., Fiil, B. K., Damgaard, R. B., Kulathu, Y., Wauer, T., Hospenthal, M. K., Gyrd-Hansen, M., Krappmann, D., Hofmann, K., and Komander, D. (2013). OTULIN antagonizes LUBAC signaling by specifically hydrolyzing Met1-linked polyubiquitin. *Cell*, 153(6):1312–1326.

[116] Kim, J., Gupta, R., Blanco, L. P., Yang, S., Shteinfer-Kuzmine, A., Wang, K., Zhu, J., Yoon, H. E., Wang, X., Kerkhofs, M., Kang, H., Brown, A. L., Park, S.-J., Xu, X., Rilland, E. Z. v., Kim, M. K., Cohen, J. I., Kaplan, M. J., Shoshan-Barmatz, V., and Chung, J. H. (2019). VDAC oligomers form mitochondrial pores to release mtDNA fragments and promote lupus-like disease. *Science*, 366(6472):1531–1536.

[117] Kim, M., Sandford, E., Gatica, D., Qiu, Y., Liu, X., Zheng, Y., Schulman, B. A., Xu, J., Semple, I., Ro, S.-H., Kim, B., Mavioglu, R. N., Tolun, A., Jipa, A., Takats, S., Karpati, M., Li, J. Z., Yapici, Z., Juhasz, G., Lee, J. H., Klionsky, D. J., and Burmeister, M. (2016). Mutation in ATG5 reduces autophagy and leads to ataxia with developmental delay. *eLife*, 5:e12245.

[118] Kim, W., Bennett, E. J., Huttlin, E. L., Guo, A., Li, J., Possemato, A., Sowa, M. E., Rad, R., Rush, J., Comb, M. J., Harper, W. J., and Gygi, S. P. (2011). Systematic and Quantitative Assessment of the Ubiquitin-Modified Proteome. *Molecular Cell*, 44(2):325–340.

[119] Kirchweger, R., Ziegler, E., Lamphear, B., Waters, D., Liebig, H., Sommergruber, W., Sobrino, F., Hohenadl, C., Blaas, D., and Rhoads, R. (1994). Foot-and-mouth disease virus leader proteinase: purification of the Lb form and determination of its cleavage site on eIF-4 gamma. *Journal of Virology*, 68(9):5677–5684.

[120] Kirisako, T., Ichimura, Y., Okada, H., Kabeya, Y., Mizushima, N., Yoshimori, T., Ohsumi, M., Takao, T., Noda, T., and Ohsumi, Y. (2000). The Reversible Modification Regulates the Membrane-Binding State of Apg8/Aut7 Essential for Autophagy and the Cytoplasm to Vacuole Targeting Pathway. *Journal of Cell Biology*, 151(2):263–276.

[121] Kirkpatrick, D. S., Gerber, S. A., and Gygi, S. P. (2005). The absolute quantification strategy: a general procedure for the quantification of proteins and post-translational modifications. *Methods*, 35(3):265–273.

[122] Kitada, T., Asakawa, S., Hattori, N., Matsumine, H., Yamamura, Y., Minoshima, S., Yokochi, M., Mizuno, Y., and Shimizu, N. (1998). Mutations in the parkin gene cause autosomal recessive juvenile parkinsonism. *Nature*, 392(6676):605–608.

[123] Kitada, T., Pisani, A., Porter, D. R., Yamaguchi, H., Tscherter, A., Martella, G., Bonsi, P., Zhang, C., Pothos, E. N., and Shen, J. (2007). Impaired dopamine release and synaptic plasticity in the striatum of PINK1-deficient mice. *Proceedings of the National Academy of Sciences*, 104(27):11441–11446.

[124] Klont, F., Bras, L., Wolters, J. C., Ongay, S., Bischoff, R., Halmos, G. B., and Horvatovich, P. (2018). Assessment of Sample Preparation Bias in Mass Spectrometry-Based Proteomics. *Analytical Chemistry*, 90(8):5405–5413.

[125] Kolitsida, P., Zhou, J., Rackiewicz, M., Nolic, V., Dengjel, J., and Abeliovich, H. (2019). Phosphorylation of mitochondrial matrix proteins regulates their selective mitophagic degradation. *Proceedings of the National Academy of Sciences*, 116(41):20517–20527.

[126] Komander, D. and Rape, M. (2012). The Ubiquitin Code. *Annual Review of Biochemistry*, 81(1):203–229.

[127] Komander, D., Reyes-Turcu, F., Licchesi, J. D. F., Odenwaelder, P., Wilkinson, K. D., and Barford, D. (2009). Molecular discrimination of structurally equivalent Lys 63-linked and linear polyubiquitin chains. *EMBO Reports*, 10(5):466–473.

[128] Kondapalli, C., Kazlauskaite, A., Zhang, N., Woodroof, H. I., Campbell, D. G., Gourlay, R., Burchell, L., Walden, H., Macartney, T. J., Deak, M., Knebel, A., Alessi, D. R., and Muqit, M. M. (2012). PINK1 is activated by mitochondrial membrane potential depolarization and stimulates Parkin E3 ligase activity by phosphorylating Serine 65. *Open Biology*, 2(5):120080.

[129] Koyano, F., Okatsu, K., Kosako, H., Tamura, Y., Go, E., Kimura, M., Kimura, Y., Tsuchiya, H., Yoshihara, H., Hirokawa, T., Endo, T., Fon, E. A., Trempe, J.-F., Saeki, Y., Tanaka, K., and Matsuda, N. (2014). Ubiquitin is phosphorylated by PINK1 to activate parkin. *Nature*, 510(7503):162–166.

[130] Koyano, F., Yamano, K., Kosako, H., Tanaka, K., and Matsuda, N. (2019). Parkin recruitment to impaired mitochondria for nonselective ubiquitylation is facilitated by MITOL. *Journal of Biological Chemistry*, 294(26):10300–10314.

[131] Kumar, A., Aguirre, J. D., Condos, T. E. C., Martinez-Torres, R. J., Chaugule, V. K., Toth, R., Sundaramoorthy, R., Mercier, P., Knebel, A., Spratt, D. E., Barber, K. R., Shaw, G. S., and Walden, H. (2015). Disruption of the autoinhibited state primes the E3 ligase parkin for activation and catalysis. *The EMBO Journal*, 34(20):2506–2521.

[132] Kumar, A., Tamjar, J., Waddell, A. D., Woodroof, H. I., Raimi, O. G., Shaw, A. M., Peggie, M., Muqit, M. M., and Aalten, D. M. v. (2017). Structure of PINK1 and mechanisms of Parkinson's disease-associated mutations. *eLife*, 6:e29985.

[133] Kunji, E. R. S., King, M. S., Ruprecht, J. J., and Thangaratnarajah, C. (2020). The SLC25 Carrier Family: Important Transport Proteins in Mitochondrial Physiology and Pathology. *Physiology*, 35(5):302–327.

[134] Kurz, M., Martin, H., Rassow, J., Pfanner, N., and Ryan, M. T. (1999). Biogenesis of Tim Proteins of the Mitochondrial Carrier Import Pathway: Differential Targeting Mechanisms and Crossing Over with the Main Import Pathway. *Molecular Biology of the Cell*, 10(7):2461–2474.

[135] Langston, J., Ballard, P., Tetrud, J., and Irwin, I. (1983). Chronic Parkinsonism in humans due to a product of meperidine-analog synthesis. *Science*, 219(4587):979–980.

[136] Lazarou, M., Jin, S. M., Kane, L. A., and Youle, R. J. (2012). Role of PINK1 binding to the TOM complex and alternate intracellular membranes in recruitment and activation of the E3 ligase Parkin. *Developmental Cell*, 22(2):320–333.

[137] Lazarou, M., McKenzie, M., Ohtake, A., Thorburn, D., and Ryan, M. (2007). Analysis of the assembly profiles for mitochondrial- and nuclear-DNA-encoded subunits into complex I. *Molecular Cell Biology*, 27(12):4228–4237.

[138] Lazarou, M., Narendra, D., Jin, S., Tekle, E., Banerjee, S., and Youle, R. (2013). PINK1 drives Parkin self-association and HECT-like E3 activity upstream of mitochondrial binding. *Journal of Cell Biology*, 200(2):163–172.

[139] Lazarou, M., Sliter, D. A., Kane, L. A., Sarraf, S. A., Wang, C., Burman, J. L., Sideris, D. P., Fogel, A. I., and Youle, R. J. (2015). The ubiquitin kinase PINK1 recruits autophagy receptors to induce mitophagy. *Nature*, 524(7565):309–314.

[140] Lee, H.-J., Na, K., Kwon, M.-S., Kim, H., Kim, K. S., and Paik, Y.-K. (2009). Quantitative analysis of phosphopeptides in search of the disease biomarker from the hepatocellular carcinoma specimen. *Proteomics*, 9(12):3395–3408.

[141] Lee, J. J., Andreazza, S., and Whitworth, A. J. (2020). The STING pathway does not contribute to behavioural or mitochondrial phenotypes in Drosophila Pink1/parkin or mtDNA mutator models. *Scientific Reports*, 10(1):2693.

[142] Lee, J. J., Sanchez-Martinez, A., Zarate, A. M., Benincá, C., Mayor, U., Clague, M. J., and Whitworth, A. J. (2018). Basal mitophagy is widespread in Drosophila but minimally affected by loss of Pink1 or parkin. *Journal of Cell Biology*, 217(5):1613–1622.

[143] Li, P. A., Hou, X., and Hao, S. (2017). Mitochondrial biogenesis in neurodegeneration. *Journal of Neuroscience Research*, 95(10):2025–2029.

[144] Li, W., Bengtson, M. H., Ulbrich, A., Matsuda, A., Reddy, V. A., Orth, A., Chanda, S. K., Batalov, S., and Joazeiro, C. A. (2008). Genome-wide and functional annotation of human E3 ubiquitin ligases identifies MULAN, a mitochondrial E3 that regulates the organelle's dynamics and signaling. *PLoS One*, 3(1):e1487.

[145] Lin, W. and Kang, U. J. (2008). Characterization of PINK1 processing, stability, and subcellular localization. *Journal of Neurochemistry*, 106(1):464–474.

[146] Liu, L., Feng, D., Chen, G., Chen, M., Zheng, Q., Song, P., Ma, Q., Zhu, C., Wang, R., Qi, W., Huang, L., Xue, P., Li, B., Wang, X., Jin, H., Wang, J., Yang, F., Liu, P., Zhu, Y., Sui, S., and Chen, Q. (2012). Mitochondrial outer-membrane protein FUNDC1 mediates hypoxia-induced mitophagy in mammalian cells. *Nature Cell Biology*, 14(2):177–185.

[147] Longo, D. L. and Archer, S. L. (2013). Mitochondrial dynamics–mitochondrial fission and fusion in human diseases. *The New England Journal of Medicine*, 369(23):2236–2251.

[148] Lundby, A., Secher, A., Lage, K., Nordsborg, N. B., Dmytriyev, A., Lundby, C., and Olsen, J. V. (2012). Quantitative maps of protein phosphorylation sites across 14 different rat organs and tissues. *Nature Communications*, 3(1):876.

[149] MacLean, B., Tomazela, D. M., Shulman, N., Chambers, M., Finney, G. L., Frewen, B., Kern, R., Tabb, D. L., Liebler, D. C., and MacCoss, M. J. (2010). Skyline: an open source document editor for creating and analyzing targeted proteomics experiments. *Bioinformatics (Oxford, England)*, 26(7):966–968.

[150] Malik, B. R., Godena, V. K., and Whitworth, A. J. (2015). VPS35 pathogenic mutations confer no dominant toxicity but partial loss of function in Drosophila and genetically interact with parkin. *Human Molecular Genetics*, 24(21):6106–6117.

[151] Manning, G., Whyte, D. B., Martinez, R., Hunter, T., and Sudarsanam, S. (2002). The Protein Kinase Complement of the Human Genome. *Science*, 298(5600):1912–1934.

[152] Marcassa, E., Kallinos, A., Jardine, J., Rusilowicz-Jones, E. V., Martinez, A., Kuehl, S., Islinger, M., Clague, M. J., and Urbé, S. (2018). Dual role of USP 30 in controlling basal pexophagy and mitophagy. *EMBO Reports*, 19(7):e45595.

[153] Martijn, J., Vosseberg, J., Guy, L., Offre, P., and Ettema, T. J. G. (2018). Deep mitochondrial origin outside the sampled alphaproteobacteria. *Nature*, 557(7703):101–105.

[154] Martin, J., Mahlke, K., and Pfanner, N. (1991). Role of an Energized Inner Membrane in Mitochondrial Protein Import. *Journal of Biological Chemistry*, 266(27):18051–18057.

[155] Martinou, J.-C. and Youle, R. J. (2011). Mitochondria in apoptosis: Bcl-2 family members and mitochondrial dynamics. *Developmental Cell*, 21(1):92–101.

[156] Martinus, R. D., Garth, G. P., Webster, T. L., Cartwright, P., Naylor, D. J., Høj, P. B., and Hoogenraad, N. J. (1996). Selective Induction of Mitochondrial Chaperones in Response to Loss of the Mitochondrial Genome. *European Journal of Biochemistry*, 240(1):98–103.

[157] Matheoud, D., Cannon, T., Voisin, A., Penttinen, A.-M., Ramet, L., Fahmy, A. M., Ducrot, C., Laplante, A., Bourque, M.-J., Zhu, L., Cayrol, R., Campion, A. L., McBride, H. M., Gruenheid, S., Trudeau, L.-E., and Desjardins, M. (2019). Intestinal infection triggers Parkinson's disease-like symptoms in Pink1-/- mice. *Nature*, 571(7766):565–569.

[158] Matheoud, D., Sugiura, A., Bellemare-Pelletier, A., Laplante, A., Rondeau, C., Chemali, M., Fazel, A., Bergeron, J. J., Trudeau, L.-E., Burelle, Y., Gagnon, E., McBride, H. M., and Desjardins, M. (2016). Parkinson's Disease-Related Proteins PINK1 and Parkin Repress Mitochondrial Antigen Presentation. *Cell*, 166(2):314–327.

[159] Matsuda, A., Suzuki, Y., Honda, G., Muramatsu, S., Matsuzaki, O., Nagano, Y., Doi, T., Shimotohno, K., Harada, T., Nishida, E., Hayashi, H., and Sugano, S. (2003). Large-scale identification and characterization of human genes that activate NF-κB and MAPK signaling pathways. *Oncogene*, 22(21):3307–3318.

[160] Matsuda, N., Sato, S., Shiba, K., Okatsu, K., Saisho, K., Gautier, C. A., Sou, Y.-s., Saiki, S., Kawajiri, S., Sato, F., Kimura, M., Komatsu, M., Hattori, N., and Tanaka, K. (2010). PINK1 stabilized by mitochondrial depolarization recruits Parkin to damaged mitochondria and activates latent Parkin for mitophagy. *Journal of Cell Biology*, 189(2):211–221.

[161] McClellan, A. J., Laugesen, S. H., and Ellgaard, L. (2019). Cellular functions and molecular mechanisms of non-lysine ubiquitination. *Open Biology*, 9(9):190147.

[162] McCullough, J., Clague, M. J., and Urbé, S. (2004). AMSH is an endosome-associated ubiquitin isopeptidase. *Journal of Cell Biology*, 166(4):487–492.

[163] McLelland, G., Soubannier, V., Chen, C. X., McBride, H. M., and Fon, E. A. (2014). Parkin and PINK1 function in a vesicular trafficking pathway regulating mitochondrial quality control. *The EMBO Journal*, 33(4):282–295.

[164] McLelland, G.-L., Goiran, T., Yi, W., Dorval, G., Chen, C. X., Lauinger, N. D., Krahn, A. I., Valimehr, S., Rakovic, A., Rouiller, I., Durcan, T. M., Trempe, J.-F., and Fon, E. A. (2018). Mfn2 ubiquitination by PINK1/parkin gates the p97-dependent release of ER from mitochondria to drive mitophagy. *eLife*, 7:e32866.

[165] McLelland, G.-L., Lee, S. A., McBride, H. M., and Fon, E. A. (2016). Syntaxin-17 delivers PINK1/parkin-dependent mitochondrial vesicles to the endolysosomal system. *Journal of Cell Biology*, 214(3):275–291.

[166] McWilliams, T. G., Barini, E., Pohjolan-Pirhonen, R., Brooks, S. P., Singh, F., Burel, S., Balk, K., Kumar, A., Montava-Garriga, L., Prescott, A. R., Hassoun, S., Mouton-Liger, F., Ball, G., Hills, R., Knebel, A., Ulusoy, A., Monte, D. A., Tamjar, J., Antico, O., Fears, K., Smith, L., Brambilla, R., Palin, E., Valori, M., Eerola-Rautio, J., Tienari, P., Corti, O., Dunnett, S. B., Ganley, I. G., Suomalainen, A., and Muqit, M. M. (2018a). Phosphorylation of Parkin at serine 65 is essential for its activation in vivo. *Open Biology*, 8(11):180108.

[167] McWilliams, T. G., Prescott, A. R., Allen, G. F. G., Tamjar, J., Munson, M. J., Thomson, C., Muqit, M. M. K., and Ganley, I. G. (2016). mito-QC illuminates mitophagy and mitochondrial architecture in vivo. *Journal of Cell Biology*, 214(3):333–345.

[168] McWilliams, T. G., Prescott, A. R., Montava-Garriga, L., Ball, G., Singh, F., Barini, E., Muqit, M. M. K., Brooks, S. P., and Ganley, I. G. (2018b). Basal Mitophagy Occurs Independently of PINK1 in Mouse Tissues of High Metabolic Demand. *Cell Metabolism*, 27(2):439–449.e5.

[169] Meissner, C., Lorenz, H., Weihofen, A., Selkoe, D. J., and Lemberg, M. K. (2011). The mitochondrial intramembrane protease PARL cleaves human Pink1 to regulate Pink1 trafficking. *Journal of Neurochemistry*, 117(5):856–867.

[170] Melber, A. and Haynes, C. M. (2018). UPRmtregulation and output: a stress response mediated by mitochondrial-nuclear communication. *Cell Research*, 28(3):281–295.

[171] Meyer, A., Laverny, G., Bernardi, L., Charles, A. L., Alsaleh, G., Pottecher, J., Sibilia, J., and Geny, B. (2018). Mitochondria: An Organelle of Bacterial Origin Controlling Inflammation. *Frontiers in Immunology*, 9:536.

[172] Michel, M., Elliott, P., Swatek, K., Simicek, M., Pruneda, J., Wagstaff, J., Freund, S., and Komander, D. (2015). Assembly and Specific Recognition of K29- and K33-Linked Polyubiquitin. *Molecular Cell*, 58(1):95–109.

[173] Michel, M., Swatek, K., Hospenthal, M., and Komander, D. (2017). Ubiquitin linkage-specific affimers reveal insights into K6-linked ubiquitin signaling. *Molecular Cell*, 68(1):233–246.e5.

[174] Mimaki, M., Wang, X., McKenzie, M., Thorburn, D. R., and Ryan, M. T. (2012). Understanding mitochondrial complex I assembly in health and disease. *Biochimica et Biophysica Acta (BBA) - Bioenergetics*, 1817(6):851–862.

[175] Mishra, P., Carelli, V., Manfredi, G., and Chan, D. C. (2014). Proteolytic cleavage of Opa1 stimulates mitochondrial inner membrane fusion and couples fusion to oxidative phosphorylation. *Cell Metabolism*, 19(4):630–641.

[176] Mizushima, N., Kuma, A., Kobayashi, Y., Yamamoto, A., Matsubae, M., Takao, T., Natsume, T., Ohsumi, Y., and Yoshimori, T. (2003). Mouse Apg16L, a novel WD-repeat protein, targets to the autophagic isolation membrane with the Apg12-Apg5 conjugate. *Journal of Cell Science*, 116(9):1679–1688.

[177] Mizushima, N., Noda, T., Yoshimori, T., Tanaka, Y., Ishii, T., George, M. D., Klionsky, D. J., Ohsumi, M., and Ohsumi, Y. (1998). A protein conjugation system essential for autophagy. *Nature*, 395(6700):395–398.

[178] Mizushima, N., Yamamoto, A., Hatano, M., Kobayashi, Y., Kabeya, Y., Suzuki, K., Tokuhisa, T., Ohsumi, Y., and Yoshimori, T. (2001). Dissection of Autophagosome Formation Using Apg5-Deficient Mouse Embryonic Stem Cells. *Journal of Cell Biology*, 152(4):657–668.

[179] Morais, V. A., Haddad, D., Craessaerts, K., Bock, P.-J. D., Swerts, J., Vilain, S., Aerts, L., Overbergh, L., Grünewald, A., Seibler, P., Klein, C., Gevaert, K., Verstreken, P., and Strooper, B. D. (2014). PINK1 loss-of-function mutations affect mitochondrial complex I activity via NdufA10 ubiquinone uncoupling. *Science*, 344(6180):203–207.

[180] Morais, V. A., Verstreken, P., Roethig, A., Smet, J., Snellinx, A., Vanbrabant, M., Haddad, D., Frezza, C., Mandemakers, W., Vogt-Weisenhorn, D., Coster, R. V., Wurst, W., Scorrano, L., and Strooper, B. D. (2009). Parkinson's disease mutations in PINK1 result in decreased Complex I activity and deficient synaptic function. *EMBO Molecular Medicine*, 1(2):99–111.

[181] Morgenstern, M., Stiller, S. B., Lübbert, P., Peikert, C. D., Dannenmaier, S., Drepper, F., Weill, U., Höß, P., Feuerstein, R., Gebert, M., Bohnert, M., Laan, M. v. d., Schuldiner, M., Schütze, C., Oeljeklaus, S., Pfanner, N., Wiedemann, N., and Warscheid, B. (2017). Definition of a High-Confidence Mitochondrial Proteome at Quantitative Scale. *Cell Reports*, 19(13):2836–2852.

[182] Murphy, M. P. (2009). How mitochondria produce reactive oxygen species. *The Biochemical Journal*, 417(1):1–13.

[183] Nakamura, N. and Hirose, S. (2008). Regulation of Mitochondrial Morphology by USP30, a Deubiquitinating Enzyme Present in the Mitochondrial Outer Membrane. *Molecular Biology of the Cell*, 19(5):1903–1911.

[184] Narendra, D., Tanaka, A., Suen, D.-F., and Youle, R. J. (2008). Parkin is recruited selectively to impaired mitochondria and promotes their autophagy. *Journal of Cell Biology*, 183(5):795–803.

[185] Narendra, D. P., Jin, S. M., Tanaka, A., Suen, D.-F. F., Gautier, C. A., Shen, J., Cookson, M. R., and Youle, R. J. (2010). PINK1 is selectively stabilized on impaired mitochondria to activate Parkin. *PLoS Biology*, 8(1):e1000298.

[186] Nargund, A. M., Pellegrino, M. W., Fiorese, C. J., Baker, B. M., and Haynes, C. M. (2012). Mitochondrial Import Efficiency of ATFS-1 Regulates Mitochondrial UPR Activation. *Science*, 337(6094):587–590.

[187] Neuhauser, N., Michalski, A., Cox, J., and Mann, M. (2012). Expert System for Computer-assisted Annotation of MS/MS Spectra. *Molecular & Cellular Proteomics*, 11(11):1500–1509.

[188] Neuspiel, M., Schauss, A. C., Braschi, E., Zunino, R., Rippstein, P., Rachubinski, R. A., Andrade-Navarro, M. A., and McBride, H. M. (2008). Cargo-selected transport from the mitochondria to peroxisomes is mediated by vesicular carriers. *Current Biology*, 18(2):102–108.

[189] Neutzner, A., Youle, R. J., and Karbowski, M. (2007). Outer mitochondrial membrane protein degradation by the proteasome. *Novartis Foundation Symposium*, 287:4–14; discussion 14–20.

[190] Newton, K., Matsumoto, M. L., Wertz, I. E., Kirkpatrick, D. S., Lill, J. R., Tan, J., Dugger, D., Gordon, N., Sidhu, S. S., Fellouse, F. A., Komuves, L., French, D. M., Ferrando, R. E., Lam, C., Compaan, D., Yu, C., Bosanac, I., Hymowitz, S. G., Kelley, R. F., and Dixit, V. M. (2008). Ubiquitin chain editing revealed by polyubiquitin linkage-specific antibodies. *Cell*, 134(4):668–678.

[191] Nezis, I. P., Simonsen, A., Sagona, A. P., Finley, K., Gaumer, S., Contamine, D., Rusten, T. E., Stenmark, H., and Brech, A. (2008). Ref(2)P, the Drosophila melanogaster homologue of mammalian p62, is required for the formation of protein aggregates in adult brain. *Journal of Cell Biology*, 180(6):1065–1071.

[192] Nguyen, T. N., Padman, B. S., Usher, J., Oorschot, V., Ramm, G., and Lazarou, M. (2016). Atg8 family LC3/GABARAP proteins are crucial for autophagosome-lysosome fusion but not autophagosome formation during PINK1/Parkin mitophagy and starvation. *Journal of Cell Biology*, 215(6):857–874.

[193] Ochoa-Ruiz, E., Díaz-Ruiz, R., Hernández-Vázquez, A. d. J., Ibarra-González, I., Ortiz-Plata, A., Rembao, D., Ortega-Cuéllar, D., Viollet, B., Uribe-Carvajal, S., Corella, J. A., and Velázquez-Arellano, A. (2015). Biotin deprivation impairs mitochondrial structure and function and has implications for inherited metabolic disorders. *Molecular Genetics and Metabolism*, 116(3):204–214.

[194] Ohtake, F., Saeki, Y., Sakamoto, K., Ohtake, K., Nishikawa, H., Tsuchiya, H., Ohta, T., Tanaka, K., and Kanno, J. (2015). Ubiquitin acetylation inhibits polyubiquitin chain elongation. *EMBO Reports*, 16(2):192–201.

[195] Okatsu, K., Kimura, M., Oka, T., Tanaka, K., and Matsuda, N. (2015a). Unconventional PINK1 localization to the outer membrane of depolarized mitochondria drives Parkin recruitment. *Journal of Cell Science*, 128(5):964–978.

[196] Okatsu, K., Koyano, F., Kimura, M., Kosako, H., Saeki, Y., Tanaka, K., and Matsuda, N. (2015b). Phosphorylated ubiquitin chain is the genuine Parkin receptor. *Journal of Cell Biology*, 209(1):111–128.

[197] Okatsu, K., Oka, T., Iguchi, M., Imamura, K., Kosako, H., Tani, N., Kimura, M., Go, E., Koyano, F., Funayama, M., Shiba-Fukushima, K., Sato, S., Shimizu, H., Fukunaga, Y., Taniguchi, H., Komatsu, M., Hattori, N., Mihara, K., Tanaka, K., and Matsuda, N. (2012). PINK1 autophosphorylation upon membrane potential dissipation is essential for Parkin recruitment to damaged mitochondria. *Nature Communications*, 3(1):1016.

[198] Okatsu, K., Uno, M., Koyano, F., Go, E., Kimura, M., Oka, T., Tanaka, K., and Matsuda, N. (2013). A dimeric PINK1-containing complex on depolarized mitochondria stimulates Parkin recruitment. *Journal of Biological Chemistry*, 288(51):36372–36384.

[199] Olichon, A., Emorine, L. J., Descoins, E., Pelloquin, L., Brichese, L., Gas, N., Guillou, E., Delettre, C., Valette, A., Hamel, C. P., Ducommun, B., Lenaers, G., and Belenguer, P. (2002). The human dynamin-related protein OPA1 is anchored to the mitochondrial inner membrane facing the inter-membrane space. *FEBS Letters*, 523(1-3):171–176.

[200] Olsen, J. V., Blagoev, B., Gnad, F., Macek, B., Kumar, C., Mortensen, P., and Mann, M. (2006). Global, In Vivo, and Site-Specific Phosphorylation Dynamics in Signaling Networks. *Cell*, 127(3):635–648.

[201] Ordureau, A., Heo, J.-M., Duda, D., Paulo, J., Olszewski, J., Yanishevski, D., Rinehart, J., Schulman, B., and Harper, J. (2015). Defining roles of PARKIN and ubiquitin phosphorylation by PINK1 in mitochondrial quality control using a ubiquitin replacement strategy. *Proceedings of the National Academy of Sciences*, 112(21):6637–6642.

[202] Ordureau, A., Paulo, J., Zhang, W., Ahfeldt, T., Cohn, E., Hou, Z., Heo, J.-M., Rubin, L., Sidhu, S., Gygi, S., and Harper, J. (2018). Dynamics of PARKIN-dependent mitochondrial ubiquitylation in induced neurons and model systems revealed by digital snapshot proteomics. *Molecular Cell*, 70(2):211–227.e8.

[203] Ordureau, A., Paulo, J. A., Zhang, J., An, H., Swatek, K. N., Cannon, J. R., Wan, Q., Komander, D., Harper, W. J., Ordureau, A., Paulo, J. A., Zhang, J., An, H., Swatek, K. N., Cannon, J. R., Wan, Q., Komander, D., and Harper, W. J. (2020). Global Landscape and Dynamics of Parkin and USP30-Dependent Ubiquitylomes in iNeurons during Mitophagic Signaling. *Molecular Cell*, 77(5):1124–1142.e10.

[204] Ordureau, A., Sarraf, S., Duda, D., Heo, J.-M., Jedrychowski, M., Sviderskiy, V., Olszewski, J., Koerber, J., Xie, T., Beausoleil, S., Wells, J., Gygi, S., Schulman, B., and Harper, J. (2014). Quantitative proteomics reveal a feedforward mechanism for mitochondrial PARKIN translocation and ubiquitin chain synthesis. *Molecular Cell*, 56(3):360–375.

[205] Osellame, L. D., Singh, A. P., Stroud, D. A., Palmer, C. S., Stojanovski, D., Ramachandran, R., and Ryan, M. T. (2016). Cooperative and independent roles of the Drp1 adaptors Mff, MiD49 and MiD51 in mitochondrial fission. *Journal of Cell Science*, 129(11):2170–2181.

[206] Padman, B., Nguyen, T., Uoselis, L., Skulsuppaisarn, M., Nguyen, L. K., and Lazarou, M. (2019). LC3/GABARAPs drive ubiquitin-independent recruitment of Optineurin and NDP52 to amplify mitophagy. *Nature Communications*, 10(408):1–13.

[207] Padman, B. S., Bach, M., Lucarelli, G., Prescott, M., and Ramm, G. (2013). The protonophore CCCP interferes with lysosomal degradation of autophagic cargo in yeast and mammalian cells. *Autophagy*, 9(11):1862–1875.

[208] Pagliarini, D. J., Calvo, S. E., Chang, B., Sheth, S. A., Vafai, S. B., Ong, S.-E., Walford, G. A., Sugiana, C., Boneh, A., Chen, W. K., Hill, D. E., Vidal, M., Evans, J. G., Thorburn, D. R., Carr, S. A., and Mootha, V. K. (2008). A mitochondrial protein compendium elucidates complex I disease biology. *Cell*, 134(1):112–123.

[209] Paisán-Ruiz, C., Guevara, R., Federoff, M., Hanagasi, H., Sina, F., Elahi, E., Schneider, S. A., Schwingenschuh, P., Bajaj, N., Emre, M., Singleton, A. B., Hardy, J., Bhatia, K. P., Brandner, S., Lees, A. J., and Houlden, H. (2010). Early-onset L-dopa-responsive parkinsonism with pyramidal signs due to ATP13A2, PLA2G6, FBXO7 and spatacsin mutations. *Movement Disorders*, 25(12):1791–1800.

[210] Park, J., Lee, S. B., Lee, S., Kim, Y., Song, S., Kim, S., Bae, E., Kim, J., Shong, M., Kim, J.-M., and Chung, J. (2006). Mitochondrial dysfunction in Drosophila PINK1 mutants is complemented by parkin. *Nature*, 441(7097):1157–1161.

[211] Penefsky, H. S. (1985). Mechanism of inhibition of mitochondrial adenosine triphosphatase by dicyclohexylcarbodiimide and oligomycin: relationship to ATP synthesis. *Proceedings of the National Academy of Sciences*, 82(6):1589–1593.

[212] Peng, J., Schwartz, D., Elias, J. E., Thoreen, C. C., Cheng, D., Marsischky, G., Roelofs, J., Finley, D., and Gygi, S. P. (2003). A proteomics approach to understanding protein ubiquitination. *Nature Biotechnology*, 21(8):921–926.

[213] Perez, F. A. and Palmiter, R. D. (2005). Parkin-deficient mice are not a robust model of parkinsonism. *Proceedings of the National Academy of Sciences*, 102(6):2174–2179.

[214] Phu, L., Rose, C. M., Tea, J. S., Wall, C. E., Verschueren, E., Cheung, T. K., Kirkpatrick, D. S., and Bingol, B. (2020). Dynamic Regulation of Mitochondrial Import by the Ubiquitin System. *Molecular Cell*, 77(5):1107–1123.e10.

[215] Pickart, C. M. and Raasi, S. (2005). Controlled Synthesis of Polyubiquitin Chains. In *Methods in Enzymology*, volume 399, pages 21–36. Academic Press.

[216] Pickrell, A. M., Huang, C.-H. H., Kennedy, S. R., Ordureau, A., Sideris, D. P., Hoekstra, J. G., Harper, J. W., and Youle, R. J. (2015). Endogenous Parkin Preserves Dopaminergic Substantia Nigral Neurons following Mitochondrial DNA Mutagenic Stress. *Neuron*, 87(2):371–381.

[217] Pimenta de Castro, I., Costa, A. C., Lam, D., Tufi, R., Fedele, V., Moisoi, N., Dinsdale, D., Deas, E., Loh, S. H. Y., and Martins, L. M. (2012). Genetic analysis of mitochondrial protein misfolding in Drosophila melanogaster. *Cell Death and Differentiation*, 19(8):1308–1316.

[218] Plecitá-Hlavatá, L., Lessard, M., Santorová, J., Bewersdorf, J., and Jezek, P. (2008). Mitochondrial oxidative phosphorylation and energetic status are reflected by morphology of mitochondrial network in INS-1E and HEP-G2 cells viewed by 4Pi microscopy. *Biochimica et Biophysica Acta (BBA) - Bioenergetics*, 1777(7-8):834–846.

[219] Pogson, J. H., Ivatt, R. M., Sanchez-Martinez, A., Tufi, R., Wilson, E., Mortiboys, H., and Whitworth, A. J. (2014). The Complex I Subunit NDUFA10 Selectively Rescues Drosophila pink1 Mutants through a Mechanism Independent of Mitophagy. *PLoS Genetics*, 10(11):e1004815.

[220] Poole, A. C., Thomas, R. E., Andrews, L. A., McBride, H. M., Whitworth, A. J., and Pallanck, L. J. (2008). The PINK1/Parkin pathway regulates mitochondrial morphology. *Proceedings of the National Academy of Sciences*, 105(5):1638–1643.

[221] Poole, A. C., Thomas, R. E., Yu, S., Vincow, E. S., and Pallanck, L. (2010). The mitochondrial fusion-promoting factor mitofusin is a substrate of the PINK1/parkin pathway. *PLoS One*, 5(4):e10054.

[222] Prudent, J., Zunino, R., Sugiura, A., Mattie, S., Shore, G., and McBride, H. (2015). MAPL SUMOylation of Drp1 Stabilizes an ER/Mitochondrial Platform Required for Cell Death. *Molecular Cell*, 59(6):941–955.

[223] Przedborski, S. and Vila, M. (2001). MPTP: a review of its mechanisms of neurotoxicity. *Clinical Neuroscience Research*, 1(6):407–418.

[224] Quirós, P. M., Prado, M. A., Zamboni, N., D'Amico, D., Williams, R. W., Finley, D., Gygi, S. P., and Auwerx, J. (2017). Multi-omics analysis identifies ATF4 as a key regulator of the mitochondrial stress response in mammals. *Journal of Cell Biology*, 216(7):2027–2045.

[225] Rakovic, A., Shurkewitsch, K., Seibler, P., Grünewald, A., Zanon, A., Hagenah, J., Krainc, D., and Klein, C. (2012). Phosphatase and tensin homolog (PTEN)-induced putative kinase 1 (PINK1)-dependent ubiquitination of endogenous Parkin attenuates mitophagy: study in human primary fibroblasts and induced pluripotent stem cell-derived neurons. *Journal of Biological Chemistry*, 288(4):2223–2237.

[226] Rambold, A. S., Kostelecky, B., Elia, N., and Lippincott-Schwartz, J. (2011). Tubular network formation protects mitochondria from autophagosomal degradation during nutrient starvation. *Proceedings of the National Academy of Sciences*, 108(25):10190–10195.

[227] Rappsilber, J., Ishihama, Y., and Mann, M. (2003). Stop and Go Extraction Tips for Matrix-Assisted Laser Desorption/Ionization, Nanoelectrospray, and LC/MS Sample Pretreatment in Proteomics. *Analytical Chemistry*, 75(3):663–670.

[228] Rappsilber, J., Mann, M., and Ishihama, Y. (2007). Protocol for micro-purification, enrichment, pre-fractionation and storage of peptides for proteomics using StageTips. *Nature Protocols*, 2(8):1896–1906.

[229] Rehling, P., Model, K., Brandner, K., Kovermann, P., Sickmann, A., Meyer, H. E., Kühlbrandt, W., Wagner, R., Truscott, K. N., and Pfanner, N. (2003). Protein Insertion into the Mitochondrial Inner Membrane by a Twin-Pore Translocase. *Science*, 299(5613):1747–1751.

[230] Reich, S. G. and Savitt, J. M. (2018). Parkinson's Disease. *The Medical Clinics of North America*, 103(2):337–350.

[231] Reiter, L. T., Potocki, L., Chien, S., Gribskov, M., and Bier, E. (2001). A Systematic Analysis of Human Disease-Associated Gene Sequences In Drosophila melanogaster. *Genome Research*, 11(6):1114–1125.

[232] Richter, B., Sliter, D. A., Herhaus, L., Stolz, A., Wang, C., Beli, P., Zaffagnini, G., Wild, P., Martens, S., Wagner, S. A., Youle, R. J., and Dikic, I. (2016). Phosphorylation of optn by tbk1 enhances its binding to ub chains and promotes selective autophagy of damaged mitochondria. *Proceedings of the National Academy of Sciences*, 113(15):4039–4044.

[233] Rijk, M. C. d., Launer, L. J., Berger, K., Breteler, M. M., Dartigues, J. F., Baldereschi, M., Fratiglioni, L., Lobo, A., Martinez-Lage, J., Trenkwalder, C., and Hofman, A. (2000). Prevalence of Parkinson's disease in Europe: A collaborative study of population-based cohorts. Neurologic Diseases in the Elderly Research Group. *Neurology*, 54(11 Suppl 5):S21–S23.

[234] Rikova, K., Guo, A., Zeng, Q., Possemato, A., Yu, J., Haack, H., Nardone, J., Lee, K., Reeves, C., Li, Y., Hu, Y., Tan, Z., Stokes, M., Sullivan, L., Mitchell, J., Wetzel, R., MacNeill, J., Ren, J. M., Yuan, J., Bakalarski, C. E., Villen, J., Kornhauser, J. M., Smith, B., Li, D., Zhou, X., Gygi, S. P., Gu, T.-L., Polakiewicz, R. D., Rush, J., and Comb, M. J. (2007). Global Survey of Phosphotyrosine Signaling Identifies Oncogenic Kinases in Lung Cancer. *Cell*, 131(6):1190–1203.

[235] Riley, B. E., Lougheed, J. C., Callaway, K., Velasquez, M., Brecht, E., Nguyen, L., Shaler, T., Walker, D., Yang, Y., Regnstrom, K., Diep, L., Zhang, Z., Chiou, S., Bova, M., Artis, D. R., Yao, N., Baker, J., Yednock, T., and Johnston, J. A. (2013). Structure and function of Parkin E3 ubiquitin ligase reveals aspects of RING and HECT ligases. *Nature Communications*, 4(1):1982.

[236] Roscoe, B. P., Thayer, K. M., Zeldovich, K. B., Fushman, D., and Bolon, D. N. A. (2013). Analyses of the effects of all ubiquitin point mutants on yeast growth rate. *Journal of Molecular Biology*, 425(8):1363–1377.

[237] Rose, C. M., Isasa, M., Ordureau, A., Prado, M. A., Beausoleil, S. A., Jedrychowski, M. P., Finley, D. J., Harper, J. W., and Gygi, S. P. (2016). Highly Multiplexed Quantitative Mass Spectrometry Analysis of Ubiquitylomes. *Cell Systems*, 3(4):395–403.e4.

[238] Rotin, D. and Kumar, S. (2009). Physiological functions of the HECT family of ubiquitin ligases. *Nature Reviews Molecular Cell Biology*, 10(6):398–409.

[239] Rubin, G. M., Yandell, M. D., Wortman, J. R., Gabor, G. L., Miklos, Nelson, C. R., Hariharan, I. K., Fortini, M. E., Li, P. W., Apweiler, R., Fleischmann, W., Cherry, J. M., Henikoff, S., Skupski, M. P., Misra, S., Ashburner, M., Birney, E., Boguski, M. S., Brody,

T., Brokstein, P., Celniker, S. E., Chervitz, S. A., Coates, D., Cravchik, A., Gabrielian, A., Galle, R. F., Gelbart, W. M., George, R. A., Goldstein, L. S. B., Gong, F., Guan, P., Harris, N. L., Hay, B. A., Hoskins, R. A., Li, J., Li, Z., Hynes, R. O., Jones, S. J. M., Kuehl, P. M., Lemaitre, B., Littleton, J. T., Morrison, D. K., Mungall, C., O'Farrell, P. H., Pickeral, O. K., Shue, C., Vosshall, L. B., Zhang, J., Zhao, Q., Zheng, X. H., Zhong, F., Zhong, W., Gibbs, R., Venter, J. C., Adams, M. D., and Lewis, S. (2000). Comparative Genomics of the Eukaryotes. *Science*, 287(5461):2204–2215.

[240] Ryan, T. A., Phillips, E. O., Collier, C. L., JB Robinson, A., Routledge, D., Wood, R. E., Assar, E. A., and Tumbarello, D. A. (2020). Tollip coordinates parkin-dependent trafficking of mitochondrial-derived vesicles. *The EMBO Journal*, 39(11):e102539.

[241] Sandoval, H., Thiagarajan, P., Dasgupta, S. K., Schumacher, A., Prchal, J. T., Chen, M., and Wang, J. (2008). Essential role for Nix in autophagic maturation of erythroid cells. *Nature*, 454(7201):232–235.

[242] Sarraf, S., Raman, M., Guarani-Pereira, V., Sowa, M., Huttlin, E., Gygi, S., and Harper, J. (2013). Landscape of the PARKIN-dependent ubiquitylome in response to mitochondrial depolarization. *Nature*, 496(7445):372–376.

[243] Sato, Y., Okatsu, K., Saeki, Y., Yamano, K., Matsuda, N., Kaiho, A., Yamagata, A., Goto-Ito, S., Ishikawa, M., Hashimoto, Y., Tanaka, K., and Fukai, S. (2017). Structural basis for specific cleavage of Lys6-linked polyubiquitin chains by USP30. *Nature Structural and Molecular Biology*, 24(11):911–919.

[244] Sauvé, V., Lilov, A., Seirafi, M., Vranas, M., Rasool, S., Kozlov, G., Sprules, T., Wang, J., Trempe, J., and Gehring, K. (2015). A Ubl/ubiquitin switch in the activation of Parkin. *The EMBO Journal*, 34(20):2492–2505.

[245] Sauvé, V., Sung, G., Soya, N., Kozlov, G., Blaimschein, N., Miotto, L., Trempe, J.-F., Lukacs, G. L., and Gehring, K. (2018). Mechanism of parkin activation by phosphorylation. *Nature Structural and Molecular Biology*, 25(7):623–630.

[246] Schapira, A. H. V., Cooper, J. M., Dexter, D., Jenner, P., Clark, J. B., and Marsden, C. D. (1989). Mitochondrial Complex I deficiency in Parkinson's Disease. *The Lancet*, 333(8649):1269.

[247] Scheperjans, F., Derkinderen, P., and Borghammer, P. (2018). The Gut and Parkinson's Disease: Hype or Hope? *Journal of Parkinson's Disease*, 8(s1):S31–S39.

[248] Scherer, W. F., Syverton, J. T., and Gey, G. O. (1953). Studies on the propagation in vitro of poliomyelitis viruses. *The Journal of Experimental Medicine*, 97(5):695–710.

[249] Schubert, A. F., Gladkova, C., Pardon, E., Wagstaff, J. L., Freund, S. M. V., Steyaert, J., Maslen, S. L., and Komander, D. (2017). Structure of PINK1 in complex with its substrate ubiquitin. *Nature*, 552(7683):51–56.

[250] Schweers, R. L., Zhang, J., Randall, M. S., Loyd, M. R., Li, W., Dorsey, F. C., Kundu, M., Opferman, J. T., Cleveland, J. L., Miller, J. L., and Ney, P. A. (2007). NIX is required for programmed mitochondrial clearance during reticulocyte maturation. *Proceedings of the National Academy of Sciences*, 104(49):19500–19505.

[251] Shaw, J. B., Malhan, N., Vasil'ev, Y. V., Lopez, N. I., Makarov, A., Beckman, J. S., and Voinov, V. G. (2018). Sequencing Grade Tandem Mass Spectrometry for Top-Down Proteomics Using Hybrid Electron Capture Dissociation Methods in a Benchtop Orbitrap Mass Spectrometer. *Analytical Chemistry*, 90(18):10819–10827.

[252] Sherer, T. B., Betarbet, R., Testa, C. M., Seo, B. B., Richardson, J. R., Kim, J. H., Miller, G. W., Yagi, T., Matsuno-Yagi, A., and Greenamyre, J. T. (2003). Mechanism of Toxicity in Rotenone Models of Parkinson's Disease. *Journal of Neuroscience*, 23(34):10756–10764.

[253] Shiba-Fukushima, K., Imai, Y., Yoshida, S., Ishihama, Y., Kanao, T., Sato, S., and Hattori, N. (2012). PINK1-mediated phosphorylation of the Parkin ubiquitin-like domain primes mitochondrial translocation of Parkin and regulates mitophagy. *Scientific Reports*, 2:1002.

[254] Shimizu, Y., Taraborrelli, L., and Walczak, H. (2015). Linear ubiquitination in immunity. *Immunological Reviews*, 266(1):190–207.

[255] Shimura, H., Hattori, N., Kubo, S.-i., Mizuno, Y., Asakawa, S., Minoshima, S., Shimizu, N., Iwai, K., Chiba, T., Tanaka, K., and Suzuki, T. (2000). Familial Parkinson disease gene product, parkin, is a ubiquitin-protein ligase. *Nature Genetics*, 25(3):302–305.

[256] Shoshan-Barmatz, V., Krelin, Y., and Shteinfer-Kuzmine, A. (2018). VDAC1 functions in Ca2+ homeostasis and cell life and death in health and disease. *Cell Calcium*, 69:81–100.

[257] Simonsen, A., Cumming, R. C., Brech, A., Isakson, P., Schubert, D. R., and Finley, K. D. (2008). Promoting basal levels of autophagy in the nervous system enhances longevity and oxidant resistance in adult Drosophila. *Autophagy*, 4(2):176–184.

[258] Sims, J. J. and Cohen, R. E. (2009). Linkage-Specific Avidity Defines the Lysine 63-Linked Polyubiquitin-Binding Preference of Rap80. *Molecular Cell*, 33(6):775–783.

[259] Singer, T. P. and Ramsay, R. R. (1990). Mechanism of the neurotoxicity of MPTP: An update. *FEBS Letters*, 274(1-2):1–8.

[260] Slater, E. C. (1973). The mechanism of action of the respiratory inhibitor, antimycin. *Biochimica et Biophysica Acta (BBA) - Reviews on Bioenergetics*, 301(2):129–154.

[261] Sliter, D. A., Martinez, J., Hao, L., Chen, X., Sun, N., Fischer, T. D., Burman, J. L., Li, Y., Zhang, Z., Narendra, D. P., Cai, H., Borsche, M., Klein, C., and Youle, R. J. (2018). Parkin and PINK1 mitigate STING-induced inflammation. *Nature*, 561(7722):258–262.

[262] Smirnova, E., Griparic, L., Shurland, D.-L., and Bliek, A. M. v. d. (2001). Dynamin-related Protein Drp1 Is Required for Mitochondrial Division in Mammalian Cells. *Molecular Biology of the Cell*, 12(8):2245–2256.

[263] Sobhian, B., Shao, G., Lilli, D. R., Culhane, A. C., Moreau, L. A., Xia, B., Livingston, D. M., and Greenberg, R. A. (2007). RAP80 Targets BRCA1 to Specific Ubiquitin Structures at DNA Damage Sites. *Science*, 316(5828):1198–1202.

[264] Soubannier, V., McLelland, G.-L., Zunino, R., Braschi, E., Rippstein, P., Fon, E. A., and McBride, H. M. (2012). A Vesicular Transport Pathway Shuttles Cargo from Mitochondria to Lysosomes. *Current Biology*, 22(2):135–141.

[265] Spence, J., Sadis, S., Haas, A. L., and Finley, D. (1995). A ubiquitin mutant with specific defects in DNA repair and multiubiquitination. *Molecular and Cellular Biology*, 15(3):1265–1273.

[266] Spillantini, M. G., Crowther, R. A., Jakes, R., Hasegawa, M., and Goedert, M. (1998). α-Synuclein in filamentous inclusions of Lewy bodies from Parkinson's disease and dementia with Lewy bodies. *Proceedings of the National Academy of Sciences*, 95(11):6469–6473.

[267] Spinelli, J. B. and Haigis, M. C. (2018). The multifaceted contributions of mitochondria to cellular metabolism. *Nature Cell Biology*, 20(7):745–754.

[268] Subramanian, A., Andronache, A., Li, Y.-C., and Wade, M. (2016). Inhibition of MARCH5 ubiquitin ligase abrogates MCL1-dependent resistance to BH3 mimetics via NOXA. *Oncotarget*, 7(13):15986–16002.

[269] Sun, N., Yun, J., Liu, J., Malide, D., Liu, C., Rovira, I. I., Holmström, K. M., Fergusson, M. M., Yoo, Y. H., Combs, C. A., and Finkel, T. (2015). Measuring In Vivo Mitophagy. *Molecular Cell*, 60(4):685–696.

[270] Surmeier, D. J., Obeso, J. A., and Halliday, G. M. (2017). Selective neuronal vulnerability in Parkinson disease. *Nature Reviews Neuroscience*, 18(2):101–113.

[271] Sutovsky, P., Moreno, R. D., Ramalho-Santos, J., Dominko, T., Simerly, C., and Schatten, G. (1999). Ubiquitin tag for sperm mitochondria. *Nature*, 402(6760):371–372.

[272] Suzuki, K., Kirisako, T., Kamada, Y., Mizushima, N., Noda, T., and Ohsumi, Y. (2001). The pre-autophagosomal structure organized by concerted functions of APG genes is essential for autophagosome formation. *The EMBO Journal*, 20(21):5971–5981.

[273] Swaney, D. L., Beltrao, P., Starita, L., Guo, A., Rush, J., Fields, S., Krogan, N. J., and Villén, J. (2013). Global analysis of phosphorylation and ubiquitylation cross-talk in protein degradation. *Nature Methods*, 10(7):676–682.

[274] Swatek, K. N., Aumayr, M., Pruneda, J. N., Visser, L. J., Berryman, S., Kueck, A. F., Geurink, P. P., Ovaa, H., Kuppeveld, F. J. M. v., Tuthill, T. J., Skern, T., and Komander, D. (2018). Irreversible inactivation of ISG15 by a viral leader protease enables alternative infection detection strategies. *Proceedings of the National Academy of Sciences*, 115(10):2371–2376.

[275] Swatek, K. N., Usher, J. L., Kueck, A. F., Gladkova, C., Mevissen, T. E., Pruneda, J. N., Skern, T., and Komander, D. (2019). Insights into ubiquitin chain architecture using Ub-clipping. *Nature*, 572(7770):533–537.

[276] Takahashi, H., Ohama, E., Suzuki, S., Horikawa, Y., Ishikawa, A., Morita, T., Tsuji, S., and Ikuta, F. (1994). Familial juvenile parkinsonism: Clinical and pathologic study in a family. *Neurology*, 44(3, Part 1):437–437.

[277] Tanaka, A., Cleland, M. M., Xu, S., Narendra, D. P., Suen, D.-F., Karbowski, M., and Youle, R. J. (2010). Proteasome and p97 mediate mitophagy and degradation of mitofusins induced by Parkin. *Journal of Cell Biology*, 191(7):1367–1380.

[278] Tanner, C. M., Kamel, F., Ross, G. W., Hoppin, J. A., Goldman, S. M., Korell, M., Marras, C., Bhudhikanok, G. S., Kasten, M., Chade, A. R., Comyns, K., Richards, M. B., Meng, C., Priestley, B., Fernandez, H. H., Cambi, F., Umbach, D. M., Blair, A., Sandler, D. P., and Langston, J. W. (2011). Rotenone, paraquat, and Parkinson's disease. *Environmental Health Perspectives*, 119(6):866–872.

[279] Teske, B. F., Fusakio, M. E., Zhou, D., Shan, J., McClintick, J. N., Kilberg, M. S., and Wek, R. C. (2013). CHOP induces activating transcription factor 5 (ATF5) to trigger apoptosis in response to perturbations in protein homeostasis. *Molecular Biology of the Cell*, 24(15):2477–2490.

[280] Timmis, J. N., Ayliffe, M. A., Huang, C. Y., and Martin, W. (2004). Endosymbiotic gene transfer: organelle genomes forge eukaryotic chromosomes. *Nature Reviews Genetics*, 5(2):123–135.

[281] Todd, A. M. and Staveley, B. E. (2008). Pink1 suppresses α-synuclein-induced phenotypes in a Drosophila model of Parkinson's disease. *Genome*, 51(12):1040–1046.

[282] Tomlinson, E., Palaniyappan, N., Tooth, D., and Layfield, R. (2007). Methods for the purification of ubiquitinated Proteins. *Proteomics*, 7(7):1016–1022.

[283] Toulorge, D., Schapira, A. H. V., and Hajj, R. (2016). Molecular changes in the postmortem parkinsonian brain. *Journal of Neurochemistry*, 139(S1):27–58.

[284] Trempe, J.-F., Brown, N. R., Lowe, E. D., Gordon, C., Campbell, I. D., Noble, M. E. M., and Endicott, J. A. (2005). Mechanism of Lys48-linked polyubiquitin chain recognition by the Mud1 UBA domain. *The EMBO Journal*, 24(18):3178–3189.

[285] Trempe, J. F., Sauve, V., Grenier, K., Seirafi, M., Tang, M. Y., Menade, M., Al-Abdul-Wahid, S., Krett, J., Wong, K., Kozlov, G., Nagar, B., Fon, E. A., and Gehring, K. (2013). Structure of Parkin Reveals Mechanisms for Ubiquitin Ligase Activation. *Science*, 340(6139):1451–1455.

[286] Trifunovic, A., Wredenberg, A., Falkenberg, M., Spelbrink, J. N., Rovio, A. T., Bruder, C. E., Bohlooly-Y, M., Gidlöf, S., Oldfors, A., Wibom, R., Törnell, J., Jacobs, H. T., and Larsson, N.-G. (2004). Premature ageing in mice expressing defective mitochondrial DNA polymerase. *Nature*, 429(6990):417–423.

[287] Truscott, K. N., Kovermann, P., Geissler, A., Merlin, A., Meijer, M., Driessen, A. J. M., Rassow, J., Pfanner, N., and Wagner, R. (2001). A presequence- and voltage-sensitive channel of the mitochondrial preprotein translocase formed by Tim23. *Nature Structural Biology*, 8(12):1074–1082.

[288] Tsuboyama, K., Koyama-Honda, I., Sakamaki, Y., Koike, M., Morishita, H., and Mizushima, N. (2016). The ATG conjugation systems are important for degradation of the inner autophagosomal membrane. *Science*, 354(6315):1036–1041.

[289] Tsuchiya, H., Burana, D., Ohtake, F., Arai, N., Kaiho, A., Komada, M., Tanaka, K., and Saeki, Y. (2018). Ub-ProT reveals global length and composition of protein ubiquitylation in cells. *Nature Communications*, 9(1):524.

[290] Tucker, K. and Park, E. (2019). Cryo-EM structure of the mitochondrial protein-import channel TOM complex at near-atomic resolution. *Nature Structural and Molecular Biology*, 26(12):1158–1166.

[291] Twig, G., Elorza, A., Molina, A. J., Mohamed, H., Wikstrom, J. D., Walzer, G., Stiles, L., Haigh, S. E., Katz, S., Las, G., Alroy, J., Wu, M., Py, B. F. F., Yuan, J., Deeney, J. T., Corkey, B. E., and Shirihai, O. S. (2008). Fission and selective fusion govern mitochondrial segregation and elimination by autophagy. *The EMBO Journal*, 27(2):433–446.

[292] Udeshi, N. D., Mani, D. R., Eisenhaure, T., Mertins, P., Jaffe, J. D., Clauser, K. R., Hacohen, N., and Carr, S. A. (2012). Methods for Quantification of in vivo Changes in Protein Ubiquitination following Proteasome and Deubiquitinase Inhibition. *Molecular & Cellular Proteomics*, 11(5):148–159.

[293] Ulrich, T., Oberhettinger, P., Schütz, M., Holzer, K., Ramms, A. S., Linke, D., Autenrieth, I. B., and Rapaport, D. (2014). Evolutionary conservation in biogenesis of β-barrel proteins allows mitochondria to assemble a functional bacterial trimeric autotransporter protein. *Journal of Biological Chemistry*, 289(43):29457–29470.

[294] Valente, E., Abou-Sleiman, P. M., Caputo, V., Muqit, M. M., Harvey, K., Gispert, S., Ali, Z., Turco, D., Bentivoglio, A., and Healy, D. G. (2004). Hereditary early-onset Parkinson's disease caused by mutations in PINK1. *Science*, 304(5674):1158–1160.

[295] Valente, E. M., Bentivoglio, A. R., Dixon, P. H., Ferraris, A., Ialongo, T., Frontali, M., Albanese, A., and Wood, N. W. (2001). Localization of a Novel Locus for Autosomal Recessive Early-Onset Parkinsonism, PARK6, on Human Chromosome 1p35-p36. *The American Journal of Human Genetics*, 68(4):895–900.

[296] Valkevich, E. M., Sanchez, N. A., Ge, Y., and Strieter, E. R. (2014). Middle-down mass spectrometry enables characterization of branched ubiquitin chains. *Biochemistry*, 53(30):4979–4989.

[297] Vargas, J. N. S., Wang, C., Bunker, E., Hao, L., Maric, D., Schiavo, G., Randow, F., and Youle, R. J. (2019). Spatiotemporal Control of ULK1 Activation by NDP52 and TBK1 during Selective Autophagy. *Molecular Cell*, 74(2):347–362.e6.

[298] Verbeck, G. F., Ruotolo, B. T., Sawyer, H. A., Gillig, K. J., and Russell, D. H. (2002). A fundamental introduction to ion mobility mass spectrometry applied to the analysis of biomolecules. *Journal of Biomolecular Techniques*, 13(2):56–61.

[299] Vijay-Kumar, S., Bugg, C. E., Wilkinson, K. D., Vierstra, R. D., Hatfield, P. M., and Cook, W. J. (1987). Comparison of the three-dimensional structures of human, yeast, and oat ubiquitin. *Journal of Biological Chemistry*, 262(13):6396–6399.

[300] Vilain, S., Esposito, G., Haddad, D., Schaap, O., Dobreva, M. P., Vos, M., Meensel, S. V., Morais, V. A., Strooper, B. D., and Verstreken, P. (2012). The Yeast Complex I Equivalent NADH Dehydrogenase Rescues pink1 Mutants. *PLoS Genetics*, 8(1):e1002456.

[301] Vilariño-Güell, C., Wider, C., Ross, O. A., Dachsel, J. C., Kachergus, J. M., Lincoln, S. J., Soto-Ortolaza, A. I., Cobb, S. A., Wilhoite, G. J., Bacon, J. A., Behrouz, B., Melrose, H. L., Hentati, E., Puschmann, A., Evans, D. M., Conibear, E., Wasserman, W. W., Aasly, J. O., Burkhard, P. R., Djaldetti, R., Ghika, J., Hentati, F., Krygowska-Wajs, A., Lynch, T., Melamed, E., Rajput, A., Rajput, A. H., Solida, A., Wu, R.-M., Uitti, R. J., Wszolek, Z. K., Vingerhoets, F., and Farrer, M. J. (2011). VPS35 Mutations in Parkinson Disease. *The American Journal of Human Genetics*, 89(1):162–167.

[302] Vincow, E. S., Merrihew, G., Thomas, R. E., Shulman, N. J., Beyer, R. P., MacCoss, M. J., and Pallanck, L. J. (2013). The PINK1-Parkin pathway promotes both mitophagy and selective respiratory chain turnover in vivo. *Proceedings of the National Academy of Sciences*, 110(16):6400–5.

[303] Vives-Bauza, C., Zhou, C., Huang, Y., Cui, M., Vries, R. L. A. d., Kim, J., May, J., Tocilescu, M. A., Liu, W., Ko, H. S., Magrané, J., Moore, D. J., Dawson, V. L., Grailhe, R., Dawson, T. M., Li, C., Tieu, K., and Przedborski, S. (2009). PINK1-dependent recruitment of Parkin to mitochondria in mitophagy. *Proceedings of the National Academy of Sciences*, 107(1):378–383.

[304] Vos, M., Esposito, G., Edirisinghe, J. N., Vilain, S., Haddad, D. M., Slabbaert, J. R., Meensel, S. V., Schaap, O., Strooper, B. D., Meganathan, R., Morais, V. A., and Verstreken, P. (2012). Vitamin K2 Is a Mitochondrial Electron Carrier That Rescues Pink1 Deficiency. *Science*, 336(6086):1306–1310.

[305] Wagner, S. A., Beli, P., Weinert, B. T., Nielsen, M. L., Cox, J., Mann, M., and Choudhary, C. (2011). A Proteome-wide, Quantitative Survey of In Vivo Ubiquitylation Sites Reveals Widespread Regulatory Roles. *Molecular & Cellular Proteomics*, 10(10):M111.013284.

[306] Wang, T., Yin, L., Cooper, E. M., Lai, M.-Y., Dickey, S., Pickart, C. M., Fushman, D., Wilkinson, K. D., Cohen, R. E., and Wolberger, C. (2009). Evidence for Bidentate Substrate Binding as the Basis for the K48 Linkage Specificity of Otubain 1. *Journal of Molecular Biology*, 386(4):1011–1023.

[307] Wang, X., Winter, D., Ashrafi, G., Schlehe, J., Wong, Y., Selkoe, D., Rice, S., Steen, J., LaVoie, M., and Schwarz, T. (2011). PINK1 and Parkin Target Miro for Phosphorylation and Degradation to Arrest Mitochondrial Motility. *Cell*, 147(4):893–906.

[308] Wauer, T. and Komander, D. (2013). Structure of the human Parkin ligase domain in an autoinhibited state. *The EMBO Journal*, 32(15):2099–2112.

[309] Wauer, T., Simicek, M., Schubert, A., and Komander, D. (2015a). Mechanism of phospho-ubiquitin-induced PARKIN activation. *Nature*, 524(7565):370–374.

[310] Wauer, T., Swatek, K. N., Wagstaff, J. L., Gladkova, C., Pruneda, J. N., Michel, M. A., Gersch, M., Johnson, C. M., Freund, S. M., and Komander, D. (2015b). Ubiquitin Ser65 phosphorylation affects ubiquitin structure, chain assembly and hydrolysis. *The EMBO Journal*, 34(3):307–325.

[311] Wenzel, D. M., Lissounov, A., Brzovic, P. S., and Klevit, R. E. (2011). UBCH7 reactivity profile reveals parkin and HHARI to be RING/HECT hybrids. *Nature*, 474(7349):105–108.

[312] Whitworth, A. J., Lee, J. R., Ho, V. M. W., Flick, R., Chowdhury, R., and McQuibban, G. A. (2008). Rhomboid-7 and HtrA2/Omi act in a common pathway with the Parkinson's disease factors Pink1 and Parkin. *Disease Models and Mechanisms*, 1(2-3):168–174.

[313] Whitworth, A. J., Theodore, D. A., Greene, J. C., Benes, H., Wes, P. D., and Pallanck, L. J. (2005). Increased glutathione S-transferase activity rescues dopaminergic neuron loss in a Drosophila model of Parkinson's disease. *Proceedings of the National Academy of Sciences*, 102(22):8024–8029.

[314] Wickliffe, K. E., Williamson, A., Meyer, H.-J., Kelly, A., and Rape, M. (2011). K11-linked ubiquitin chains as novel regulators of cell division. *Trends in Cell Biology*, 21(11):656–663.

[315] Witoelar, A., Jansen, I. E., Wang, Y., Desikan, R. S., Gibbs, J. R., Blauwendraat, C., Thompson, W. K., Hernandez, D. G., Djurovic, S., Schork, A. J., Bettella, F., Ellinghaus, D., Franke, A., Lie, B. A., McEvoy, L. K., Karlsen, T. H., Lesage, S., Morris, H. R., Brice, A., Wood, N. W., Heutink, P., Hardy, J., Singleton, A. B., Dale, A. M., Gasser, T., Andreassen, O. A., Sharma, M., and Investigators, International Parkinson's Disease Genomics Consortium (IPDGC), North American Brain Expression Consortium (NABEC), and United Kingdom Brain Expression Consortium (UKBEC) (2017). Genome-wide Pleiotropy Between Parkinson Disease and Autoimmune Diseases. *JAMA Neurology*, 74(7):780.

[316] Woodroof, H. I., Pogson, J. H., Begley, M., Cantley, L. C., Deak, M., Campbell, D. G., Aalten, D. M. F. v., Whitworth, A. J., Alessi, D. R., and Muqit, M. M. K. (2011). Discovery of catalytically active orthologues of the Parkinson's disease kinase PINK1: analysis of substrate specificity and impact of mutations. *Open Biology*, 1(3):110012.

[317] Wriessnegger, T., Gubitz, G., Leitner, E., Ingolic, E., Cregg, J., Delacruz, B., and Daum, G. (2007). Lipid composition of peroxisomes from the yeast Pichia pastoris grown on different carbon sources. *Biochimica et Biophysica Acta (BBA) - Molecular and Cell Biology of Lipids*, 1771(4):455–461.

[318] Xu, M., Skaug, B., Zeng, W., and Chen, Z. J. (2009). A Ubiquitin Replacement Strategy in Human Cells Reveals Distinct Mechanisms of IKK Activation by TNFα and IL-1β. *Molecular Cell*, 36(2):302–314.

[319] Xu, S., Peng, G., Wang, Y., Fang, S., and Karbowski, M. (2011). The AAA-ATPase p97 is essential for outer mitochondrial membrane protein turnover. *Molecular Biology of the Cell*, 22(3):291–300.

[320] Yamano, K., Fogel, A. I., Wang, C., Bliek, A. M. v. d., and Youle, R. J. (2014). Mitochondrial Rab GAPs govern autophagosome biogenesis during mitophagy. *eLife*, 3(0):e01612.

[321] Yamano, K., Kikuchi, R., Kojima, W., Hayashida, R., Koyano, F., Kawawaki, J., Shoda, T., Demizu, Y., Naito, M., Tanaka, K., and Matsuda, N. (2020). Critical role of mitochondrial ubiquitination and the OPTN–ATG9A axis in mitophagy. *Journal of Cell Biology*, 219(9):e201912144.

[322] Yamano, K., Wang, C., Sarraf, S. A., Münch, C., Kikuchi, R., Noda, N. N., Hizukuri, Y., Kanemaki, M. T., Harper, W., Tanaka, K., Matsuda, N., and Youle, R. J. (2018). Endosomal Rab cycles regulate Parkin-mediated mitophagy. *eLife*, 7:e31326.

[323] Yamano, K. and Youle, R. J. (2013). PINK1 is degraded through the N-end rule pathway. *Autophagy*, 9(11):1758–1769.

[324] Yau, R. G., Doerner, K., Castellanos, E. R., Haakonsen, D. L., Werner, A., Wang, N., Yang, W. X., Martinez-Martin, N., Matsumoto, M. L., Dixit, V. M., and Rape, M. (2017). Assembly and Function of Heterotypic Ubiquitin Chains in Cell-Cycle and Protein Quality Control. *Cell*, 171(4):918–933.e20.

[325] Ye, Y. and Rape, M. (2009). Building ubiquitin chains: E2 enzymes at work. *Nature Reviews Molecular Cell Biology*, 10(11):755–64.

[326] Yonashiro, R., Ishido, S., Kyo, S., Fukuda, T., Goto, E., Matsuki, Y., Hoshino, M., Sada, K., Hotta, H., and Yamamura, H. (2006). A novel mitochondrial ubiquitin ligase plays a critical role in mitochondrial dynamics. *The EMBO Journal*, 25(15):3618–3626.

[327] Yoo, Y.-S., Park, Y.-Y., Kim, J.-H., Cho, H., Kim, S.-H., Lee, H.-S., Kim, T.-H., Kim, Y. S., Lee, Y., Kim, C.-J., Jung, J. U., Lee, J.-S., and Cho, H. (2015). The mitochondrial ubiquitin ligase MARCH5 resolves MAVS aggregates during antiviral signalling. *Nature Communications*, 6(1):7910.

[328] Yoshii, S. R., Kishi, C., Ishihara, N., and Mizushima, N. (2011). Parkin mediates proteasome-dependent protein degradation and rupture of the outer mitochondrial membrane. *Journal of Biological Chemistry*, 286(22):19630–19640.

[329] Yun, J., Puri, R., Yang, H., Lizzio, M. A., Wu, C., Sheng, Z.-H., and Guo, M. (2014). MUL1 acts in parallel to the PINK1/parkin pathway in regulating mitofusin and compensates for loss of PINK1/parkin. *eLife*, 3:e01958.

[330] Zalk, R., Israelson, A., Garty, E. S., Azoulay-Zohar, H., and Shoshan-Barmatz, V. (2005). Oligomeric states of the voltage-dependent anion channel and cytochrome c release from mitochondria. *Biochemical Journal*, 386(1):73–83.

[331] Zhang, J., Montine, T. J., Smith, M. A., Siedlak, S. L., Gu, G., Robertson, D., and Perry, G. (2002). The mitochondrial common deletion in Parkinson's disease and related movement disorders. *Parkinsonism & Related Disorders*, 8(3):165–170.

[332] Zhao, Q., Wang, J., Levichkin, I. V., Stasinopoulos, S., Ryan, M. T., and Hoogenraad, N. J. (2002). A mitochondrial specific stress response in mammalian cells. *The EMBO Journal*, 21(17):4411–4419.

[333] Zheng, X. and Hunter, T. (2013). Parkin mitochondrial translocation is achieved through a novel catalytic activity coupled mechanism. *Cell Research*, 23(7):886–897.

[334] Zhou, D., Palam, L. R., Jiang, L., Narasimhan, J., Staschke, K. A., and Wek, R. C. (2008). Phosphorylation of eIF2 Directs ATF5 Translational Control in Response to Diverse Stress Conditions. *Journal of Biological Chemistry*, 283(11):7064–7073.

[335] Zhou, H., Palma, S. D., Preisinger, C., Peng, M., Polat, A. N., Heck, A. J. R., and Mohammed, S. (2012). Toward a comprehensive characterization of a human cancer cell phosphoproteome. *Journal of Proteome Research*, 12(1):260–271.

[336] Zimprich, A., Benet-Pagès, A., Struhal, W., Graf, E., Eck, S. H., Offman, M. N., Haubenberger, D., Spielberger, S., Schulte, E. C., Lichtner, P., Rossle, S. C., Klopp, N., Wolf, E., Seppi, K., Pirker, W., Presslauer, S., Mollenhauer, B., Katzenschlager, R., Foki, T., Hotzy, C., Reinthaler, E., Harutyunyan, A., Kralovics, R., Peters, A., Zimprich, F., Brücke, T., Poewe, W., Auff, E., Trenkwalder, C., Rost, B., Ransmayr, G., Winkelmann, J., Meitinger, T., and Strom, T. M. (2011). A Mutation in VPS35, Encoding a Subunit of the Retromer Complex, Causes Late-Onset Parkinson Disease. *The American Journal of Human Genetics*, 89(1):168–175.

[337] Ziviani, E., Tao, R. N., and Whitworth, A. J. (2010). Drosophila Parkin requires PINK1 for mitochondrial translocation and ubiquitinates Mitofusin. *Proceedings of the National Academy of Sciences*, 107(11):5018–5023.

[338] Zubarev, R. A., Horn, D. M., Fridriksson, E. K., Kelleher, N. L., Kruger, N. A., Lewis, M. A., Carpenter, B. K., and McLafferty, F. W. (2000). Electron Capture Dissociation for Structural Characterization of Multiply Charged Protein Cations. *Analytical Chemistry*, 72(3):563–573.